NSTX UPGRADE
CONCEPTUAL DESIGN REPORT

October 2009

Edited by: Erik Perry

Table of Contents

Section 1: Overview

NSTX Upgrade CDR

October 2009

Lead Author: Erik Perry

A. Purpose

The CD-0 Mission Need for the NSTX Upgrade Project was approved by the Deputy Director of Science Program of the Office of Science, Dr. Patricia Dehmer on February 23, 2009. The NSTX Upgrade Project will include an upgrade of the NSTX central magnets ("centerstack") and the installation of a second Neutral Beam Injection (NBI) plasma heating and current drive system which will significantly expand the NSTX device and plasma parameters closer to next-step Spherical Torus (ST) conditions and provide a broader physics basis for the successful operation of ITER.

B. Mission Need

The mission of the NSTX program is to explore the properties of compact and high normalized pressure "spherical torus" (ST) magnetic fusion plasmas. The compact and accessible ST configuration is potentially advantageous for the development of fusion energy and also broadens and improves the scientific understanding of plasma confinement in ITER. The plasma confinement capability, and the achievable plasma temperature, scale strongly with plasma current in the tokamak and ST. Plasma current in the range of 1 million amperes (1 mega-ampere) is required to access plasma temperatures needed to understand ST physics under fusion-relevant conditions. The only existing DOE facility capable of producing mega-ampere-class ST plasmas is the NSTX facility.

The ST shares many features in common with the conventional tokamak, but several important differences have also been identified – for example the scaling of turbulent energy transport with the frequency of inter-particle collisions. Understanding the causes of these differences is important not only to ST research, but also for developing a predictive capability for magnetic confinement generally. The new centerstack would double the NSTX toroidal magnetic field to 1 Tesla and enable a doubling of the maximum plasma current to 2 MA (million amperes) for the first time in STs. The centerstack upgrade combined with the installation of a second Neutral Beam Injection (NBI) will enable operation at higher magnetic field, current, and plasma temperature, thereby reducing the plasma collisionality to values substantially closer to those projected for next-step ST facilities and for ITER. Access to reduced collisionality will extend the plasma physics understanding of the ST and aid in the development of predictive capability for plasma confinement. Further, controllable fully-non-inductive current-sustainment is predicted to be provided by the second NBI, and would enable tests of the potential for steady-state ST operation and contribute to assessing the ST as a cost-effective path to fusion energy.

The ST is particularly well suited to provide a cost effective test-bed to bridge several gaps from successful ITER operation to a demonstration fusion power plant (Demo) as identified in the Fusion Energy Sciences Advisory Committee (FESAC) report issued October 2007 and entitled: "Priorities, Gaps and Opportunities: Towards A Long-Range Strategic Plan for Magnetic Fusion Energy". More recently, in November 2008, the "Report of the FESAC Toroidal Alternates Panel" also found that the ST offers the potential for an attractive test facility for developing fusion components. Upgrading the NSTX facility could significantly narrow or close capability gaps identified above. In support of these upgrades, the NSTX collaborative research team developed its Five Year Program Plan for 2009-2013 which was favorably peer reviewed and strongly endorsed in DOE-OFES reviews conducted on July 28–31, 2008. The review panel specifically endorsed NSTX upgrade plans which form the central elements of the NSTX Five Year Program Plan.

Advantages of upgrading NSTX include cost and schedule savings from utilization of the existing NSTX facility and related available infrastructure while minimizing the disruption to ongoing ST research. NSTX was originally designed for upgradable centerstack and the second NBI capability. Most existing diagnostic systems are compatible with these upgraded capabilities. Construction of a new ST facility with similar capability could offer increased flexibility and/or design improvements, however it would require significantly higher cost and time as the NSTX site credit is significant ~ $200 M, and the disruption to ongoing ST research if existing ST facilities were not operated during the design and construction phase of a new ST facility. Based on the above considerations, upgrading the existing NSTX facility is the most promising and practical path to close ST capability gaps in a timely and cost-effective manner.

C. Project Preliminary Scope Baseline

The NSTX centerstack upgrade entails the replacement of the slender central column, which holds a subset of the NSTX magnets, with a wider column (by ~ 13 cm in radius), capable of ~ 2x higher confining magnetic fields to bring NSTX to within approximately a factor of two of next-step STs and longer pulses to validate physics at current relaxed conditions ("physics" steady-state). The NSTX centerstack is replaceable as an integrated assembly such that the work to remove the existing center-stack and install the new one can be carried out in a few months. The original NSTX General Requirements Document anticipated a new centerstack with longer pulse and higher field, and the design of NSTX includes suitable provision in related components (toroidal field (TF) outer legs, poloidal field (PF) coils, power supplies, etc.). The key technical approach for the NSTX centerstack upgrade project is the fabrication and assembly of a new centerstack assembly, consisting of the inner legs of the toroidal field (TF) coil, the ohmic heating (OH) solenoid, the centerstack casing, the centerstack plasma facing components, the inboard plasma facing components, and the inboard PF-1 coils. The project scope also includes associated sensors (TF joint sensors, magnetic sensors and thermocouples), reconfiguration of the TF power supplies for higher current operations, and enhancements of support structures for higher field and higher current operation.

The NSTX second NBI entails moving a TFTR Neutral Beam heating and current drive system to NSTX, thereby doubling the NSTX neutral beam power and injecting more tangentially, similar to the injection geometry proposed for next-step STs. The NSTX second NBI project task is similar to the first NBI system installed in FY2000. The project will largely utilize one of the existing four TFTR NBI systems. The second NBI will be installed at Bay K where the vacuum vessel Bay K port area will be modified. The new duct will require new circular and rectangular bellows and an appropriate set of protective shields. The new duct will also incorporate a vacuum pump duct. Prior to the second NBI installation, the NSTX Test Cell Bay K area must be cleared which includes the Bay L pump duct, Bay K diagnostics, existing platforms, diagnostic and vacuum system racks, and gas injection system racks. Following the second neutral beam installation, the vacuum pumping and gas injection control racks will be relocated and brought back to an operational state. For this second NBI upgrade, decontamination of the TFTR beam line (a large high-vacuum stainless steel box enclosure containing various NBI components including cryogenic-panels, beam dump, bending magnets, calorimeter, etc.) will take place prior to refurbishment. This decontamination work will take place in the appropriately equipped TFTR Test Cell where it is currently stored. Replacement components will be fabricated for items which can not be satisfactorily decontaminated.

D. Project Preliminary Cost and Schedule Baseline

The Office of Project Assessment has been charged by the Office of Fusion Energy Science to conduct a review to validate the NSTX Upgrade Project conceptual design and cost range for CD-1 on Dec. 15-16, 2009. The project and documentation will be reviewed and judged as to whether they are ready for CD-1. This Conceptual Design Report will be judged on its completeness as well as whether it is comprehensive and the cost and schedule ranges appropriate.

The preliminary cost range at for the NSTX Upgrade Project is $77-94M unconstrained and $81– 98M when constrained to match anticipated budget guidance. The currently planned unconstrained preliminary funding profile, which will allow the completion of the project by fiscal year 2014, is given in Table 1 below. The final scope for CD-2 will depend on the updated CD-2 cost and schedule, which will be being developed in accordance with the funding profile guidance, and the Total Project Cost (TPC) expectation. The CD-2 baseline will incorporate the results of several on-going cost reduction and value engineering studies.

Table 1. NSTX Upgrade Project Unconstrained Preliminary Funding Profile

Fiscal Year	2009	2010	2011	2012	2013	2014
ROM (Lower Range)	$ 5.2M	$11.8M	$13.4M	$31.3M	$13.1M	$ 2.0M
ROM (Upper Range)	$ 5.2M	$13.0M	$15.7M	$39.9M	$17.8M	$ 2.1M

The following list is a preliminary unconstrained schedule of critical decision milestones for the NSTX Upgrade Project.

Submit CD-1, Alternative Selection & Cost Range	December 2009
Submit CD-2, Performance Baseline	July 2010
Submit CD-3, Start of Construction	April 2011
Submit CD-4, Start of Operations	May 2014

E. Acquisition Strategy

An Acquisition Strategy (AS) will be approved by the Acquisition Executive and reviewed by the DOE Science Office of Project Assessment (OPA) as a prerequisite for CD-1.

F. Environmental Strategy

The NSTX Upgrade Project has undergone review under the National Environmental Policy Act (NEPA) and the DOE has determined that this project meets the requirements for a Categorical Exclusion (CX) under Appendix B to Subpart D of the DOE NEPA Implementing Procedure Rule (10CFR1021). Activities involving potential radiological exposures will be conducted in accordance with existing radiological safety requirements, which are in compliance with relevant DOE rules, including 10 CFR 835.

The NSTX Upgrade Project will incorporate the institutional Integrated Safety Management (ISM) Plan that has been approved by DOE.

G. Risk Management

The NSTX Upgrade Project Environmental Safety & Health (ES&H) risks have been identified on the NSTX Upgrade Project preliminary hazard assessment document. These are addressed via institutional line management ES&H programs, such as PPPL's Integrated Safety Management program.

The NSTX Upgrade Project has developed a Risk Management Plan as part of the Preliminary Project Execution Plan. The project will manage risks as a line responsibility. Risks are identified by WBS Level 2 managers based on probability of occurrence and impact/consequence. The NSTX Upgrade Project management team reviews the identified risks, and as well as the risk mitigation plans, and tracks the implementation of the mitigations using a Risk Registry.

The completion of the NSTX Upgrade Project is projected to be in FY 2014, including six months of schedule contingency, assuming the optimum funding profile. Achievement of this schedule depends largely on receiving the necessary funding. Project plans and milestones will need to be adjusted accordingly if the funding profile is changed.

Section 2: Centerstack Upgrade Overview

NSTX Upgrade CDR

October 2009

Lead Author: Larry Dudek

1. Introduction

The purpose of the NSTX Centerstack upgrade is to expand the NSTX operation space and thereby the physics basis for the next-step ST Facilities. The upgrade will achieve higher levels of performance and pulse duration. The table 1 below lists the operational requirements the design is based on.

	NSTX	NSTX-CSU
Plasma Major Radius [m]	0.8540	0.9344
Aspect Ratio	1.266	1.500
Plasma Current, I_P [MA]	1.0	2.0
Toroidal Field B_t [T]	0.55	1.0
Pulse Length, T_{pulse} [s]	1.0	5.0
Rep Rate $T_{repetition}$ [s]	600	2400
Center Stack Radius$R_{centerstack}$ [m]	0.1849	0.3148
Antenna Rad, $R_{antenna}$ [m]	1.5740	1.5740

Table 1. Operational Requirements

2. Centerstack Upgrade Scope

The changes to the central core include the following component upgrades (Figure 1):

1. A new Toroidal Field (TF) inner leg bundle including flags, hubs, and flexible connectors
2. A new Ohmic Heating (OH) coil
3. New Poloidal Field (PF) coils PF1A Upper, PF1A Lower, and PF1B
4. Replace Microtherm thermal insulation
5. A new Center Stack Casing (CSC)
6. Replace Plasma Facing Components (PFC) associated with CSC including the Inboard Divertor (IBD)
7. New TF, OH, PF1A Upper (PF1AU), PF1A Lower (PF1AL), and PF1B Lower (PF1BL) coil electrical leads
8. New CS and Supply piping for heating and cooling of CSC and

IBD The following structural upgrades will be made to the machine structures:

1. TF outer leg supports
2. PF coil supports
3. Pedestal which supports Center Stack Assembly from floor
4. Vacuum vessel if required (VV)

The following Electrical Systems will be upgraded as part of the centerstack upgrade:

1. Power Systems (Upgrade TF power supply to support full field capability of ~1T. (At ~1T, ~2.5s flattop every 20 min and up to ~5 s every 40 min)
2. CS Bakeout system
3. I&C systems

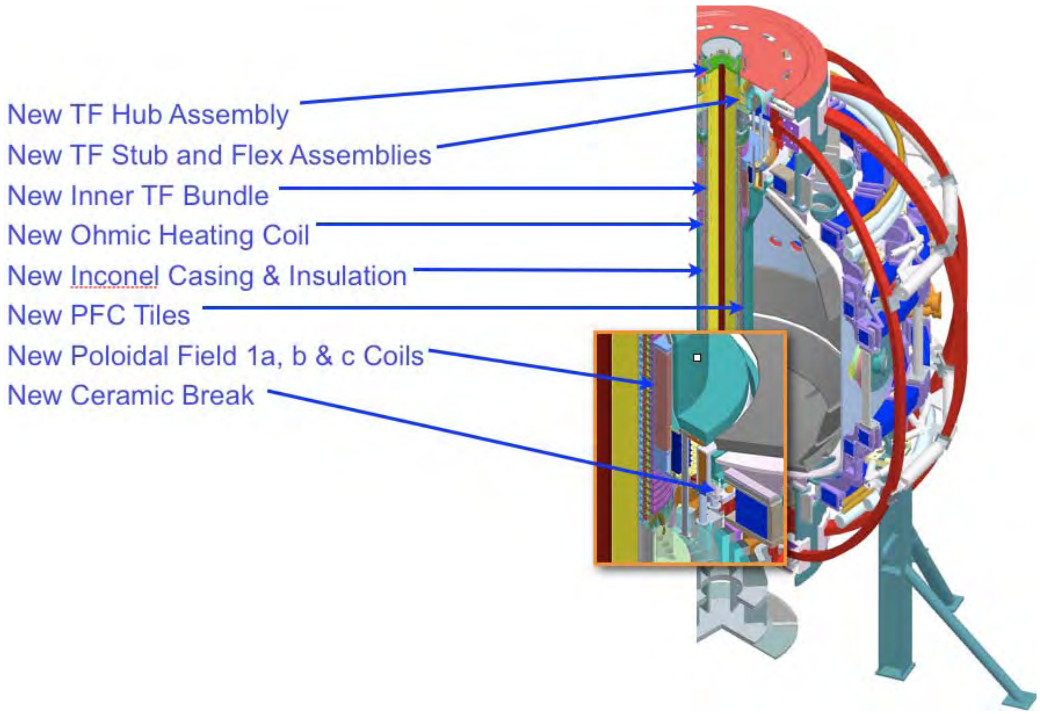

Figure 1. Core Upgrades

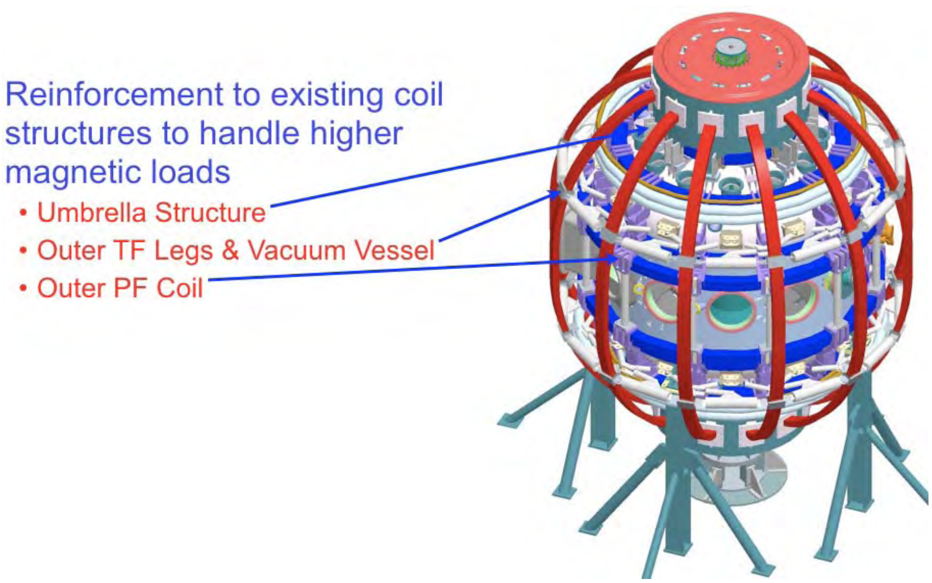

Figure 2. Structural Upgrades to the Coil Structures

In addition to the above upgrades the Center Stack Diagnostics Sensors (Rogowski Coils, Mirnov Coils, Flux Loops, Langmuir Probes & Thermocouples) will be relocated to the new centerstack and replaced with new parts. The Auxiliary systems will be upgraded to support the new centerstack by modifying the water system to improve the cooling for the new OH coil which include an increase in cooling water pressure by upgrading the pump to provide 600 psig (up from 400 psig).

3. Peer Review

A peer review of the centerstack design was held in mid August at Princeton. The reviewers included engineers from outside the lab. Presentations included technical details on the analysis and the design concept. At this review 40 Chits were generated and have been dispositioned. Most of the chits were written in the area of analysis recommendations and TF Inner to outer joint design. The project has responded to these chits and the closeout is being tracked.

4. Milestone Summary Schedule

Figure 3 shows the summary milestone schedule for the NSTX Centerstack Upgrade. The copper procurement for the TF bundle is planned for early procurement in order to complete it in time for installation. The copper which is on the critical path must be procured, machined a stub is friction stir welded onto both ends before epoxy impregnation.

5. Cost Estimates

Cost estimates were generated by the Job Managers with input from engineers closest to the work. Estimates are conservative and are "middle of the error bar" estimates. Depending on the work estimated, they are based on previous NSTX construction, quotes from Vendors or suppliers engineering Judgement, or published cost data (eg RS Means).

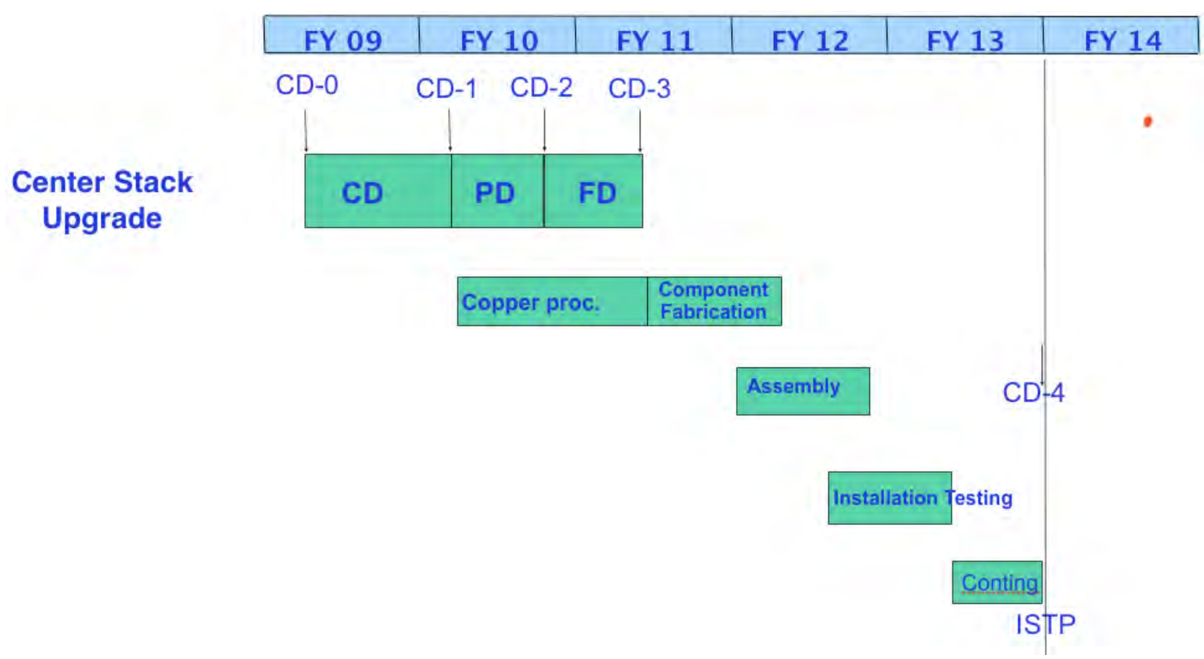

Figure 3. NSTX Centerstack Upgrade Milestone Summary

6. Risks

The risks of greatest concern at CD-0 were those listed in Table 2 below.

Risk	Mitigation
Aability to find a cost effective TF Joint that works at higher fields.	The selected design has been verified through analysis to be far superior to the existing design for current capacity and liftoff
Little room to re-enforce outer TF Legs and Umbrella Structure to handle higher loads.	The original concept of a diamond brace has evolved to a "radius rod concept"

Table 2. CD-0 Risks

The latest Risk Registry now has 34 risks identified which are broken down as follows:

- •Vendor Performance (9)
- •Coil Fabrication (8)
- •Installation Difficulty (7)
- •Design error (4)
- •Analysis (3)
- •Other (3)

Risk	Mitigation
OTF and PF Support Installation Difficulty	1. Design is being tailored to improve installation by making the parts modular and utilizing space occupied by the existing supports 2. Coordinate carefully with the NB upgrade 3. Proceduralize the removal of the existing equipment

Table 3. Risk of Most Concern

Section 3: Centerstack Upgrade and Magnet Systems

NSTX Upgrade CDR

October 2009

Lead Author: Jim Chrzanowski

1.0 Centerstack Assembly Components

The upgrades to the Centerstack assembly involve numerous components that will be discussed in this document. The components include:

1.1 Inner Toroidal Field Coil bundle
1.2 Ohmic Heating Solenoid
1.3 Centerstack Casing & bellows Assembly
1.4 Ceramic Break Assembly
1.5 Plasma Facing Components
1.6 Inner Poloidal Field Coils

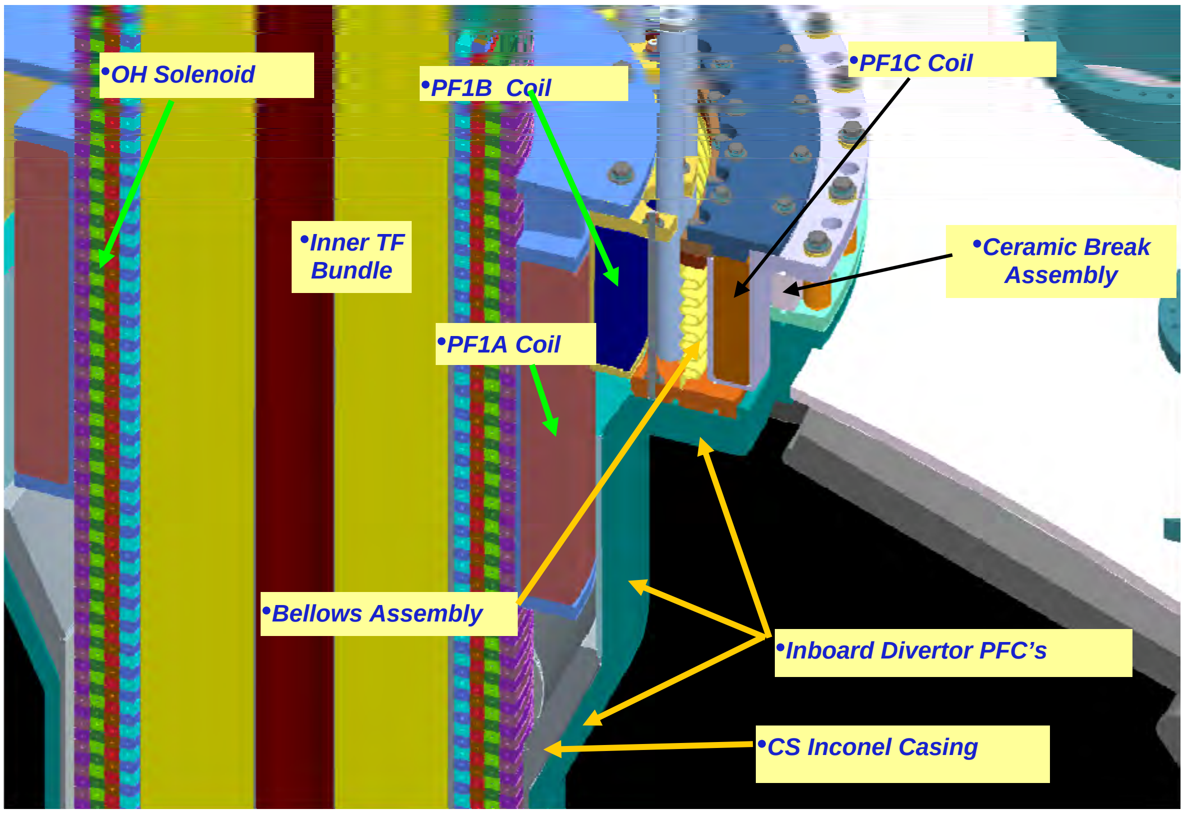

Figure 1- Centerstack Assembly Components

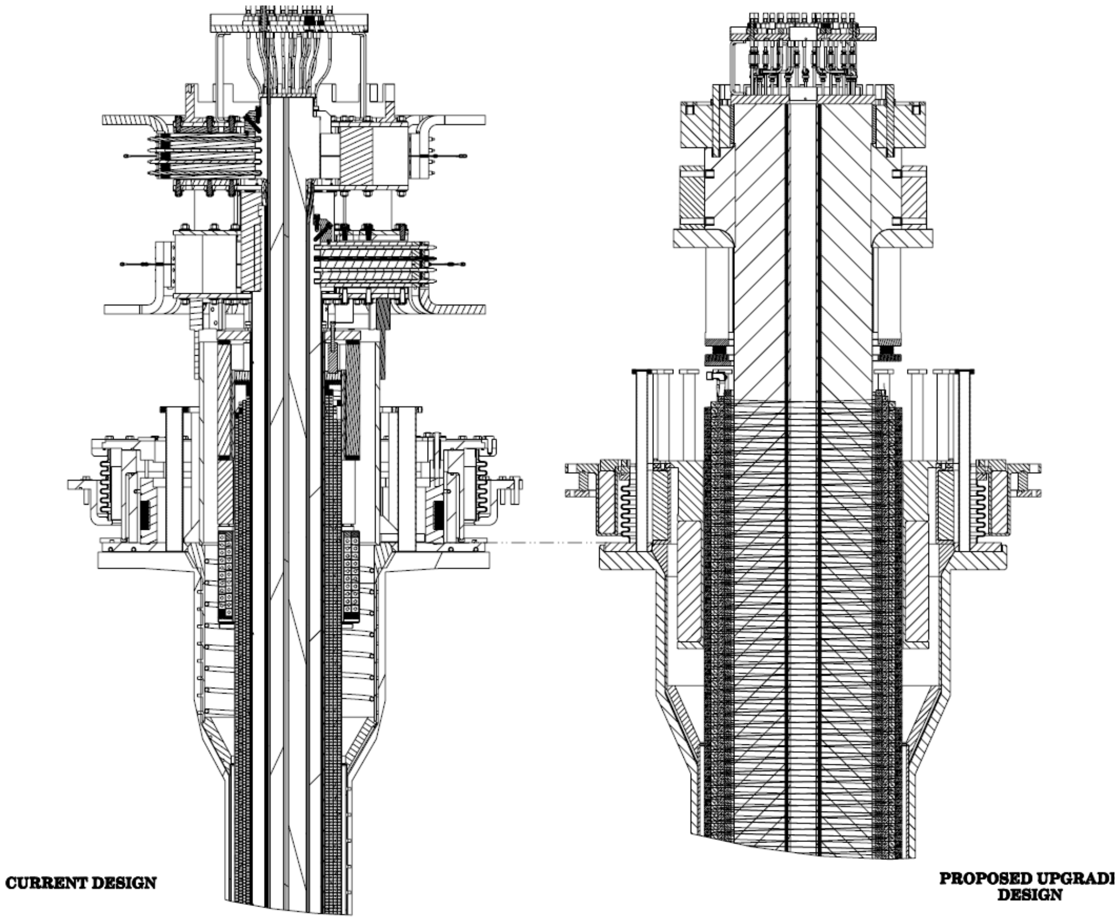

Figure 2- Comparison between Original & Upgrade CS

2.0 Inner Toroidal Field Bundle

The TF bundle forms the inner legs of the Toroidal Field coil system. The Inner TF Bundle turns will be linked to the Outer TF coils via flexible bus connections that will not be discussed in this section.

2.1 Design Description

The inner TF bundle consists of 36 individual coil turns that will operate at 129 KA. The original TF bundle design was constructed with two layers of turns- 12 inner and 24 outer turns. The upgrade design has a single layer of wedge shaped conductors [See figure 3].

The coil will be constructed using water-cooled copper conductors that are insulated with S-2 glass tape and then Vacuum-pressure-impregnated (VPI) using CTD-101K resin system.

The physical size of the upgraded Inner TF Bundle has nearly doubled. The diameter has increased from 7.9 to 15.8 inches and the copper weight from 2300 to 10,900 pounds. Table 1 gives the design comparison between the original and upgraded Inner TF bundle.

Table 1- Inner TF Bundle Design Comparison

	Base Design	Upgrade Design
Operating Voltage	1013 volts	1013 volts
Number of turns	36	36
Number of layers	2	1
Cooling	Water	Water
Operating current	71,168 amps	129,778 amps
Turn insulation	0.0324 in.	0.0324 in.
Dielectric strength- turn insulation		3.8 KV [3] half-lapped layer glass
Groundwall insulation	0.054 in.	0.090 in.
Copper mass	2260 lbs	10,900 lbs
Outside diameter	7.866 in.	15.752 in.
Insulation scheme	B-stage CTD-112	S-2 glass and VPI CTD-101K
Cooling hole size ID	0.186 in.	0.305 in.

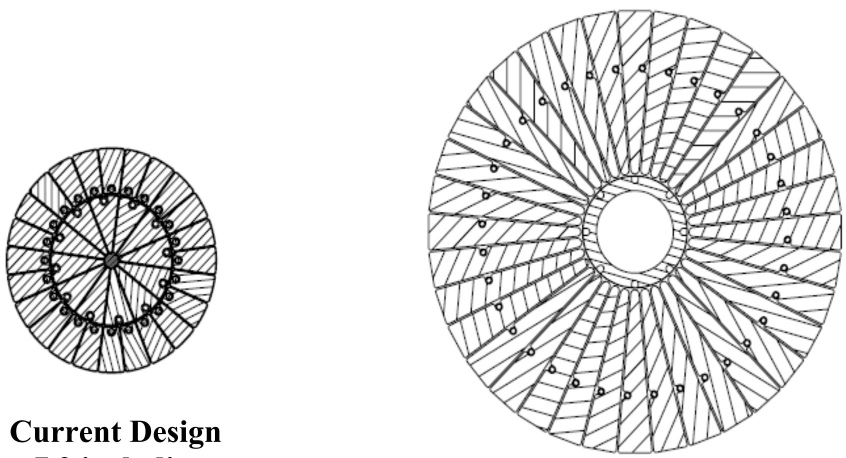

Current Design
7.9 inch dia.

Upgrade Design- 15.7 inch dia.

Figure 3- Size Comparison of TF Bundle

2.2 Inner TF Conductor:

The conductor will be procured as wedge shaped copper extrusions. The copper grade will be C10700 [oxygen-free w/silver] or equivalent. Due to the geometry of the conductor, the conductor manufacturers require the conductor to be extruded oversize and not to final tolerance [See Figure 4- Rough TF Extrusion]. This will result in a second operation of final machining that will also include machining the cooling groove as well as a relief for the coil leads [See Figure 5- TF Extrusion after Machining]. The coil leads will then be attached to the conductor using a Friction Stir Weld [FSW] process [See Figure 6- TF Extrusion w/ Lead Extension]. The coil leads will be constructed using high strength copper alloy C18100- [Copper-Chromium-Zirconium]. This high strength alloy will enhance the pull out strength of the inserts at the TF joint.

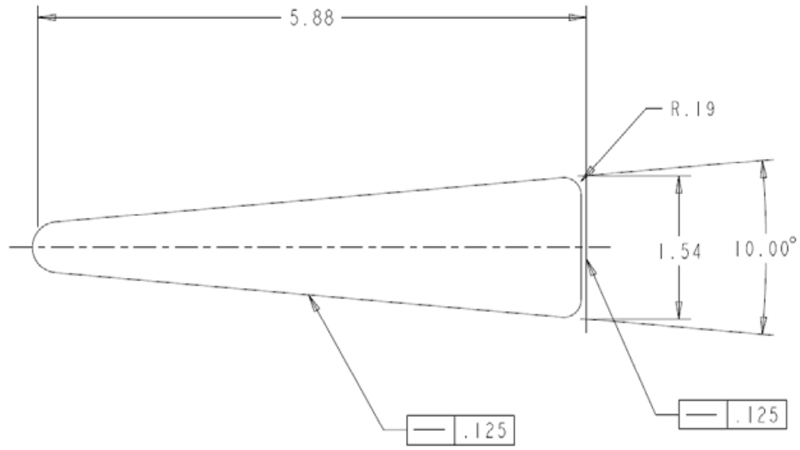

Figure 4- Rough TF Extrusion

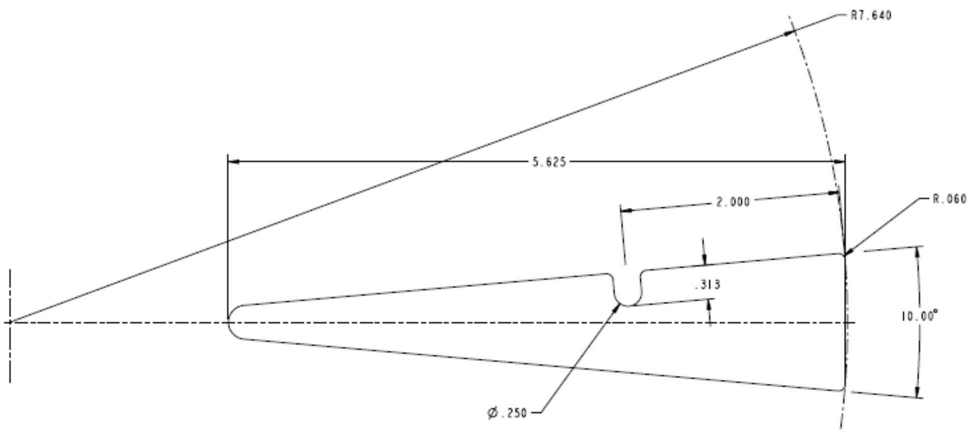

Figure 5- TF Extrusion after Machining

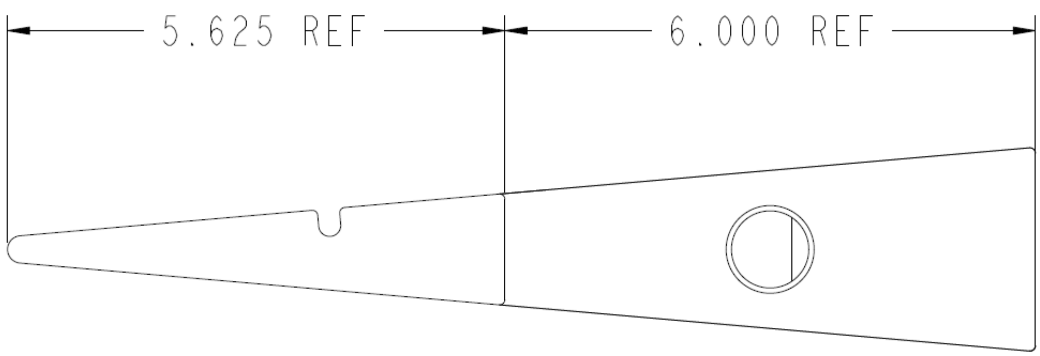

Figure 6- TF Extrusion w/ Lead Extension

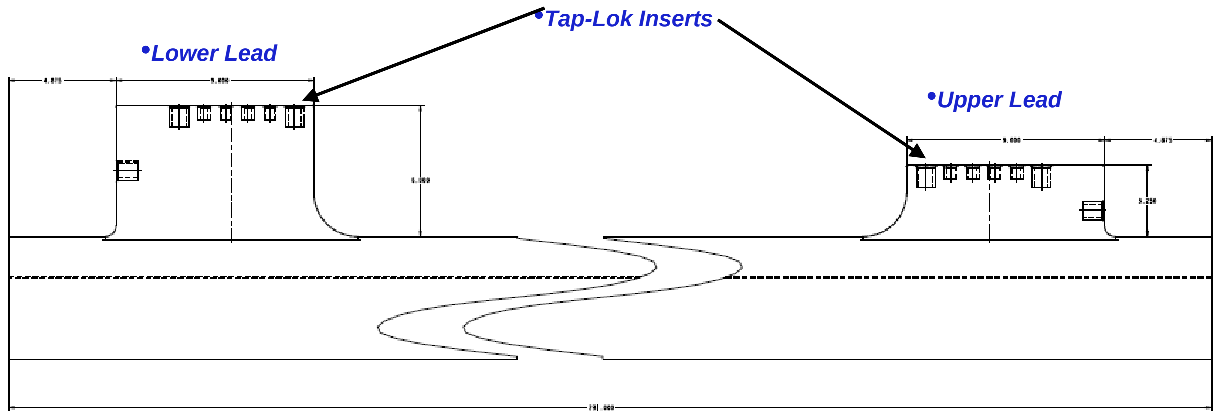

Figure 7- TF Conductor w/Leads

The upper coil lead is shorter in height than the lower to allow for the installation and assembly of the PF1A coils and the Centerstack casing.

2.2.1 Friction Stir Welding (FSW) Tests:

Tests have been performed by Edison Welding Institute to qualify the procedure for joining the leads to the conductor. Additional test need to be performed joining the C18100 to the C10700.

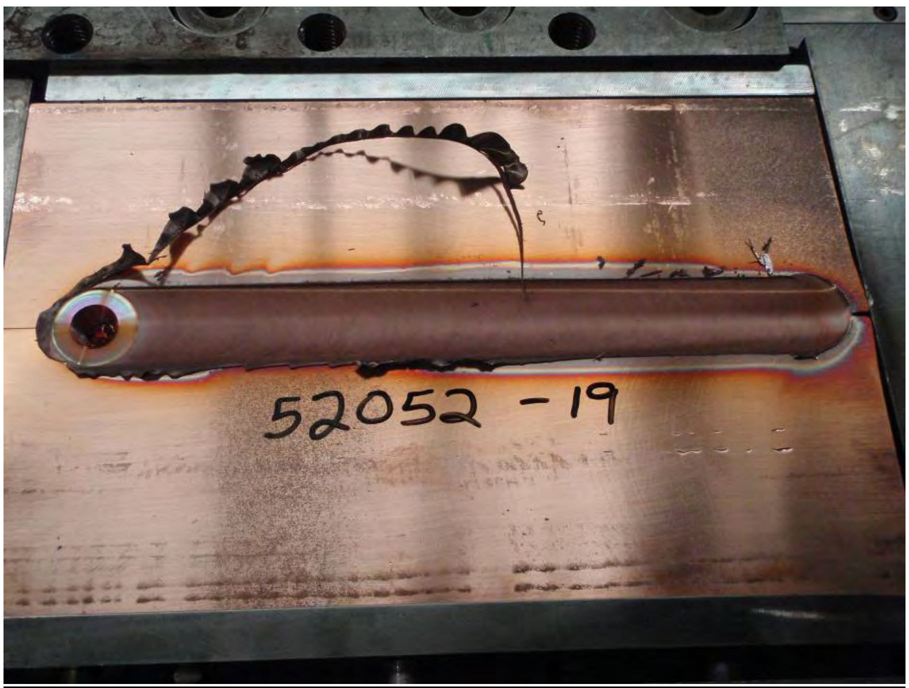

Figure 8- View of FSW Sample produce by Edison Welding Institute.

Figure 9- FSW Rotating Pin

2.2.2 Conductor Procurement Plan:

The plan is to procure [80] TF extrusions following a Conductor Peer Review that will be held in January 2010. This will include sufficient conductor for 2 bundles plus conductor for process development. Only 45 conductors will be completely finished with final machining and lead extensions.

2.3 Resin System

The resin system that has been selected for all of the upgrade coils is CTD-101k a product of Composite Technology Development Inc. 101K is a three component epoxy system that has long working time and low viscosity. The material was well characterized by the ITER project as well as for NSCX where is was used to VPI the Modular and Toroidal Field Coils.

2.3.1 Cure Cycle:

5 hours @ 100º C [Cure]

16 hours @ 125º C [Post Cure]

2.4 TF Bundle End Details:

Figures 9 and 10 show some of the details of the ends of the TF bundle. Between each conductor at the lead area will be a Kapton/G-10 flash shield that will enhance the tracking distances between joints.

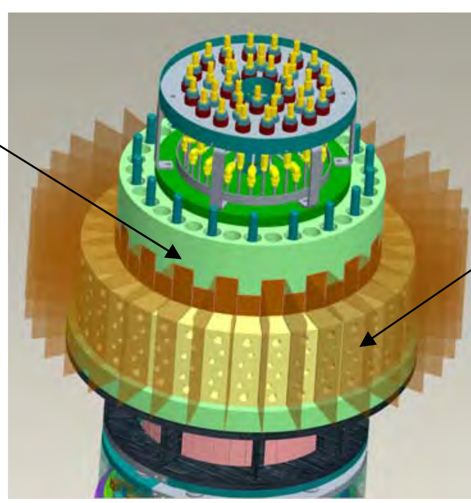

Figure 10- Details of Upper End of TF Bundle

A G-10 spline will be used to transfer any twisting loads to the umbrella.

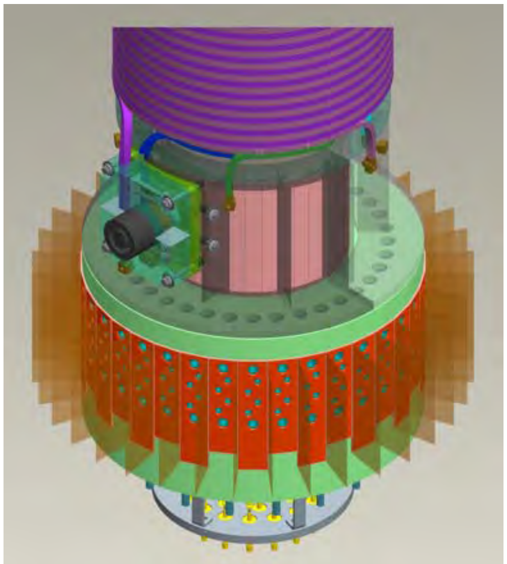

Figure 11- Details of Lower End of TF Bundle

2.5 Manufacturing Plan

The present plan is to manufacture the Inner TF bundle at PPPL. This is based on the degree of manufacturing difficulty as well as to maintain quality control.

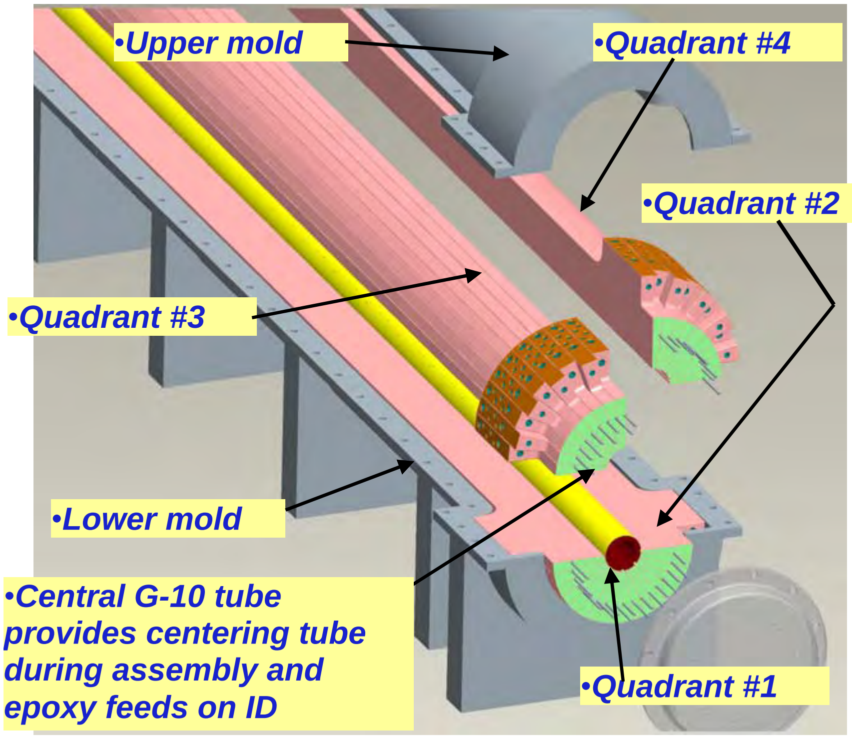

Figure 12- Inner TF Bundle Assembly

2.5.1 Proposed Manufacturing Sequence:

2.5.1.1 Solder the copper cooling tubes in place.

2.5.1.2 Sandblast and prime conductors
2.5.1.3 Assemble conductors into a 9 turn quadrant
2.5.1.4 VPI Quadrant
2.5.1.5 Repeat process for all 4 quadrants.
2.5.1.6 Assemble together the 4-quadrants with fiberglass between quadrants.
2.5.1.7 Overwrap full bundle with fiberglass groundwrap.
2.5.1.8 VPI full TF bundle.
2.5.1.9 Remove from mold, clean and perform final acceptance tests.

3.0 Ohmic Heating Solenoid [OH]

The OH solenoid is a continuous solenoid winding extending above and below the mind-plane of the NSTX device. The OH solenoid will be wound directly over the upgraded Inner TF bundle between the upper and lower TF joint extensions.

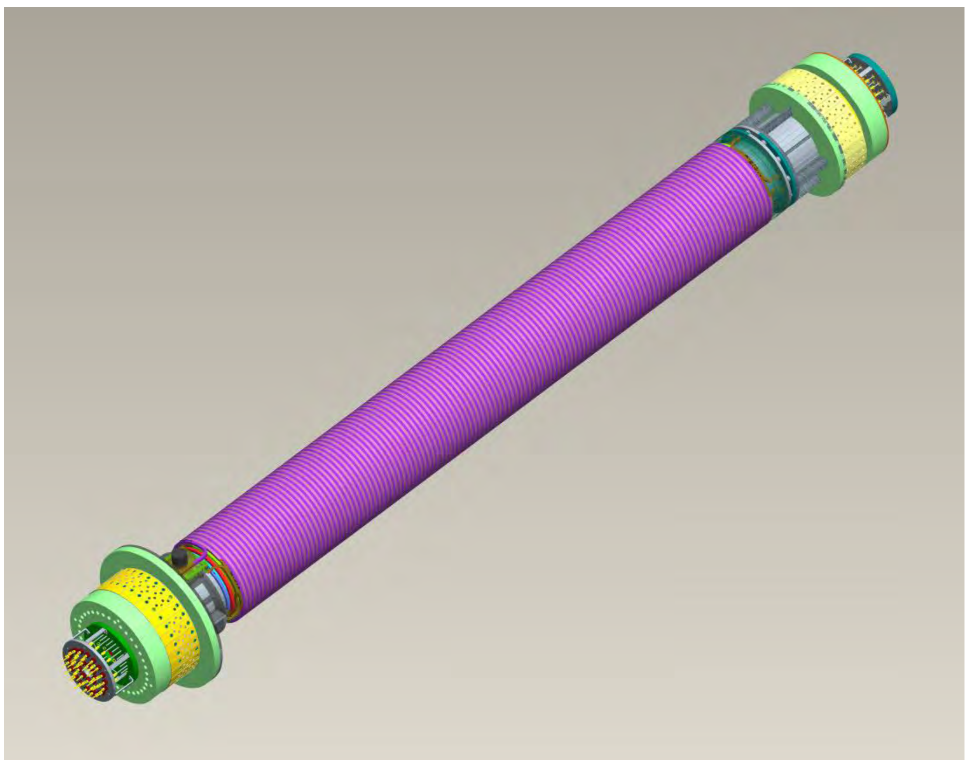

Figure 13- OH Solenoid

3.1 Design Description:

The OH coil consists of four layers wound two-in-hand for a total of eight windings. There are a total of 1148 turns total, and will operate at a maximum +24 to -24 KA. Multiple layers of Teflon tape will be installed onto the OD of the TF bundle to provide a slip plane for thermal growth between the OH coil and TF bundle. The coil will be constructed using water cooled copper conductor that will be insulated with Kapton/S-2 glass tape and vacuum pressure impregnated (VPI) in place using CTD-101K resin system.

The upgraded OH solenoid has nearly doubled in physical size increasing from 12.3 to 22.1 inch diameter and in copper weight from 2300 to 6400 pounds.

	Base Design	Upgrade Design
Operating Voltage	6077 volts	8100 volts
Number of turns	964	1148
Number of layers	4	4
Cooling hole diameter	0.188 in	0.175 in
Operating current	24,000 amps	24,000 amps
Groundwall insulation	0.054 in.	0.090 in.
Turn insulation	0.0268 in	0.0480 in
Turn insulation dielectric strength		16.4 KV
Outside diameter	12.304 in	22.10 in
Copper mass	2340 lbs	6400 lbs
Cooling paths	8	8

Table 2- OH Solenoid Design Comparison

3.2 Design Improvements/Features:

There are a number of design improvements over the original OH solenoid. These include:

3.2.1 *Coil Lead Location:* the leads have been relocated to the bottom of the machine to minimize motion in the lead to bus area

3.2.2 *Coil Lead Design:* The leads will use a coaxial design to minimize any stray fields/forces as a result of the lead to bus connections.

3.2.3 *Winding Surface:* No tension tube will be used. The OH will be wound directly onto the OD of the inner TF bundle.

3.2.4 *Cooling Connections:* Improvements have been made to enhance the reliability of the cooling connections.

3.2.5 *Slip Plane:* A slip plane will be provided between the Inner TF bundle and OH to allow for relative thermal growth between coils.

3.2.6 *Ground Planes:* Ground planes will be provided on both the inner and outer surfaces of the OH solenoid.

3.2.6.1 Inner: Corona shield C215.51 tape [von-Rolla]

3.2.6.2 Outer: Conductive paint

3.2.7 *Braze Joints:* Two types of conductor braze joints

3.2.7.1 *In*-line: Induction Brazed joints

3.2.7.2 *Layer to Layer*: TIG Braze joints

3.2.8 *OH Removal:* Even though the OH is trapped, in case of an OH failure, the coil can be cut off from the TF bundle and a new OH wound and VPI'd.

3.3 OH Conductor

The OH conductor will be procured as a copper extruded conductor w/cooling hole. The copper alloy will be C10700 [oxygen-free w/silver] or equivalent. The conductor cross-section will be trapezoidal in shape to accommodate any "Keystoning" that may occur as a result of the small diameter. Tests were performed to determine the correct trapezoidal cross section that would be required to maintain coil build tolerances.

A total of 5000 feet of copper conductor will be required.

- Layer 1: 555 feet each x 2
- Layer 2: 603 feet each x 2
- Layer 3: 653 feet each x 2
- Layer 4: 702 feet each x 2

Procurement of the copper conductor will occur following the Preliminary Design Review. A total of 12,000 feet will be procured that includes sufficient conductor for two coils plus development process material.

3.4 OH End Details:

3.4.1 *Upper End:* A stainless steel support structure will be installed between the OH solenoid and the upper TF lead extension. A Belleville washer assembly between the OH and TF will be used to maintain the pre-load on the coil. [Required pre-load analysis is presently being performed].

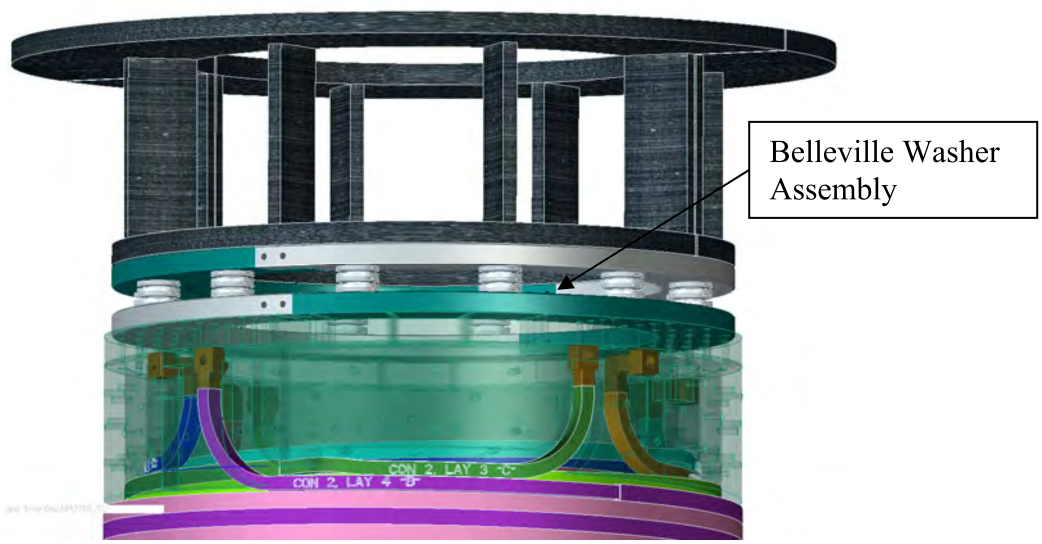

Figure 14- Upper OH Details

3.4.2 *Lower End:* The coaxial OH coil leads are located on the bottom of the solenoid to minimize motion on the leads. A stainless steel support structure will be installed between the OH solenoid and the lower TF lead extension that will support the leads and the end of the OH solenoid. [See Figure 15- Lower OH Details]

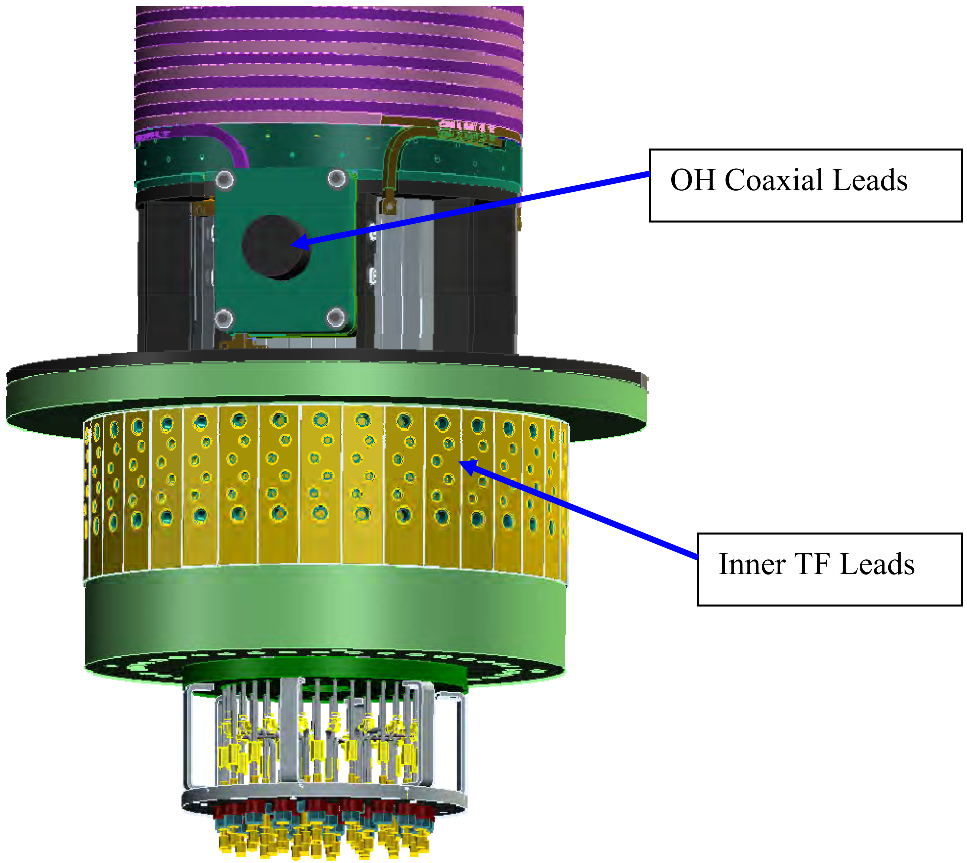

Figure 15- Lower OH Details

3.5 Braze Joints:

There are three types of braze joints that will be used in the construction of the OH solenoid.

3.5.1 *Layer to Layer:* "TIG Braze"

The layer to layer joints are performed at the ends of the OH solenoid when jumping from one layer to the next. A method developed- "TIG Braze" will be used. This method provides adequate joint strength and minimizes annealing of the joint area. and provides a means to independently cool each layer of the solenoid.

This method has been used successfully on the original OH and as well as the rebuilt OH produced by ASIPP in Heifi, China.

3.5.1.1 *TIG-Braze Procedure:*

3.5.1.1.1 Pre-tin the overlapping joint surfaces using the 96%/4 % tin-silver soft-solder. The conductors shall not be heated above 260 °C [500°F].

3.5.1.1.2 Each end of the conductors shall be TIG brazed, by a qualified operator, using Sil-Fos braze material with helium shield gas. (12-18 seconds at 135 amps per end) [**Note: TIG brazing heat input MUST be carefully controlled to minimize annealing of the copper conductor.]**

3.5.1.1.3 The maximum joint temperature and the time required to complete the TIG operation must be monitored and documented.

3.5.1.1.4 Each lap joint shall be visually inspected for full flow and whetting of the braze material.

3.5.1.1.5 Remove the clamps from the previous operation. Apply flux to the pre-tinned joint and solder with 96%/ 4% Tin-Silver soft-solder with a melt temperature of 221°C (430°F) using pre-approved procedure and technique.

3.5.1.1.6 Carefully clean the joint with hot water, assuring that no water gets into the surrounding insulation, and remove excess solder using a file and hand sanding.

3.5.1.1.7 A visual inspection of the finished joint shall be made to ascertain complete flow of solder/braze material into the joint area and joint quality.

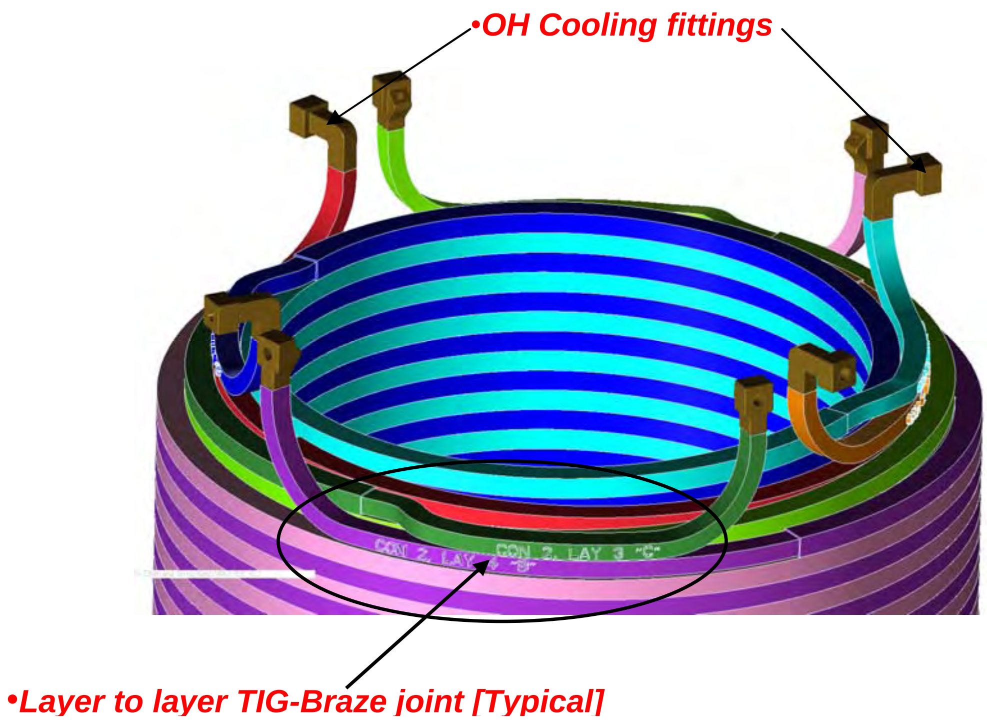

Figure 16- OH Layer to Layer TIG-Braze Joint

3.5.1.2 *R&D Testing:*

Successful tests have been performed to verify procedure using proposed conductor sizes.

Figure 17- Layer to Layer Specimens

3.5.2 In line Braze:

In line brazes are used to join together conductors during the winding process. These will be induction brazed using Sil-Fos braze material. After each braze, the joint will be tested by a helium leak testing while applying a hydraulic load to the joint.

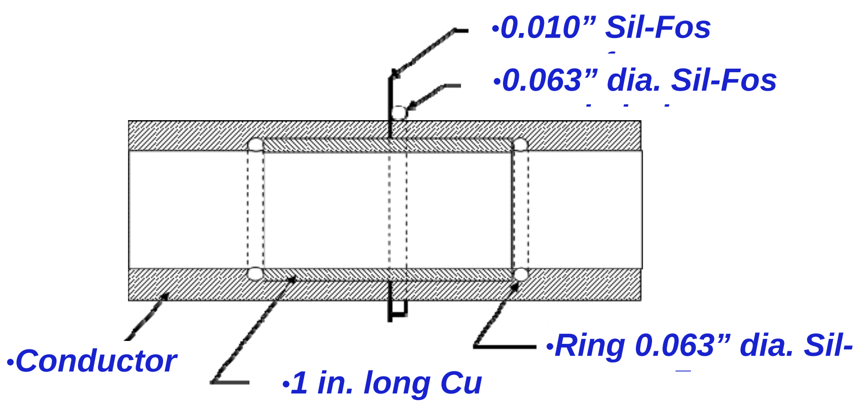

Figure 18- Proposed In-Line Braze Joint

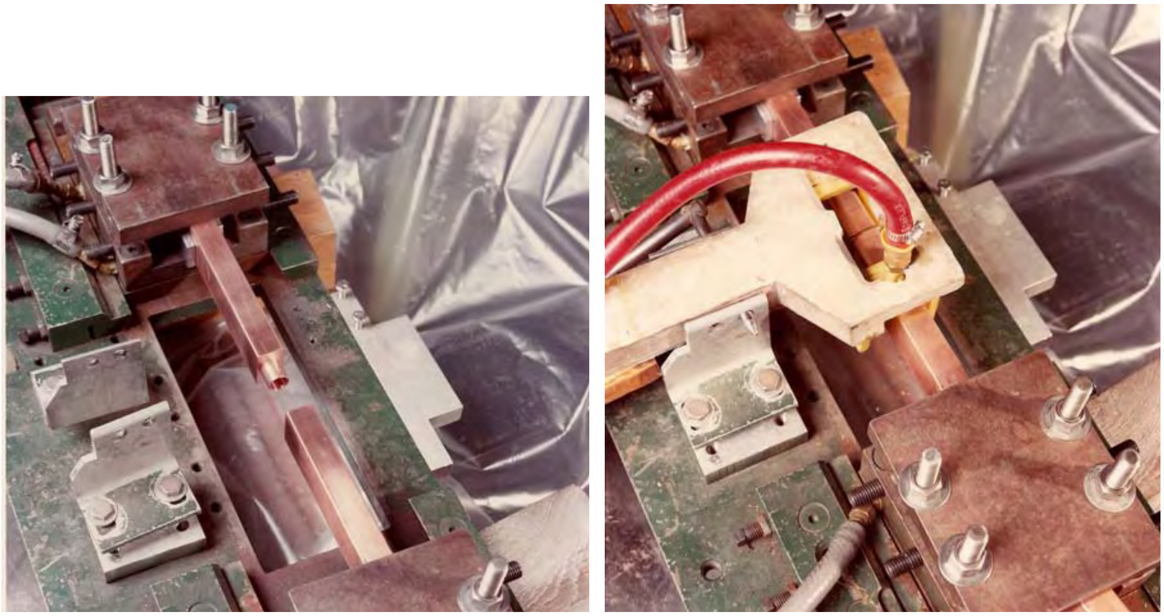

Figure 19- Typical Induction Braze Process

3.5.3 Lead and Cooling Fittings:

The cooling fittings and lead connections will be joined to the conductor by either torch or induction brazing process. Sil-Fos will be used as the braze material.

3.6 OH Coil Leads:

The OH solenoid leads will be located at the lower section of the coil and be a coax design. This will minimize both motion and stray fields in the vicinity of the joint.

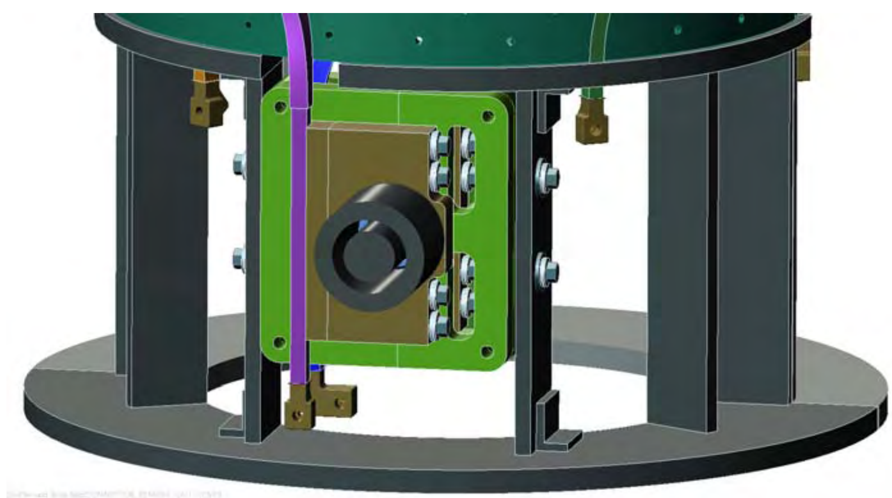

Figure 20- OH Lead Area

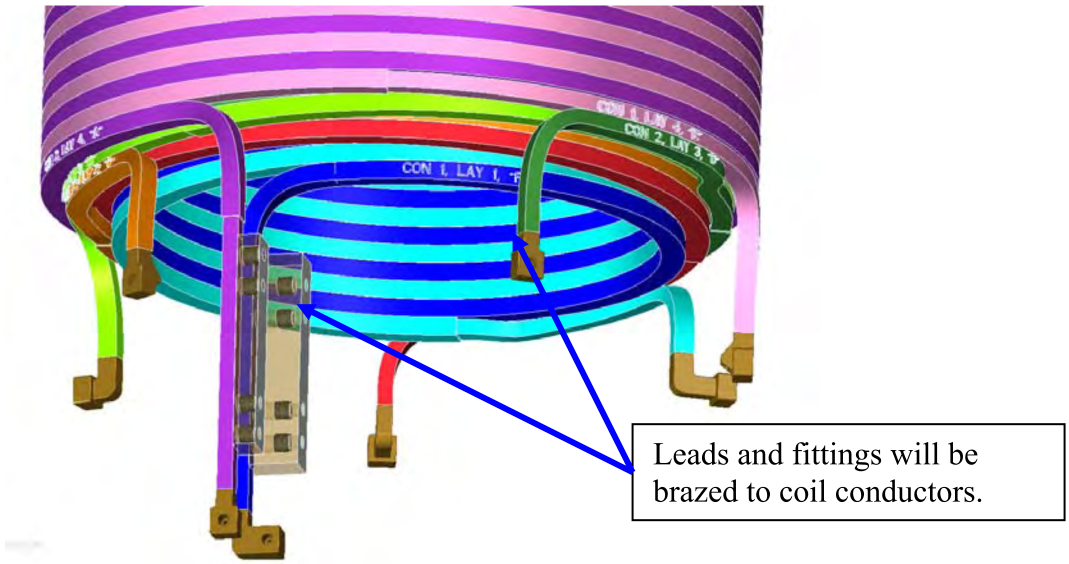

Figure 21- OH Lead to Conductor

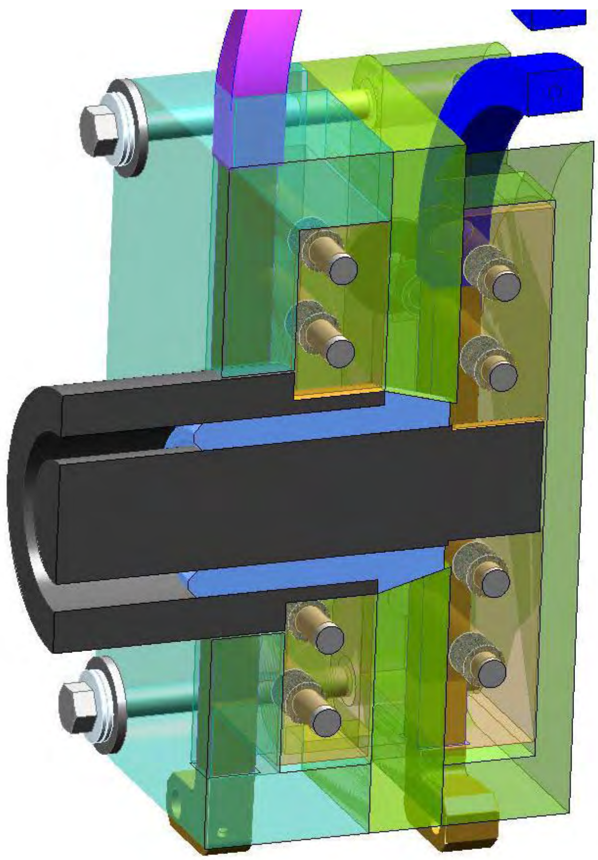

Figure 22- Cutaway of OH Coax Joint

3.7 OH Manufacturing Plan:

The present plan is to manufacture the OH solenoid at PPPL. This is based on the degree of manufacturing difficulty as well as to maintain quality control.

3.7.1 Proposed Manufacturing Sequence:

3.7.1.1 Mount the completed TF bundle into winding fixture.
3.7.1.2 Apply Teflon "Slip Plane" onto the OD of the TF bundle.
3.7.1.3 Apply ground plane tape and groundwall insulation.
3.7.1.4 Wind 4 layers of OH solenoid directly onto TF bundle.
3.7.1.5 Brazes – Layer to Layer and In-line brazes will be required.
3.7.1.6 Apply outer groundwrap insulation.
3.7.1.7 Install mold
3.7.1.8 Vacuum-pressure-impregnate OH solenoid.
3.7.1.9 Perform final electrical and pressure tests on both OH and TF inner bundle.
3.7.1.10 Apply outer ground plane
3.7.1.11 Apply surface diagnostics
3.7.1.12 Install "Micro-Therm" thermal blanket

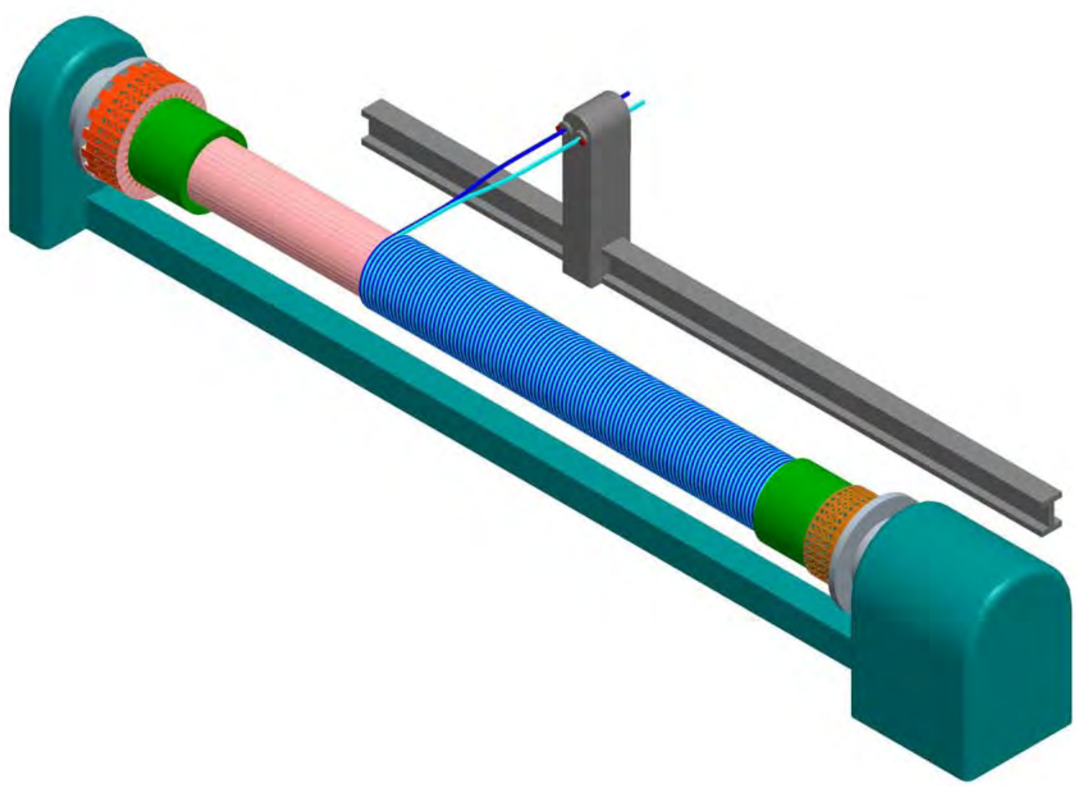

Figure 23- Winding OH Solenoid

4.0 Centerstack Casing Components:

The Centerstack Assembly is comprised of numerous components including:

- Centerstack Casing:
- Bellows Assembly
- Ceramic Break Assembly
- Plasma Facing Components
- Inner PF Coils [PF1A thru PF1B]

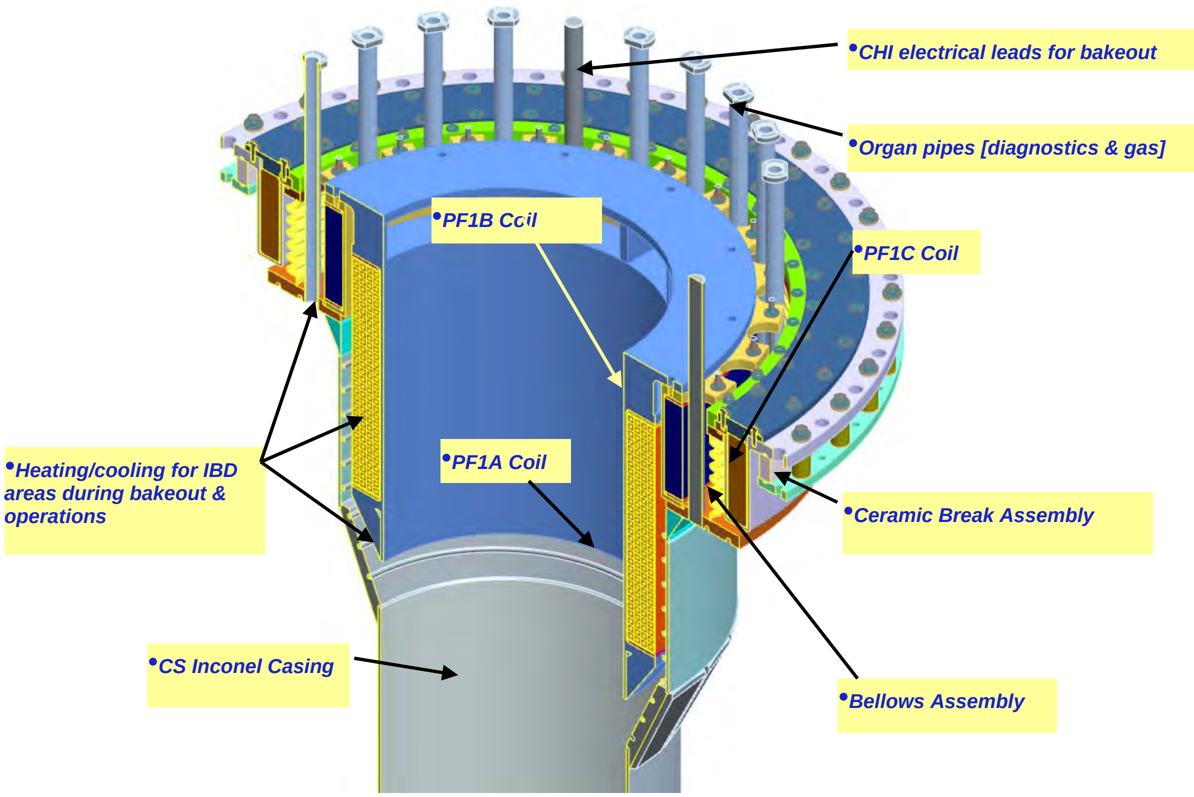

Figure 24- Overview of Centerstack Casing Components

4.1 Centerstack Casing & Bellows:

The Centerstack casing and bellows are fabricated using Inconel 625 and provides the inner vacuum vessel wall for the NSTX vacuum vessel. It also provides the structural support for the plasma facing components and surface diagnostics. Active cooling in the IBD regions has been incorporated in the upgrade.

	Center section Dia. [in.]	Wall Thick. [in.]	Material	Length [in.]	Flange Diameter [in.]	Bellows	Organ Pipes
Original	13.162	0.157	Inconel 625	132.25	43.75	Inconel 625	Yes
Upgraded	23.29	0.25	Inconel 625	133.83	43.75	Inconel 625	Yes

Table 3- CS Case Design Comparison

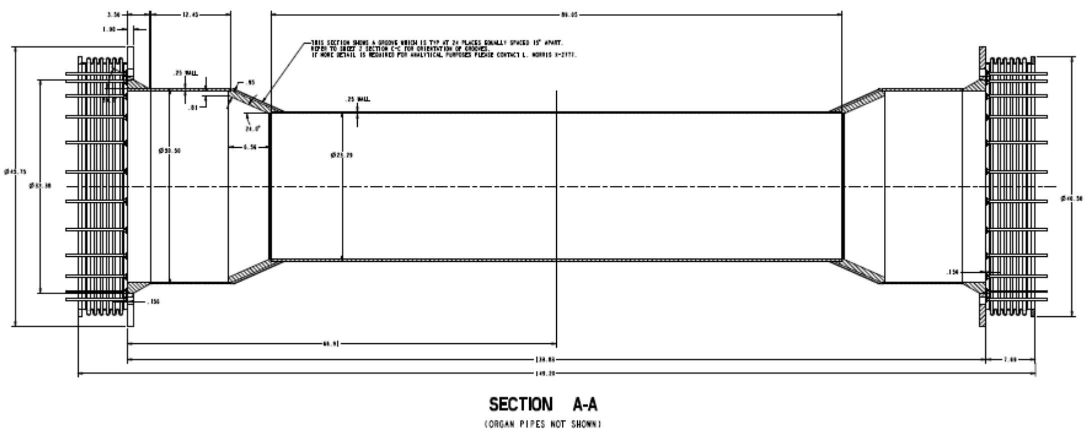

4.1.1 Centerstack Casing Organ Pipe & Casing Supports

4.1.1.1 The casing has a number of features "Organ Pipes" that provide VV access for diagnostics, gas injection and Inboard Divertor (IBD) cooling.

4.1.1.1.1 *Upper Organ Pipes*:

4.1.1.1.1.1 (3) CHI leads for bakeout

4.1.1.1.1.2 (4) IBD Cooling

4.1.1.1.1.3 (2) Gas Injection

4.1.1.1.1.4 (15) Diagnostic feeds

4.1.1.1.2 *Lower Organ Pipes*:

4.1.1.1.2.1 (3) CHI leads for bakeout

4.1.1.1.2.2 (4) IBD Cooling

4.1.1.1.2.3 (6) Casing Supports

4.1.1.1.2.4 (11) Diagnostic feeds

4.1.2 The organ pipe sizes 1.25 inch D x 1.125 inch ID.

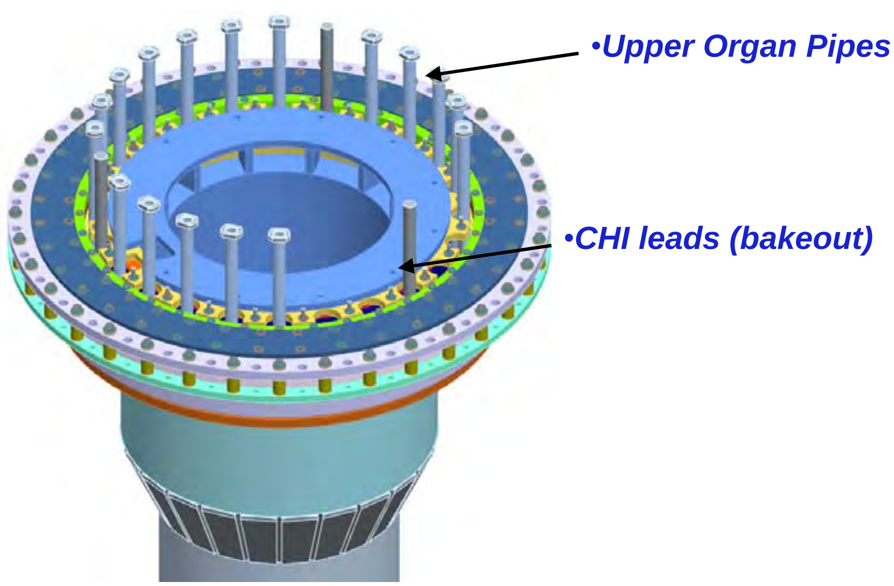

Figure 25- Upper Casing Organ Pipes

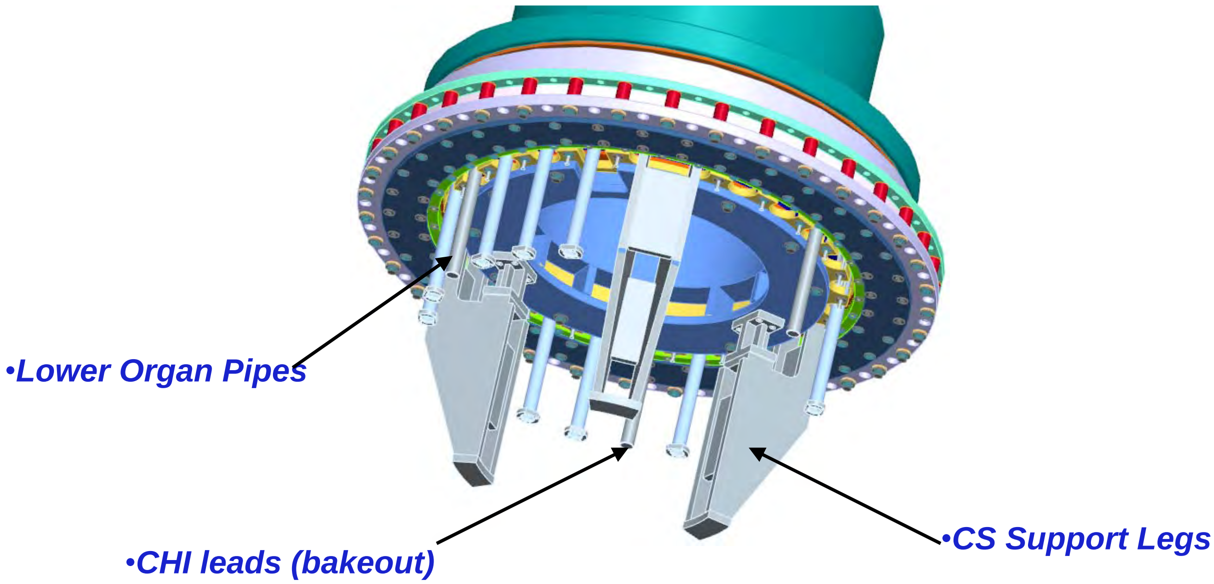

Figure 26- Lower Casing Organ Pipes and Supports

4.1.3 Centerstack Casing Manufacturing Plan:

4.1.3.1 All of the Inconel components will be procured from outside vendors.

4.1.3.2 Final assembly and welding will be completed at PPPL.

4.1.3.3 Inconel studs will be fastened to the casing wall to provide an anchor point for the PFC's.

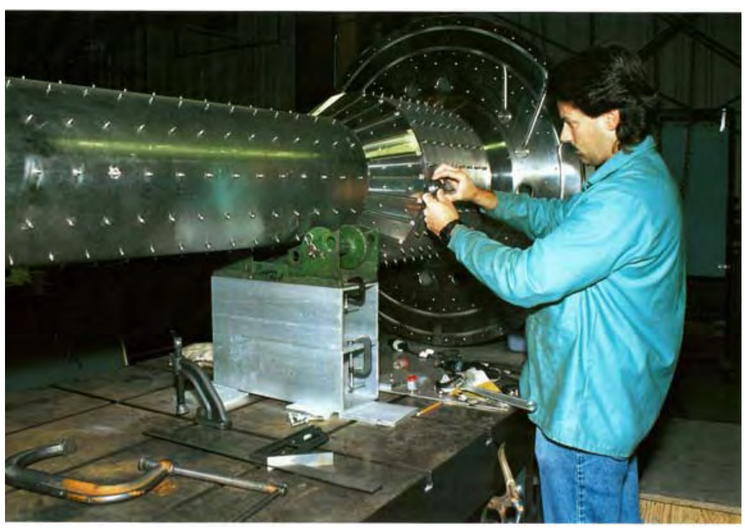

Figure 27- Installation of Inconel Studs

4.2 Ceramic Break Assembly:

The ceramic break assembly provides the electrical isolation between the inner and outer vacuum vessel assemblies. The assembly includes the ceramic insulator and structural member that connects the OVV to the IVV bellows. The structure also houses the PF-1C coils.

4.2.1 *Materials*:

4.2.1.1 **Ceramic Insulator:** Either AD96 Alumina or high strength porcelain. [47.5 inch ID x 49.5 OD x 2 inch high]

4.2.1.1.1 Dielectric Strength**:** 200 V/mil

4.2.1.1.2 Compression strength: 50,000 psi

4.2.1.1.3 Tensile strength: 5,000 psi

4.2.1.2 **Structure:** 316 Stainless Steel

4.2.1.3 **VV Insulators:** G-11

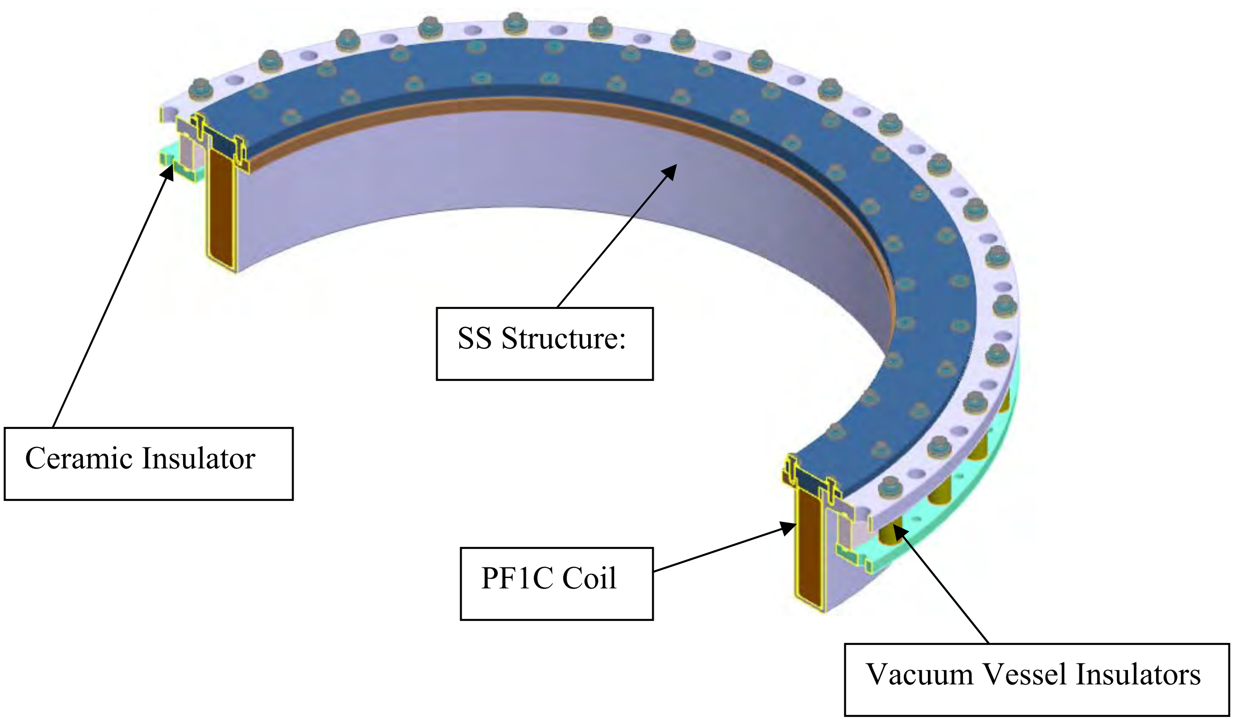

Figure 28- Ceramic Break Assembly

4.3 Centerstack Plasma Facing Components:

The plasma facing components [PFC] cover the surface of the casing and in-board divertor to protect the Centerstack from the plasma temperatures. Even though the diameter has increased, there will be fewer individual tiles (600) vs. the original design (900).

4.3.1 *PFC Features:*

4.3.1.1 **Materials**: Moving toward carbon fiber composite

4.3.1.1.1 Wider range of thermal properties [thermal shock & oxidation thresholds]

4.3.1.1.2 Better mechanical properties for attachment

4.3.1.1.3 Material Selection: pending completion of analysis studies.

4.3.1.2 **Surface Coverage**:

4.3.1.2.1 Vertical casing- Use low-k tiles to limit the heat load to the CS

4.3.1.2.2 Inboard Divertor Surfaces- Use high-k tiles/ Active surface cooling is required

4.3.1.3 **Tile Thickness**:

4.3.1.3.1 Vertical CS: 0.75 inch thick

4.3.1.3.2 Vertical IBD: 1 inch thick

4.3.1.3.3 Horizontal IBD: 2 inch thick

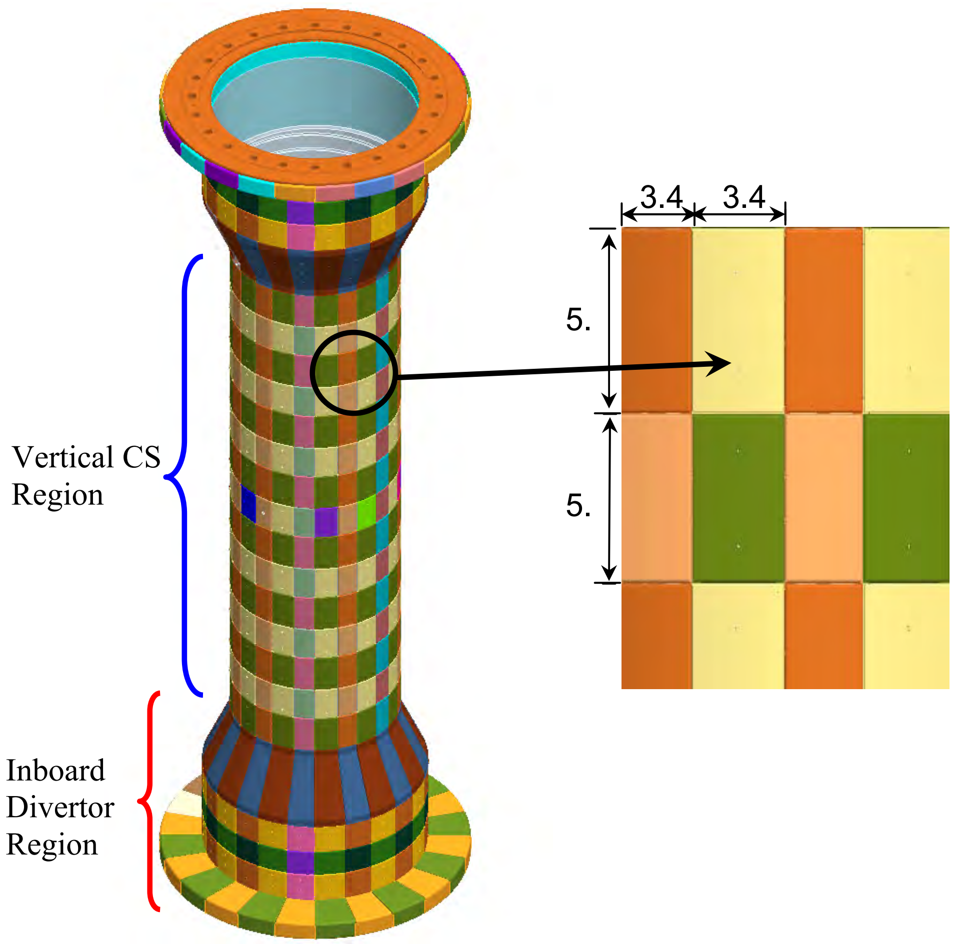

Figure 29- Layout of PFC's

4.3.1.4 **Tile Fastening Scheme**:

The PFC tile assemblies will be secured to the Centerstack casing using rails and T-bars. The upgrades will correct any reoccurring issues that were encountered with the original design during installation and fit up.

4.3.1.5 **Diagnostics**:

Diagnostics and gas injection capabilities will be incorporated in the design and layout of the PFC's.

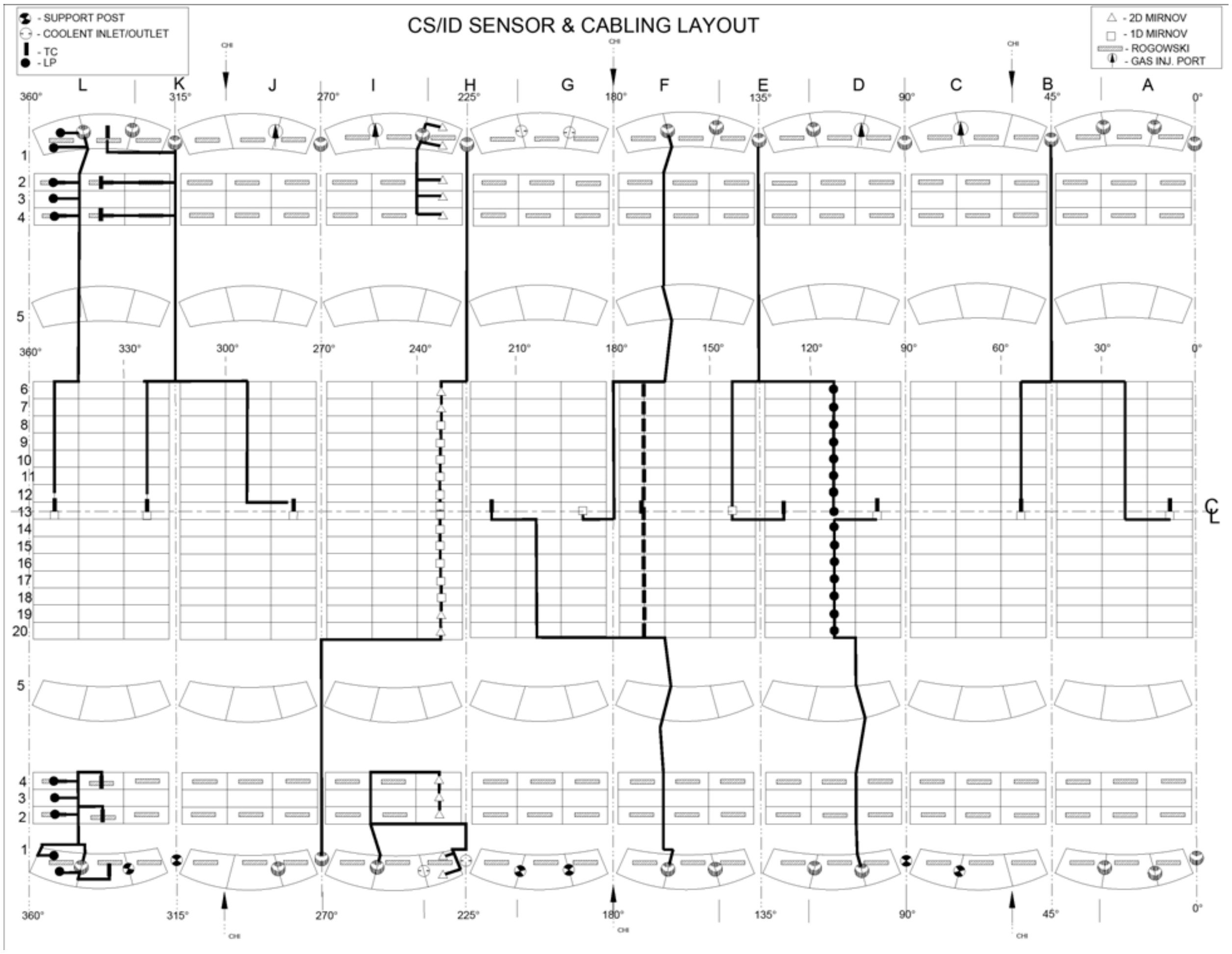

Figure 30- Layout of Diagnostic Cabling

5.0 Inner Poloidal Field Coils:

The Centerstack Upgrades include (3) pairs of new inner Poloidal Field Coils that are positioned near the ends of the Centerstack casing.

5.1 Design Description

The coils are constructed of C10700 extruded copper conductor w/cooling hole and are insulated with half-lapped layers of S2 glass tape. The coils will then vacuum pressure impregnated using CTD-101k. PF1A and PF1B will be wound directly onto their support structures and then VPI'd in place. The PF1C will be wound on a mandrel and VPI'd. The coil will then be placed into its support structure which is part of the ceramic break assembly.

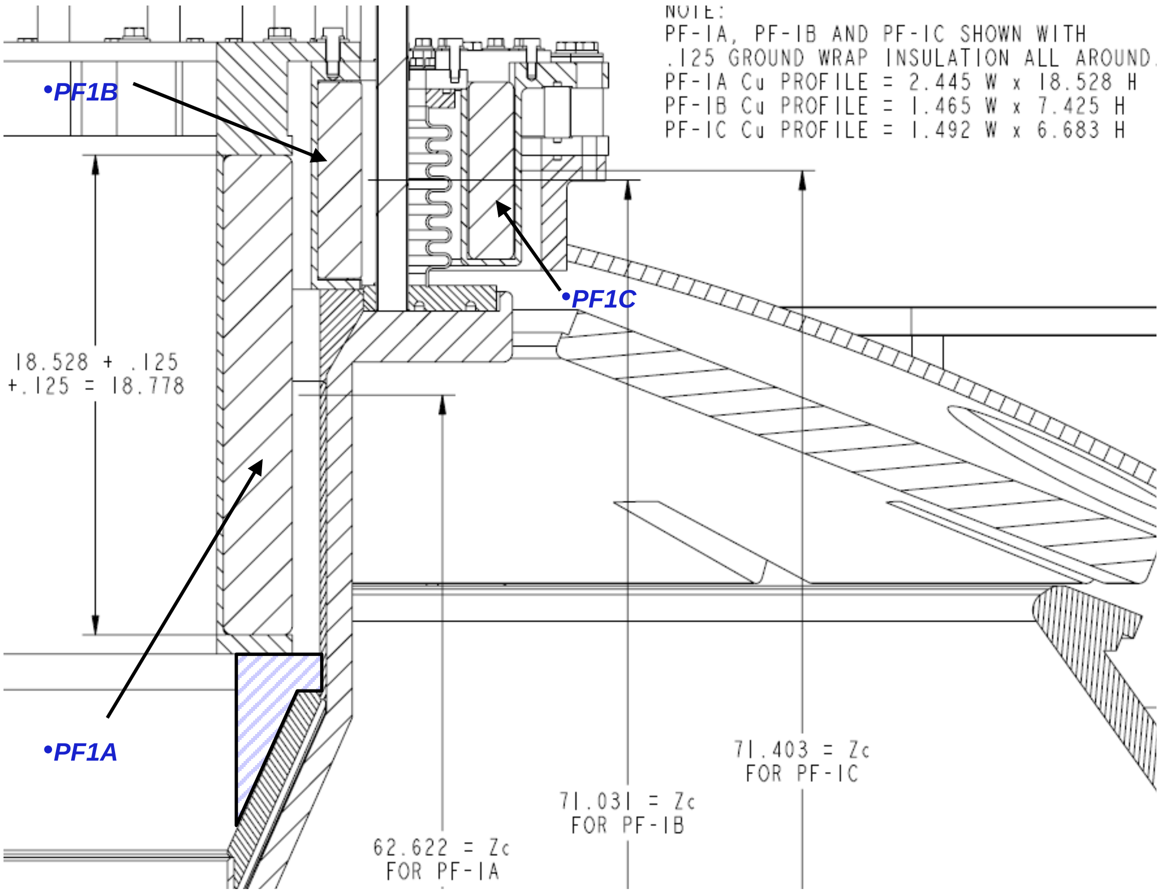

Figure 31- Position of Inner PF Coils

		PF1A	PF1B	PF1C
Voltage	Volts	1013	1013	1013
Current	Amps	1464	270	372.6
T/T Voltage	Volts	8.4	5.6	6.3
Number of Turns	n	120	180	162
ESW	sec	5.5	5.5	5.5
Conductor Width	In.	0.591	0.220	0.220
Conductor Height	In.	0.591	0.220	0.220
Cooling Hole Diameter	In.	0.217	0.098	0.098
Turn insulation thickness	In.	0.018	0.018	0.018
Ground insulation thickness	In.	0.108	0.108	0.108

Table 4 - Inner PF Coil Parameters

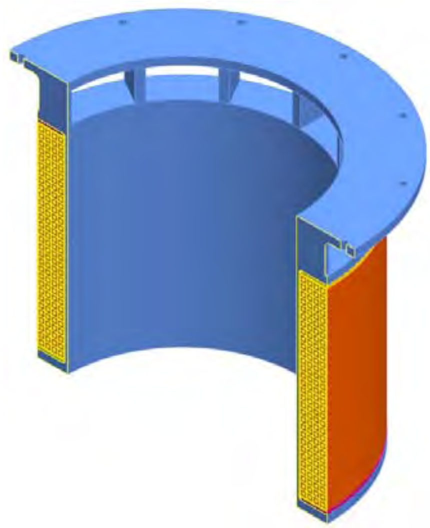

Figure 32 - PF1A Coil

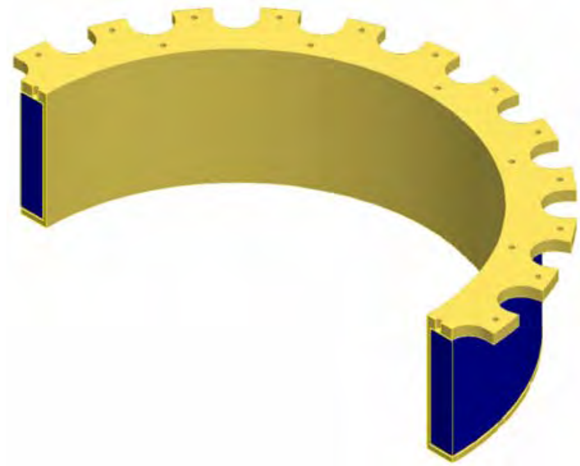

Figure 33- PF1B Coil

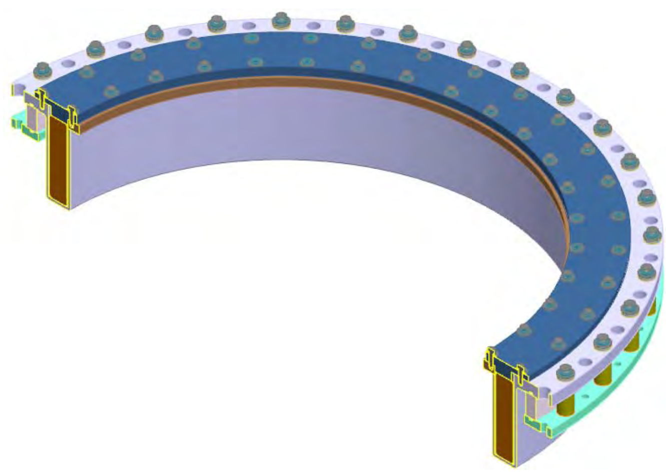

Figure 34- PF1C Coil

Section 4: TF Flex Joint and TF Bundle Stub

NSTX Upgrade CDR

October 2009

Lead Author: Thomas Willard

The objectives of this analysis of the NSTX Upgrade TF Flex Strap and TF Bundle Stub design were: 1.) to determine if the design is adequate to meet the requirements specified in the NSTX Structural Design Criteria, specifically, if the flex strap lamination stresses and the copper lead extension thread stresses meet the requirements for fatigue, yield, and buckling, under worst-case/ power supply-limit load conditions: 130,000 amps/ strap, 0.3 T poloidal field, and 1.0 T toroidal field; and 2.) to verify that the local contact pressure in the bolted electrical joints is a minimum of 1500 psi, sufficient to maintain the joint contact electrical conductance above the design goal, based on the current-design development tests, of 1.0E06 siemens/in^2.

The results of the ANSYS multiphysics finite element analysis - electric, transient thermal, magnetostatic, and static structural - show that: 1.) the maximum equivalent stress in the laminations is 27.5 ksi, which is 25.5 ksi below the fatigue allowable for the full-hard C15100 copper-zirconium strip; 2.) the maximum equivalent stress in the copper threads is 29.1 ksi, which is 32.9 ksi below the fatigue allowable for the full-hard C18150 copper-chromium-zirconium plate; 3.) the minimum average contact pressure is >6500 psi, and the minimum local contact pressure is >2500 psi, which is 1000 psi above the design goal; and 4.) the lamination minimum linear buckling load multiplier factor (LMF) is > 58, which is approximately 10x the minimum allowable specified in the NSTX Design Criteria document.

1.0 NSTX Upper Umbrella Assembly Upgrade Design Solid Model

The solid model of the Upper Umbrella Assembly Upgrade Design is shown in Figure 1.0. The design is cyclic symmetric, with twelve 3-strap TF coil segments evenly spaced around the circumference. The solid model for a Single Segment 3-Strap Assembly is shown in Figure 1.1.

Figure 1.0 - NSTX Upper Umbrella Assembly Upgrade Design

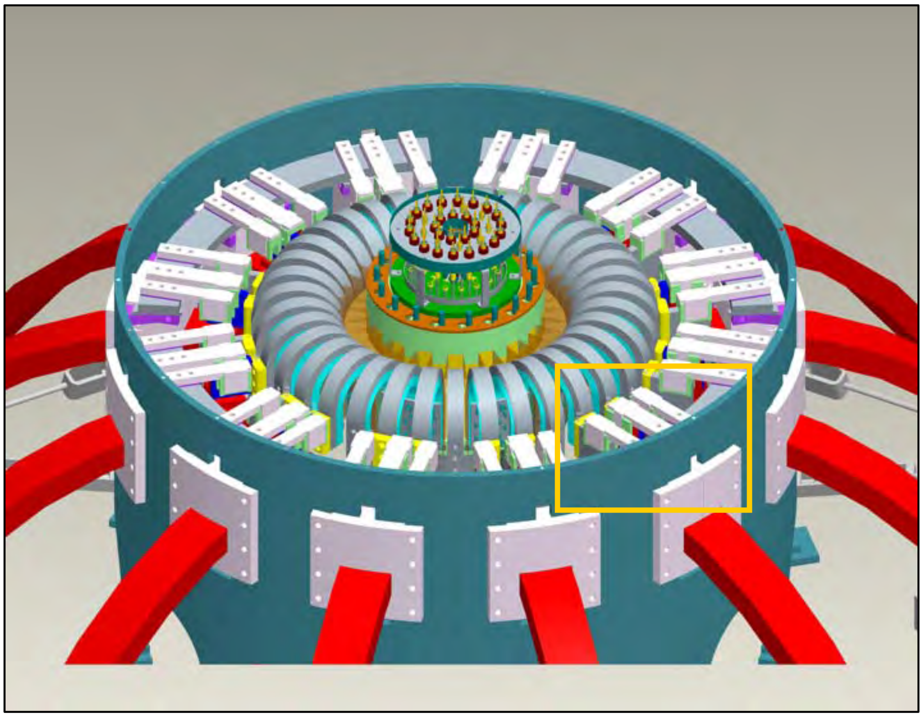

Figure 1.1- Single Segment 3-Strap Assembly

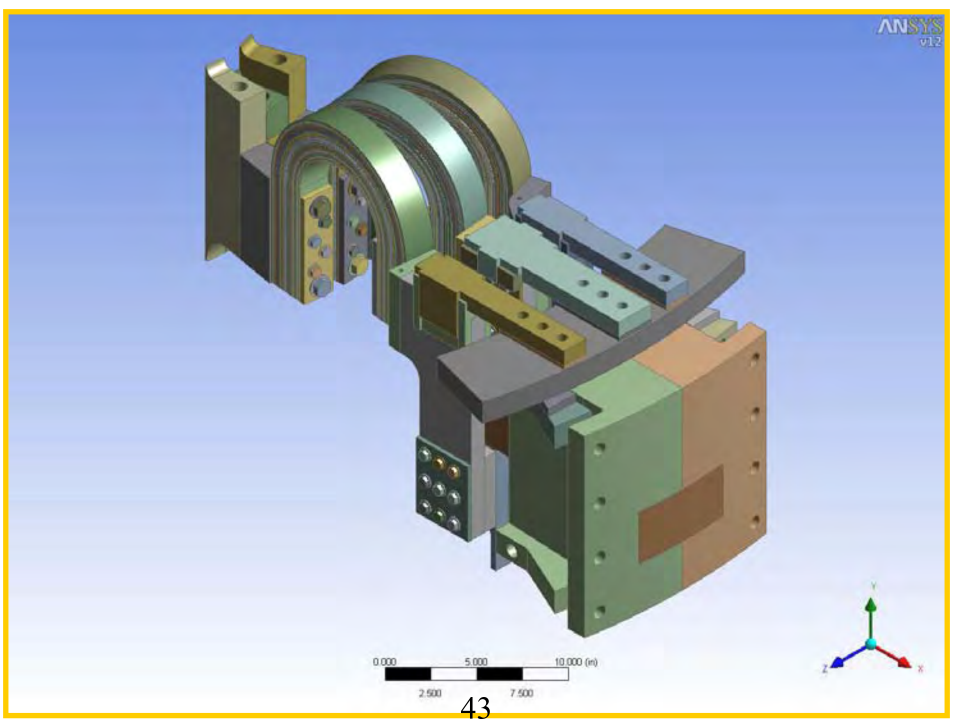

1.1 Single Strap Assembly Solid Model Description

The solid model of a Single Strap Assembly is shown in Figure 1.2. The strap assembly consists of an inner assembly of 19X .060” thick laminations, and an outer assembly of 12X .090” thick laminations; the gap between each lamination is .005”. The material is fully-hardened C15100 H04 copper zirconium alloy, chosen for its high-temperature (>450 C) resistance to softening (see Appendix), and for its high-temperature fatigue strength (241 MPa for 300 E06 cycles).

1.2 Boundary Conditions: Thermal & EM Displacements, Currents, and Applied Magnetic Fields

The boundary conditions applied to each strap assembly, for the worst-case, power supply-limit conditions, are also shown in Figure 1.2. Electromagnetic forces result when the total current of 130,000 kA crosses with the poloidal field of .3 T and the toroidal field of 1 T. Electromagnetic forces acting on the TF coil legs also apply a twist to the center stack (CS) relative to the vessel wall, resulting in a torsional displacement of .10”. In addition to the electromagnetic forces, thermal expansion of the CS produces a .3” vertical and a .018” radial displacement of the TF Bundle Stub-end of the strap assembly, and the heat generated from high current densities produces temperature gradients, resulting in thermal strains.

Figure 1.2 - Single Strap Assembly Solid Model and Boundary Conditions

2.0 Comparison of Current TF Joint Design versus Upgrade Design

The current TF bundle stub-end joint design is shown in Figure 2.1. The 12” long, C10700 silver-bearing copper TF Radial Flags are bolted to the C10700 lead extensions using four 3/8-16 Inconel 718 threaded rods, pretensioned to 5000 lbf/ea. Medium length (.562”) Tap-Lok self-tapping inserts are installed in the mating face of the lead extensions.

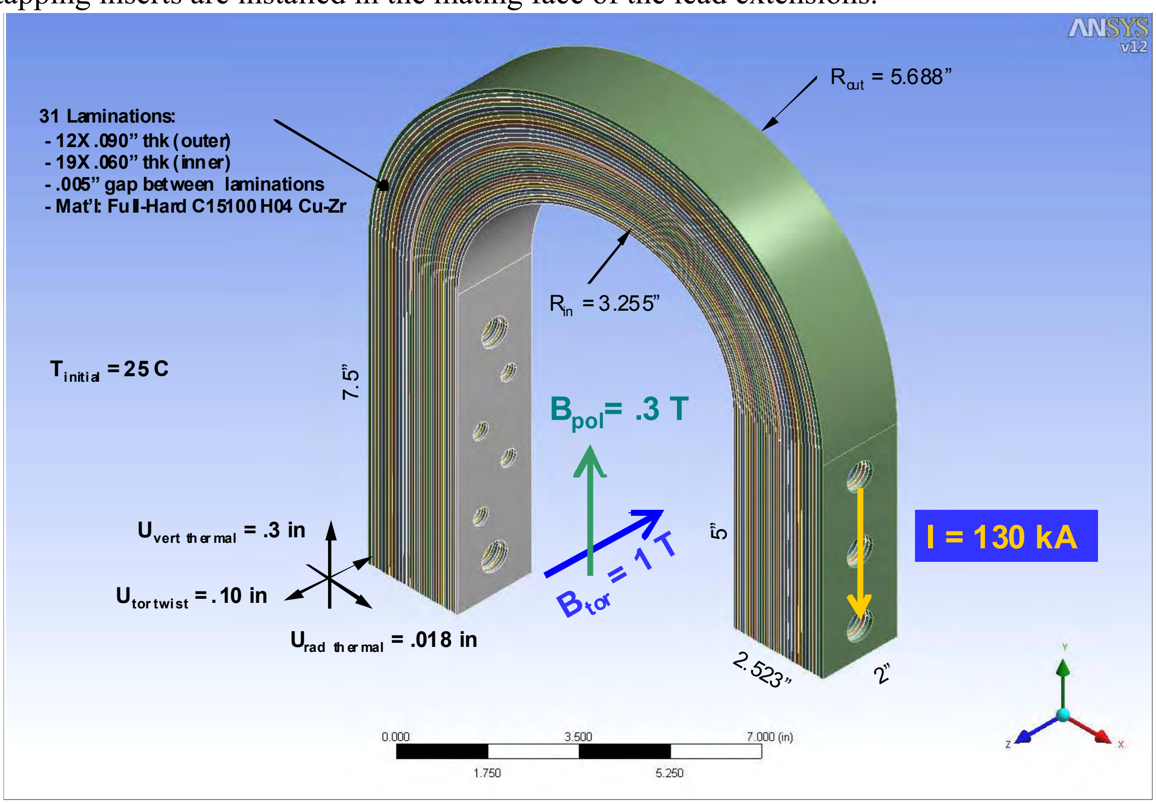

Figure 2.1 – Current Joint Design: TF Radial Flag

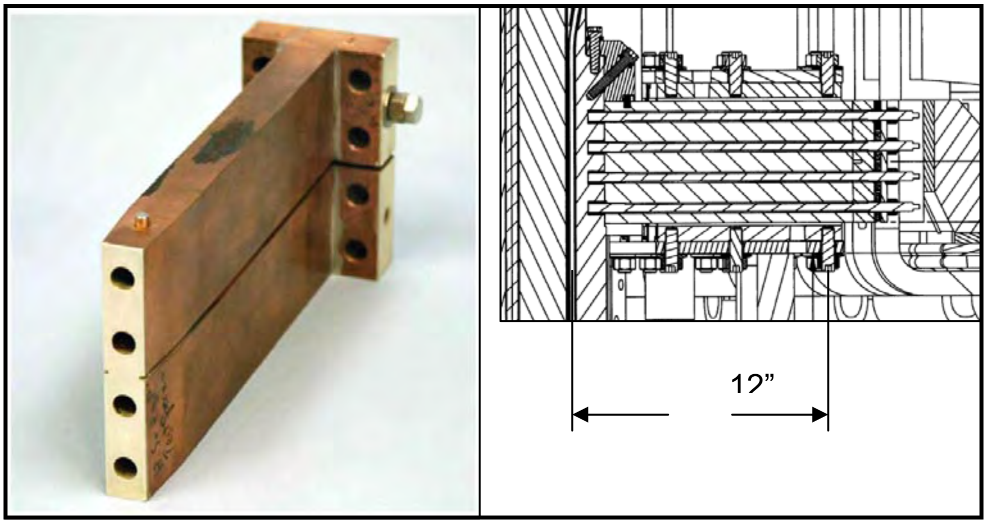

2.1 Current Joint Design Development Tests

A series of development tests were performed on the current TF joint design and included: 1.) insert cyclic pull-out tests, to determine the maximum permissible bolt pretension to prevent shear fatigue failure of the copper threads; 2.) static friction coefficient measurement of a silver-plated C10700 copper joint; and 3.) electrical contact resistance versus pressure measurements. All measurements were made at the maximum expected operating temperature: 100C.

2.1.1 Insert Cyclic Pull-Out Tests

Figure 2.2 shows the set-up for the insert cyclic pull-out tests. An Instron tensile test machine was used to determine the static pull-out strength as well as to establish the fatigue strength curve of the bolted joint. The results showed that the copper threads always failed first, and that the maximum permissible bolt pretension to prevent fatigue failure within 60,000 cycles, with the additional operational cyclic load of 2000 lbf applied, was 5000 lbf.

Figure 2.2 - 3/8-16 Tap-Lok Insert/ C10700 Copper Thread Pull-Out Test

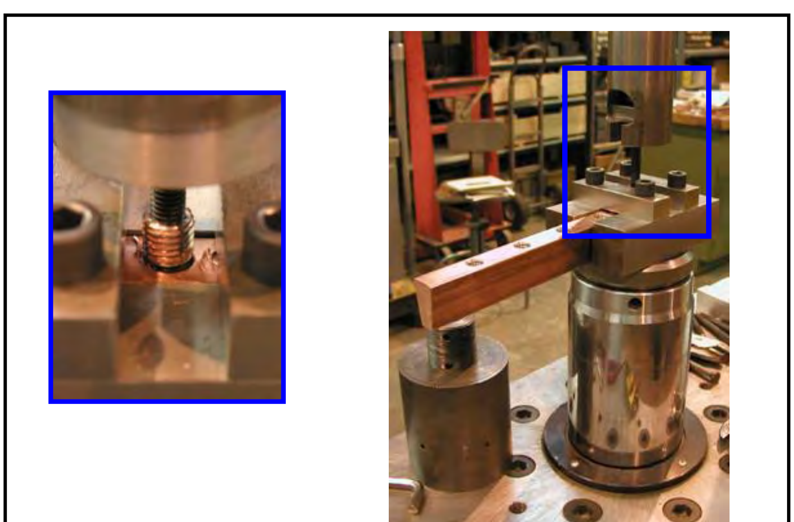

2.1.2 Static Coefficient of Friction of Silver-Plated Copper Joint

The static coefficient of friction of a silver-plated copper joint was measured using the test set-up shown in Figure 2.3. The Instron tensile test machine was used to apply a known lateral force to the center plate of the 3-plate stack; a load cell was used to measure the clamping force applied to the stack. The results show that the coefficient was .40, measured at the point just before sliding occurred.

Figure 2.3 - Static Coefficient of Friction Test

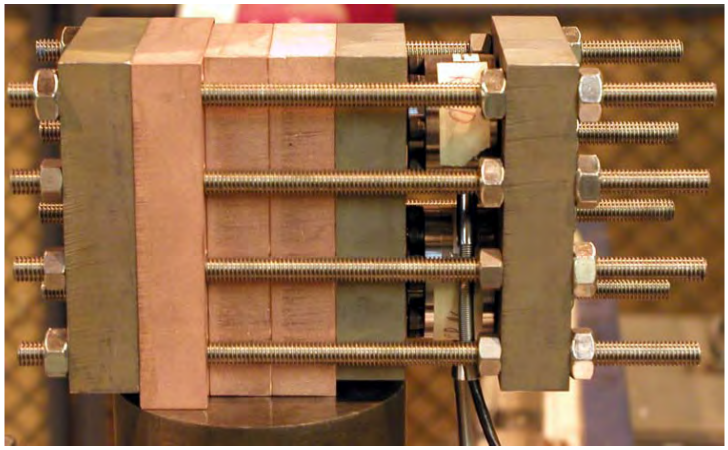

2.1.3 Electrical Contact Resistivity versus Pressure

The electrical contact resistivity versus pressure was measured using the test set-up shown in Figure 2.4. The Instron tensile test machine was used to apply a known axial force to the test fixture. The 100 A test current was applied using the large diameter bolts at the ends of the copper test plates. Probes on either side of the joint measured the voltage drop across the joint. The results show a sharp knee in the curve at ~1500 psi: above this pressure, the contact resistivity is a weak function of pressure. Above 4000 psi, the resistivity can be assumed to be a constant of .5 μohm m-in^2.

Figure 2.4 - Electrical Contact Resistivity versus Pressure

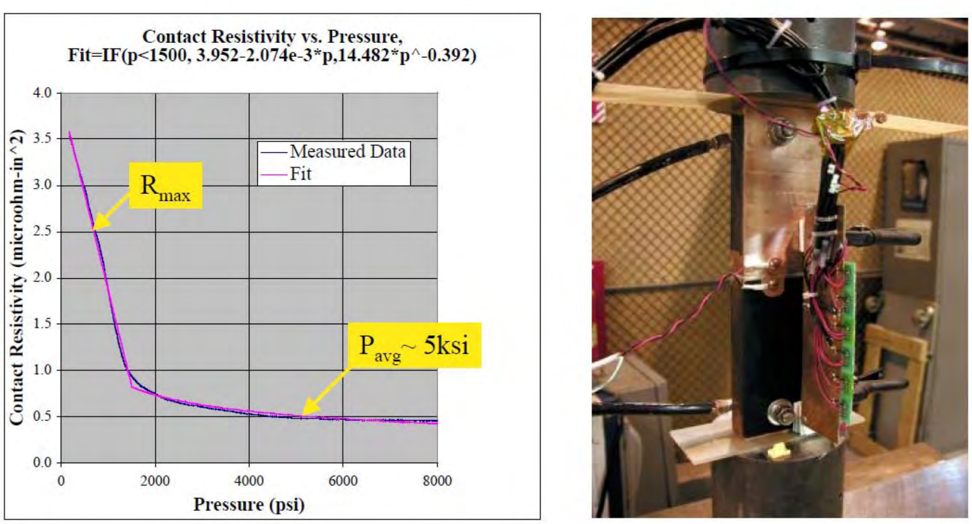

2.2 Issues with Current TF Joint Design

In-situ, operational measurements of the current-design TF joint electrical contact resistivity indicate that the joints on the levels closest to the plasma (four levels of joints: two in the top umbrella, two in the bottom umbrella) begin to separate or lift-off when the TF field strength is greater than .45 T. As the joints separate, interruption of the high current induces arcing, resulting in pitting damage on the extension-lead side of the joints. To prevent this damage from occurring over more than 25% of the joint surface, the operational TF field is limited to .55 T, instead of the design point of .6 T.

This lift-off was investigated in a separate, direct-coupled ANSYS multiphysics model of the TF Radial Flag and joint (R. Woolley, 2005), where it was shown that approximately 30% of the joint separates when the TF field strength is .6 T, as shown in Figure 2.4. This was later confirmed with a bench test of a bolted joint where daylight was observed between the halves of the joint when a .6 T simulated prying moment was applied to the TF Radial Flag.

Photographs of the joints, taken after 2 years of operation, show close correspondence between the observed pitting damage and the ANSYS-predicted lift-off areas (see Figure 2.4). No pitting damage was observed in the joints on the levels furthest from the plasma, where the field strength is 1/3 the maximum value and operational voltage measurements show no signs of separation.

Figure 2.5 – Joint Lift-Off and Pitting Damage Areas

2.3

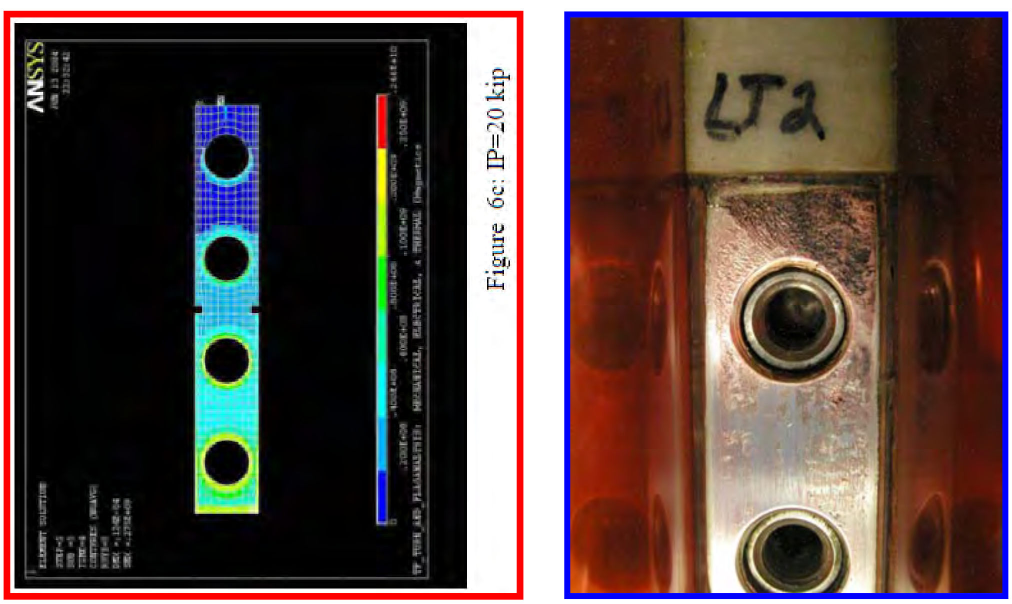

ANSYS Results: Contact Pressure   Lift-off Pitting Damage - 2005

Design Operating Point Comparison

A comparison of the design operating point - TF current/ turn, TF and PF field strengths, and maximum pulse duration - for the current and upgrade designs is shown in Table 2.1. From the table, it is clear that the upgrade design operating point conditions are much more severe. However, it will be shown below that improvements in the upgrade design result in larger margins, even under the more severe operating conditions.

Table 2.1 - Design Operating Point Comparison				
Design	Total Current (A)	Maximum TF (Tesla)	Maximum PF (Tesla)	On-Time Pulse Duration (sec)
Current	72,000	0.6	0.1	0.5
Upgrade	130,000	1.0	0.3	7.0

2.4 Joint Mechanical Parameters Comparison

A comparison of the mechanical parameters of the TF lead-extension bolted joint designs is shown in Table
2.2. From the table, it is clear that the upgrade design is much more robust.

The joint is located further from the CS winding, so the joint contact area is much wider. It is also taller, so the contact area is approximately 4x larger. The number of bolts/ joint has increased, and there is a mix of 3/8 and 5/8 bolts, with the 5/8 bolts located furthest from the bolt centroid. The lead-extension material has been changed to a high strength copper alloy C18150 copper-chromium-zirconium, so that the bolt pretension is limited by the strength of the bolts and not the shear strength of the copper threads. All of this results in a nearly 5x increase in total bolt force, a 50% increase in initial contact pressure, and a large positive lift-off torque margin. Since there is no lift-off, the local contact pressure never falls below a minimum value, determined in the ANSYS analysis below to be > 2500 psi.

Table 2.2 - Joint Mechanical Parameters Comparison							
Design	Joint Contact Area (in^2)	Total Bolt Force (lbf)	Average Initial Contact Pressure (psi)	Minimum Operating Local Contact Pressure (psi)	Calculated In-Plane Mating Torque (in-lbf)	Max. TF In-Plane Separating Torque (in-lbf)	Lift-off Torque Margin
Current	3.382	20,000	5,914	0	12,500	17,500	-0.29
Upgrade	12.739	94,000	7,379	~2500	90,875	30,143	2.01

2.5 Joint Electrical/ Thermal Parameters Comparison

A comparison of the electrical and thermal parameters of the joints is shown in Table 2.3. Though the total current is higher in the upgrade design, the current density is only 1/2 the density in the current design. The initial (closed joint) electrical resistance and heat generated in both designs is small, as is the estimated temperature rise across the joints, assuming no thermal capacitance.

Table III - Joint Electrical/ Thermal Parameters Comparison						
Design	Current Density (A/in^2)	Initial Electrical Resistance (W)	Heat Generated I^2R (W)	Thermal Power Density (W/in^2)	Initial Thermal Resistance (W/C)	Zero-Heat Capacity Temperature Rise (C)
Current	21,289	1.48E-07	7.66E+02	2.27E+02	1.18E-02	9.1
Upgrade	10,205	3.93E-08	6.63E+02	5.21E+01	3.14E-03	2.1

2.6 Static Bolt Strengths and Insert Pull-Out Loads Comparison

A comparison of the static bolt strengths and insert pull-out loads of the two joint designs is shown in Table 2.4. From the table, it can be seen that the shear strength of the C10700 copper threads in the current design limits the 3/8 bolt pretension to below the maximum allowable bolt load. When the estimated 2000 lbf operational cyclic load is considered, the allowable bolt pretension is reduced to only 5000 lbf: a 2000 lbf reduction due to the cyclic load, and a 3000 lbf reduction due to the reduced shear strength of the copper for fatigue at 60,000 cycles.

The upgrade design uses high strength C18150 copper-chromium-zirconium, with more than twice the shear strength of the C10700 copper, for the lead-extensions,. Also, because the extensions are longer, a longer 3/8 insert is used, with a larger shear area. This results in the copper thread strength being greater than the bolt tensile strength, so the maximum allowable bolt pretension is limited by the strength of the bolt. The bolt reactions from the ANSYS analysis below indicate that the cyclic load is small (10-15% of the bolt pretension), so can be reduced to nearly zero with the use of Belleville washers. To maximize the contact pressure and lift-off margin, without exceeding the maximum allowable bolt loads, the following bolt pretensions were chosen for the upgrade design: 10,000 lbf for the 3/8 bolts; and 27,000 lbf for the 5/8 bolts.

Table IV - Static Bolt Strength and Insert Pull-Out Load Comparison

Design	Bolt Size	Qty/ Joint	Bolt Mat'l	Bolt Yield Strength (psi	Bolt NSTX D.C. Allowable (psi)	Tensile Stress Area (in^2)	Max. Bolt Load	Tap-Lok Insert Outer Thread	Insert Length (in)	Effective Shear Area (in^2)	Copper Alloy	Yield Strength (psi)	Shear Strength (psi)	Insert Pull-out Load (lbf)
Current	3/8-16	4	Inconel 718	185,000	138,750	0.0775	10,753	9/16-16	0.562	0.4864	C10700	36,000	20,772	10,104
Upgrade	3/8-16	4	Inconel 718	185,000	138,750	0.0775	10,753	9/16-16	0.687	0.608	C18150	75,000	43,275	26,311
	5/8-11	2				0.226	31,358	29/32-11	1.125	1.61				120,750

2.7 Comparison Summary

In summary, joint pitting damage in the current design occurs with TF fields > .45 T, in lift-off areas predicted by an ANSYS direct-coupled model and verified by in-situ measurements of joint resistivity. No pitting damage occurs in joints further from the plasma that do not lift-off. Bolt pretension, limited to 5000 lbf due to the low shear fatigue strength of the copper threads, is not sufficient to prevent lift-off, given the long lever arm of the TF Radial Flag.

The upgrade flex strap design reduces the lever arm length, minimizing the prying torque. The more robust design , with bolt pretensions limited by the strength of the bolts, also increases the mating torque, resulting in a large positive lift-off margin. A description of the ANSYS multiphysics analysis, used to determine the stresses in the laminations and the minimum local contact pressure in the joints, follows.

3.0 ANSYS Multiphysics Analysis

3.1 Sequential Multiphysics Model Description

The block diagram of the ANSYS multiphysics analysis used to evaluate the design is shown in Figure 3.1.
Note: This sequential, one-way coupled model is valid only if the bolted joints do not lift-off, and if the electrical and thermal contact resistances are a weak function of pressure, which is true here if the local contact pressure is above 1500 psi.

A current of 130 kA/strap assembly was applied in an Electric analysis to determine the voltage, the current density (JS), and the Joule heating (Heat Gen) throughout the model. Next, the current density results were used in a Magnetostatic analysis, along with the toroidal field (Bz) and the poloidal field (By) strengths, to determine the nodal Lorentz forces. In parallel, the Joule heat results were used in a Transient Thermal analysis (initial temperature T_{int} = 22 C, time duration t = 7 seconds), to determine the nodal temperatures. Finally, the Lorentz forces and temperatures were used in a Static Structural analysis, along with the displacements due to the CS thermal expansion and twist, to determine the lamination and thread stresses, and the contact status and pressure distributions on the bolted joints. A separate linear static and buckling analysis was also performed to determine the buckling load multiplier factor (LMF) of the laminations.

Figure 3.1- ANSYS Multiphysics Analysis Block Diagram

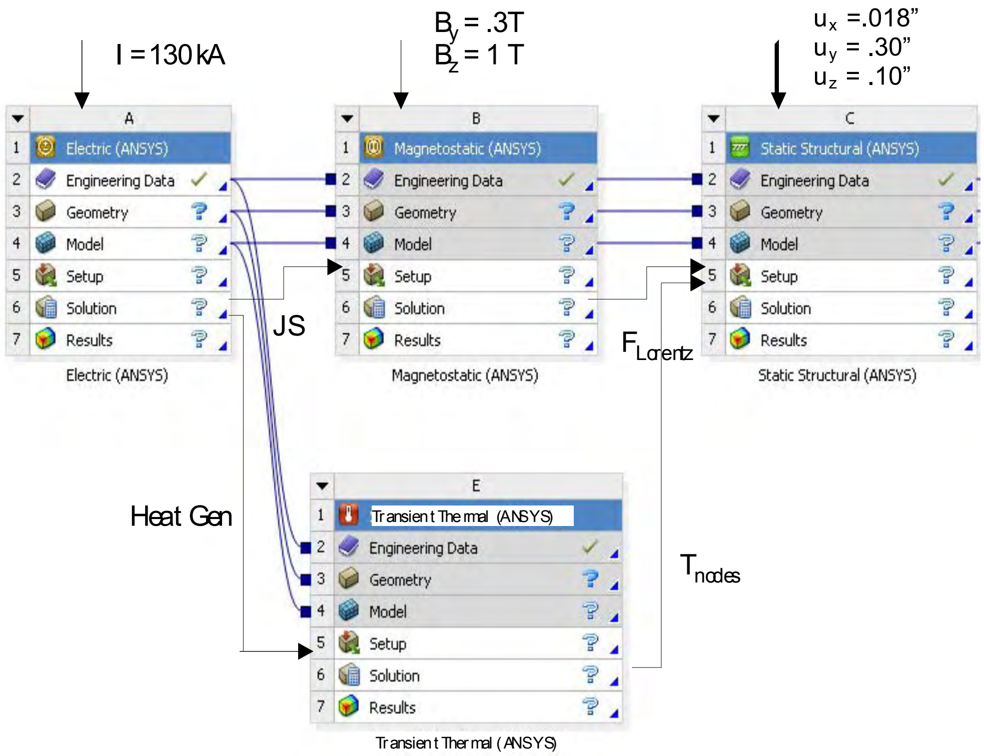

3.2 - Finite Element Model Mesh

The finite element mesh of the model is shown in Figure 3.2. The hex-dominant mesh consists of 2,902,672 nodes and 580,846 elements. The strap laminations were meshed using the automatic thin sweep feature, with 3 divisions in the thru-thickness direction to accurately model the bending behavior.

3.3 Electric Analysis Results

3.3.1 Voltage Results

The voltage results from the Electric analysis are shown in Figure 3.3.1. The results show there is approximately a 1 volt drop across the assembly, with half the drop occurring across the strap laminations.

3.3.2 Current Density Results

The current density results from the Electric analysis are shown in Figure 3.3.2. The results show that the current through the laminations is not uniform, with the shorter, inner laminations carrying more current than the outer, even though the inner laminations are 50% thinner.

3.3.1 Joule Heat Results

The Joule heat results from the Electric analysis are shown in Figure 3.3.3. The results show that, due to the higher current densities, there is more heating of the inner laminations than the outer. The inside corners of the TF coil lead extensions, where current crowding is occurring, also experience high heat generation.

Figure 3.2 - Finite Element Mesh

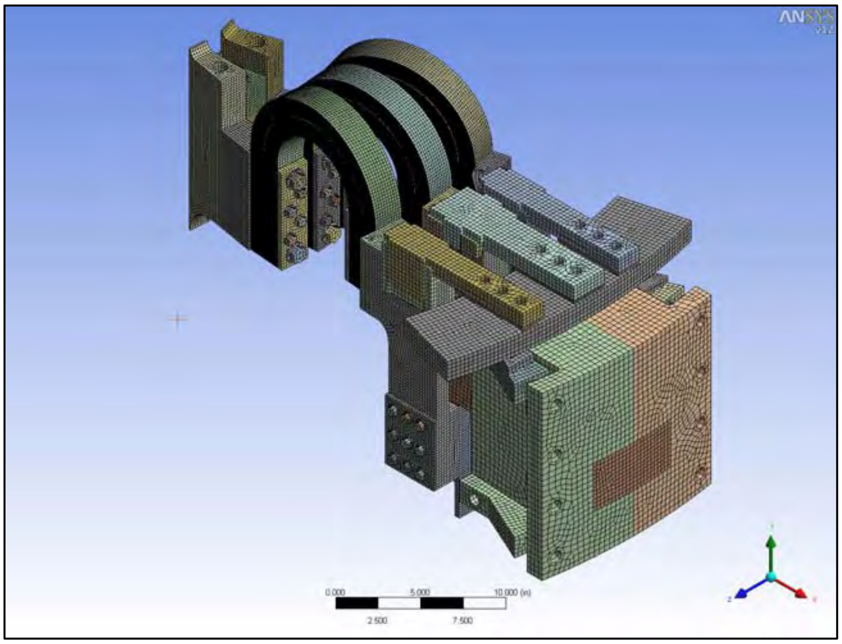

Figure 3.3.1 – Electric Analysis Results: Voltage

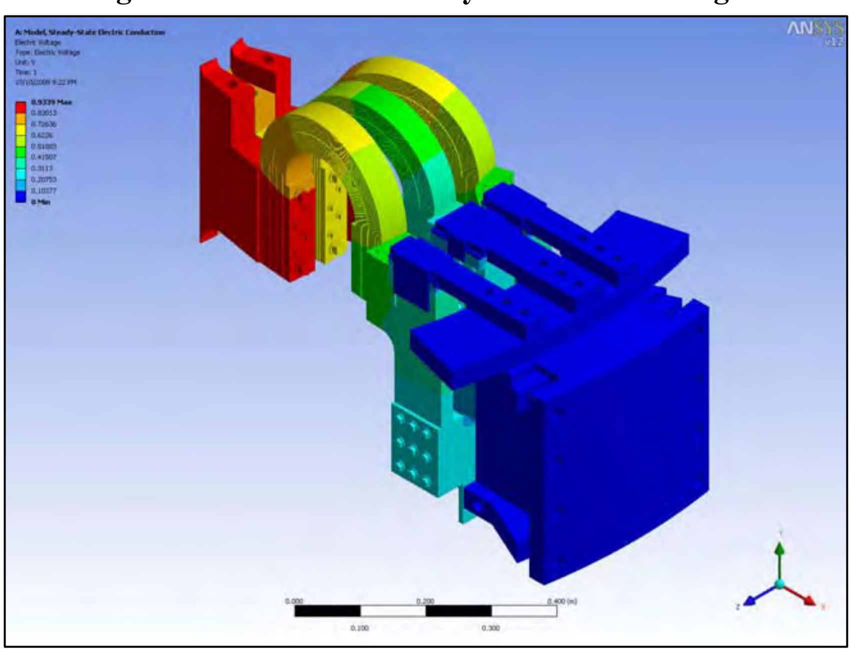

Figure 3.3.2 – Electric Analysis Results: Current Density

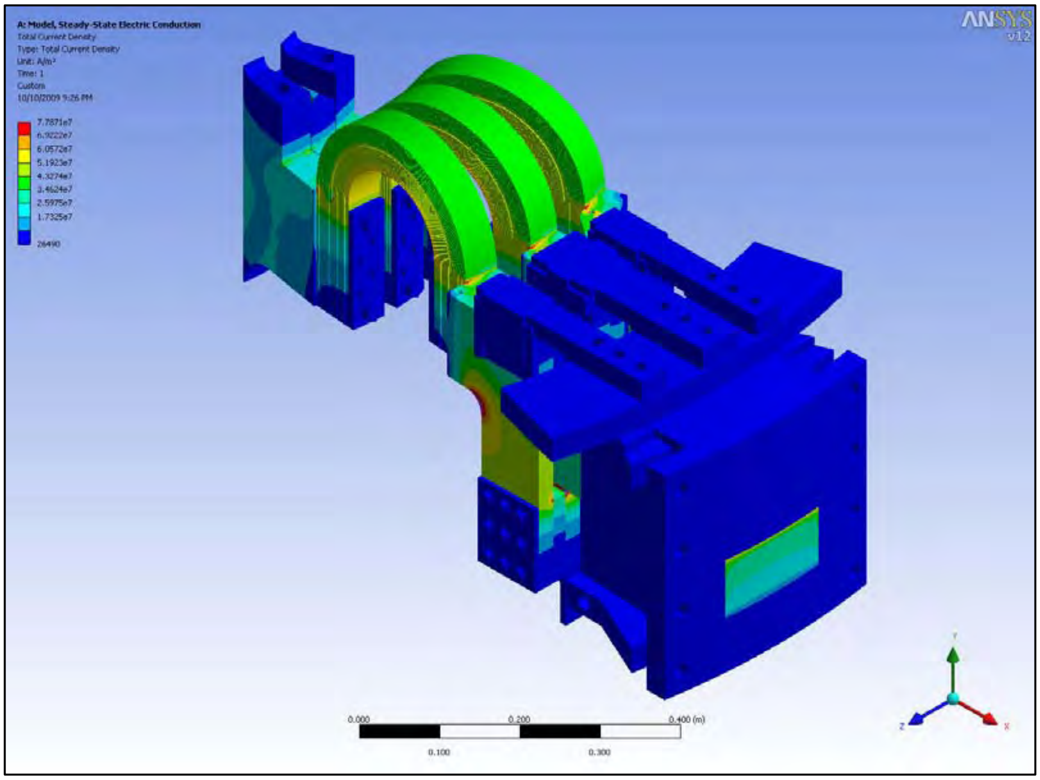

Figure 3.3.3 – Electric Analysis Results: Joule Heat

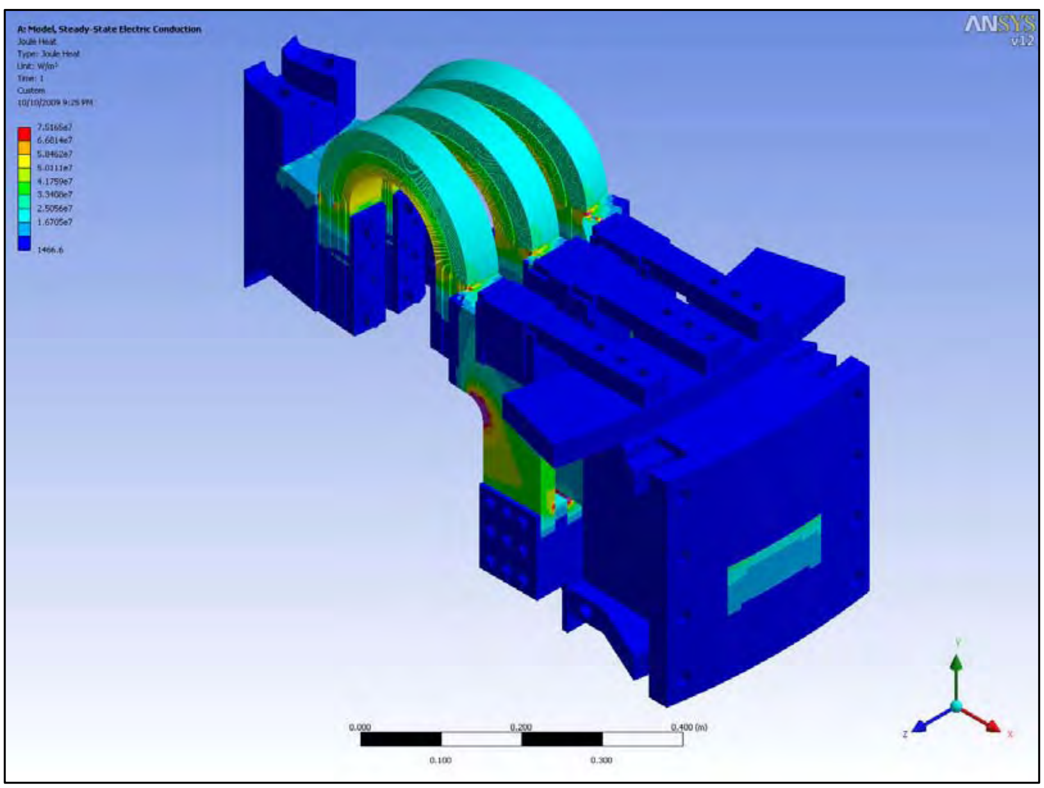

3.4 Magnetostatic Analysis Results

A vector plot of the Lorentz forces from the Magnetostatic analysis is shown in Figure 3.4. A close-up view of the laminations show that the forces act predominantly outward in a radial direction, resulting in a hoop stress in the laminations, but also have an out-of-plane (OOP) component, resulting in an OOP bending stress.

3.5 Transient Thermal Analysis Results

The temperature results, for time = 7 seconds, from the Transient Thermal analysis is shown in Figure 3.5. The results show the maximum temperature of 156 C occurs in the innermost strap lamination, where the current density is the highest, and where the heat conduction path to the 'thermal sink' of the cool, large copper plates is the longest. Significant heating also occurs in the corner radii of the TF lead extensions, where the current density and Joule heating are again high. The softening temperature of both the C15100 and C18150 copper alloys used is over 500 C, so the strength of the laminations and the lead extensions should not be affected by this heating.

3.6 Static Structural Analysis Results

3.6.1 Overall Stress Results

A plot of the von Mises stress results for the overall assembly from the Static Structural analysis is shown in Figure 3.6.1. The results show high stresses in the 304 stainless steel supports used to stabilize the tops of the TF lead extensions, as well as in the square-corner of the longest TF lead extension (close-up view).

The design will be changed to eliminate these high stresses by: 1.) optimizing the shape of the supports to reduce the bending stresses, and changing the support material to Inconel 718; and 2.) adding a corner radius to the long TF lead extension.

3.6.2 Lamination Stress Results

A plot of the worst-case von Mises stress results, for both the inner and outer laminations, from the Static Structural analysis is shown in Figure 3.6.2. From the figure, the maximum stress is 27,575 psi and occurs on the outside edge of the inner lamination at the point where the lamination shape transitions from straight to curved. The maximum stress in the outer lamination is 22,171 psi and also occurs at the transition point.

Note: In a separate MathCAD analysis, not included here, it was shown that the stress in the outer laminations is dominated by the OOP bending stress due to the PF field, while the stress in the inner laminations is dominated by the in-plane bending stress due to the thermal expansion of the CS.

3.6.3 Copper Lead Extension Thread Stress Results

A plot of the von Mises stresses in the copper threaded lead extensions (outer straps) from the Static Structural analysis is show in Figure 3.6.3. Note: It wasn't possible to include enough detail in this model to accurately determine the local copper thread stresses. Instead, the average thread stress for each bolt size, based on the insert vendor's (Tap-Lok) specified effective shear areas, were used, along with the initial bolt pretensions, to determine the copper thread shear stresses. The shear stresses were then converted to the equivalent (von Mises) stresses listed in Figure 3.6.3, with the maximum of 29,047 psi occurring in the 5/8-size insert copper threads.

3.6.4 Contact Status and Pressure

Plots of contact status and pressure results for the TF lead extension joints (worst-case) from the Static Structural analysis are shown in Figure 3.6.4. The results show that no lift-off occurs in the joints, and that the minimum local contact pressure is 2500 psi, occurring over less than 5% of the joint area: the average contact pressure in the joints is greater than 6500 psi.

Figure 3.4– Magnetostatic Analysis Results: Lorentz Forces

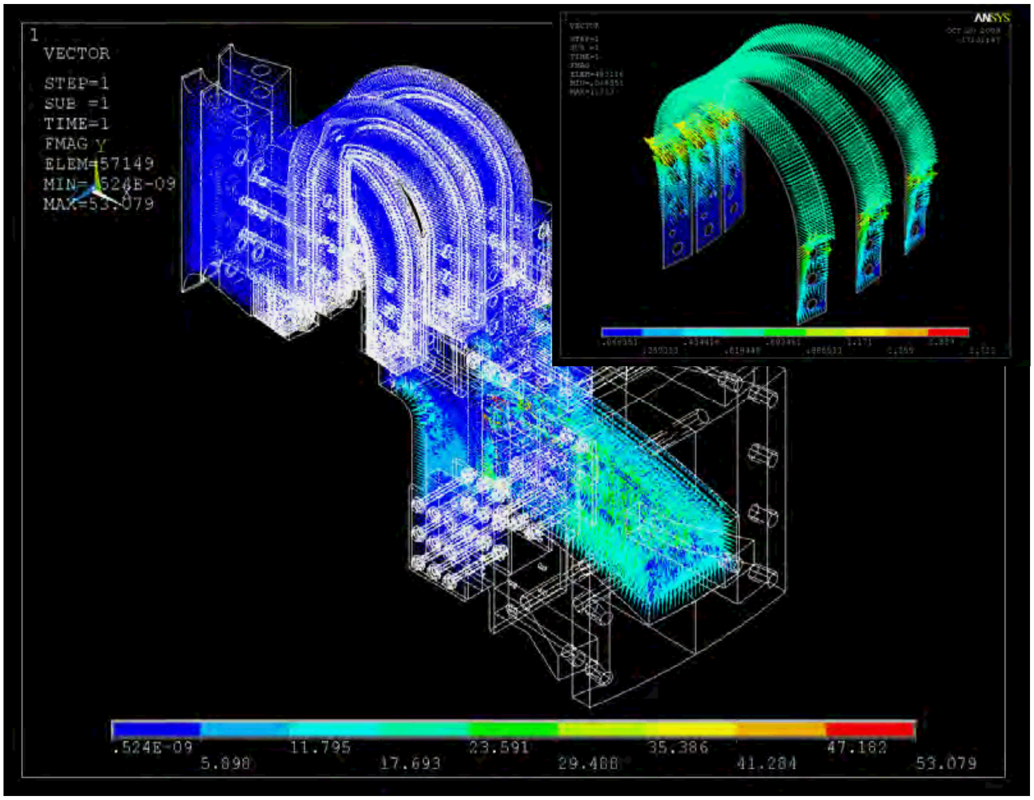

Figure 3.5 – Transient Thermal Analysis Results: Temperatures

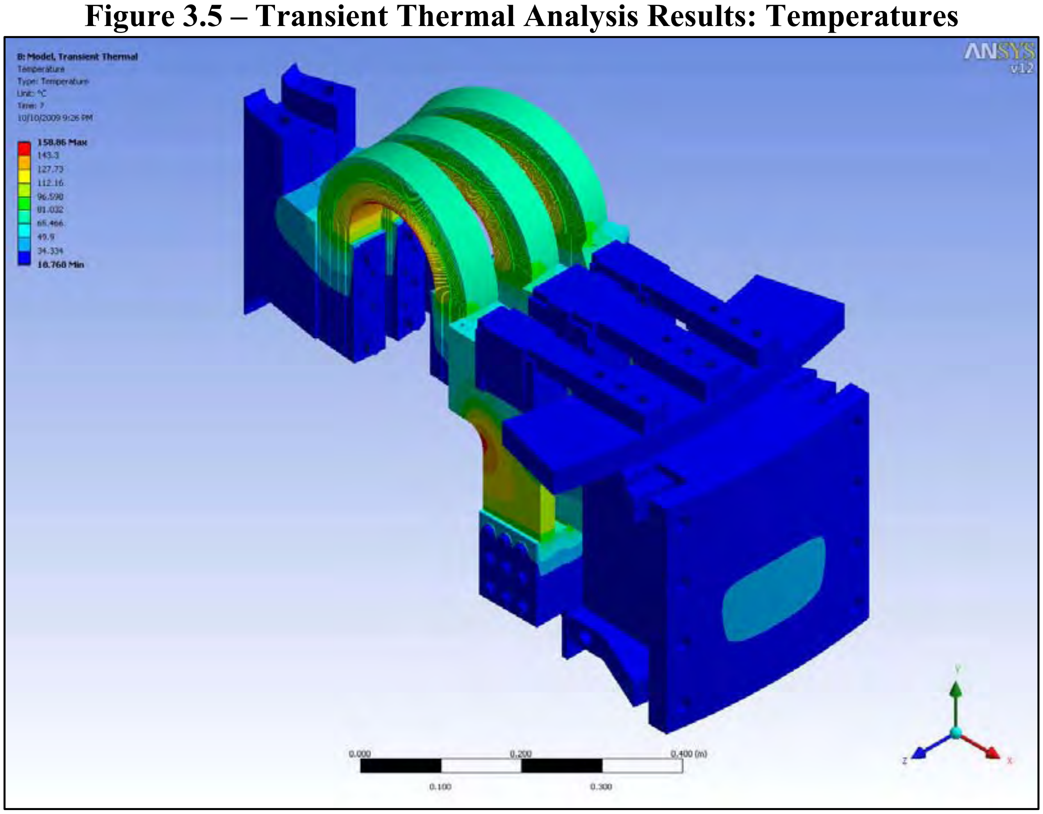

Figure 3.6.1 – Static Structural Analysis Results: von Mises Stress: Overall

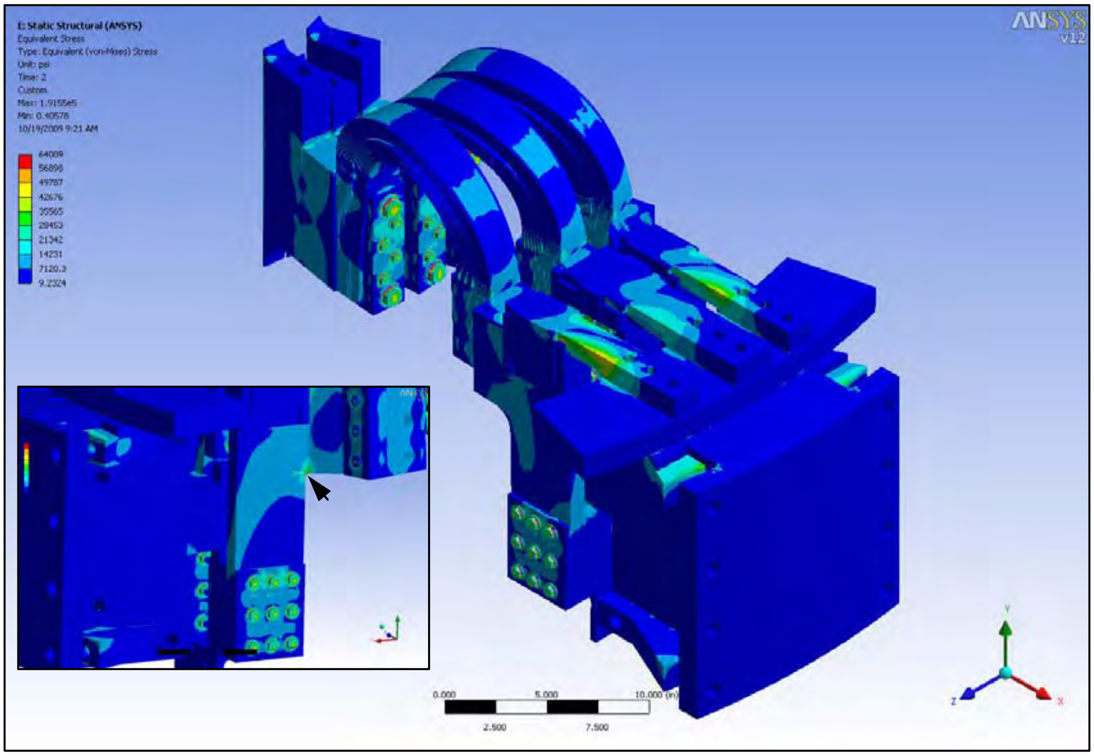

Figure 3.6.2 – Static Structural Analysis Results: von Mises Stress: Laminations

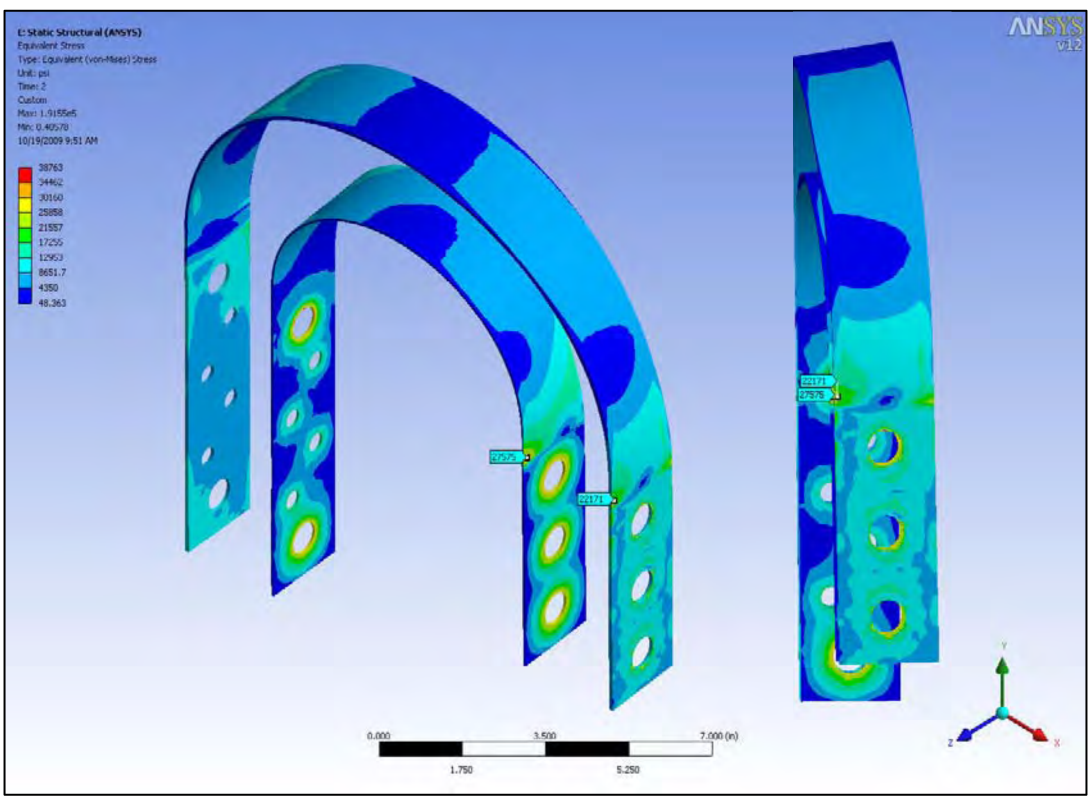

Figure 3.6.3 – Static Structural Analysis Results: von Mises Stress: Threads

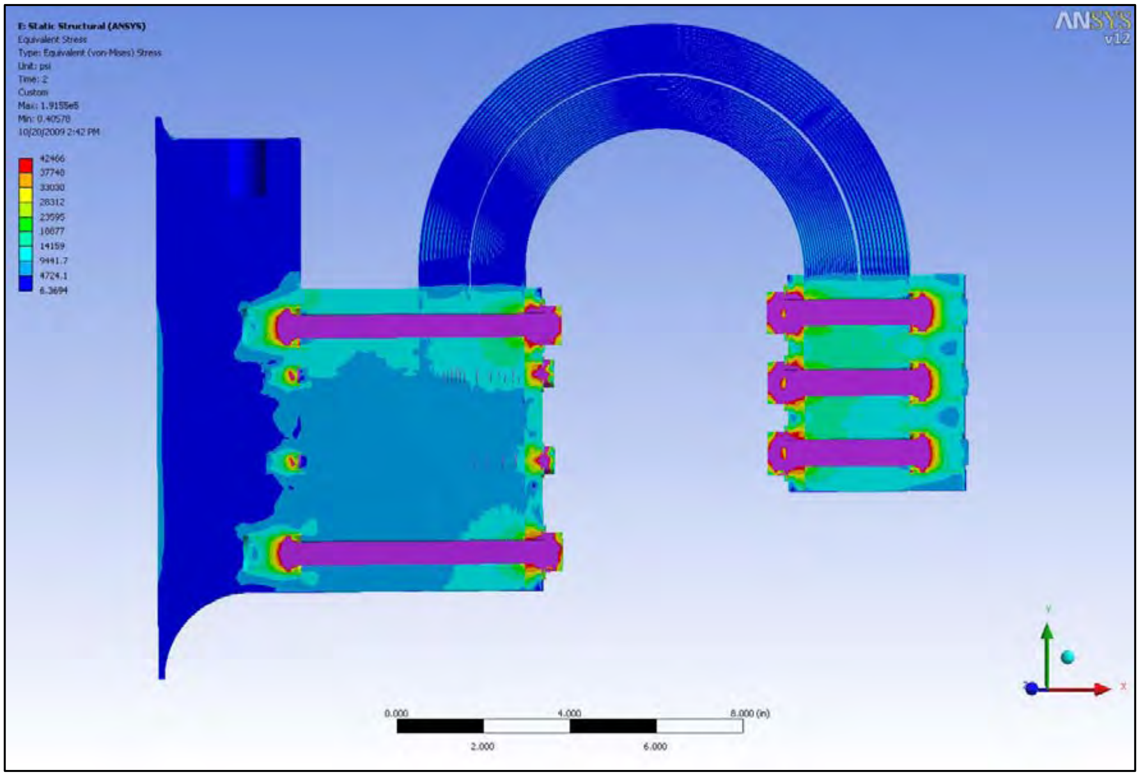

Figure 3.6.4 – Static Structural Analysis Results: TF Bundle Stub Bolted Joint Contact Pressure

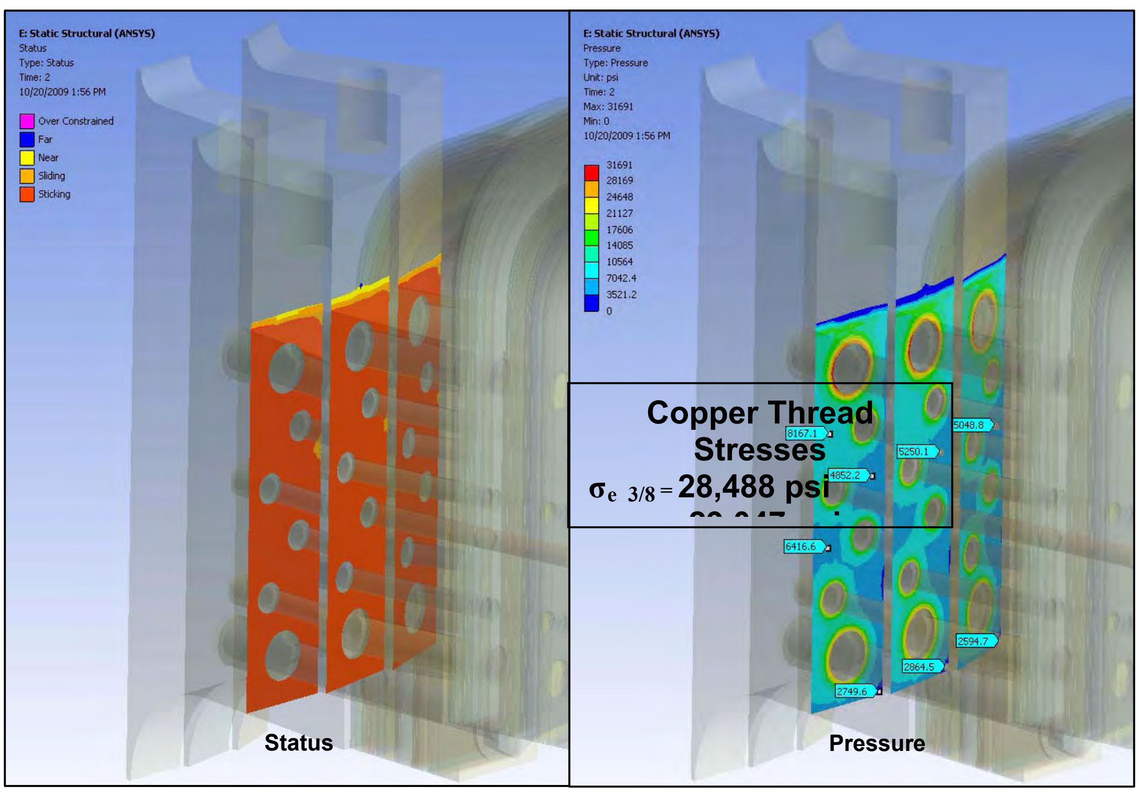

3.7 Linear Buckling Analysis Results

The results of the Linear Buckling analysis for the outer-most lamination are shown in Figure 3.7. The results show that buckling occurs in the same straight-to-curved transition area as where the stresses were shown to be the highest. The first-mode load multiplier factor (LMF), or scaling factor applied to all the static structural analysis lamination loads required to produce buckling, is 58.4. This value is so much greater than the margin in yield or ultimate strength of the laminations that mechanical failure will occur well before buckling.

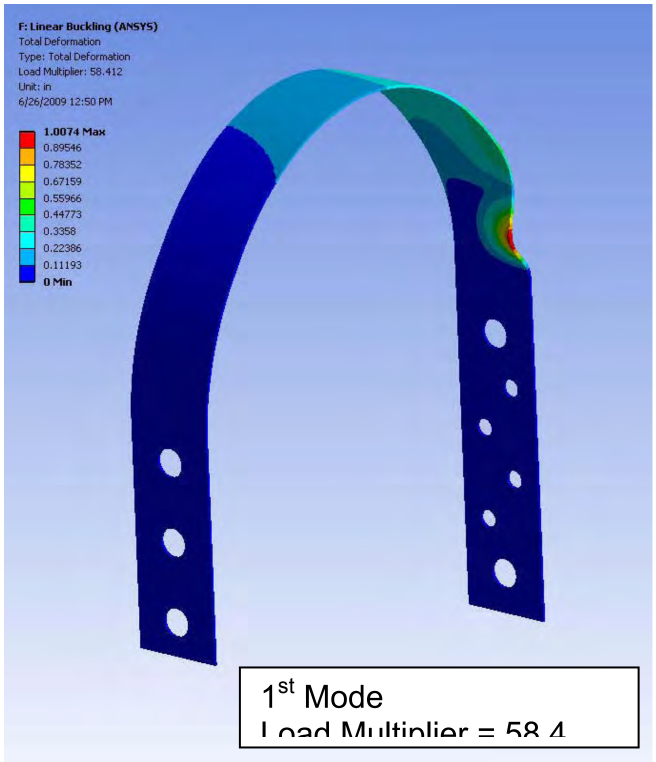

Figure 3.7 – Linear Buckling Analysis Results: Load Multiplication Factor (LMF)

4.0 Conclusions

From Figure 3.6.2, the maximum equivalent (von Mises) stress in the laminations is 27.5 ksi. To satisfy the requirements of the NSTX Structural Design Criteria, the fatigue strength at 3000 cycles must be greater than twice this stress (factor of safety = 2), or the fatigue strength at 60000 cycles (20x N) must be equal to or greater than this stress, whichever is the more severe requirement. Figure 4.1 shows the estimated fatigue S-N curve for C15100 copper-zirconium, including plots of full power and 2/3 full power stresses at N = 3000 cycles, and N = 60000 cycles. With the factor of safety of 2 applied, the design stress level at full power slightly exceeds the fatigue strength at 3000 cycles. Because this stress was determined under worst-case power supply fault conditions, considered an extremely rare event, the design stress is judged to be acceptable and to meet the requirements of the Design Criteria. A fatigue test of a single strap assembly, under simulated worst-case load conditions, is recommended to confirm this assessment.

From Figure 3.6.3, the maximum equivalent stress in the copper threads is 29.1 ksi. Figure 4.2 shows the estimated fatigue S-N curve for C181500 copper-chromium-zirconium, including plots of full power and 2/3 full power stresses at N = 3000 cycles, and N = 60000 cycles. From the figure, it can be seen that the design stress meets the requirements of the Design Criteria.

Reference: “Analysis of NSTX TF Voltage Measurements”, R.Woolley, PPPL memo, 2005

Figure 4.1 – Flex Strap Lamination Fatigue Life

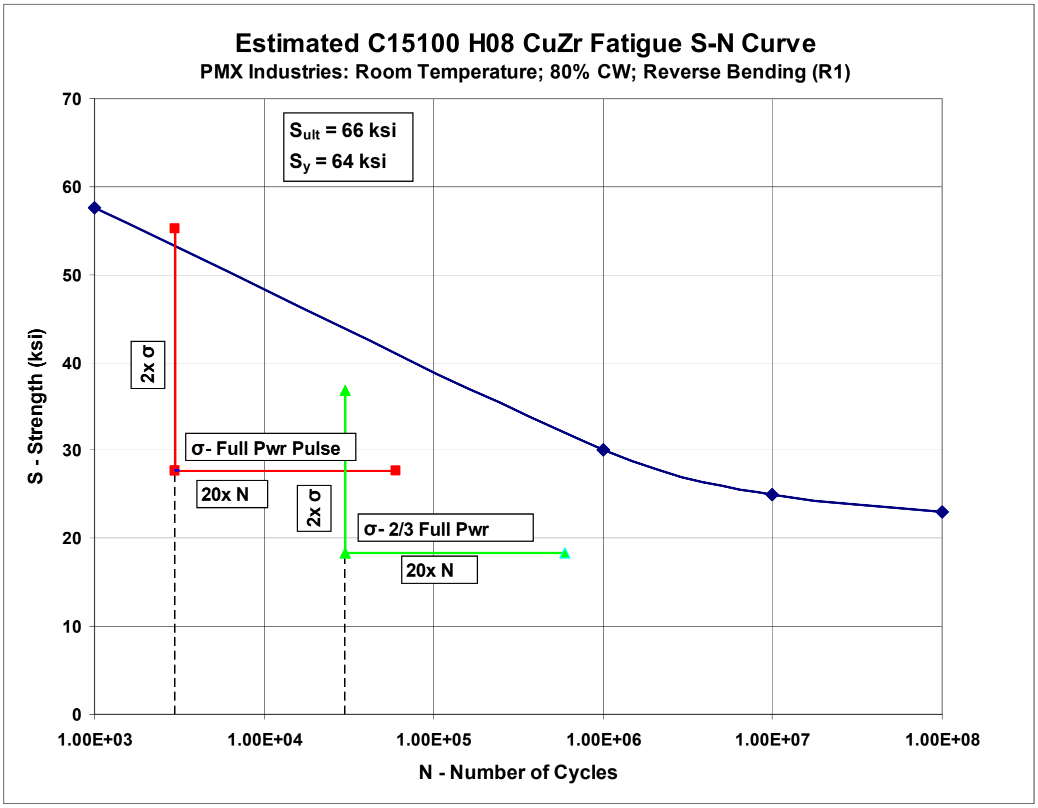

Figure 4.2 – Bolted Joint Copper Thread Fatigue Life

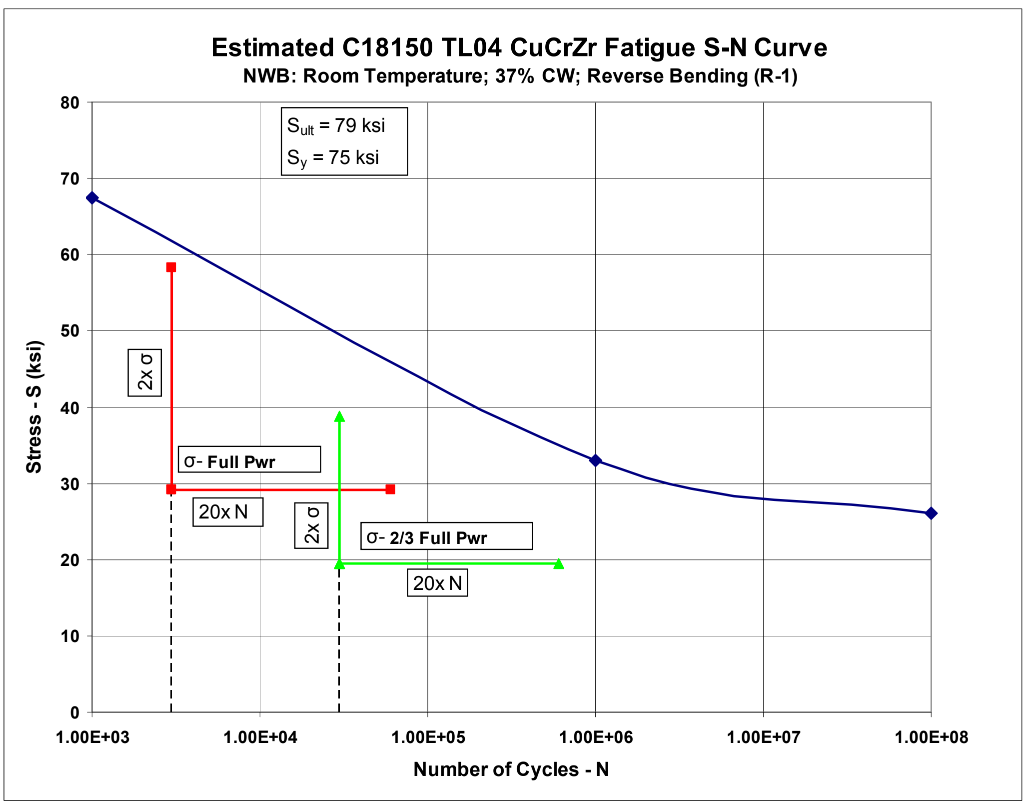

Appendix

Properties of some Copper Alloys

(Outokumpu Poricopper Oy)

Name	CDA	Acronym	Thermal Conductivity at 20 C [W/(m*K)]	Electrical Resistivity at 20 C [μOhm*cm]	Yield Strength Cold Worked 84% 24 C [MPa]	Yield Strength Annealed 24 C [MPa]	Fatigue Strength Cold Worked Number of Cycles[300x10^6]
Oxygen-free Copper	C10200	Cu-OF	394	1.7241-1.70	341	54.5	117
Silver-Bearing Oxygen-free Copper	C10400	Cu-OFS	394	1.74-1.71	373	-	103
Electrolytic Tough-Pitch Copper	C11000	Cu-ETP	394	1.7241-1.70	345	49.6	117
Copper-Chromium	C18200	Cu-Cr1	301-343	2.3-2.0	520	-	193
Cadmium Copper	C16200		360	1.92	474	83	205
Cupro-Nickel		Cu Ni25	33.5	34	530	140	269
Aluminum Bronze		Cu Al5	75.4-83.7	10	441	186	131
Zirconium Copper	C15000	Cu-Zr	367	1.86	414	80	241

Effect of temperature on the softening of copper alloys

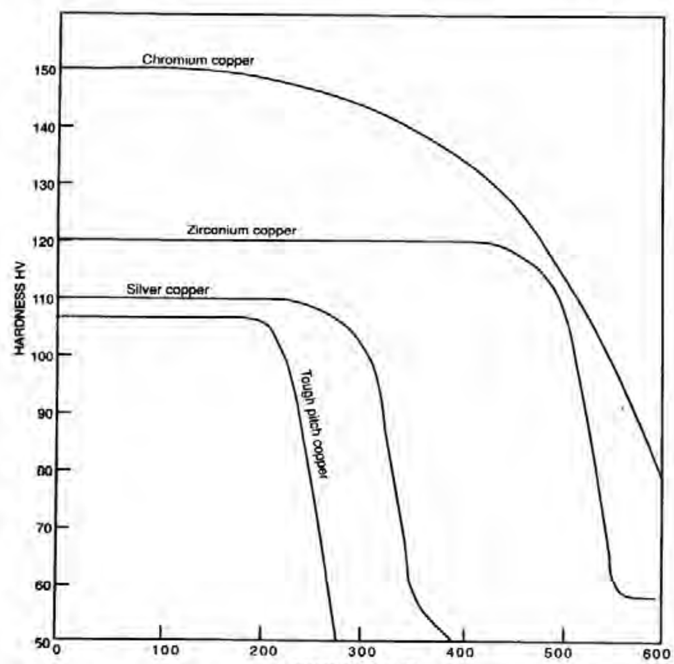

Hardness values as influenced by softening temperatures of typical tough pitch high conductivity copper, silver copper, chromium copper and zirconium copper

Section 5: Coil Structures

NSTX Upgrade CDR

October 2009

Lead Author: Danny Mangra

1. Structural Design

The NSTX Centerstack upgrade will increase the magnetic fields and electromagnetic forces on the PF and TF coils. This WBS will cover the design and fabrication of those modifications. The scope of this work includes the design of reinforcements to the umbrella structure, centerstack pedestal, TF outer leg structures, supports for PF coils 2, 3, 4 and 5 upper and lower.

The modifications must resist the forces generated by the upgraded coils (Table 1). The coil support modification must interface with the existing legacy equipment and fit into the real estate available. The supports should allow for the coils to be aligned with a tolerance of 5 mm. The stress levels in the structural components should be within the requirements set forth by NSTX Design Criteria. The individual components to be installed will be

Cage Links	Power Supply Limit		Operational Limit	
	Max (lbs)	Min (lbs)	Max (lbs)	Min (lbs)
PF 3 Upr to PF 4 Upr	272,631	-314,951	103,217	-150,417
PF 5 Upr to PF 5 Lwr	665,724	-666,010	258,062	-239,821
PF 4 Lwr to PF 3 Lwr	116,805	-471,392	35,711	-150,441
Upper dome load	194,759	-369,644	59,209	-59,365
Lower dome load	191,694	-194,844	44,531	-59,250
Load by vessel to 4 legs to	495,107	-495,329	58,722	-65,529

Table 1. PF Cage Force Inputs

modularized such that they can be handled easily (<100#/ part) without the aid of an overhead crane when possible. Care shall be taken to minimize the impact to the existing NSTX hardware and diagnostic experiments during installation and once installed.

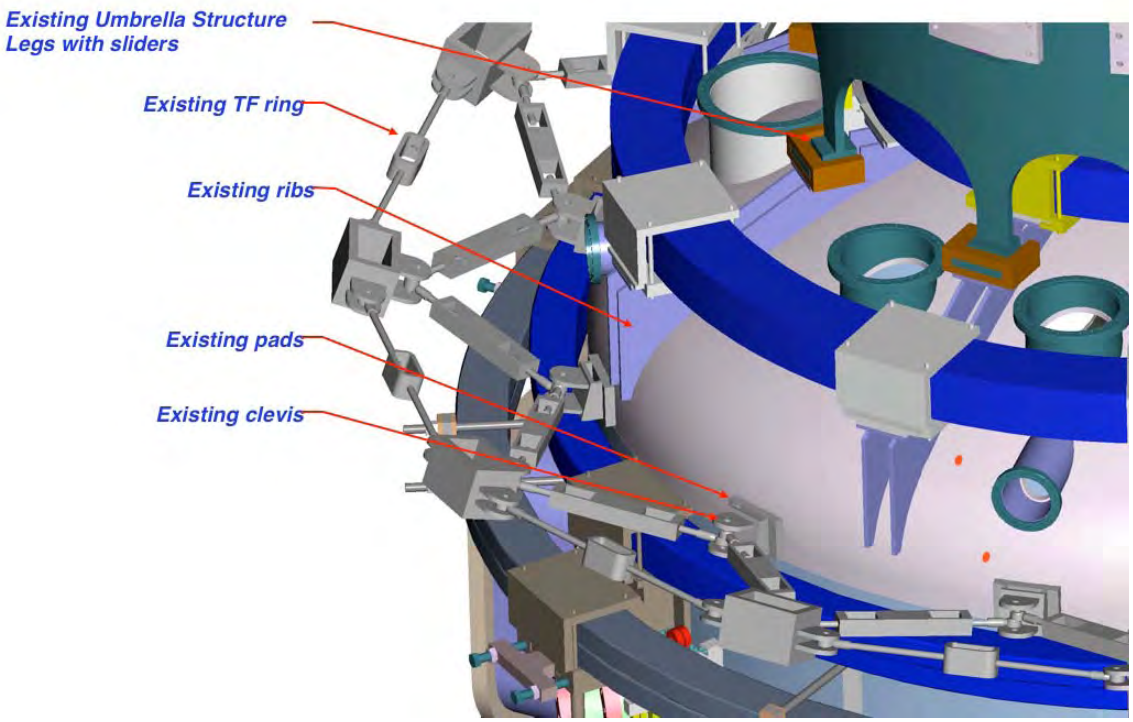

Figure 1. Existing TF Structure

2. Outer TF Leg Coil Supports

The existing outer TF coil supports (Figure 1) utilize space between the outer leg and vacuum vessel at elevations several feet above and below the machine midplane. The upgraded supports for the outer TF legs are designed to utilize the same space (Figure 2) occupied by the existing TF Outer leg turnbuckle system. The new structure will make use of tubular structural members to create a toroidal ring to support the outer legs against the magnetic forces acting outward in a radial direction. There are two of these rings, one located above the midplane ports and one located below. To react the against the tangential magnetic forces a system of radius rods is used inside the rings to that support is given in the tangential direction but the vacuum vessel is allowed to expand radially during bakeout without adding loads to the TF outer legs. Adjustments for alignment during installation will be provided. Spherical rod end connections at the vacuum vessel provide for minor misalignment and compliance in the vertical direction. Insulated bushings made from G-10 or G-11 provide breaks in the toroidal direction to prevent parasitic current loops.

3. PF Coil Support Cage

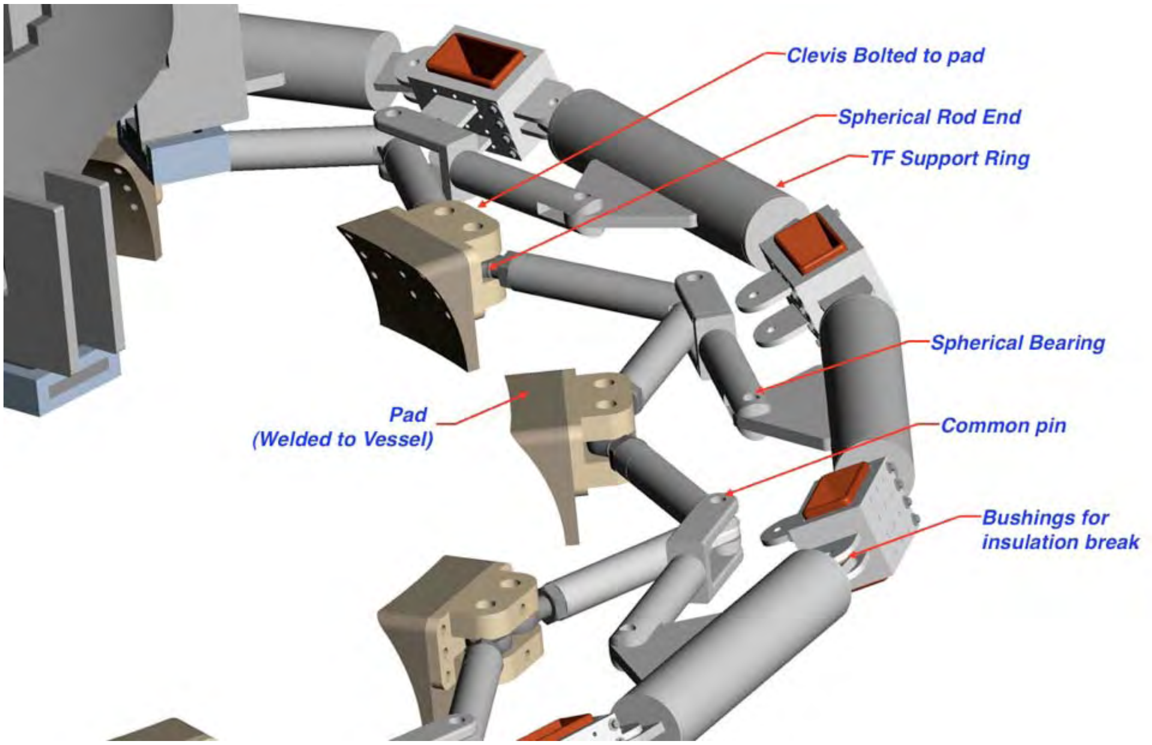

Figure 2. Outer TF Support Structure

The outer PF coils (PF3, 4, & 5) are provided with a support cage (Figure 3) to remove the loads from the vacuum vessel where they are supported in the existing design. This provides additional margin in the vacuum vessel so it may provide support to the outer TF legs against the higher magnetic fields. The existing dome ribs, on which the PF2 and 3 coils are supported, need to be modified (Figure 4) so they are free of the PF coils. The new PF cage will be installed in small lightweight modules (Figure 5). The PF loads are carried down into the floor through a set of four (4) new legs. A stabilizer (Figure 6) to connect the PF cage to the TF outer leg assembly is also provided for registration and damping.

4. Umbrella Structure Modifications

The umbrella structure connections to the outer TF legs will also be reinforced (Figure 7) by adding plates behind the aluminum castings at the TF end support connections. The umbrella legs to the vacuum vessel connections will also be reinforced against tangential loads by welding gussets to the umbrella. The cover to the umbrella structure will be simplified by eliminating the existing splined connection and replacing it with a one piece lid which is designed for compliance in the vertical direction but rigid in the tangential direction.

The centerstack pedestal is designed to be stronger to resist the higher OH coil launching loads. A larger base is provided to reduce the force per unit area to an acceptable level for the test cell floor. The pedestal is designed with a joint at the middle to allow it to be installed in pieces. Gussets at the base are provided with bolted joints so they may be removed for access to the centerstack.

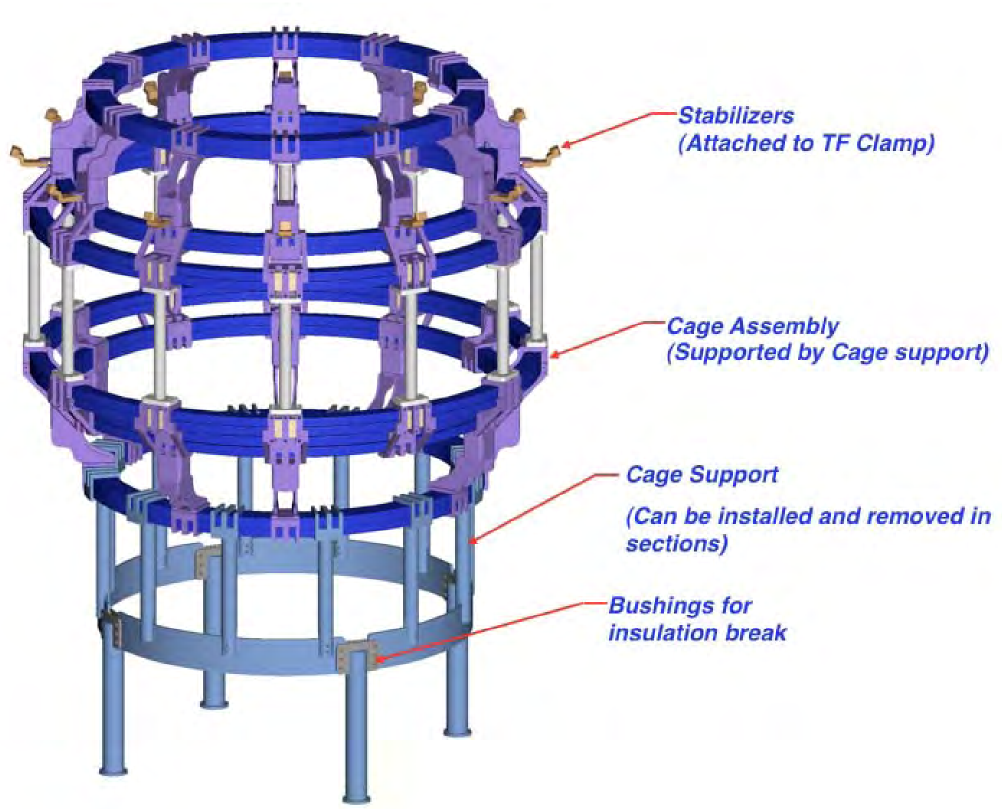

Figure 3. Outer PF Coil Support Structure

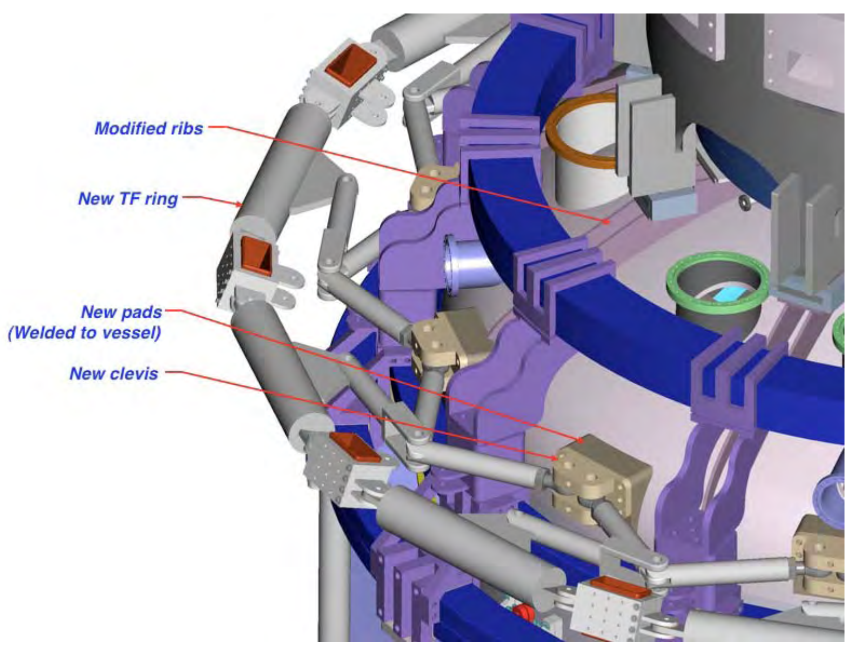

Figure 4. PF Support Ribs and Outer TF Supports

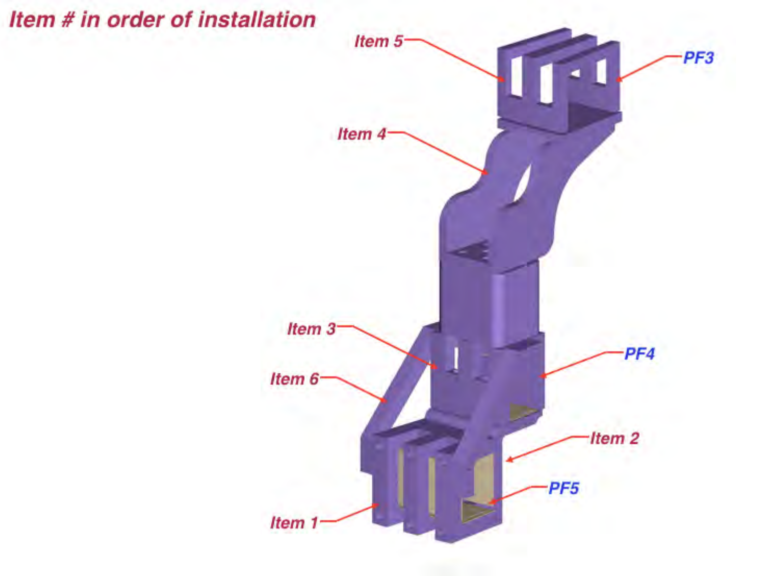

Figure 5 The PF coil support links are designed in small segments to ease installation

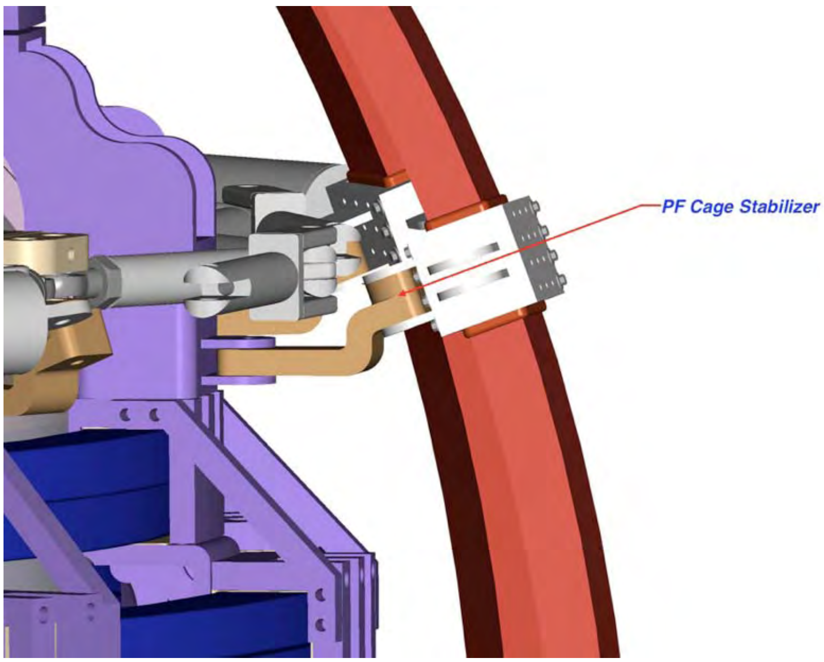

Figure 6. A PF Cage Stabilizer is provided for registration to the Outer TF Legs

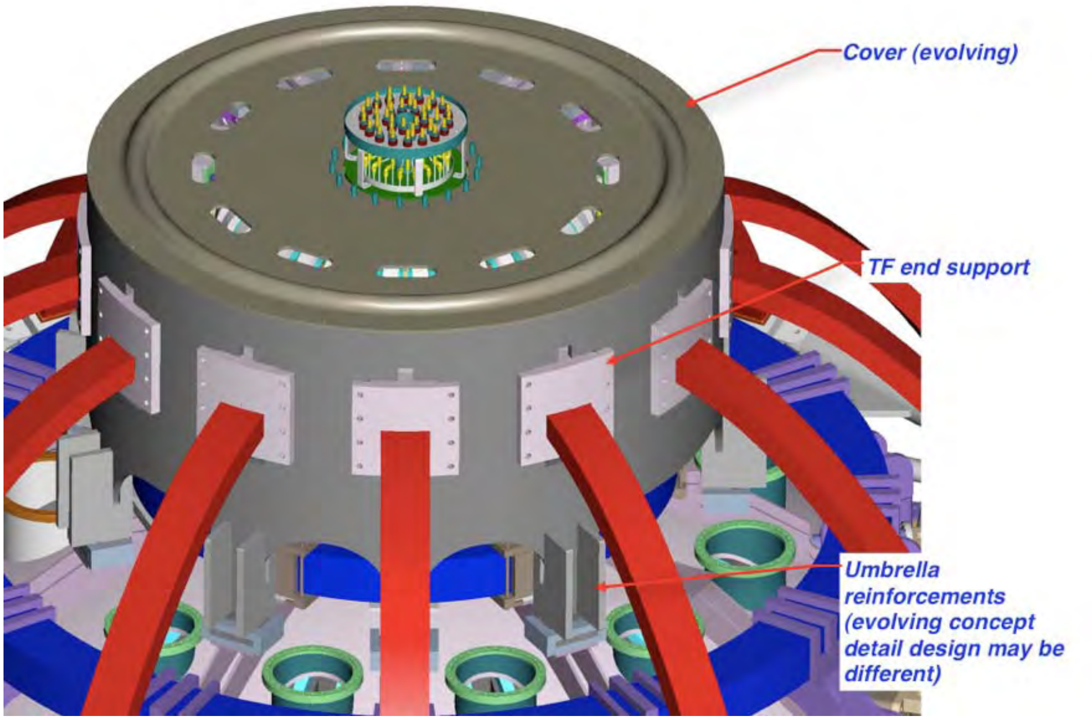

Figure 7. The Umbrella Structure is reinforced at the Outer TF Leg Connection and the Legs

5. Installation Procedure Plan

The installation of the PF Cage needs to be carefully planned in order to minimize the cost and the impact to the existing experiment and diagnostics. The sequence plan to install the PF cage and coils is as follows:

1. Install Shaping fixtures on PF5 coils
2. Remove existing coil clamps on PF5 and PF4
3. Upper PF5/PF4 are raised & Lower PF5/PF4 are lowered
4. Inspect coils for needed repairs (leaks etc) & repair if needed
5. Reposition upper PF5 & install PF5 cage clamps
6. Link PF4 to PF5 via mechanical supports
7. Add columns to PF5 and repositioned lower PF5
8. Process continued on the lower coils
9. Each coil is mechanical aligned for concentricity
10. Leg system for the cage is attached
11. Alignment system relative to legs of vessel is installed
12. Cage system can be slid on ground (grouting plate to be designed)
13. Align cage and bolt to ground/grouted plate
14. Remove shaping fixture & alignment fixture
15. Address electrical isolation/grounding needs

Job	Estimate ($K)
Job: 1200 - Vacuum Vessel & Structural Support	$776
Job: 1201 - Outer TF Structures	$689
Job: 1202 - Outer PF Coil Structures	$1,111
Job: 1203 - Umbrella Structural Reinforcement	$397
Job: 1204 - CS Support Pedestal	$197
Job: 1205 - Misc VV Structural Support	$252

Table 2. Cost Estimate by subassembly

6. Installation Resources for PF & TF Supports

Below is the estimated resources required for the installation of the PF and TF support structures:

1. Equipment Removals (398 mday)
2. Cage Support (88 mday)
3. Upper Half Installation (923 mday)
4. Lower Half Installation (835 mday)
5. Center Stack Pedestal (48 mday)
6. Reinstall Equipment (650 mday)

7. Cost Estimate

The cost estimates for the PF and TF Coils structures were developed using a combination of dollar per pound of hardware for the fabrication cost and a dollar per model and drawing to estimate the labor for the preliminary and final design of the supports. The estimate by subassembly is shown in Table 2.

8. Issues

The following issues have been identified and will be resolved during the preliminary design:

1. The launching loads on the vessel exceed the capability of the existing vessel connections of the vacuum vessel legs so some reinforcement will need to be implemented. The plan is to implement a set of welded gussets to increase the margin.
2. The PF 2 coils supports will also likely require reinforcement however since the increase in loads in minimal the modifications can be implemented by changing the fasteners in the existing supports.
3. The PF cage support is still evolving and being evaluated against all of the operational scenarios. The design presented is conservative and can support the coils against the maximum forces generated by the coils at the power supply limits. The PF 5 column Supports are installed inside the Outer TFs in 12 locations. Optimization may allow reductions.

4. The centerstack pedestal capacity is limited by the connection provided to the centerstack (18-3/8" bolts) which is 126 KIPS. High strength fasteners will be required to achieve that capability.
5. The dome ribs will require significant modification insitu to install the new PF cage support system. Careful planning will be required to minimize the impact and cost.
6. Clevises on vessel must be removed and replaced with stronger versions to provide the restraint required for the outer TF leg support system.

9. Summary

The conceptual design of the PF TF support structures is based on the worst case power supply limit loads. The PF cage is modularized so it can be installed easily with minimum impact to the experiment and can be optimized for operational limits by removing sections to save cost and schedule.

Section 6: Analysis

NSTX Upgrade CDR

October 2009

Lead Author: Peter Titus

Introduction

The NSTX [1] is the world's highest performance spherical torus (ST) research facility and is the centerpiece of the U.S. ST research program. Since starting operation in 1999, NSTX has established the attractiveness of the low-aspect-ratio tokamak ST concept characterized by strong intrinsic plasma shaping and enhanced stabilizing magnetic field line curvature. The purpose of the NSTX Center Stack Upgrade project is to expand the NSTX operational space and thereby the physics basis for next-step ST facilities. The plasma aspect ratio (ratio of major to minor radius) of the upgrade is increased to 1.5 from the original value of 1.26. The higher value of A matches the value found to be optimal in studies of future ST devices, and also increases the cross sectional area of the center stack by a factor of ~ 3 and makes possible higher levels of performance and pulse duration. The new center stack will provide a toroidal magnetic field at the major radius R_0 of 1 Tesla (T) compared to 0.55T in the existing NSTX device, and will enable operation at plasma current I_p up to 2 Mega-Amp (MA) compared to the 1MA rating of the existing. Plasma flat top duration is extended to 5.0 seconds from the present 0.5 second capability. This extension benefits substantially from another upgrade project which will add a second Neutral Beam Injection (NBI) line to NSTX such that flat-top current sustainment can be achieved non-inductively using NBI current drive.

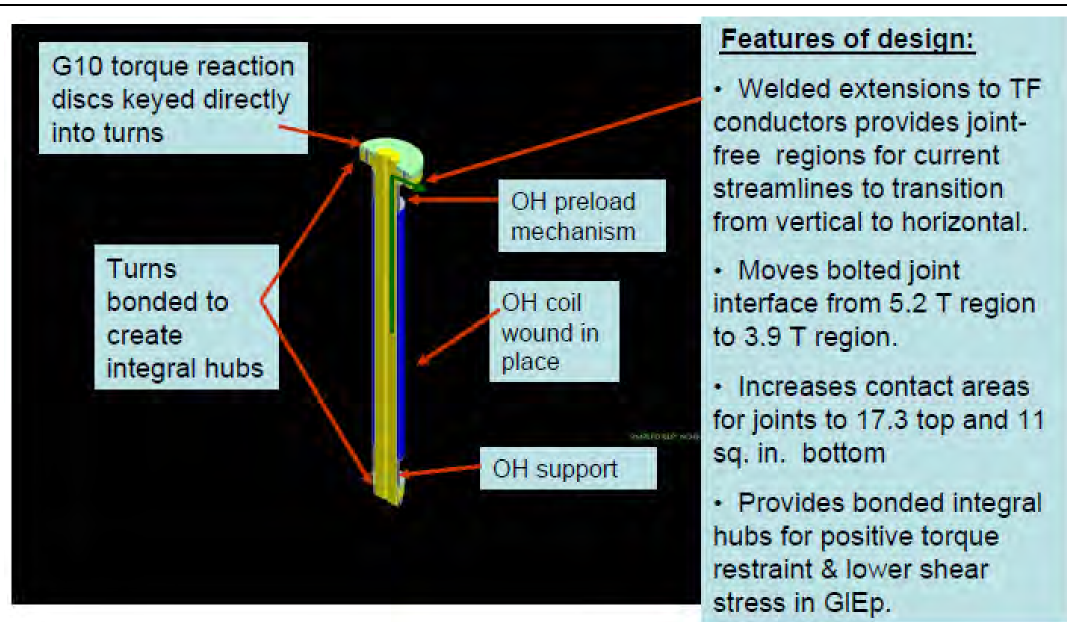

The NSTX center stack (CS) consists of the inner legs of the toroidal field (TF) coil surrounded by an ohmic heating (OH) solenoid and a several poloidal field (PF) shaping coils, all encased in a vacuum-tight metallic center stack casing (CSC) covered by plasma facing tiles. Since the TF coils include a demountable joint between the inner and outer legs, and the CSC includes a bellows and vacuum seal connection to the outer vacuum vessel, the entire center stack assembly is removable as a modular unit. Thus the upgrade will be accomplished by replacing the existing CS with an entirely new assembly with new TF inner legs, OH and PF coils, CSC, and plasma facing tiles. The TF outer legs, originally designed with an upgrade in mind, are retained but with enhancements to their structural supports.

This document describes the analytic effort performed to support the conceptual design effort. Analyses build on a strong document package qualifying the original NSTX design. Operational history also contributed to understanding weaknesses in the design and afforded an opportunity to expand the engineering qualification more uniformly throughout the machine. Calculations which support thte original design may be found at:

http://nstx.pppl.gov/nstx/Engineering/NSTX_Eng_Site/Technical/General/Calculations/NSTX_Engr_Calcs.html

Calculations that support the conceptual design of the centerstack upgrade may be found at:

http://nstx-upgrade.pppl.gov/Engineering/WBS_Specific_Info/Design_Basis_Documentation/Calculations/index_Calcs.htm

Summary of the CDR Analysis Status

The design basis loading is evolving because of GRD guidance on Worst Case vs Normal +Machine Protection System. Cost savings are likely as we remove extreme load scenarios via inclusion in MPS.

TF Inner Joint Field and displacement boundary conditions have been passed to a detailed model of the joint (T. Willard's Calculation [4])

TF reinforcements for in-plane and out-of plane loads have been designed to Worst Case loads and remain in the territory currently used by the present TF supports – Loosening or disassembly is not required for bake-out. Reinforcements of the umbrella structure are needed.
Centerstack TF and OH assembly meets normal operational loads, Belleville support system maintains OH coil contact at lower support to eliminate motion at leads and coolant connections.

As of the CDR no modifications of the vessel or passive plates are needed for disruption loads. More disruption cases are being run, and more detailed models of the passive plate support hardware are being modeled.
Active cooling being incorporated into the new centerstack divertor areas has been sized. Tile surface temperatures for long pulse full power operation are high and require further evaluation.

Inner PF's and structure are undergoing improvements as a part of the normal design process to meet Normal and Halo loads.

Analysis work continues to complete treatment of all details of the design and optimize and economize the design concepts.

Design Input

Some of the Upgrade parameters are repeated here for convenience. An up-to-date complete listing of the Upgrade characteristics are in the design point spreadsheet available on the NSTX Upgrade engineering website.

		NSTX BASE	NSTX CSU
Ro	m	0.854	0.934
Ip	MA	1.0	2.0
Bt@Ro	T	0.6	1.0
OH Flux Swing Total	Wb	0.7	1.9
Initiation Vloop	V	2.9	4.7
Ip Flat Top Time	s	0.5	5.0
Ip Ramp Up Rate	MA/s	5.0	2.0
Ip Ramp Down Rate	MA/s	10.0	4.0
Ro+a	m	1.477	1.504
A_95		1.4	1.6
a	m	0.623	0.570
R0-a	m	0.231	0.365
Zmax	m	1.371	1.424
Rzmax	m	0.480	0.593
Ip Duration	s	0.8	6.5
OH Single Swing Flux	Wb	0.4	1.4
OH Flux Initiation	Wb	0.1	0.1
OH Flux Ramp	Wb	0.5	1.3
OH Flux Flat Top	Wb	0.1	0.5

		NSTX BASE	NSTX CSU
TF Rcuinner	m	0.0072	0.0260
TF Rcuouter	m	0.0977	0.1941
TF �Zcu	m	5.3300	5.3300
TF #turns	turns	36	36
TF #layers	layers	2	1
TF Ground insulation	m	0.0014	0.0024
TF Turn insulation	m	0.0008	0.0008
TF Cooling hole diameter	m	0.0047	0.0047
TF Conductor corner radius	m	0.0010	0.0010
TF Packing fraction		0.8169	0.8900
TF Voltage	V	1013	1013
TF Current	Amp	71168	129778
TF Tesw (L/R Decay)	s	1.38	7.57
TF Action (L/R Decay)	A^2-s	7.01E+09	1.27E+11
TF Voltage stress max turn-turn	kv/mm	0.6231	0.6231
TF Voltage stress max turn-ground	kv/mm	0.4637	0.3190
TF Inlet Coolant Temp	C	12	12
TF Inner leg maximum temp (L/R Decay)	C	99	100

TF Outer leg maximum temp (L/R Decay)	C	17	50
Total Copper Mass TF Inner Legs	Tonne	1.2	0.0
Total Copper Mass TF Outer Legs	Tonne	8.4	0.0

		NSTX BASE	NSTX CSU
TF Rcuinner	in	0.2819	1.0220
TF Rcuouter	in	3.8469	7.6398
TF □Zcu	in	209.8425	209.8425
TF #turns	turns	36	36
TF #layers	layers	2	1
TF Cooling hole diameter	in	0.1860	0.1860
TF Conductor corner radius	in	0.0390	0.0390
TF Packing fraction		0.8169	0.8900
TF Voltage	V	1013	1013
TF Current	Amp	71168	129778
TF Tesw (L/R Decay)	s	1.38	7.57
TF Action (L/R Decay)	A^2-s	7.01E+09	1.27452E+11
TF Voltage stress max turn-turn	volt/mil	16	16
TF Voltage stress max turn-ground	volt/mil	12	8
TF Inlet Coolant Temp	C	12	12
TF Inner leg maximum temp (L/R Decay)	C	99	100
TF Outer leg maximum temp (L/R Decay)	C	17	50
Total Copper Mass TF Inner Legs	lbs	2560	0
Total Copper Mass TF Outer Legs	lbs	18495	0

Criteria

For the conceptual design of NSTX Centerstack Upgrade, a structural criteria specific to the project, has been adopted. This and the General Requirements document provide the criteria for design of the upgrade. Both the GRD and the criteria document may be accessed through the NSTX Upgrade engineering web page. Summaries are included here:

Allowables for Coil Copper Stresses

The TF copper ultimate is 39,000 psi or 270 MPa . The yield is 38ksi (262 MPa). Sm is 2/3 yield or 25.3ksi or 173 MPa – for adequate ductility, which is the case with this copper which has a minimum of 24% elongation. Note that the ½ ultimate is not invoked for the conductor (It is for other structural materials) . These stresses should be further reduced to consider the effects of operation at 100C. This effect is estimated to be 10% so the Sm value is 156 MPa.

- From: I-4.1.1 Design Tresca Stress Values (Sm), NSTX_DesCrit_IZ_080103.doc
- • (a) For conventional (i.e., non-superconducting) conductor materials, the design Tresca stress values (Sm) shall be 2/3 of the specified minimum yield strength at temperature, for materials where sufficient ductility is demonstrated (see Section I-4.1.2). *
- It is expected that the CS would be a similar hardness to the TF so that it could be wound readily. For the stress gradient in a solenoid, the bending allowable has been used for initial sizing. The bending allowable is 1.5*156 or 233MPa, Membrane or average tresca stress in the coil section should meet the membrane stress allowable.

Room Temperature Allowables for 316 and 304 SST

Material	Sm	1.5Sm
316 LN SST	183Mpa (26.6 ksi)	275Mpa (40ksi)
316 LN SST weld	160MPa(23.2ksi)	241MPa(35ksi)

Mill Certs for the 304 Vessel Show a 45 ksi Yield

05/19/1998 13:53 6174720409 NEWENGLANDSTEELTANK PAGE 03

Avesta Sheffield

Avesta Sheffield Plate Inc.

Certificate of Analysis and Tests

OUR ORDER 106101 - 01 HEAT & PIECE 87893-3B 5/13/98

PSI MIC NO. C992

SOLD TO: PROCESS SYSTEMS INTERNATIONAL
20 WALKUP DRIVE
WESTBOROUGH MA 01581

SHIP TO: NEW ENGLAND STEEL TANK
111 BROOK ROAD
SOUTH QUINCY MA 02169
737001-06

---------------------------------- YOUR ORDER & DATE ----------------------------------

558635 3/18/98 TAG# PART #V077P001

---------------------------------- ITEM DESCRIPTION ----------------------------------

HEAT & PIECE 87893 - 3B 3A
WEIGHT 3002
FINISH 1
GRADE 304 UNS-S30400
DIMENSIONS .625 X 76.000 X 212.000 EXACT

---------------------------------- SPECIFICATIONS ----------------------------------

THE PRODUCTS LISTED ON THIS MILL TEST REPORT SATISFY PREFERENCE CRITERION B AS DEFINED IN ARTICLE 401 OF THE NORTH AMERICAN FREE TRADE AGREEMENT. COUNTRY OF ORIGIN IS USA

ASTM A240-96A ASMESA240-96AD
NO WELD REPAIR ON MATERIAL
ASTM A262-93A PRAC A

ASTM A480-96,ASMESA480-96AD
MAG PERM <1.05 ASTM A342 (6)
ASTM A262-93A PRAC E

PLATES & TEST PCS SOLUTION ANNEALED @ 1950 DEGREES FARENHEIT MINIMUM.
THEN WATER COOLED OR RAPIDLY COOLED BY AIR
FREE OF MERCURY CONTAMINATION
HOT ROLLED, ANNEALED & PICKLED (HRAP)

---------------------------------- MECHANICAL & OTHER TESTS ----------------------------------

HARDNESS RB	81
GRAIN SIZE	5
YIELD STRENGTH (PSI)	45256 ✓
TENSILE STRENGTH (PSI)	91368 ✓
BEND	OK ✓
INTERGRANULAR CORROSION	OK ✓
ELONGATION % IN 2"	63.6 ✓
REDUCTION OF AREA %	72.5

Insulation Shear Stress Allowable

- ***From Dick Reed Reports/Conversations:***
- Shear strength, short-beam-shear, interlaminar
- **Without Kapton 65 MPa (TF, PF1 a,b,c)**
- **With Kapton 40 MPa (CS)**
- **Estimated Strength at Copper Bond 65 MPa/2 =32.5 MPa (All Coils)**

- ***From Criteria Document:***

- ***I-5.2.1.3 Shear Stress Allowable***
- The shear-stress allowable, Ss, for an insulating material is most strongly a function of the particular material and processing method chosen, the loading conditions, the temperature, and the radiation exposure level. The shear strength of insulating materials depends strongly on the applied compressive stress. Therefore, the following conditions must be met for either static or fatigue conditions:
- Ss = [2/3 to]+ [c2 x Sc(n)]
-

2/3 of 32.5 MPa = 21.7 MPa

5ksi=34 MPa
2/3 of this is 23 MPa
C2~=.1 (not .3)

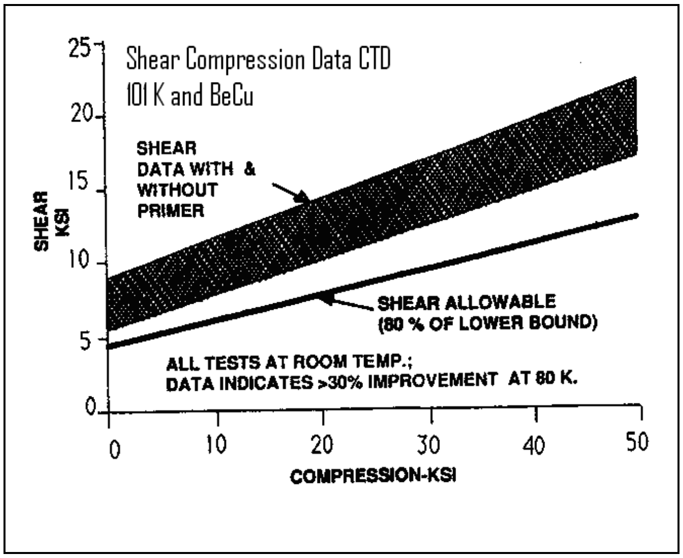

NSTX Fatigue Criteria Document Content:

NSTX CSU is designed for approximately 3000 full power and 30,000 two-thirds power pulses. A fatigue strength evaluation is required for those NSTX CSU components with undetectable flaws that are either cycled over 10,000 times or are exposed to cyclic peak stresses exceeding yield stress.
Any NSTX component without cyclic tensile loading and loaded only in compression shall not require a fatigue evaluation.

For engineering purposes, number of NSTX pulses, after implementing the Center Stack Upgrade, shall be assumed to consist of a total of ~ 60,000 pulses based on the GRD specified pulse spectrum.
Fatigue has not been considered extensively during the CDR, The Criteria and GRD need to be reconciled. A definition of the aged condition for “used” components needs tro be developed. Because of the increase in loads, Minors Rule and Non-Linearity of Fatigue, previous stress cycles will add little in the cumulative damage evaluation ,

Design Loads

Lorentz Loads from coil currents are a major loading on NSTX. A range of identified operational current equilibria constitute the normal operating loads. These are included in the published design point, accessed through the NSTX Upgrade web page[1]. A plot of the currents is included in figure 0.18 . A modest 10% "headroom is used in the current specs to provide for some scenario flexibility.

A challenging requirement in the GRD was to evaluate worst power supply loads and attempt to design to these. If the resulting designs are difficult or costly to implement, then the load combination that produces the "onerous" loading is to be addressed in the Machine Protection System (MPS). The magnitudes of the worst case combinations of loads have made it hard to design any of the structures to meet the worst case load criteria.

The TF self load effects i.e. the centering load in the centerstack and the tension loads in the outer legs have been designed with the maximum terminal current planned for the upgrade. It is the poloidal field coils that potentially combine in uncertain ways to produce large unanticipated loads. The outer leg reinforcements have been designed to the worst out-of-plane loads, and the hardware to react these loads does not appear excessive. On the other hand, support of the outer PF coils to resist the worst possible extremes in loading appears to be a costly and time consuming proposition. This area is one of the prime candidates for relaxing load requirements and obtaining some significant cost savings.

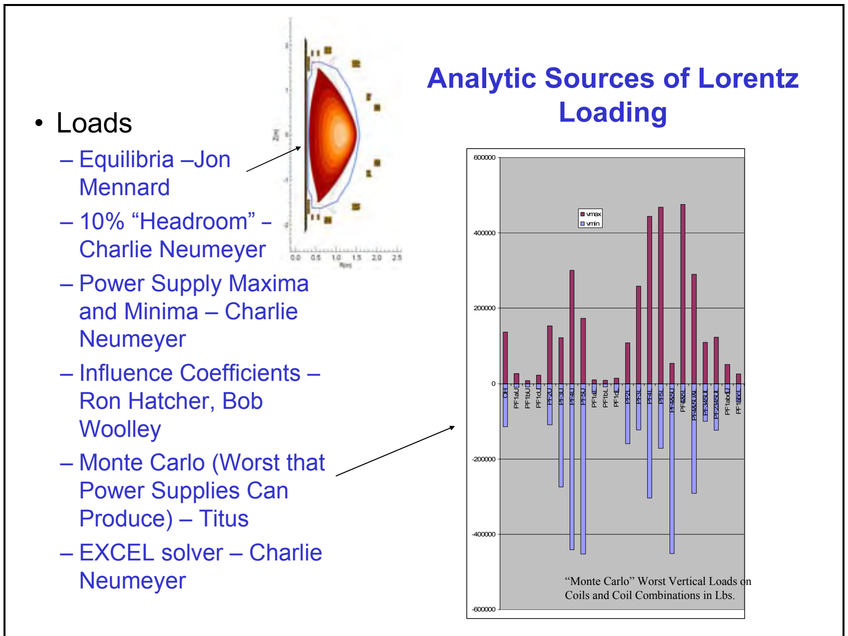

Figure 0.18-1

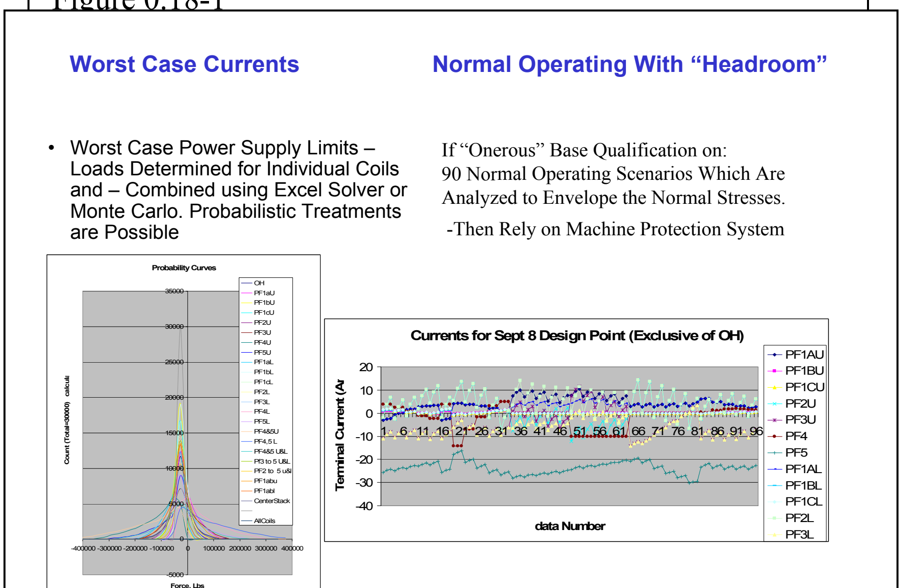

Figure 0.18-2

The specifics of the load spec for the poloidal field coils were still evolving at the time of the CDR. One approach is to rely exclusively on the machine protection system, and abandon designing to coil current overage, If this is chosen , the criteria, and the GRD need to be changed. One proposal is to add a probabalistic approach, this would remain within the GRD, and Criteria framework by describing what a reasonable level of over current loading should be. - essentially putting a spec on "onerous" During the CDR, J. Minerviini suggested a ITER like categorization of loads – MED is working to this on the ELM coils, port plugs etc. Excerpts from our NSTX criteria document were provided to the review committee. ITER uses a load spec that assigns "Anticipated" "Unlikely" etc. to loading - but no probabilities. The present NSTX Centerstack Upgrade criteria quotes probabilities. The NSTX CSU GRD and Criteria provides a better framework to categorize loads than ITER, but there is some consistency in approach and there would be an advantage in retaining a framework of load qualification used on other projects. The solution for these difficulties is to commit to building a robust Machine Protection System and shifting the worst case currents evaluation from an "Unlikely" category to an "Extremely Unlikely Category" In the structural design criteria, the load spec will be clarified. Load categorizations will be based on an update of the NSTX Failure Modes and Effects Analysis (FMEA) Numerical probabilities will not be assessed. A rigorous reliability analysis is not judged appropriate for the NSTX CSU experimental device. A draft proposal follows:

Criteria Document Paragraph I-2.0 LOAD COMBINATIONS

The NSTX structural systems shall be designed for both normal operating conditions and off-normal events. These conditions are:

- Normal Events - Events that are planned to occur regularly in the course of facility operation. ***Normal EM loading shall consist of the 96 currently (Nov 2009) defined current scenarios, identified in the NSTX Upgrade Design Point, and other normal operating current scenarios identified as required for the NSTX Centerstack Upgrade mission, and included in the Design Point***

- Anticipated Events - Events of moderate frequency which may occur once or more in the lifetime of a facility. ***Anticipated EM loading shall consist of Normal loads plus disruptions judged to be common or anticipated.***

- Unlikely Events - Events which are not anticipated but may occur during the lifetime of a facility.

EM Loading for Unlikely Events can result from:

  - ***TBD – The Failure Modes and Effects Analysis (FMEA) will be re-evaluated by WAF cognizant Engineers for the Upgrade Design Point. A qualitative evaluation of the likelyh0od of the failure and the severity of the consequences will be combined in a qualitative manner and be assigned to the list of "Unlikely" and "Extremely Unlikely" events***
  - ***Disruption Events that are judged to be unlikely***

- Extremely Unlikely Events - Events which are not expected to occur during the lifetime of a facility but are postulated because of their safety consequences.

EM Loading for Extremely Unlikely Events can result from

  - ***Machine Protection System(MPS) failure. Lower level power supply controls remaining intact, with random or pegged currents resulting, Consequences of current control failure shall be within the damage limits described in the table in section 1.2.6***

- ***Other TBD events from the FMEA***
- ***Catastrophic Disruption Events if identified for NSTX***

- Incredible Events - Events of extremely low probability of occurrence or of non-mechanistic origin.

Criteria Document Paragraph I-2.6 Damage Limits and Recovery From Events

Condition	Functional and damage limit for the experimental facility	Damage limits to component or support	Recovery from damage
Normal	All the safety related structures, systems, and components are functional.	The component or support should maintain specified service function.	Within specified operational limit. Anticipated maintenance and minor adjustment.
Anticipated	All the safety related structures, systems, and components are functional.	The component or support must withstand this loading without significant damage requiring repair.	Within specified operational limit. Anticipated maintenance and minor adjustment
Unlikely	In addition to the challenged component, inspection may reveal localized large damage, which may call for repair of the affected components.	Material plasticity, local insulation failure or local melting which may necessitate the removal of the component from service for inspection or repair of damage to the component or support.	The facility may require major replacement of faulty component or repair work.
Extremely Unlikely	Gross damage to the affected system or component. Nevertheless the facility maintains the specified minimum safety function.	Gross general deformations, local melting and extensive insulation damage requiring repair, which may require removal of component from service.	Magnet system may be so damaged that repair is not considered economic.

Monte Carlo

This analysis and the procedures for quantifying worst case loads may still find some usefulness in identifying loads for the "Extremely Unlikely" Category.

Vertical and Radial force influence matrices were provided by Ron Hatcher(1). These were used in a Monte Carlo simulation which varied the coil current's within their allowable ranges and computed forces on the individual coils. The maximums and minimums were determined for 10,000 sets of randomly selected coil currents. This yields the worst case loading the power supplies can produce, and ignores the likely loading during plasma shots. The resulting loads and hoop stresses are useful in providing an upper limit on the mechanical loads on the coils. Forces on coil groups, such as PF4 and 5 upper can be summed and maxima and minima determined to provide design loads for specific structural elements or regions.

The "random" results are similar to those obtained in the design point spreadsheet with EXCEL solver or Hatchers procedure to rack up max loads. Typically the Monte Carlo simulation with 10,000 simulations misses some of the peaks and captures more with a higher number of simulations. Modeling "pegged" currents extends the likelihood that the Monte Carlo simulation will capture the low probability max loads because currents are modeled as either at a max or a min, rather than simulations many intermediate currents.

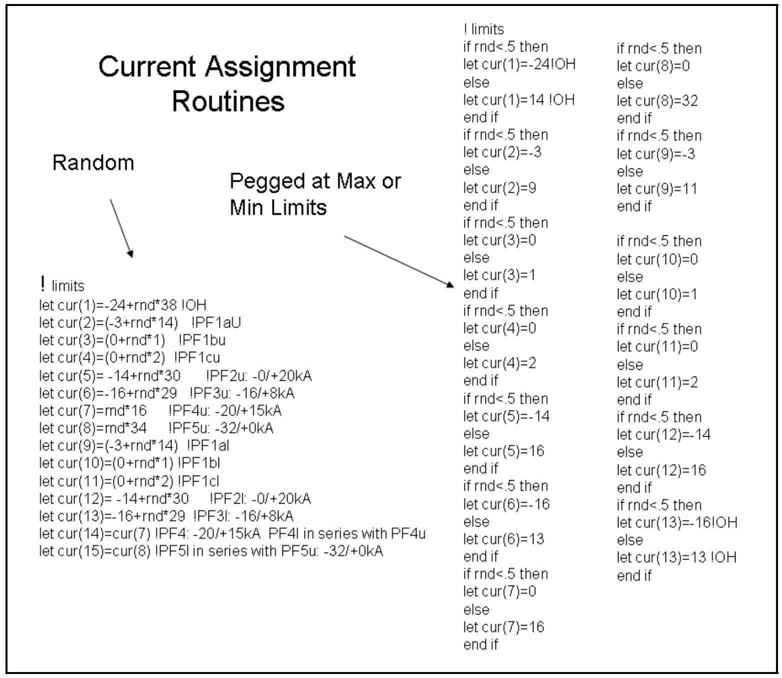

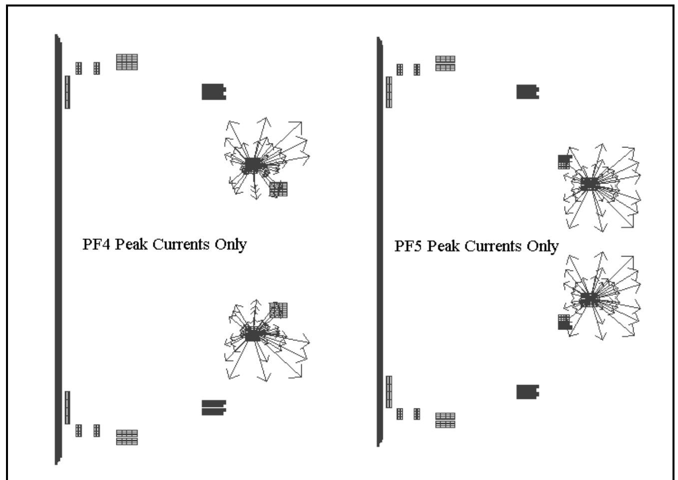

An example of the simple axisymmetric analyses used in computing influence coefficients

List of References

[1] Charles L. Neumeyer, http://www.pppl.gov/~neumeyer/NSTX_CSU/Design_Point.html, dated 7-29-2009.

[2] NSTX-CALC-13-001-00, Global Model – Model Description, Mesh Generation, Results

[3] Disruption Analysis Of Vacuum Vessel and Passsive Plates NSTX-CALC-12-001-00, S. Avasarala

[4] Tom Willard, "TF Flex Joint and TF Bundle Stub", NSTX-CALC-132-06-00, 2009.

[5] Robert D. Woolley, "TF Joint Pressure VS Temperature In NSTX CSU Upgrade", CSU-CALC-132-090211-RDW-01, 2009.

[6] Peter Titus, "Coupled Electromagnetic-Thermal Analysis (04072009)", *NSTX-CALC-132-01-00*, 2009.

[7] Peter Titus, "Coupled Electromagnetic-Thermal Analysis (04202009)", NSTX-CALC-132-02-00, 2009.

1.0.0 Global Modeling

The Global model of NSTX Center Stack Upgrade (NSTX-CSU) provides a simulation of the overall behavior of the machine. It provides boundary conditions for local models and sub Models , or allows inclusion of the detailed models of components in the global model. In many cases it has been built from from other available model segments – The upper and lower head sections of the vessel model come from H.M. Fan's early vessel models. The cylindrical shell that contains the mid plane ports comes from a vessel model built by Srinivasa Avasarala from the Pro–E model of the vessel. In some instances parts of the global model were exported to be evaluateds in more detail. Multiple scenarios from the NSTX design point are run using the global model. The design points are publised on the web and are maintained by C. Neumeyer. As of this issue of the calculation, 70 of the 90 normal operating current sets published in the July 2009 design point have been run in the global model. The September 8 design point has a revision to the OH current variations and these have not yet been run. Loads from normal operating current sets are in general much less severe than loads that are based on worst case power supply currents. In order to compare the global model results with some of the local models that have been run, some of the "worst case" currents have been run in the global model. The outer TF reinforcements are an example of this. Results reported in sub paragraphs of section 8 have been used to qualify components, check results and guide the need for further analyses. The outer TF leg reinforcements discussed in section 8.3 and in NSTX calculation number 132-04-00 are based on two pairs of current sets. These are intended to maximize the out-of-plane loading on the TF outer legs for an up-down symmetric loading and an up-down asymmetric loading that causes large net torques on the outer legs. These two current sets were included in the loading analyzed in the global model. Behavior of the two analyses is consistent. Section 8.3 of Ref [2] discusses these results and adds a qualifiucationn of

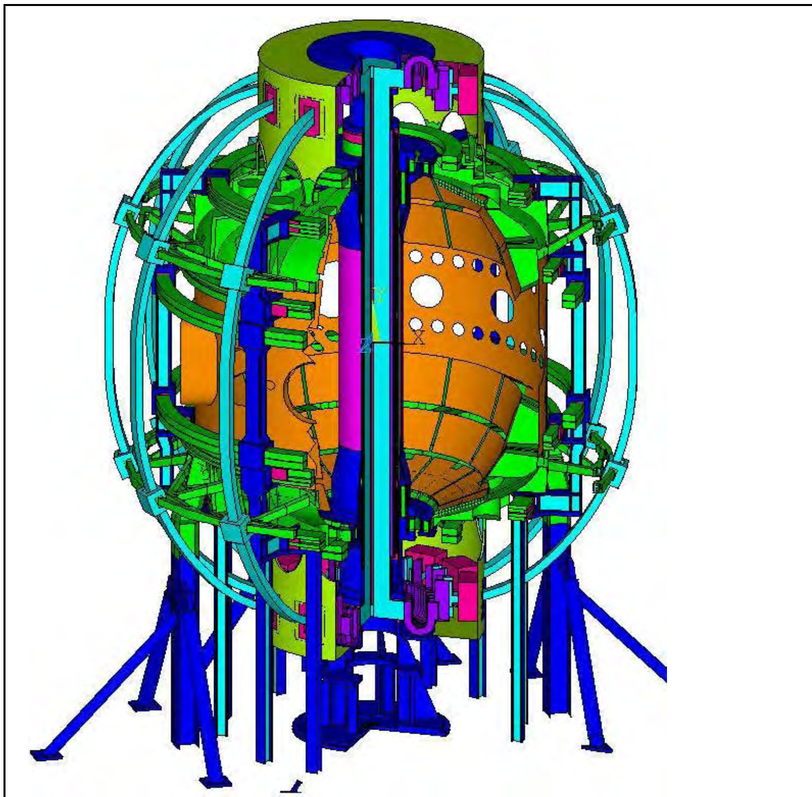

Figure 1.0.0-1

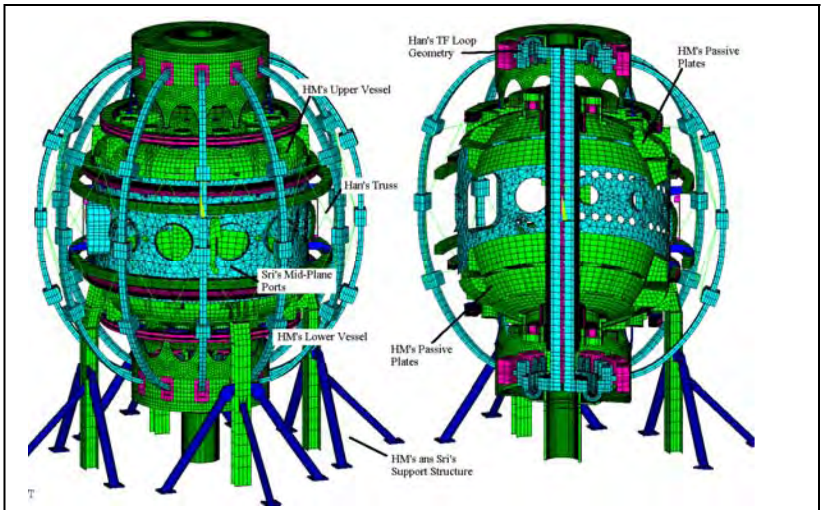

Figure 1.0.0-2 Global Model Status as of June 22 2009

the bending related bond shear in the TF outer leg. Section 8.1 documents the acceptable stresses in the diaphram plate that replaces the gear tooth torsional connection between the centerstack and the outer umbrella structure.Section 8.5 of Ref [2] provided global displacements to the detailed analysis of the flex joint [4] Section **1.3.2.3 or Secion 8.6** of Ref [2] is to date, the only treatment that shows acceptability of the torsional shear in the inner leg. Section ____ similarly profided guidance on global twist in the evaluation of the centerstack OH support details. Section 8.8 shows the stresses and loading around the I beam column attachmeents to the vessel and points to the need to evaluate the weld details of this connection.

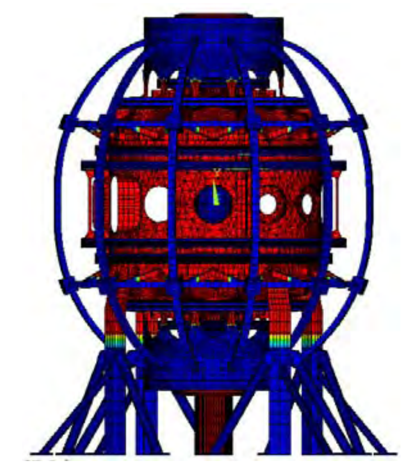

Figure 1.0.0-3 -1
350C Bake-Out Temp

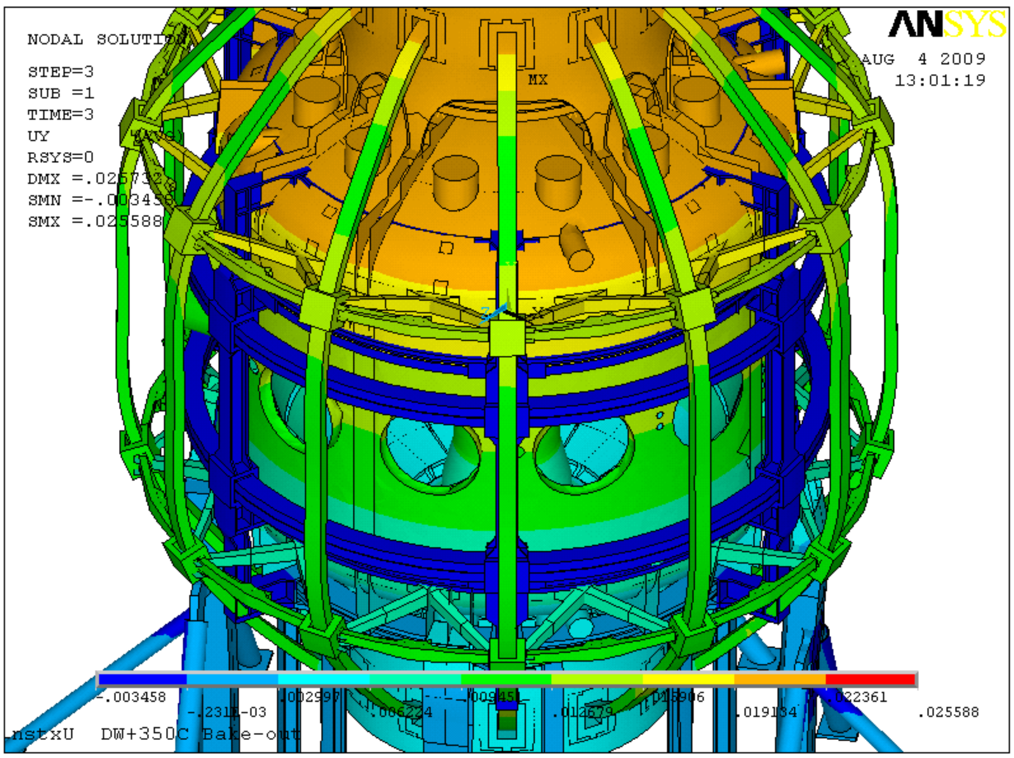

Figure 1.0.0-4 Outer PF Support "Cage" is Not Connected to the Vessel During Normal Operation or Bake-Out

1.1.1 Plasma Facing Components

1.1.1.1 Heat Balance and Heat Loads on PFCs

A thermal analysis of the NSTX CSU was done to demonstrate that the adequacy of proposed active cooling of the CS, in conjunction with radiation cooling to outboard components, to limit the maximum temperatures and thermal gradients in the CS Casing to protect the CS coils and O-rings joints. Output of the thermal analysis were used in a first cut thermal stress analysis of the graphite tiles. The impact of anticipated Lithium Coating on ratcheted temperatures was also investigated.

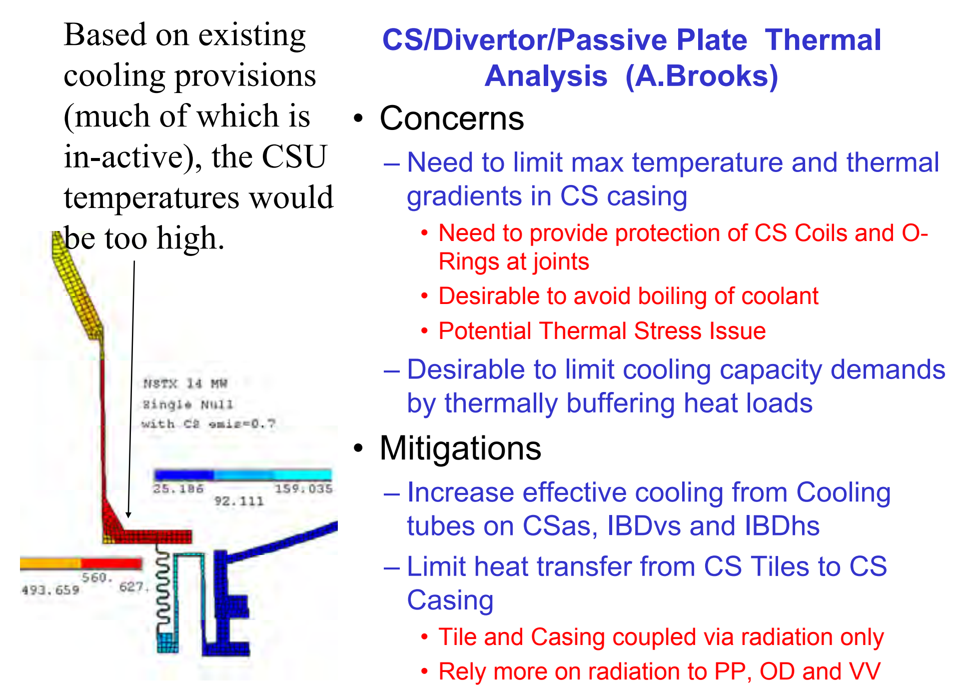

Figure 1.1,1-1 Heat Balance Summary Slide from the CDR

Results of the analysis were used to guide the design. In particular, it was found advantageous to thermally isolate as much as possible the CS tiles from the CS casing to limit the thermal ratcheting of the casing and thermal gradients with the actively cooled inboard divertor region. This does lead to higher temperatures in the graphite (in excess of 2000 C) which needs to be assessed by the project as to whether the increased carbon sublimation can be tolerated or if alternate materials (i.e. molybdenum) should be considered.

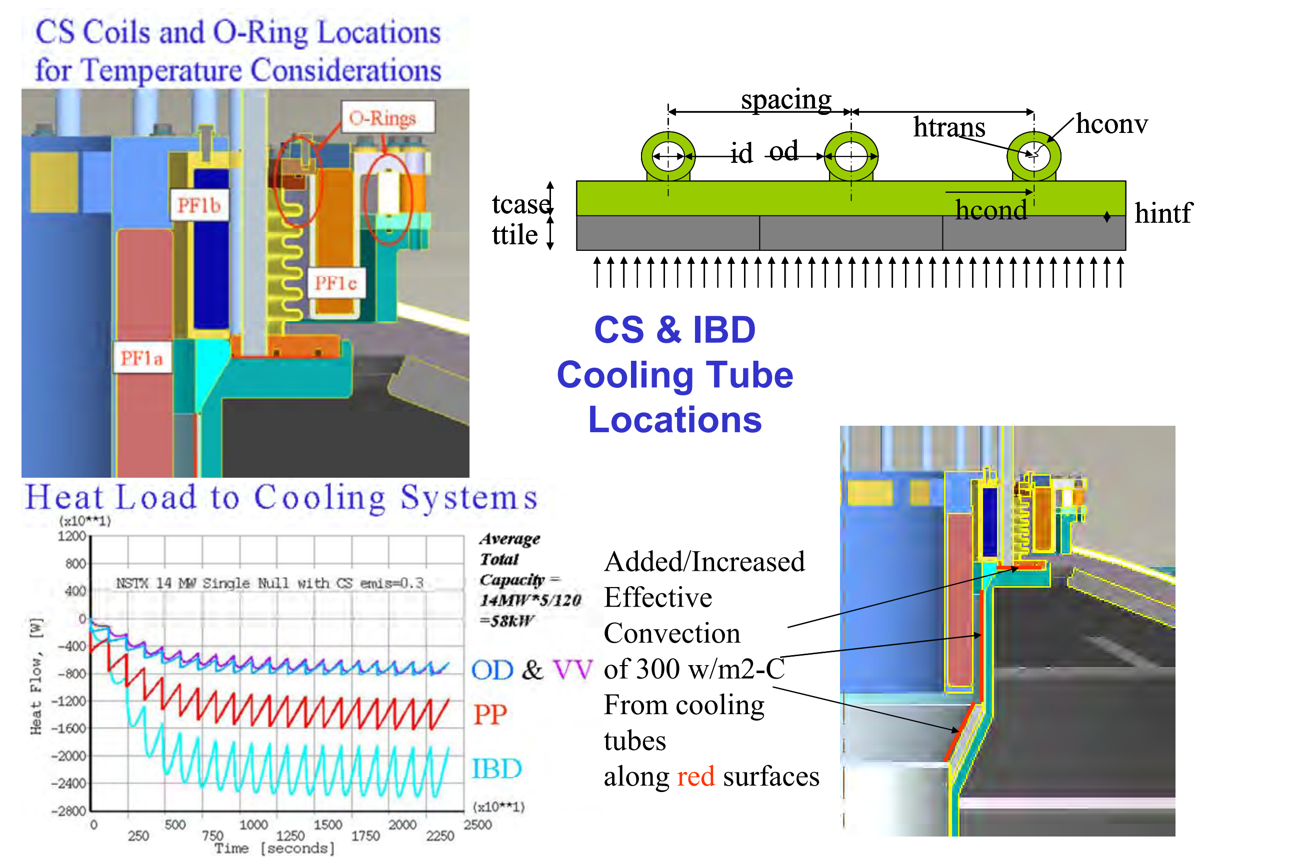

Figure 1.1,1-2 Heat Balance Summary Slide – Critical Areas Requiring Cooling

Tile Stress Analysis

The initial thermal stress analysis the inboard divertor tile assuming ATJ graphite at those temperatures appear marginally adequate. Efforts to increase margin by considering CFC's or by better characterizing the ATJ thermal-stress properties at temperature are needed.

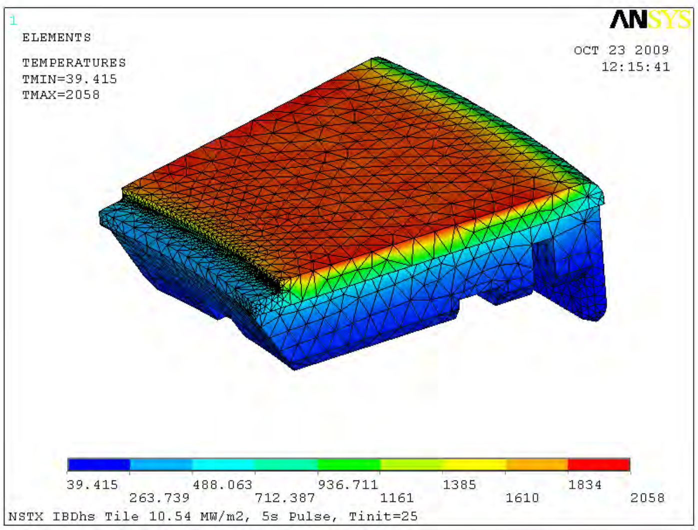

End of First Pulse Temperature Distribution

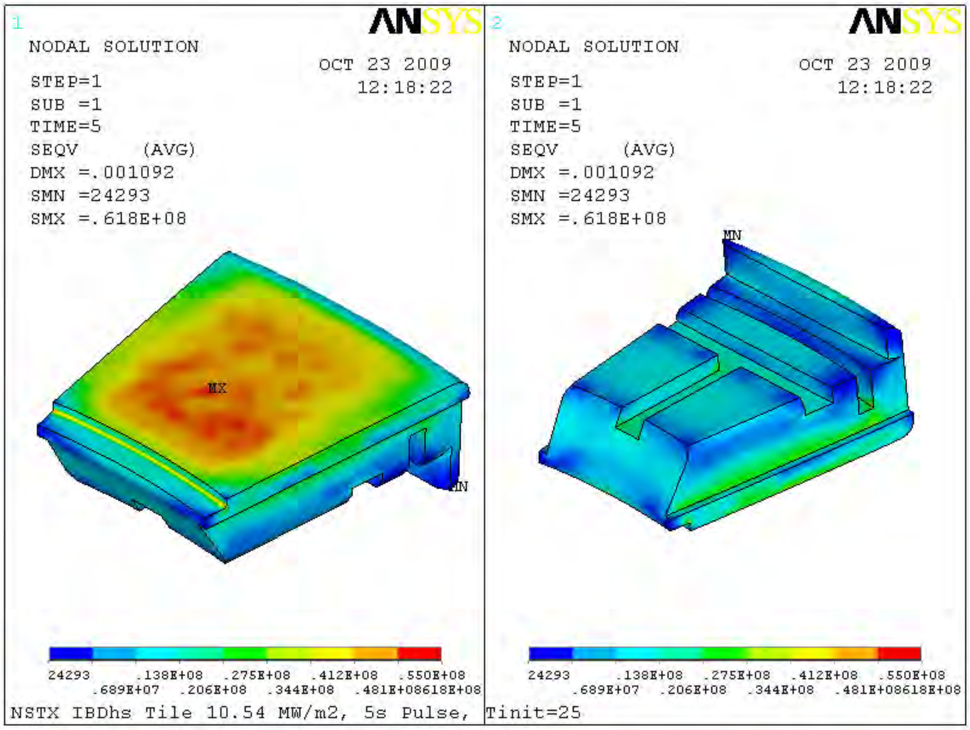

Tile Stress Results Summary

	Inboard Divertor Horizontal Section Tile		
	Thermal and Structural Response Summary		
		Max	Min
1st Pulse	Temp, C	2058	39
	Sx, Mpa	9.5	-51.7
	Sy	20.9	-64.0
	Sz	15.6	-63.7
	Sxy	13.3	-13.5
	Syz	13.6	-13.5
	Sxz	18.2	29.6
	Seqv	61.8	0.0
		Max	Min
Last Pulse	Temp, C	2516	623
	Sx, Mpa	11.1	-60.2
	Sy	25.0	-71.8
	Sz	20.0	-72.4
	Sxy	15.8	-16.0
	Syz	15.7	-15.6
	Sxz	21.8	-35.4
	Seqv	72.2	0.0
	Note: y is normal to tile, z is radial, x is toroidal		

No Data on Shear Stress Limit

	Ten Str. (//)	Comp. Str.
units	MPa	MPa
GraphTech ATJ Graphite	26	66
CGW Iso Graphite	31.4	77.5
CGC Iso Graphite	34.3	86.3

RT Tensile and Compressive Strength Values From Kelsey Tresemer

Flexural Strength vs T (below) suggests Graphite gets stronger at higher T

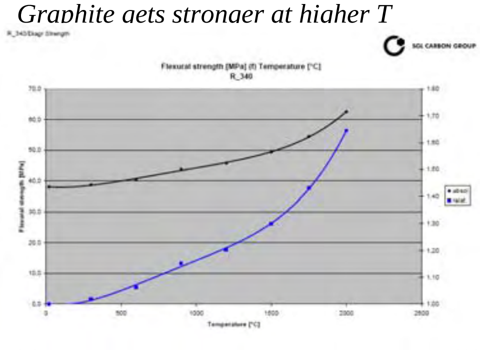

1.1.1. **Disruption Analysis, Passive Plate Disruption Stress**

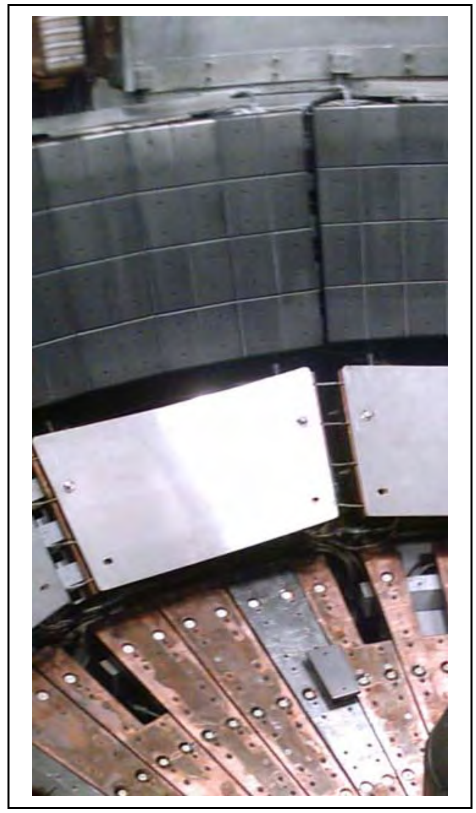

The objective of this analysis is to estimate the stresses in the vacuum vessel and passive plates caused by the plasma disruption. The Vector Potential solution for a 2D axisymmetric simulation of disruption in OPERA is imposed on the 3-D model in ANSYS to obtain the eddy currents and Lorentz forces. A static and dynamic stress pass is then run and the stresses are computed. Only the outboard diverter disruption scenario is discussed in this report.

The solid models of the vessel, umbrella structure, port extensions and support legs are imported from Pro-E. The model retains all the complex 3-D geometry but the port extensions, legs and the vessel are merged together to form one solid. The umbrella structure is a separate solid. This model is meshed with 8 node bricks in workbench and the mesh is carried into ANSYS classic. To get around the DOF compatibility issues, the mesh is rebuilt in ANSYS classic, retaining the number of nodes and elements and the connectivity. A vector potential gradient is then applied on this model to see if the model works. Eddy currents and Lorentz forces obtained agreed with intuition. An approximate model of the passive plates, in agreement with the 2-D model used in OPERA, is modeled in ANSYS. This is tied to the vessel using constraint equations. The degree of freedom coupled is Volt during the E-mag run and Displacement during the structural run.

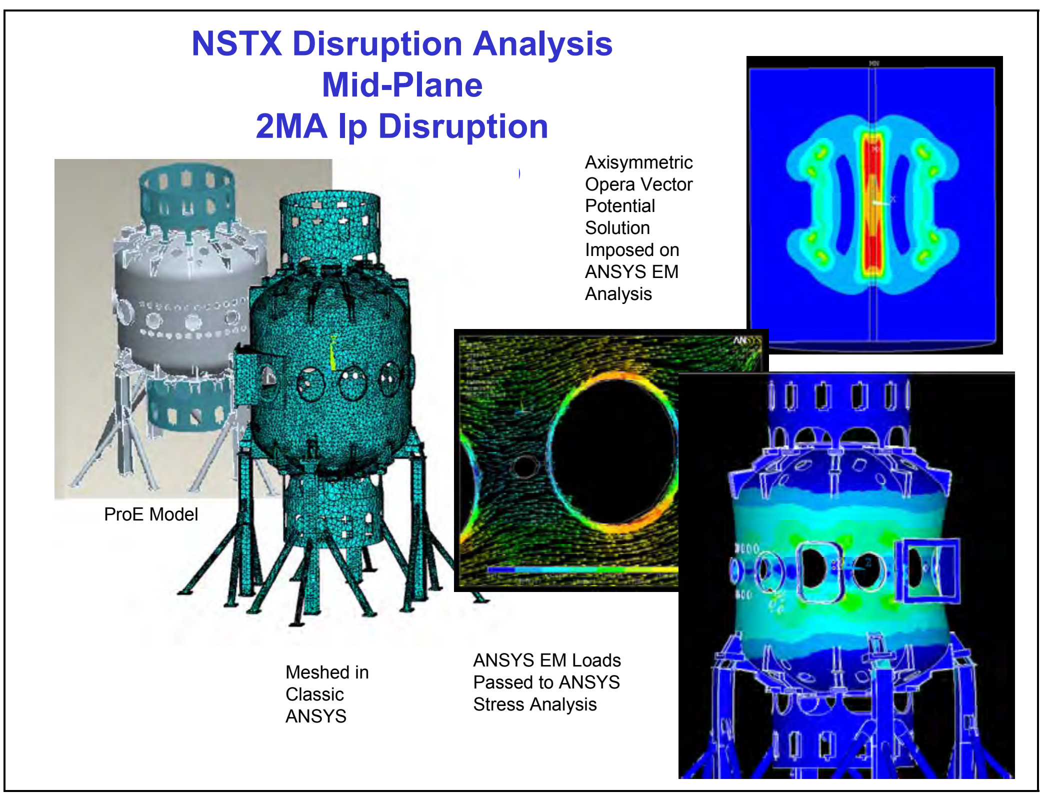

The analysis uses a vector potential solution. Grad A is B:

$$\mathbf{B} = \nabla \times \mathbf{A}.$$

Vector potentials obtained from OPERA are arranged in 80x80 tabular form so that they can be fed into ANSYS. The first 11 tables are considered for the study and these tables are spaced 0.5 ms apart. Macros are developed that read these values into ANSYS. The meshes in OPERA and ANSYS are dissimilar, but since ANSYS interpolates the tables between two adjacent indices, proper indexing of the coordinates yields a reasonable approximation of the Vector Potentials. The element type used was SOLID 97 and the material properties used are that of Stainless Steel except for the passive plates which are made up of Copper. This model is then solved for eddy currents and Lorentz forces..

The model is then converted into a structural model by switching the SOLID 97s into SOLID 45s. 11 load steps, 5ms apart are written for the stress pass. Forces are read from the earlier E-mag results fie using LDREAD command and both the Static and Dynamic analyses are performed. A 0.5% damping factor is used in the dynamic run.

The maximum stress obtained during the static analysis (ignoring the sharp corners) is 1600 Mpa and that from the dynamic analysis is 290 Mpa. Four nodes are picked in the model to compute the DLFs and the stresses seem to have reduced by a factor of 0.18-0.23.

The method employed uses the vector potential solution from an axisymmetric OPERA run and applies it to a mode complex model of the vessel and passive plates. In order to ensure the solution is in geometric registration with the passive plates, the coordinates that were used in the OPERA analysis were used to generate the passive plate mesh.

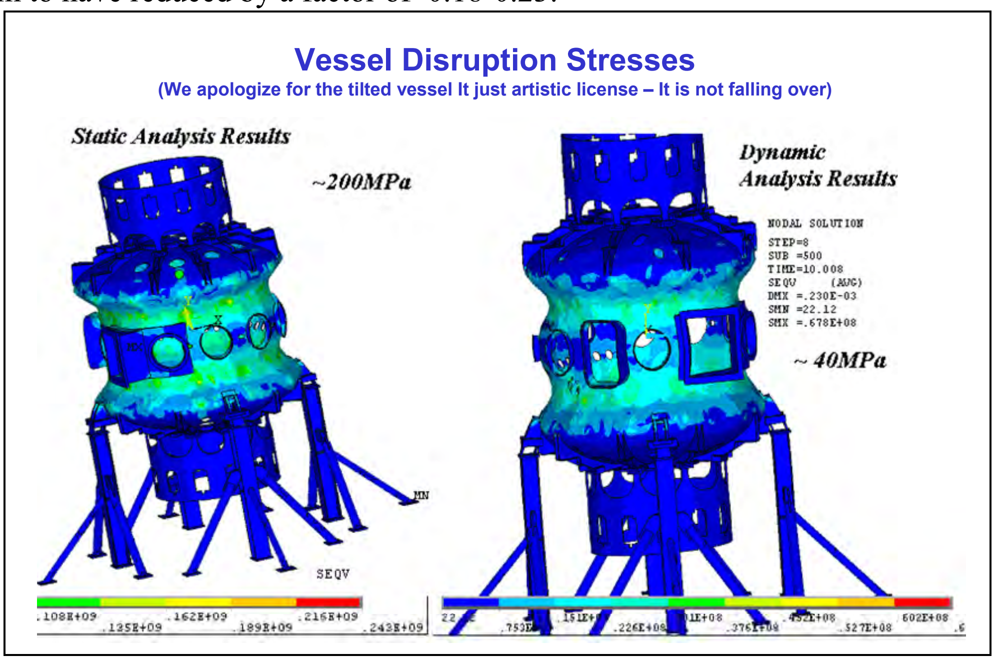

- The Dynamic Load Factors are found to less than 0.25
- The stresses are under acceptable limit.
- Macros developed here have been used for other models to simulate disruption stresses.
- This method (of imposing Vector Potentials) circumvents the modeling of air and other complexities involving complex 3-D geometry.
- The disruption scenario studied here is just the Outboard Diverter disruption. The other two scenarios : Primary Passive Plate and Secondary Passive Plate will be studied.
- All the high stress modes of vibration might not have been picked up by the dynamic analysis because of memory limitations of PC
- CAD model of the Passive Plates is yet to be obtained and integrated into the model

Primary Passive Plate Coordinates
X=1.3600 Y=1.0056
X=1.5092 Y=0.5530
X=1.5213 Y=0.5569
X=1.3720 Y=1.0095
Secondary Passive Plate
X=1.0640 Y=1.4447
X=1.3399 Y=1.0543
X=1.3503 Y=1.0617
X=1.0744 Y=1.4520
Outboard Divertor
x=0.6208 y=1.6390
x=1.2056 y=1.4092
x=1.2149 y=1.4185
x=0.6301 y=1.6483

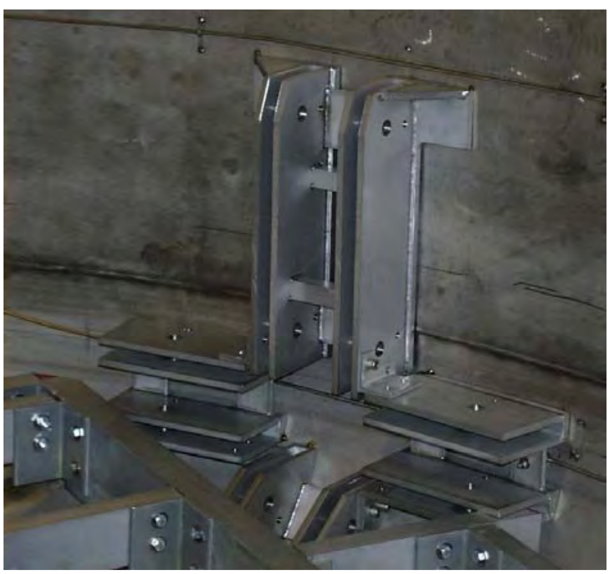

Photo of Passive Plate Attachment Details. As of November 9 the ProE model of the mounting hardware is available

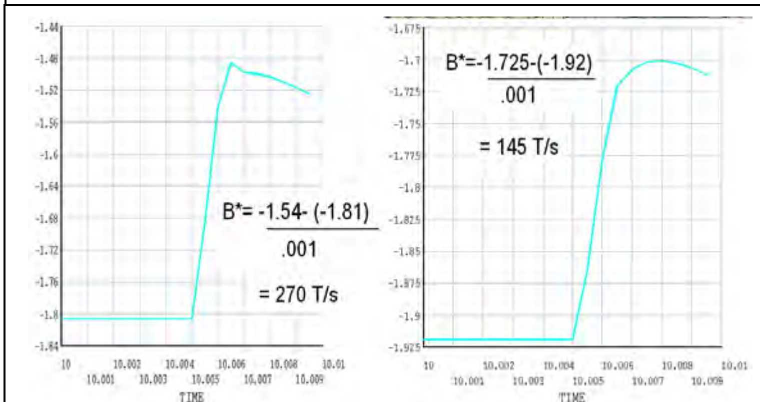

As a cross check of the results, The vertical Bdot in the outer area of the vessel near the mid plane was compared with the results reported for the High Harmonic Fast Wave (HHFW) discussed in section 2.1. The passive plate analysis yielded a vertical field transient or Bdot of 250 T/sec and the HHFW analyses yielded 280 Tesla/sec. Both were for 2Megamp 1millisecond disruptions. The HHFW analysis was for a simple linear rampdown in plasma current. The passive plate analysis is for a more complex simulation of a the disruption at the divertor distuption.

Results of the passive plate analysis show no significant non-cyclic symmetry resulting from the distribution of differing ports at the equatorial plane. The current plan is to perform a detailed analysis of only a 60 degree sector of the vessel, divertor, and passive plates to allow an adequately detailed modeling of the actual mounting hardware. .

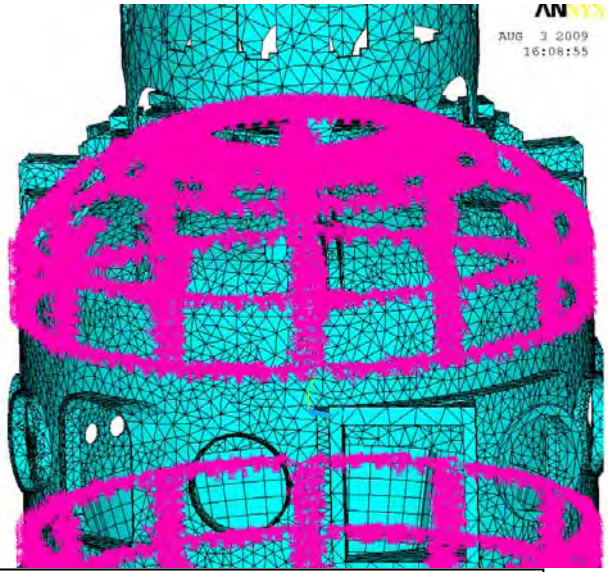

Constraint Equations that stitch the passive plate structure to the vessel. These were created with the CEINTF command

1.2 Vacuum Vessel & Support Structure

The vacuum vessel is a major component in many individual analyses because it is the major support structure for most of the outboard components of NSTX. The vessel supports the passive plates for which disruption loads are the major loading. The vessel participates in the electromagnetic response to the disruption, and is included in the disruption analysis discussed in section ___. The vessel provides in-plane support of the TF outer legs at the umbrella structure. The vessel also provides the support for OOP loads on the TF outer legs via connections through tangential radius rods just above the upper and below the lower head intersection with the cylindrical part of the shell. The vessel is included in the analysis of the TF outer legs. The global model includes a model of the vessel and attempts to bring all the loading together and addresses bake-out, operating temperatures and Lorentz Loads

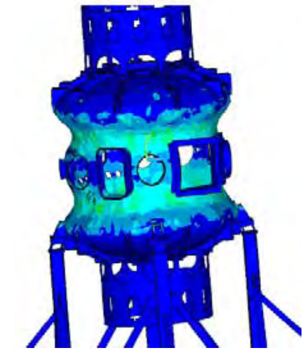

Vessel Respose to a disruption discussed in section ___

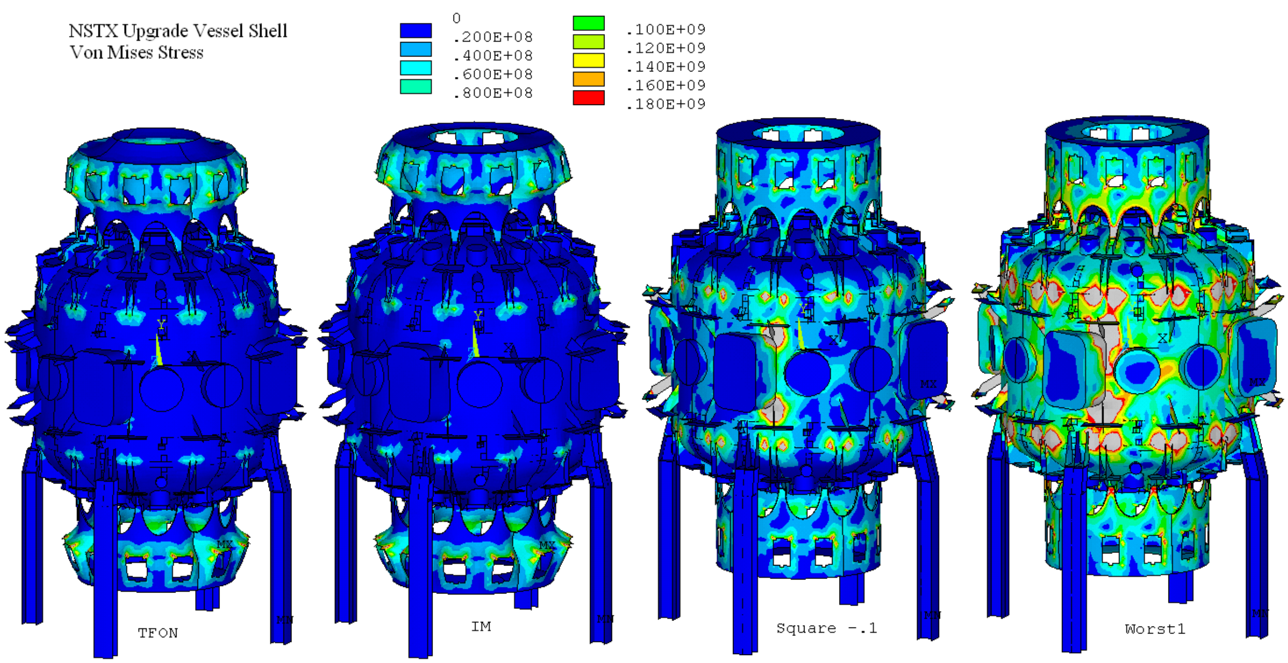

Global model results

1.2.3.1 Vessel Outer Leg Connection

The main beam gusset plates are 1.5 inches thick . Visually scaling the welds, they are about 2 inches long and maybe 3/8 fillets.
Joe indicate that the weld seem to about 3/8", definitely less than ½ " and more than ¼ ".
He will measure to confirm.
I will ask Jim about the drawings instructions.

There are 3 on each outside edge and 3 inside- maybe more on the underside

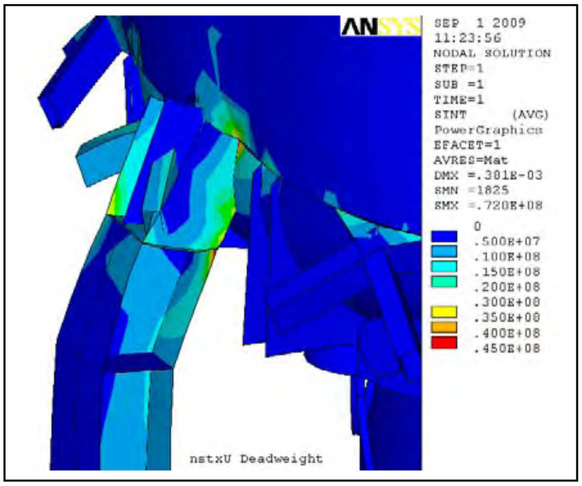

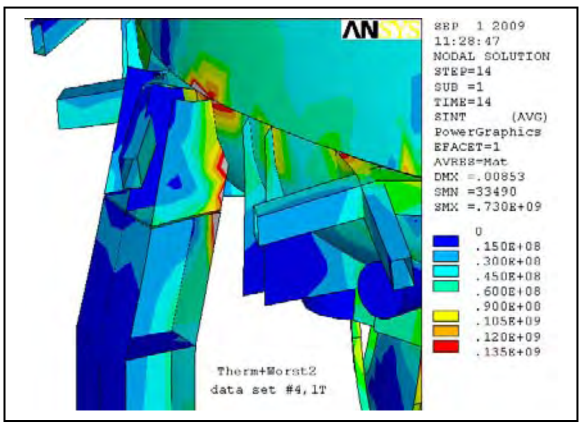

Figure 1.2.3.1-2

1.2.3.2 Upper Diaphragm/Cover/Flex

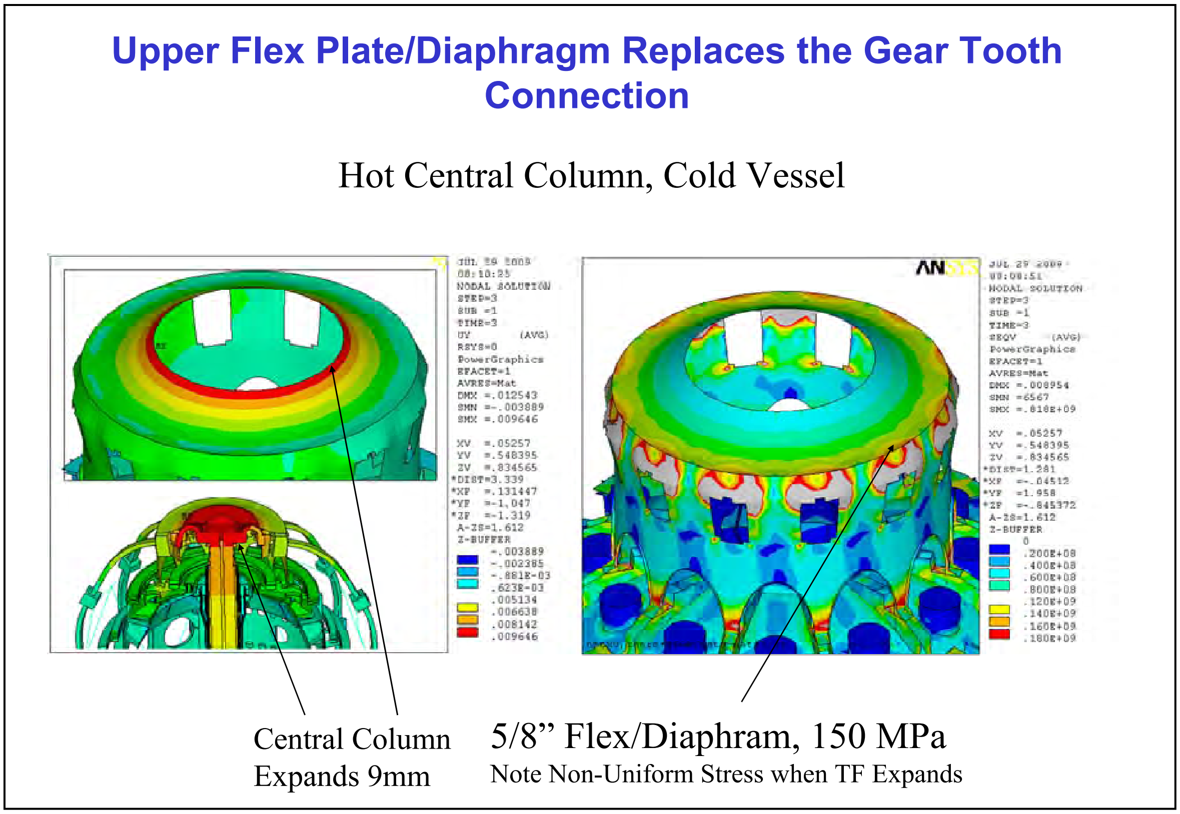

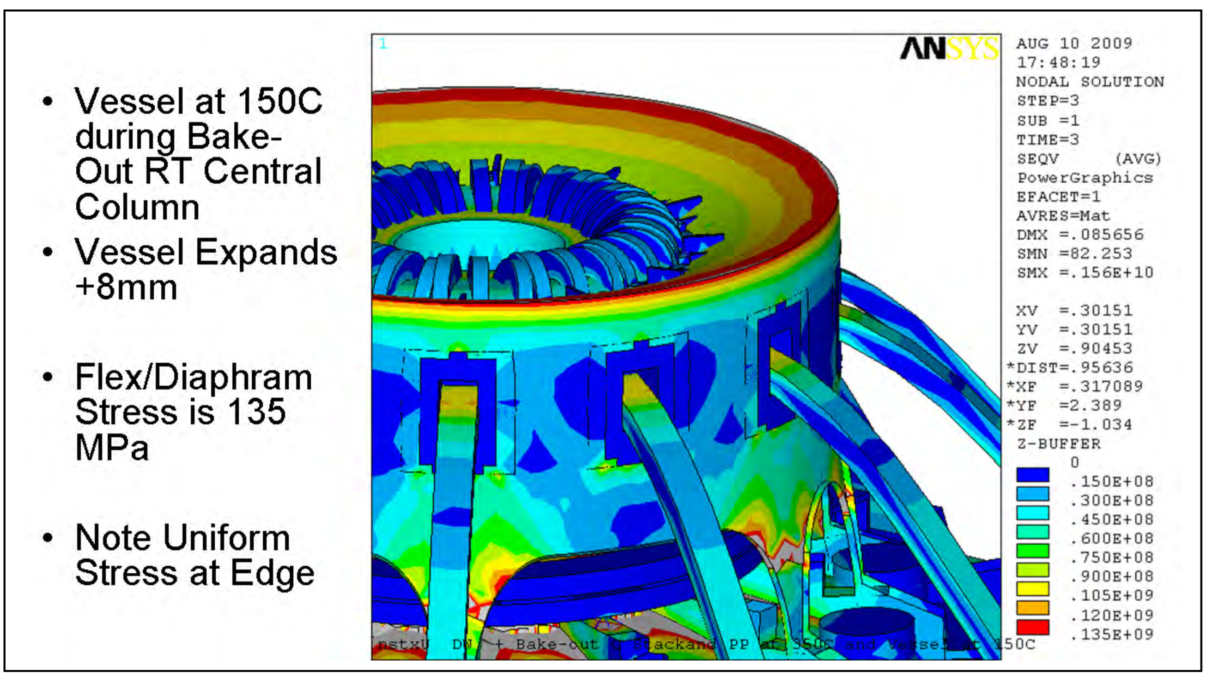

1.2.3.3 Umbrella Structure

The Umbrella structure appears in a number of models. The figures shown here are from an early analysis of the TF outer leg loads on the aluminum block and bolting. The conclusion of this analysis is that there are some modest reinforcements needed to improve the capacity of the aluminum block bolting to take the TF tension. Loads were applied on the bolt hole locations in the umbrella structure. Out-of plane were applied as shear loads. Further analysis of the umbrella loads are presented in section 1.3.2.2

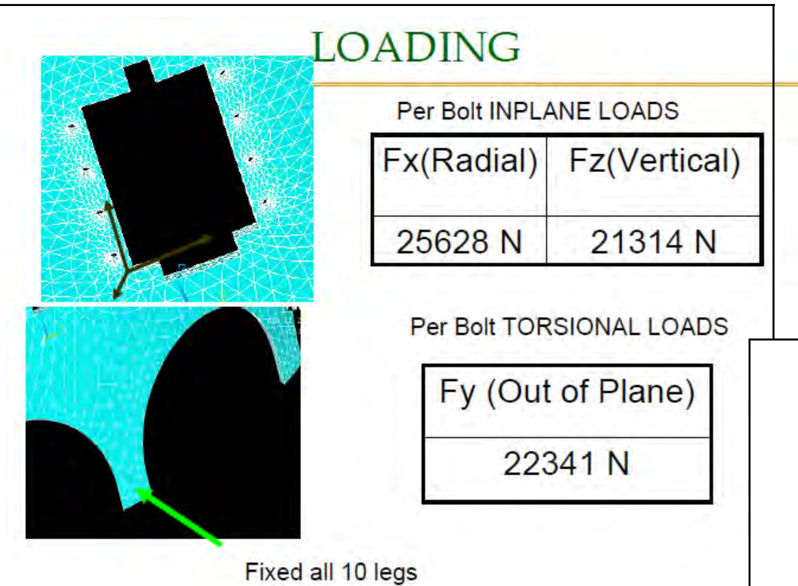

Figure 1.3.3.3-1 Umbrella Structure Loading

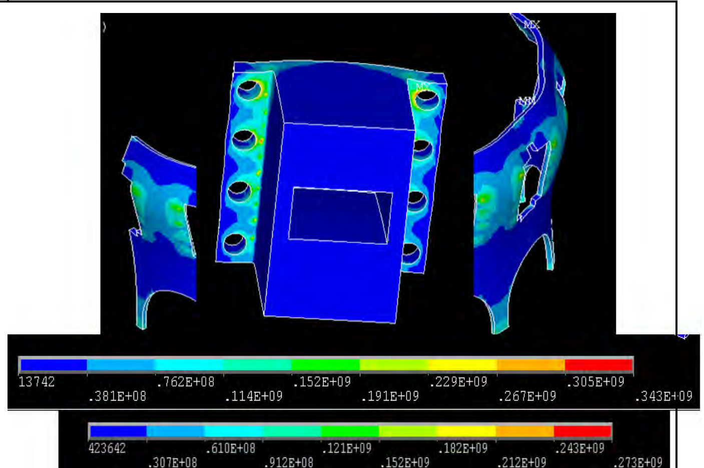

Figure 1.3.3.3-2 Aluminum Block Analysis Results

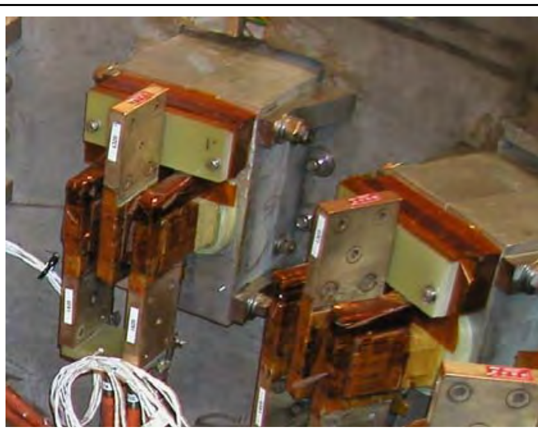

Figure 1.3.3.3-3 View Inside Umbrella Structure. Plates will be added to distribute bolt loads into the shell more effectively

Figure 1.3.3.3-41View from Outside the Umbrella Structuree

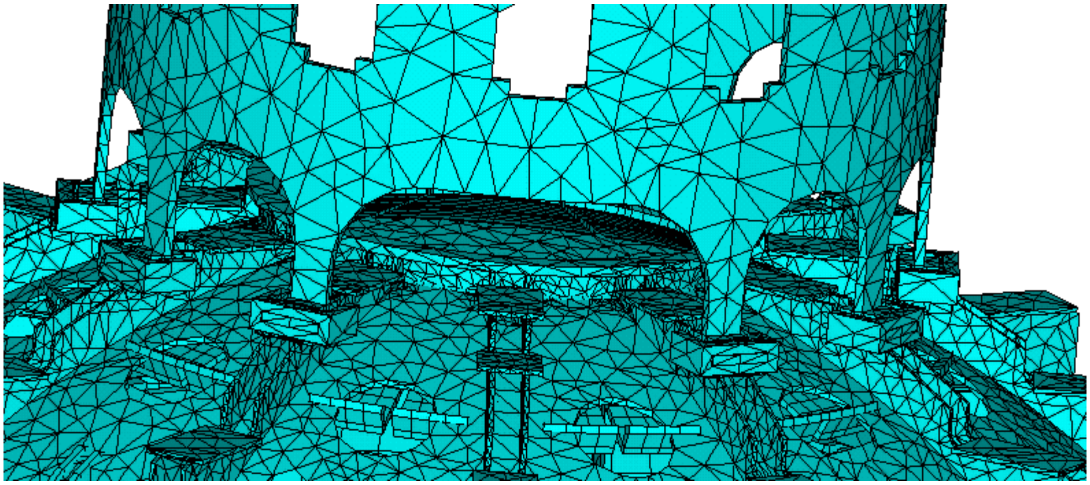

1.3.3.3-4 FEA model of the umbrella structure showing large span arch

.

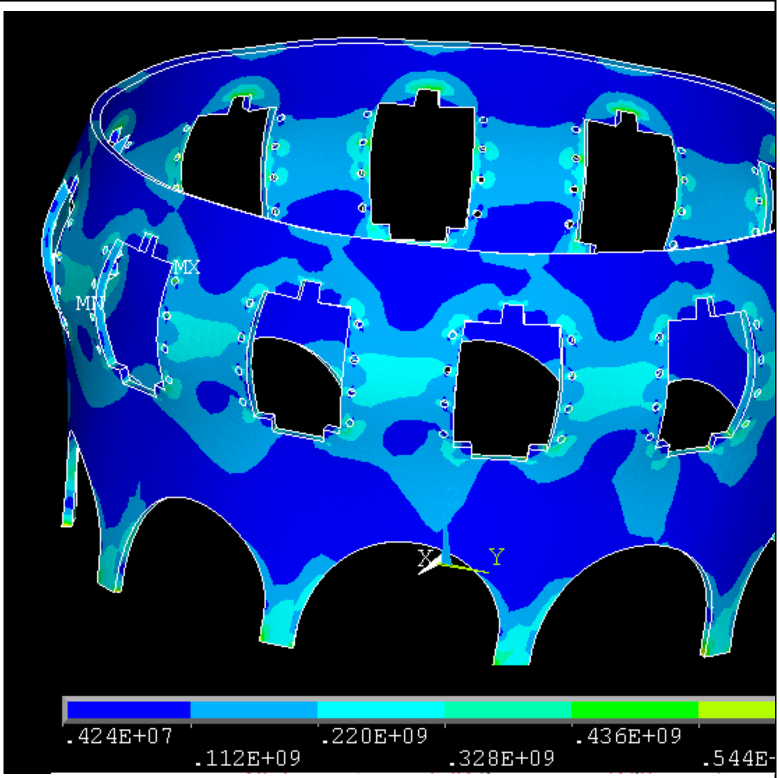

1.3.3.3-5 Umbrella Structure response to In-Plane Loads from the TF outer legs

1.2.3.4 Center Stack Casing

There are a number of concerns to address in the design of the centerstack casing. It supports the inner PF's – PF1a, and b. This is discussed in Section 1.3.3.3 . It supports the plasma facing components – tiles and backing plates for the central column and for the inner upper and lower divertor. Consequently it is exposed to the heat loads from these components. Current is run vertically through the casing to heat it during bake-out to 350 degrees C. Operationally, early estimates were that the casing could go to 500C or higher. This posed a problem for the support of the inner PF coils and local stresses in the and the halo current loads Figure 1.2.3.4.0-1 shows the upper end of the casing showing PF1a,and B, and PF1c which sit on the outboard side of the bellows and is supported by the vessel

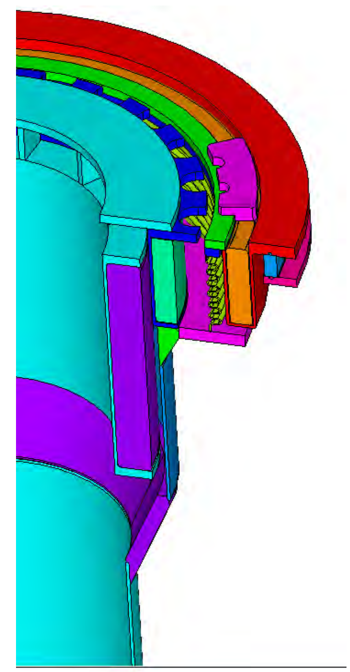

Figure 1.2.3.4.0-1 Centerstack Casing

1.2.3.4.1 Centerstack Casing Thermal Loads

Heat balance calculations in Section 1.1.1.1 quantify the temperatures that result from plasma

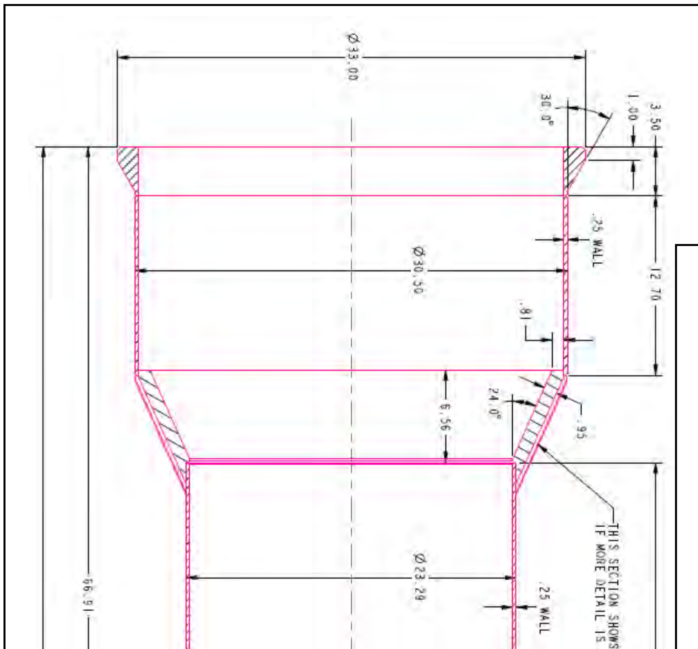

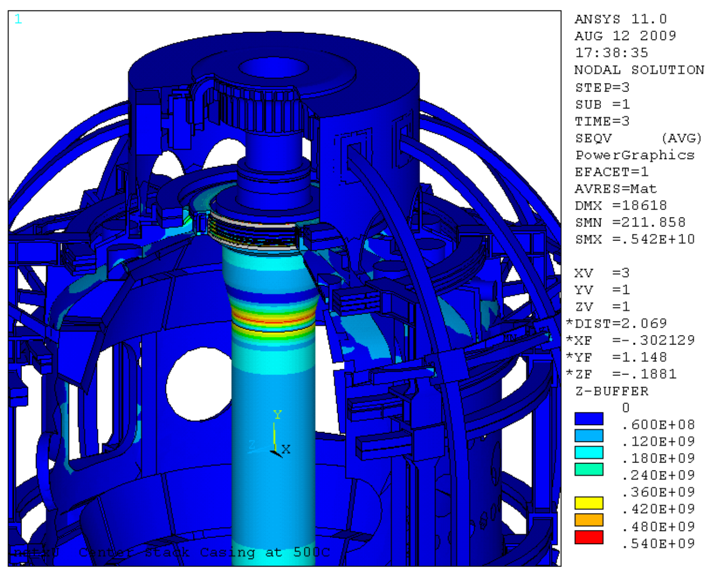

Figure 8.12-1 Casing Stress Estimate with the Case at 500C peak operating temperature, and the PF Support area maintained at 100C

1.2.3.4.2 Centerstack Casing Halo Loads

From the NSTX_CSU-RQMT-GRD rev. 0 10 March 30, 2009**:**

"A peak poloidal halo current up to 10% of the maximum plasma current prior to the disruption, with a toroidal peaking factor of 2:1; that is, the toroidal dependence of the halo current is $[1 + \cos(\phi - \phi_0)]$, for all toroidal phase angles ϕ_0 from 0 to $2*\pi$. Halo current entry/exit locations shall assume a separation of 1.0m with vertical displacement + or - 0.25m about the midplane
Location of Disrupting Plasmas & Halo Current Entry/Exit Points
Current and field directions (referring to Figure 2.2-2) shall be as follows:

- Plasma current Ip into the page (counter-clockwise in the toroidal direction,
viewed from above)
- Halo current exits plasma and enters the structure at the entry point, exits the structure and re-enters the plasma at the exit point (counter-clockwise poloidal current, in the view of the figure)
- Toroidal field into the page (clockwise in the toroidal direction, viewed from above)

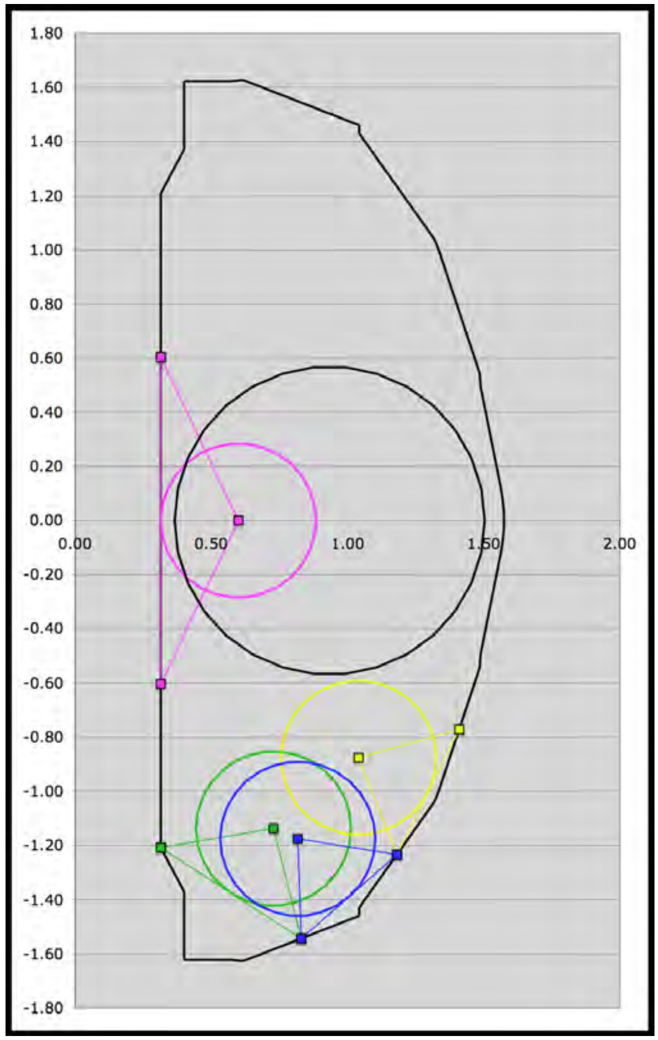

GRD Figure 2.2-2

Disruption and Halo Current Analysis Procedure and Results

Halo current [MA]	n.a	20%=	35%=	35%=	35%=
		400kA	700kA	700kA	700kA
Halo current entry point (r,z) [m]	n.a	0.3148	0.3148	0.8302	1.1813
		0.6041	-1.2081	-1.5441	-1.2348
Halo current exit point (r,z) [m]	n.a	0.3148	0.8302	1.1813	1.4105
		-0.6041	-1.5441	-1.2348	-0.7713

Sri Avasarala and Ron Hatcher's disruption analyses were used to provide a vector potential "environment" for a model of the center stack casing. Sri has developed a procedure which starts with Ron Hatcher's OPERA disruption simulation, and transfers the axisymmetric vector potential results into a 3 D model of the vessel and passive plates. With modest changes any of the internal components can be evaluated with this procedure. A model of the center stack casing was input to Sri's electromagnetic analysis. The results are shown in Figures 1 and 2

Lorentz loads from these current entry and exit points were calculated assuming a peaking factor of 2. At present, only the equatorial plane halo current distribution has been evaluated. The acceptability of the results depends on the Dynamic Load Factor. Static str4uctural analysis produces unacceptable results. Dynamic analysis produced manageable results, with further evaluation of the net loads action on the support legs and bellow, needing qualification.

INCONEL 625

Test Temperature, °F(°C)	Ultimate Tensile Strength, ksi (MPa)	Yield Strength at 0.2% offset,ksi (MPa)	Elongation in 2" percent
Room	138.8 (957)	72.0 (496)	38
200	133.3 (919)	67.3 (464)	41
400	129.4 (892)	62.2 (429)	44
600	125.6 (866)	59.5 (410)	45
800	122.2 (843)	59.2 (408)	45
1000	119.9 (827)	58.8 (405)	46
1200	119.6 (825)	57.0 (393)	47

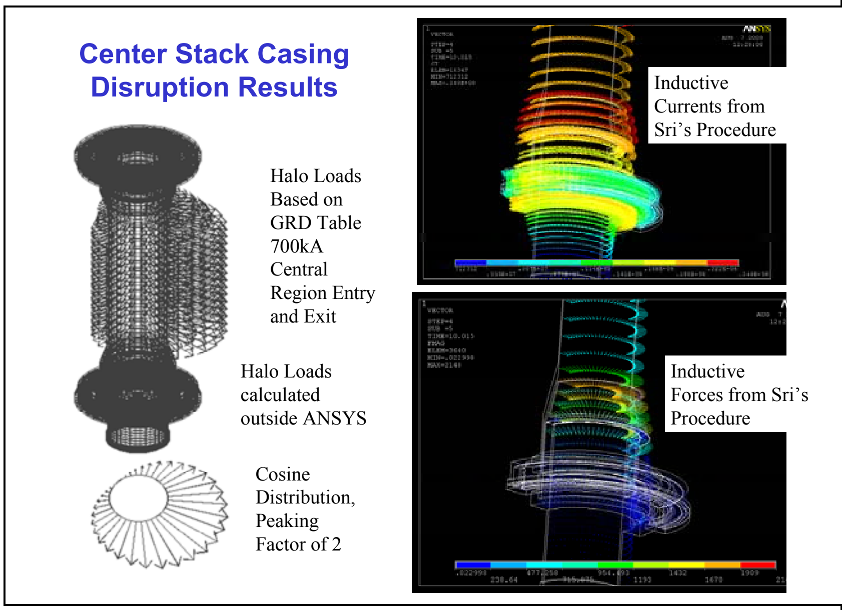

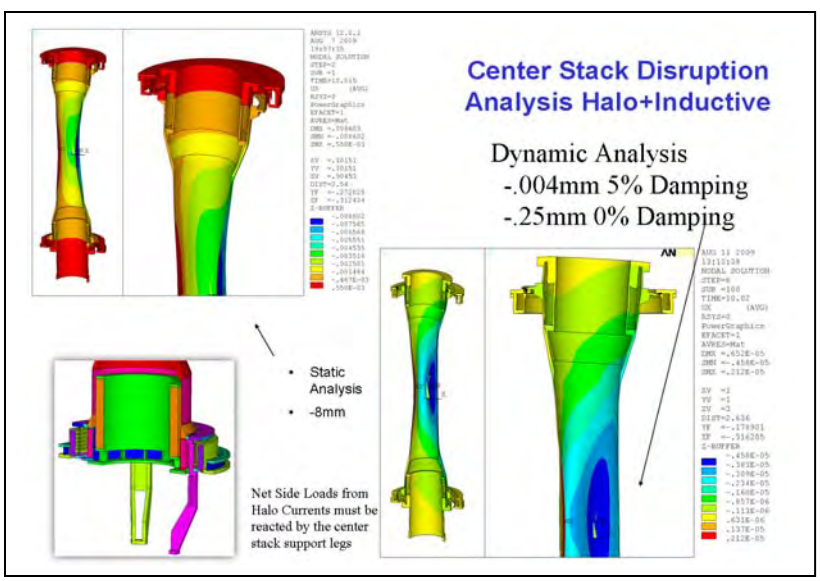

1.3 Magnet Systems

1.3.1.1 Coil Builds

The latest coil builds are included inn the design point spreadsheet available on the NSTX engineering website. The builds tabulated here are from an early equilibrium flexibility based on “squareness” that was published by J. Menard. These builds were used in the global model described in section 1.0.0

Coil Builds
#33 is the Plasma

#			r	z	dr	dz	nx	nz
1	CS		.2344	.0021	.01	4.3419	2	20
2	CS		.2461	.0067	.01	4.2803	2	20
3	CS		.2577	.0022	.01	4.2538	2	20
4	CS		.2693	-.0021	.01	4.1745	2	20
5	PF1aU	28	.3239	1.5906	.0413	.3265	4	4
6	PF1bU	10	.4142	1.8252	.042	.1206	4	4
7	PF1cU	10	.56	1.8252	.042	.1206	4	4
8	PF2U	14	.7992	1.8526	.1627	.068	4	4
9	PF2U	14	.7992	1.9335	.1627	.068	4	4
10	PF3U	7	1.4829	1.5696	.1631	.034	4	4
11	PF3U	8	1.4945	1.5356	.1864	.034	4	4
12	PF3U	7	1.4829	1.6505	.1631	.034	4	4
13	PF3U	8	1.4945	1.6165	.1864	.034	4	4
14	PF4U		1.795	.8711	.0922	.034	4	4
15	PF4U		1.8065	.9051	.1153	.034	4	4
16	PF4U		1.7946	.8072	.0915	.068	4	4
17	PF4L		1.795	-.8711	.0922	.034	4	4
18	PF4L		1.8065	-.9051	.1153	.034	4	4
19	Pf4L		1.7946	-.8072	.0915	.068	4	4
20	PF5U	12	2.0118	.6489	.1359	.0685	4	4
21	PF5U	12	2.0118	.5751	.1359	.0685	4	4
22	PF5L	12	2.0118	-.6489	.1359	.0685	4	4
23	PF5L	12	2.0118	-.5751	.1359	.0685	4	4
24	PF3L	7	1.4829	-1.5696	.1631	.034	4	4
25	PF3L	8	1.4945	-1.5356	.1864	.034	4	4
26	PF3L	7	1.4829	-1.6505	.1631	.034	4	4
27	PF3L	8	1.4945	-1.6165	.1864	.034	4	4
28	PF2L	14	.7992	-1.8526	.1627	.068	4	4
29	PF2L	14	.7992	-1.9335	.1627	.068	4	4
30	PF1cL	10	.56	-1.8252	.042	.1206	4	4
31	PF1bL	10	.4142	-1.8252	.042	.1206	4	4
32	PF1aL	28	.3239	-1.5906	.0413	.3265	4	4
33	Ip		.9344	0	.5696	1	6	8

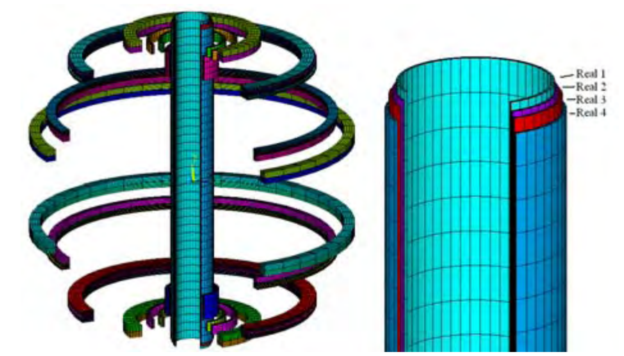

Figure 1.3.1.1-1 PF Coil s

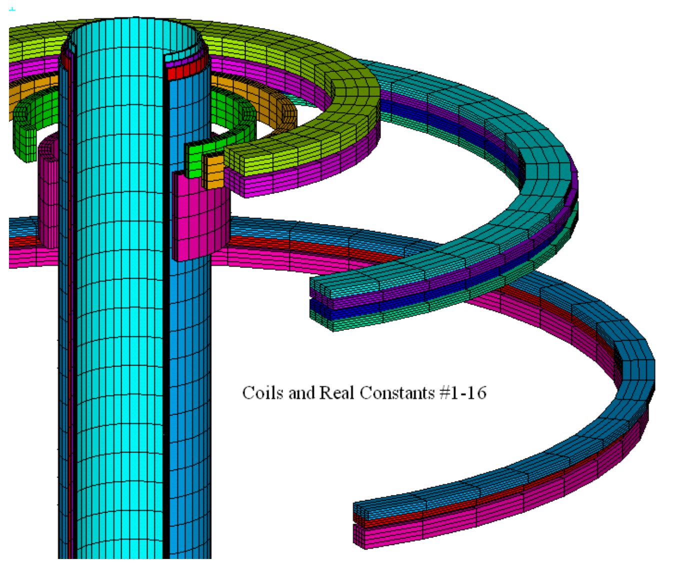

Figure 1.3.1.1-2 PF Coils

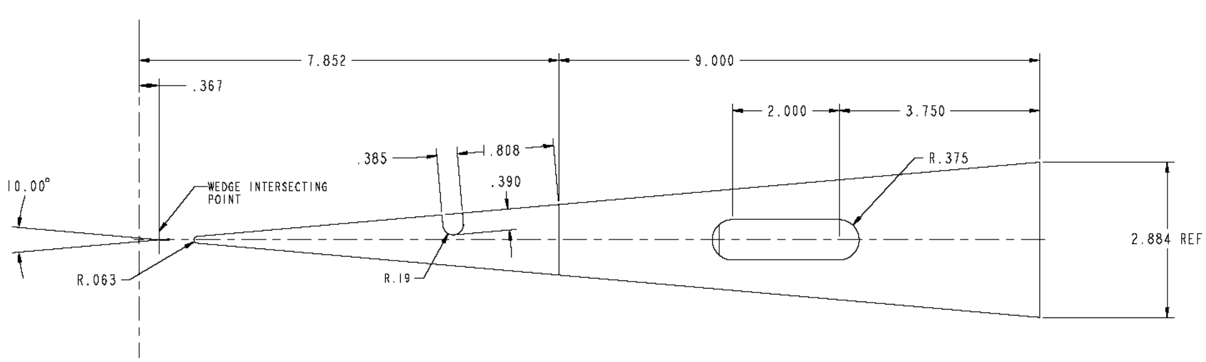

Figure 1.3.1.1-3 TF Build (Including Flag)

1.3.1.2 PF Currents

The latest design poiint on the NSTX engineering website includes 96 current scenarios. This table is included because it is consistent with the coil build table above.

PF Scenario Currents In Mat

Coil #	TFON	IM	-0.1	-0.05	0	0.05	0.1	Worst 1	Worst 2	Worst3	Worst4	Worst5
Step	2	3	4	5	6	7	8	9	10	11	12	13
	Nst1	Nst2	Nst3	Nst4	Nst5	Nst6	Nst7	Nsw3	Nsw4	Nsw5	Nsw6	Nsw7
1	0	5.88	.000	.000	.000	.000	.000	-5.88	5.88	5.88	-1.47	-1.47
2	0	5.808	.000	.000	.000	.000	.000	-5.808	5.808	5.808	-5.808	-1.452
3	0	5.76	.000	.000	.000	.000	.000	-5.76	5.76	5.76	-5.76	-1.92
4	0	5.664	.000	.000	.000	.000	.000	-5.664	5.664	5.664	-5.664	-1.416
5	0	0	7.172	7.196	7.234	7.348	7.452	0.784	0.784	0.784	0.784	0.784
6	0	0	-5.650	-4.763	-3.628	-2.331	-.946	0.12	0.12	0.12	0.12	0.12
7	0	0	-4.922	-4.014	-2.936	-1.755	-.517	0.2	0.2	0.2	0.2	0.2
8	0	0	4.484	4.307	3.941	3.401	2.772	0.168	0.168	0.168	0.168	0.168
9	0	0	4.484	4.307	3.941	3.401	2.772	0.168	0.168	0.168	0.168	0.168
10	0	0	-1.058	-1.426	-1.655	-1.720	-1.690	-0.112	-0.112	-0.112	-0.112	-0.112
11	0	0	-1.058	-1.426	-1.655	-1.720	-1.690	-0.128	-0.128	-0.128	-0.128	-0.128
12	0	0	-1.058	-1.426	-1.655	-1.720	-1.690	-0.112	-0.112	-0.112	-0.112	-0.112
13	0	0	-1.058	-1.426	-1.655	-1.720	-1.690	-0.128	-0.128	-0.128	-0.128	-0.128
14	0	0	-2.388	-1.183	-.206	.488	.923	-0.08	-0.08	-0.08	-0.08	-0.08
15	0	0	-2.388	-1.183	-.206	.488	.923	-0.1	-0.1	-0.1	-0.1	-0.1
16	0	0	-2.388	-1.183	-.206	.488	.923	-0.16	-0.16	-0.16	-0.16	-0.16
17	0	0	-2.388	-1.183	-.206	.488	.923	-0.08	-0.08	-0.08	-0.08	-0.08
18	0	0	-2.388	-1.183	-.206	.488	.923	-0.1	-0.1	-0.1	-0.1	-0.1
19	0	0	-2.388	-1.183	-.206	.488	.923	-0.16	-0.16	-0.16	-0.16	-0.16
20	0	0	-3.374	-4.340	-5.139	-5.771	-6.210	-0.384	-0.384	-0.384	-0.384	-0.384
21	0	0	-3.374	-4.340	-5.139	-5.771	-6.210	-0.384	-0.384	-0.384	-0.384	-0.384
22	0	0	-3.374	-4.340	-5.139	-5.771	-6.210	-0.384	-0.384	-0.384	-0.384	-0.384
23	0	0	-3.374	-4.340	-5.139	-5.771	-6.210	-0.384	-0.384	-0.384	-0.384	-0.384
24	0	0	-1.058	-1.426	-1.655	-1.720	-1.690	-0.112	-0.112	-0.112	-0.112	-0.112
25	0	0	-1.058	-1.426	-1.655	-1.720	-1.690	-0.128	-0.128	-0.128	-0.128	-0.128
26	0	0	-1.058	-1.426	-1.655	-1.720	-1.690	-0.112	-0.112	-0.112	-0.112	-0.112
27	0	0	-1.058	-1.426	-1.655	-1.720	-1.690	-0.128	-0.032	-0.128	-0.128	-0.128
28	0	0	4.484	4.307	3.941	3.401	2.772	0.168	0.168	0.168	0.168	0.168
29	0	0	4.484	4.307	3.941	3.401	2.772	0.168	0.168	0.168	0.168	0.168
30	0	0	-4.922	-4.014	-2.936	-1.755	-.517	0.2	0.2	0.2	0.2	0.2
31	0	0	-5.650	-4.763	-3.628	-2.331	-.946	0.12	0.12	0.12	0.12	0.12
32	0	0	7.172	7.196	7.234	7.348	7.452	0.784	0.784	0.784	0.784	0.784
33	0	0	2.000	2.000	2.000	2.000	2.000	2	2	2	2	2

1.3.1.3 Lorentz Force Plots – TF and TF+OH

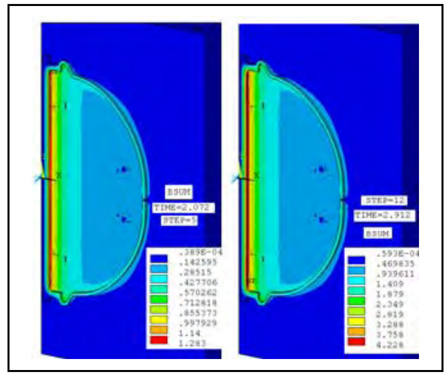

The peak toroidal field from the load files used in the global model is 4.9T. The peak field from the electromagnetic current diffusion model is 4.2T. They used different TF inner leg dimensions from different design point published throughout the CDR2009

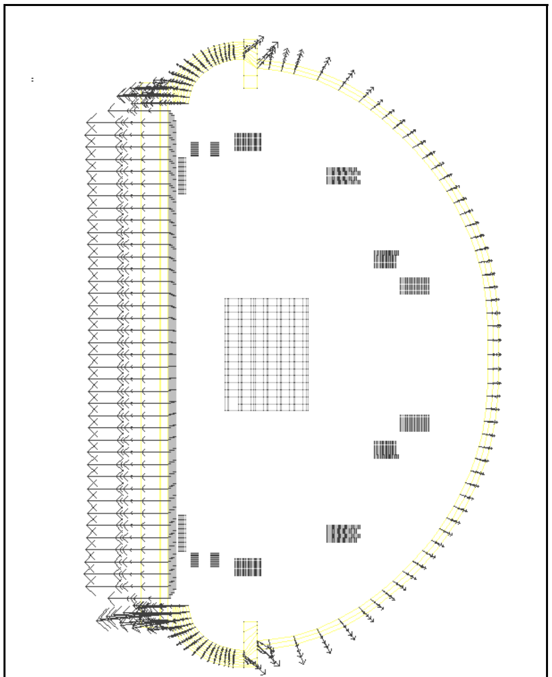

TFON

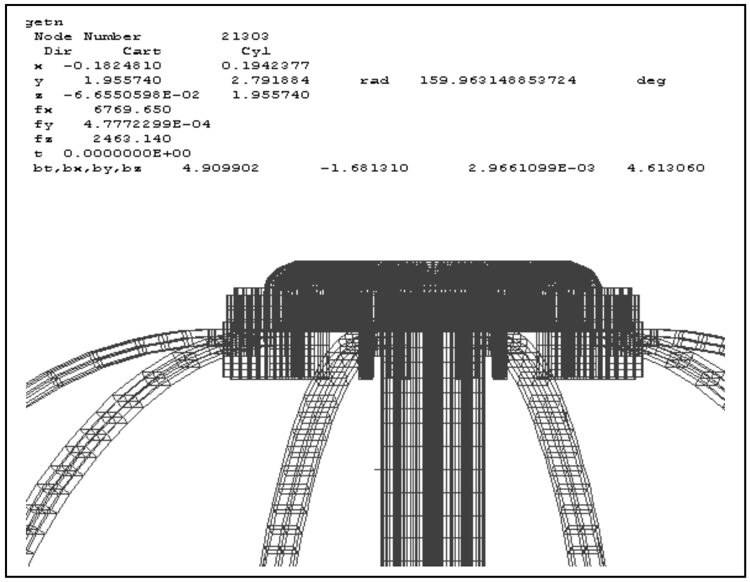

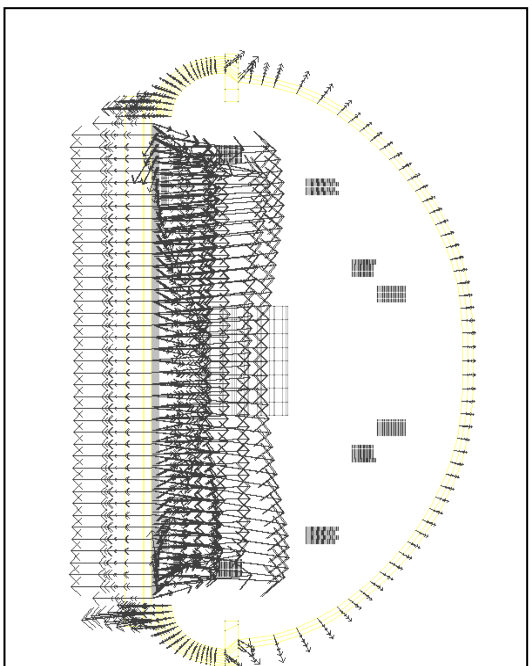

IM

```
TF Current Spec ( L/R decay )
*if,b_0,eq,3,then
!    NSTX Faulted Pulse
NumSteps=51
t1= .1   $ i1= 0
t2= .2   $ i2= 0
t3= 1.952   $ i3= 15690.906
t4= 2.072   $ i4= 38658.746
t5= 2.192   $ i5= 58169.054
t6= 2.312   $ i6= 74742.32
t7= 2.432   $ i7= 88820.681
t8= 2.552   $ i8= 100779.71
t9= 2.672   $ i9= 110938.46
t10= 2.792   $ i10= 119567.93
t11= 2.912   $ i11= 126898.33
t12= 3.032   $ i12= 129777.84
t13= 4.00   $ i13= 129777.84
t14= 5.00   $ i14= 129777.84
t15= 6.00   $ i15= 129777.84
t16= 7.00   $ i16= 129777.84
t17= 8.00   $ i17= 129777.84
t18= 9.512   $ i18= 129777.84
t19= 9.632   $ i19= 113132.22
t20= 9.752   $ i20= 98621.613
t21= 9.872   $ i21= 85972.17
t22= 9.992   $ i22= 74945.174
t23= 10.136   $ i23= 63563.326
t24= 10.256   $ i24= 55410.543
t25= 10.376   $ i25= 48303.454
```

```
t27= 10.616   $ i27= 36707.073
t28= 10.736   $ i28= 31998.937
t29= 10.856   $ i29= 27894.677
t30= 10.976   $ i30= 24316.839
t31= 11.096   $ i31= 21197.903
t32= 11.216   $ i32= 18479.01
t33= 11.336   $ i33= 16108.848
t34= 11.456   $ i34= 14042.689
t35= 11.576   $ i35= 12241.54
t36= 11.696   $ i36= 10671.411
t37= 11.816   $ i37= 9302.6701
t38= 11.936   $ i38= 8109.4875
t39= 12.056   $ i39= 7069.3453
t40= 12.176   $ i40= 6162.6142
t41= 12.296   $ i41= 5372.1826
t42= 12.416   $ i42= 4683.1337
t43= 12.536   $ i43= 4082.4638
t44= 12.656   $ i44= 3558.8372
t45= 12.776   $ i45= 3102.3723
t46= 12.896   $ i46= 2704.4546
t47= 13.016   $ i47= 2357.5748
t48= 15.0   $ i48= 1000
t49= 20.0   $ i49= 100
t50= 40.0   $ i50= 0.0
t51= 1000.0   $ i51= 0.0
*endif
```

1.3.2 Toroidal Field Coils

The TF inner leg is sized mainly based on the inertial cooling requiremnents and not on stress limits. At the equatorial plane, the stress is modest – only 40 to 50 Mpa. This provides a conservative stress in the copper including ample allowance for the cooling holes, but minimal wedge pressure to augment the shear capacity.

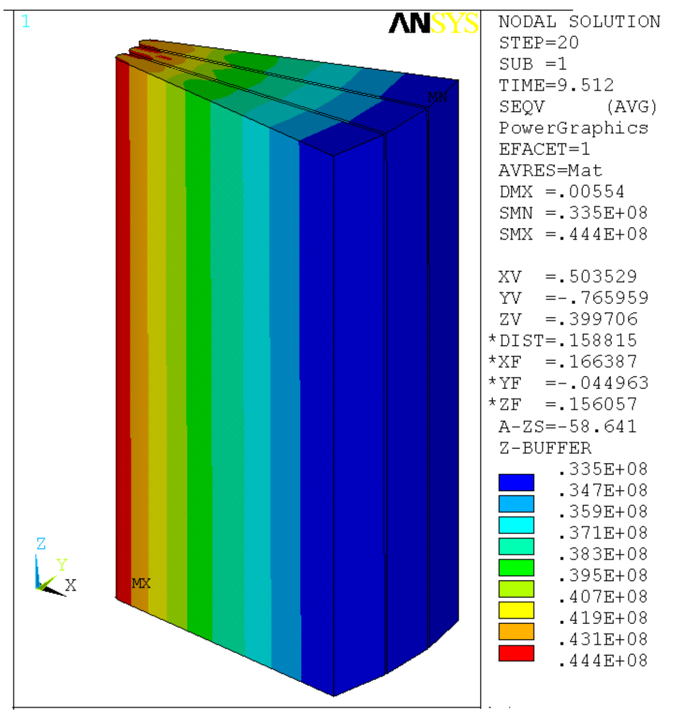

Figure 1.3.2-1 Results from the Electromagnetic-Thermal Model

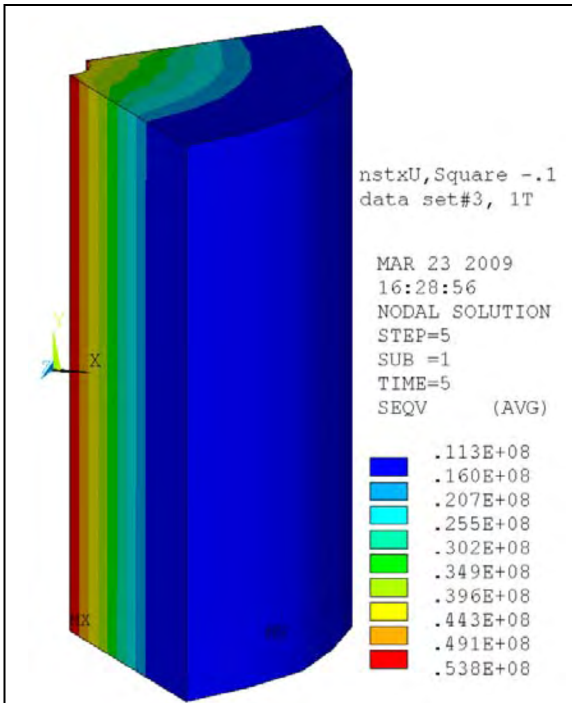

Figure 1.3.2-2 Results from the Global Analysis

1.3.2.1 Coupled Electromagnic-Thermal Analysis

The objective of this analysis is to calculate the temperature and stresses during TF coil ramp up, flat top and ramp down (Fig. 1). PF field is not considered. This analysis is based on the coupled field electromagnetic and thermal analysis for a simple model by P. Titus [1], [2].

The distribution of current in TF coil depends on the resistance, inductance and contact pressure in the contact area. Coil temperature reaches highest at the end of the pulse, i.e., 10.136s for normal operation. Maximal temperature is 117ºC, at the inner side of arch and inner TF leg. Comparing with C. Neumeyer's result (101 ºC temperature rise [3]) this analysis with current diffusion effect results in a little higher temperature. But within this temperature range, active cooling is not necessary. Max coil temperature is 47 ºC at the end of pulse. But the temperature at the end of the coil can reach 65 ºC because it connects to the arch which has higher temperature.

In this model, the arch is modeled by two solid pieces. But in reality, they are made of many straps. So the arches in this model have anisotropic material properties (mechanical properties are based on the local structure model results of T. Willard [4]), Current density, magnetic flux density and temperature from this analysis have been provided to T. Willard for his detailed simulation of the joint.

Using high strength copper (80% IACS) in the flag extension increases the temperature only by < 1ºC. Thus high strength copper can be used if required to increase the pressure of joint bolt insert over the capacity of pure copper.

The central beam has maximal hoop tension stress of 72.7MPa at 9.512s (i.e. the end of flat top) and 58.5MPa at 10.136s (i.e. the end of pulse), similar to Titus's result [2]. But there is another even higher hoop stress point of 95.5MPa at 9.512s, at the connection between central beam and flag, which is due to the L-shape connection part between the arch and TF outer leg.

Toroidal field contours have been provided for use in other calculations—in particular the background field in the antenna calculation.

Structure response at the joint has been included for comparison with more detailed modeling of the joint [4].

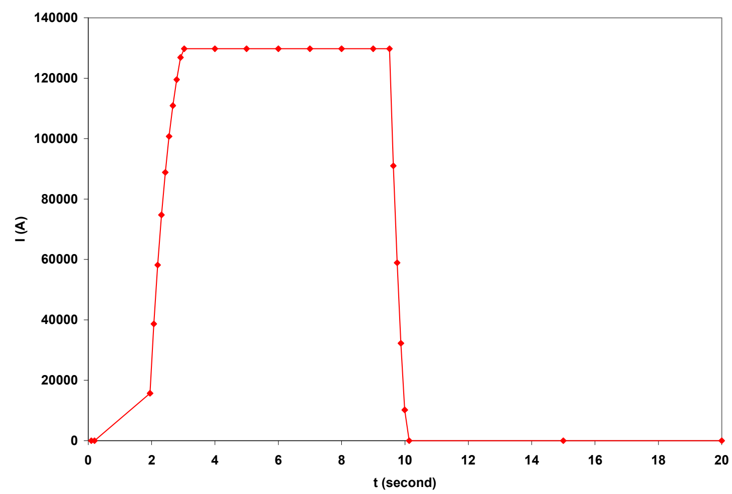

Figure 1.3.2.1-1: NSTX normal operation waveform.

Analysis Method

This is a transient and coupled field analysis. An electromagnetic model (Fig. 2) is used to calculate current diffusion effect and transfer the generated heat and Lorenz force to thermal and structural model. The thermal and structural model calculates the temperature, displacement, thermal stress, contact pressure at contact areas, and then transfer these data back to electromagnetic model. The materials have temperature dependent material properties, including electrical resistivity, thermal conductivity, specific heat, coefficients of thermal expansion. The arches have anisotropic resistivity and thermal conductivity to simulate the straps. Because the arch is made of many straps and not a solid copper, it becomes much more compliant. The modulus of the arch is based on the results of T. Willard [4]. The upper flag uses high strength copper which has 1/0.8 resistivity and 80% thermal conductivity of pure copper. In next section, the results show that using high-strength copper or pure copper doesn't have much difference. The lower flag uses pure copper. In the electromagnetic model, the contact regions have pressure dependent resistivity and the data are from R. Woolley [5] (Table 1).

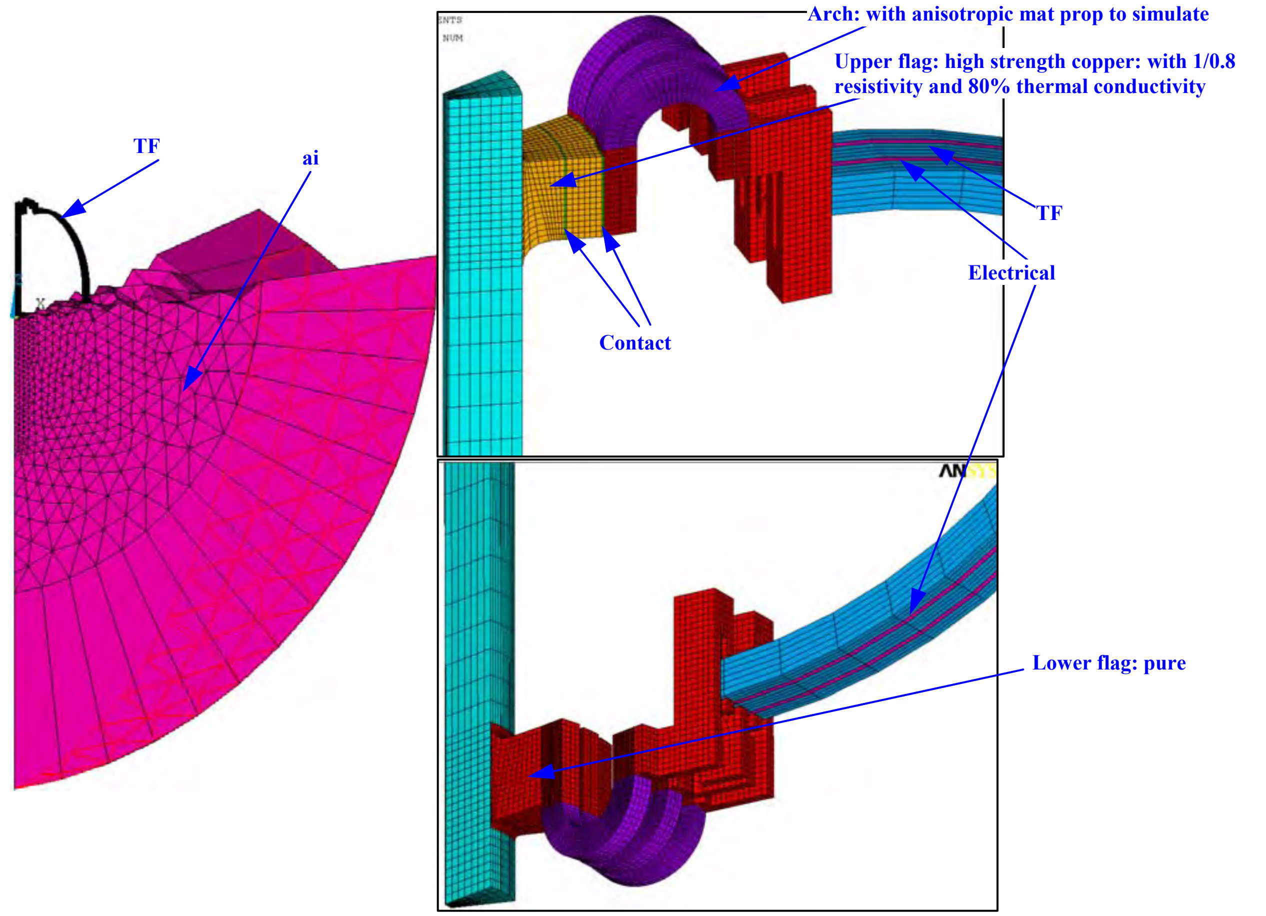

Figure 1.3.2.1-3 NSTX Electromagnetic Model , Including Air

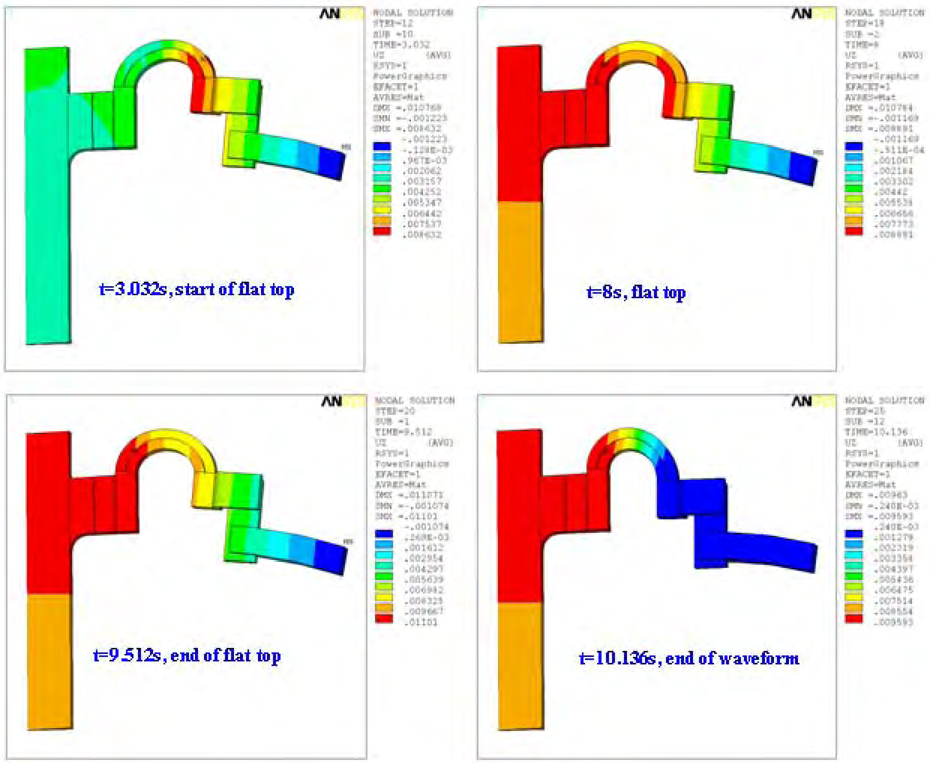

Displacements from the Electromagnetic Current Diffusion Model

Inner Leg Temperature, L/R Fault

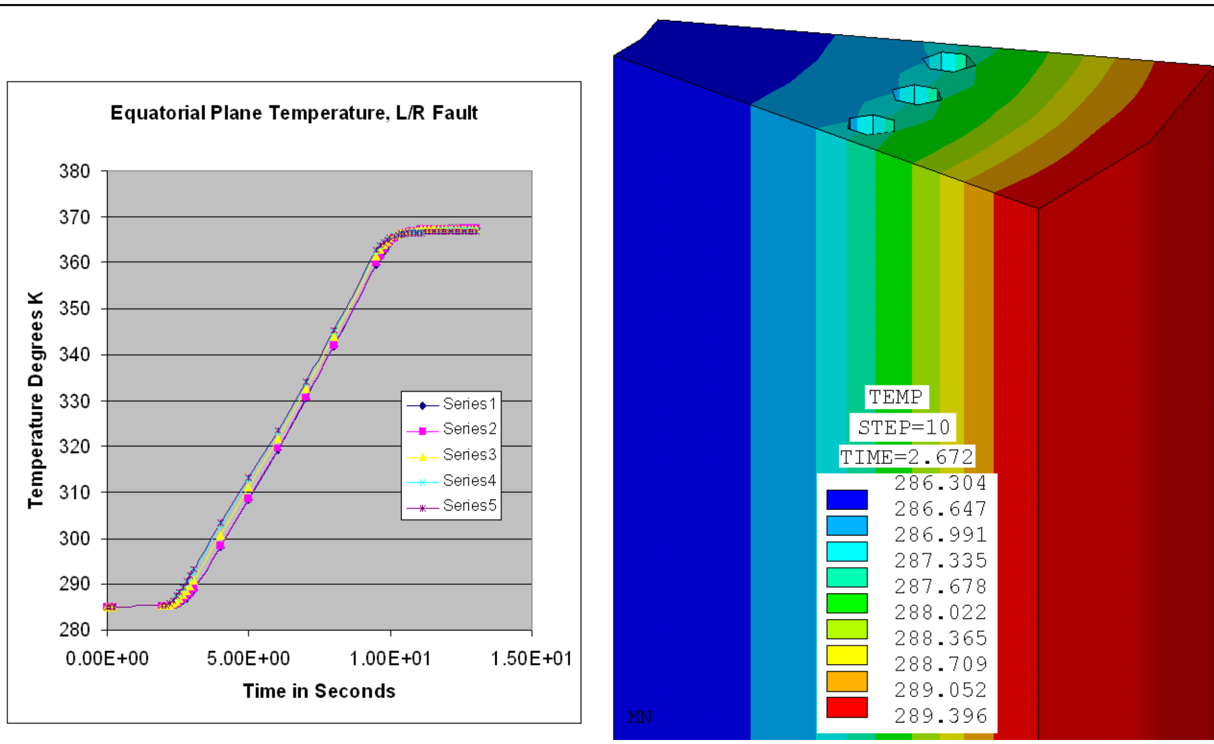

Figure 23 Equatorial Plane Time History. End average temperature is 367.15, Ref [6],{7]

12.2.1 Extended Hub Structural Pass

Structural Pass

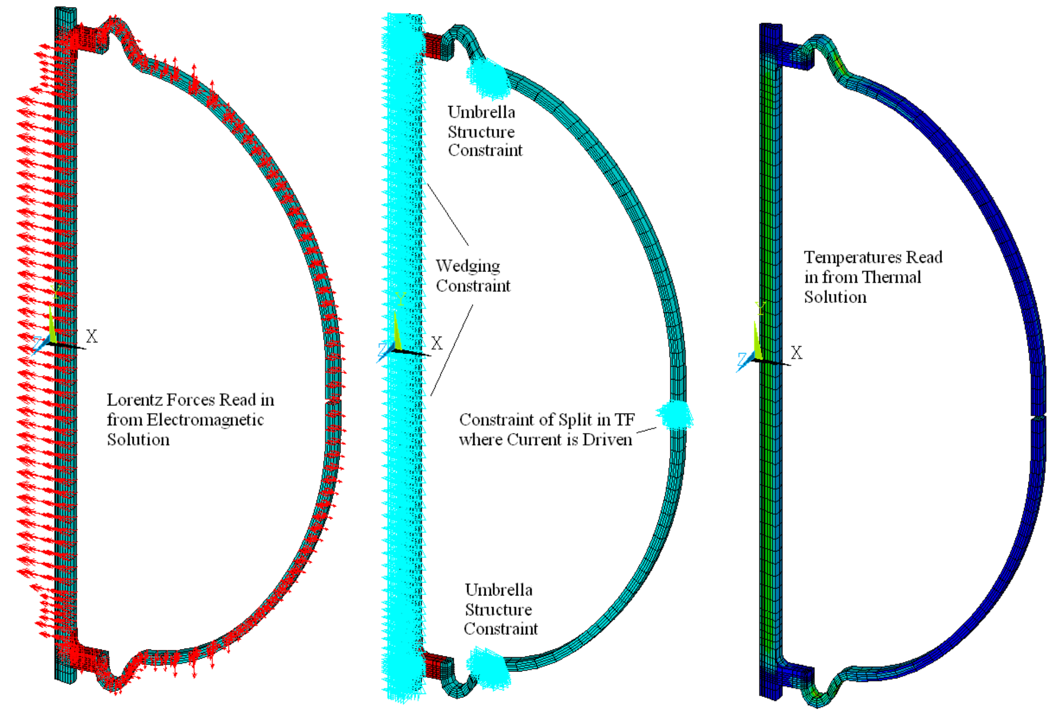

Figure 24 Structural Pass Forces, Constraints, and Temperatures

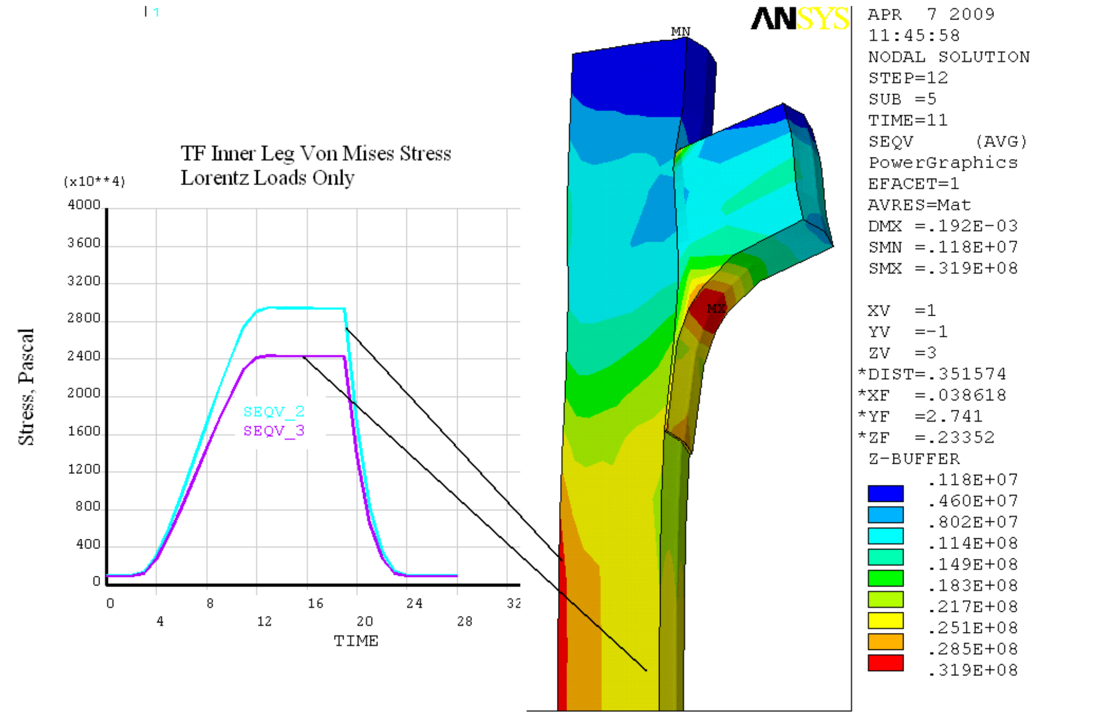

Figure 27 Inner Leg Stress Time History – No Thermal Stresses

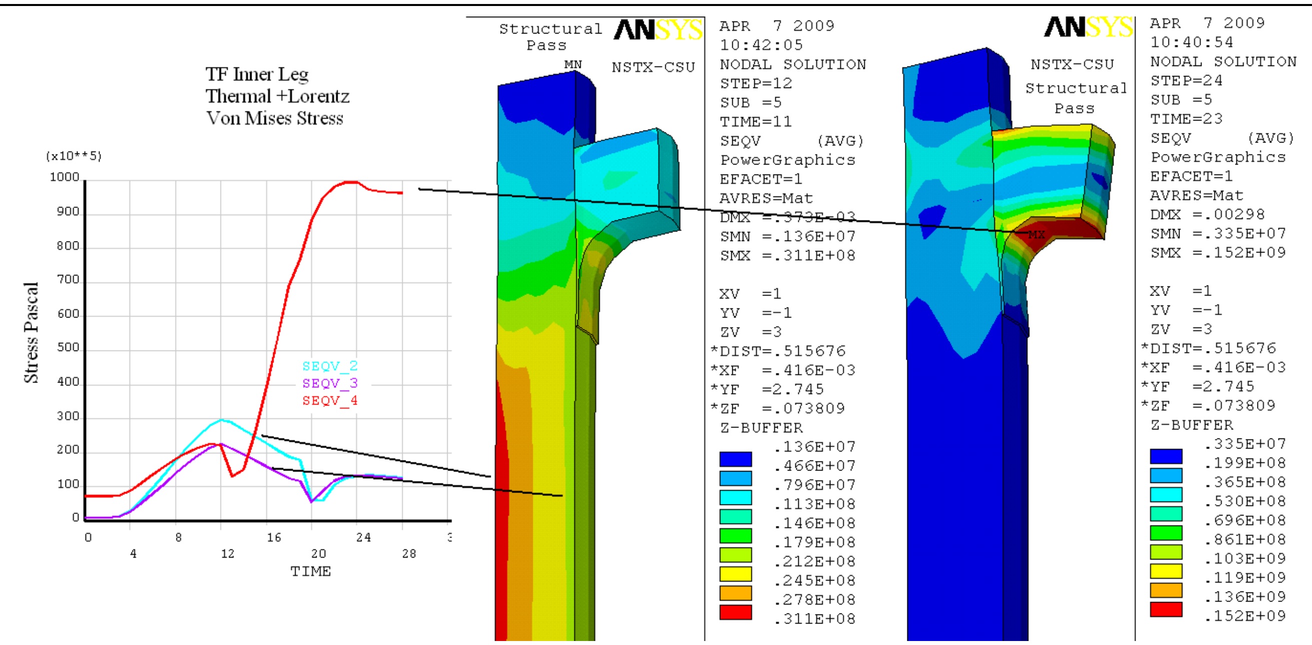

Figure 28 Inner Leg Von Mises Stress Time History – With Thermal Stress. The higher stress at the end of the pulse results from the restraint of center stack thermal expansion by a stiff modeling of the joint loop. This for the Nominal TF Current Profile.

1.3.2.1 Joint Option Studies

The demountable inner leg of the ST is a key feature which is also very challenging [2]. The current density is quite high and adequate contact pressure must be maintained at the joint under all conditions of electromagnetic loading. Currents, fields, and forces are quite high and in some cases bidirectional. The TF inner leg assembly experiences substantial axial thermal which has to be accommodated by the radial limbs without causing high stresses or moments which would spoil the contact pressure at the joint. The area is quite congested and access to fasteners is difficult. The radial limbs must make up for fabrication tolerances on the inner legs and assembly tolerances on the outer legs.

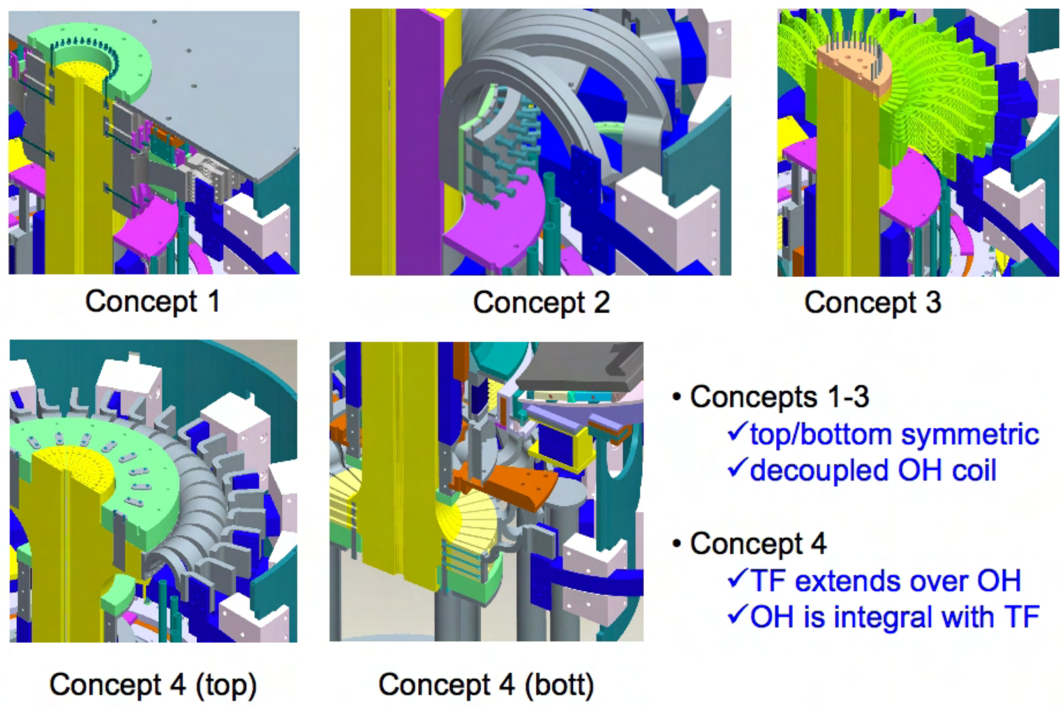

Figure 1.3.2.1- 35 Concepts for TF Joint

In order to develop a robust solution for the NSTX center stack upgrade four concepts have been independently developed and are now under assessment as shown in Figure 1.3.2.1- 35. Concepts 1-3 are basically different than 4 since the TF inner legs do not include any extensions at the ends so that the OH coil can be separately manufactured and installed/removed repeatedly. In concept 4, radial extensions would be e-beam welded to the wedge shaped turns yielding the advantage of jointing at a greater radius (lower field, greater surface area) but the disadvantage of the fabrication of the TF and OH being linked, and the OH coil being trapped.

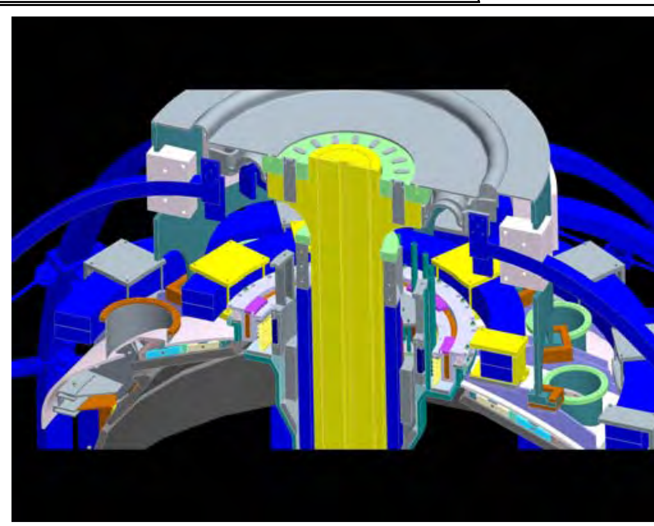
Figure1.3.2.1 Concept 4 , Extended Hub Concept

The essential features of the joint concepts are:

Concept 1: Bolted joint with inserts, constant tension shaped radial, flexibility both in-plane & out-of-plane, torque transmitted to lid

Concept 2: Jacking ring joint connection, flexibility in-plane, self-supported against torque

Concept 3: Jacking ring joint connection, constant tension shaped radial, flexibility in-plane, self-supported against torque

Concept 4: e-beam welded extensions, bolted joints with inserts, flexibility in-plane, torque transmitted to lid

Concept 4 was chosen for the conceptual design effort.

1.3.2.2 TF Joint Qualification

1.3.2.2.1 TF Joint Qualification Boundary Conditions

The TF joint is part of the larger NSTX structural system and has many interfaces. The outer flags are attached to the umbrella structure aluminum blocks which in turn are supported by the vessel umbrella structure and are loaded by the TF outer leg loads. The connection at the centerstack assembly sees the 8 mm vertical thermal growth of the joule heated TF inner leg. The inner and outer attachment points of the joint are held in toroidal registration by the upper and lower diaphragms described and analyzed ion section 1.2.3.2

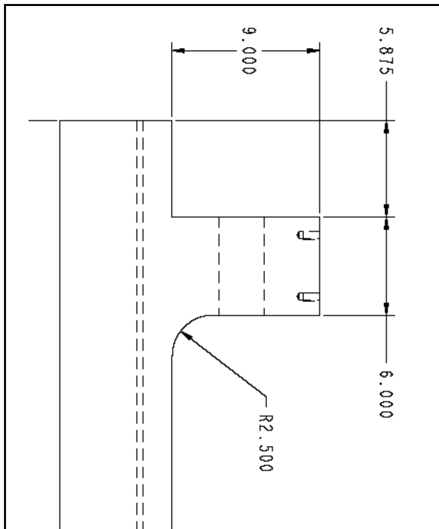

Figure **12.2**-2

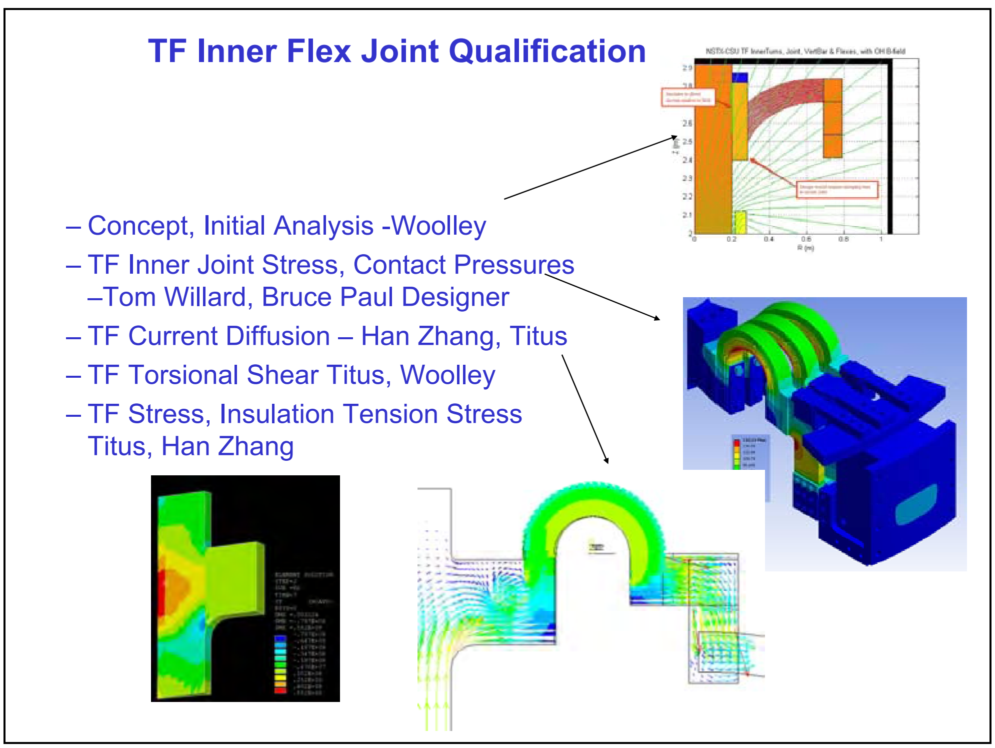

Current Diffusion Model was Used to Qualify CuCrZn Flag Extensions and Allow Stronger Inserts and Bolts

NSTX-CSU Coupled Transient Electromagnetic-Thermal Analysis – With a Structural Pass – Used to Provide TF Field at the Strap, Inductively Driven Current Densities and Temperatures (H. Zhang)

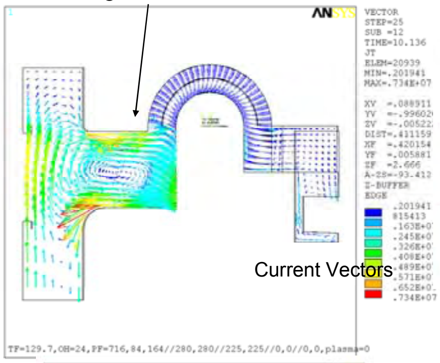

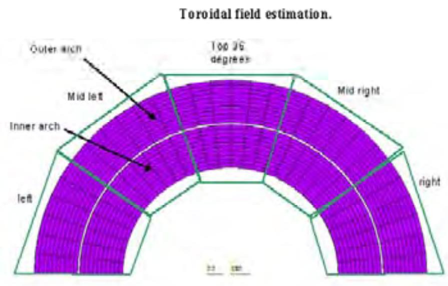

EM Model

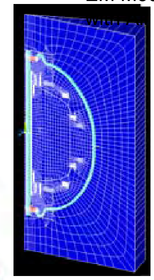

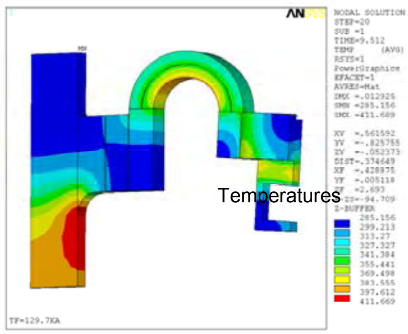

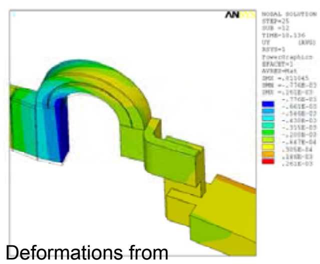

Deformations from Structural Pass

Thermal De-Wedged Region - Through Thickness Insulation Tension Stress

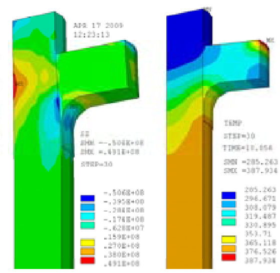

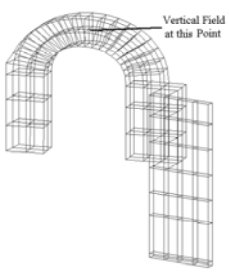

Max Vertical Field at TF Straps

Ron Hatcher Gave us the Worst Vertical Field , .3T, to Design the Strap to:

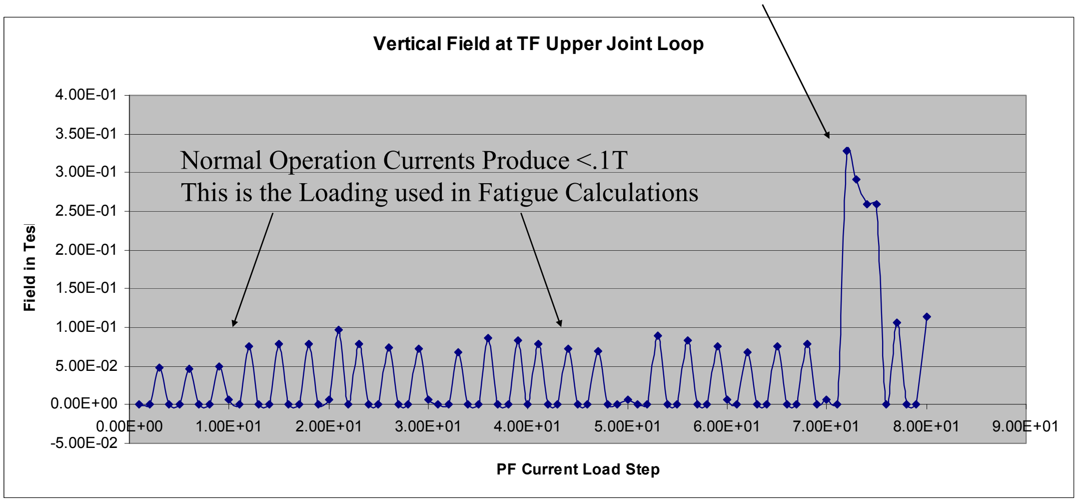

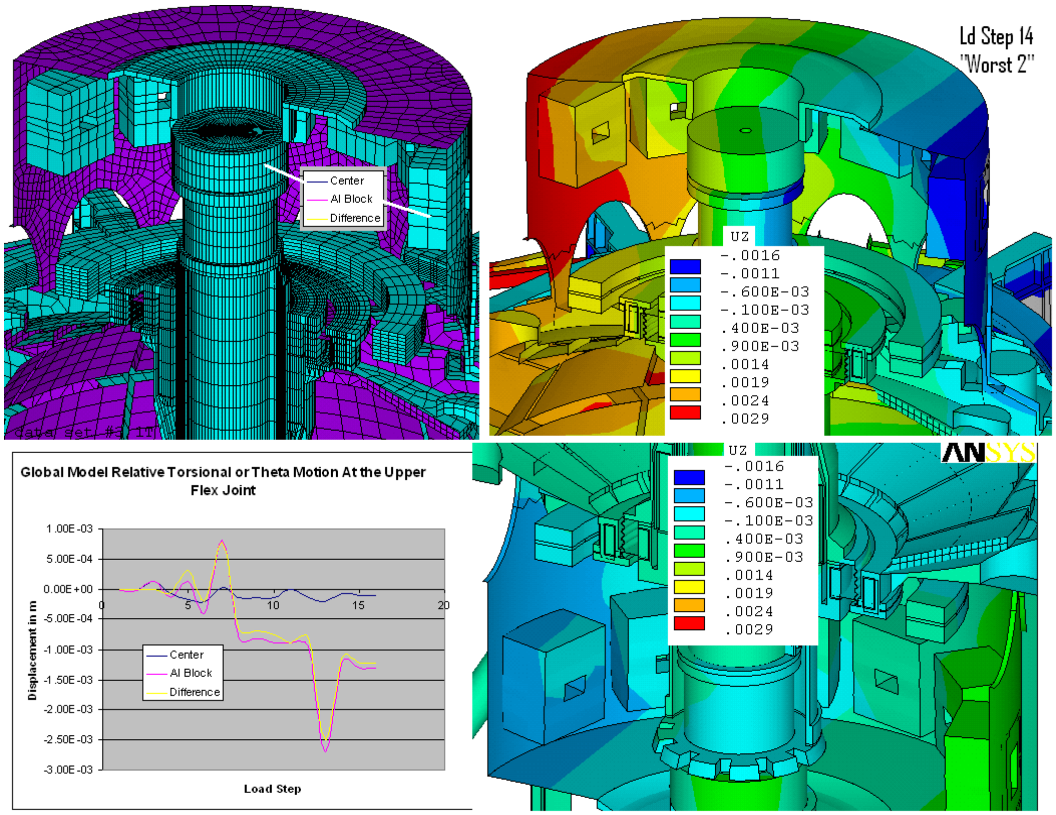

Toroidal Displacements at the Flex Joint

1.3.2.3TF Joint Local Model

A complete treatment of this analysis may be found on the NSTX Centerstack Upgrade Engineering Web page and is documented in ref [4]

The objectives of this analysis of the NSTX Upgrade TF Flex Strap and TF Bundle Stub design were: 1.) to determine if the design is adequate to meet the requirements specified in the NSTX Structural Design Criteria, specifically, if the flex strap lamination stresses and the copper lead extension thread stresses meet the requirements for fatigue, yield, and buckling, under worst-case/ power supply-limit load conditions: 130,000 amps/ strap, 0.3 T poloidal field, and 1.0 T toroidal field; and 2.) to verify that the local contact pressure in the bolted electrical joints is a minimum of 1500 psi, sufficient to maintain the joint contact electrical conductance above the design goal, based on the current-design development tests, of 1.0E06 siemens/in^2.

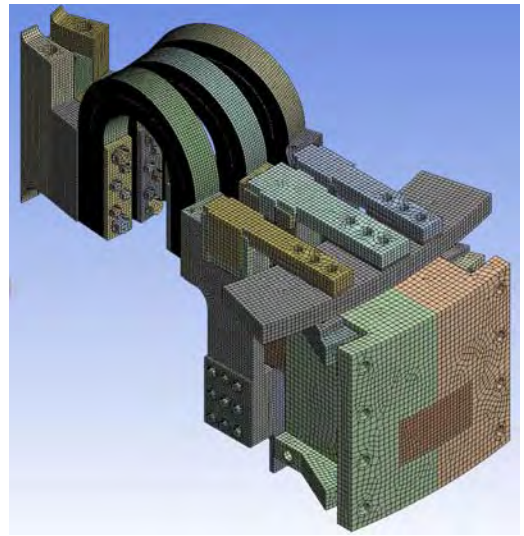

Figure 1.3.2.3-1 TF Joint Model

The results of the ANSYS multiphysics finite element analysis - electric, transient thermal, magnetostatic, and static structural - show that: 1.) the maximum equivalent stress in the laminations is 27.5 ksi, which is 25.5 ksi below the fatigue allowable for the full-hard C15100 copper-zirconium strip; 2.) the maximum equivalent stress in the copper threads is 29.1 ksi, which is 32.9 ksi below the fatigue allowable for the full-hard C18150 copper-chromium-zirconium plate; 3.) the minimum average contact pressure is >6500 psi, and the minimum local contact pressure is >2500 psi, which is 1000 psi above the design goal; and 4.) the lamination minimum linear buckling load multiplier factor (LMF) is > 58, which is approximately 10x the minimum allowable specified in the NSTX Design Criteria document.

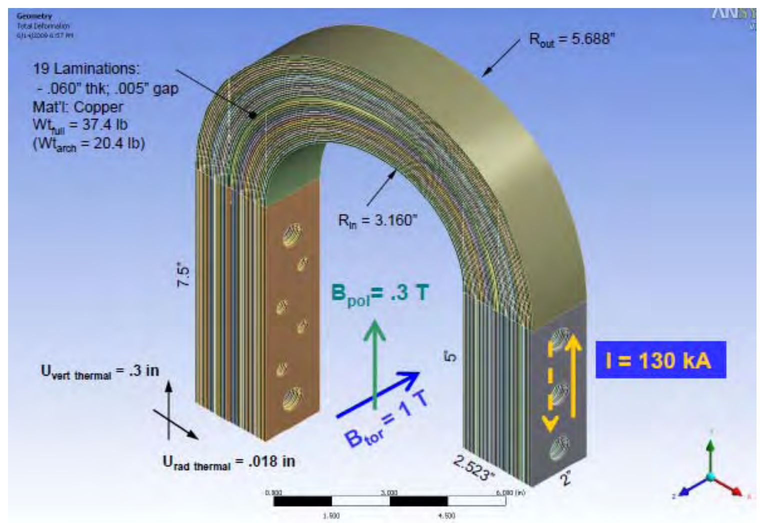

Table 2.1 - Design Operating Point Comparison				
Design	Total Current (A)	Maximum TF (Tesla)	Maximum PF (Tesla)	On-Time Pulse Duration (sec)
Current	72,000	0.6	0.1	0.5
Upgrade	130,000	1.0	0.3	7.0

1.3.2.3Joint Mechanical Parameters Comparison

A comparison of the mechanical parameters of the TF lead-extension bolted joint designs is shown in Table 2.4-2.22
2.2. From the table, it is clear that the upgrade design is much more robust.

The joint is located further from the CS winding, so the joint contact area is much wider. It is also taller, so the contact area is approximately 4x larger. The number of bolts/ joint has increased, and there is a mix of 3/8 and 5/8 bolts, with the 5/8 bolts located furthest from the bolt centroid. The lead-extension material has been changed to a high strength copper alloy C18150 copper-chromium-zirconium, so that the bolt pretension is limited by the strength of the bolts and not the shear strength of the copper threads. All of this results in a nearly 5x increase in total bolt force, a 50% increase in initial contact pressure, and a large positive lift-off torque margin. Since there is no lift-off, the local contact pressure never falls below a minimum value, determined in the ANSYS analysis below to be > 2500 psi.

Table 2.2 - Joint Mechanical Parameters Comparison

Design	Joint Contact Area (in^2)	Total Bolt Force (lbf)	Average Initial Contact Pressure (psi)	Minimum Operating Local Contact Pressure (psi)	Calculated In-Plane Mating Torque (in-lbf)	Max. TF In-Plane Separating Torque (in-lbf)	Lift-off Torque Margin
Current	3.382	20,000	5,914	0	12,500	17,500	-0.29
Upgrade	12.739	94,000	7,379	~2500	90,875	30,143	2.01

1.3.2.3 Joint Electrical/ Thermal Parameters Comparison

A comparison of the electrical and thermal parameters of the joints is shown in Table 2.3. Though the total current is higher in the upgrade design, the current density is only 1/2 the density in the current design. The initial (closed joint) electrical resistance and heat generated in both designs is small, as is the estimated temperature rise across the joints, assuming no thermal capacitance.

Table III - Joint Electrical/ Thermal Parameters Comparison

Design	Current Density (A/in^2)	Initial Electrical Resistance (W)	Heat Generated I^2R (W)	Thermal Power Density (W/in^2)	Initial Thermal Resistance (W/C)	Zero-Heat Capacity Temperature Rise (C)
Current	21,289	1.48E-07	7.66E+02	2.27E+02	1.18E-02	9.1
Upgrade	10,205	3.93E-08	6.63E+02	5.21E+01	3.14E-03	2.1

2.6 Static Bolt Strengths and Insert Pull-Out Loads Comparison

A comparison of the static bolt strengths and insert pull-out loads of the two joint designs is shown in Table 2.4. From the table, it can be seen that the shear strength of the C10700 copper threads in the current design limits the 3/8 bolt pretension to below the maximum allowable bolt load. When the estimated 2000 lbf operational cyclic load is considered, the allowable bolt pretension is reduced to only 5000 lbf: a 2000 lbf reduction due to the cyclic load, and a 3000 lbf reduction due to the reduced shear strength of the copper for fatigue at 60,000 cycles.

The upgrade design uses high strength C18150 copper-chromium-zirconium, with more than twice the shear strength of the C10700 copper, for the lead-extensions,. Also, because the extensions are longer, a longer 3/8 insert is used, with a larger shear area. This results in the copper thread strength being greater than the bolt tensile strength, so the maximum allowable bolt pretension is limited by the strength of the bolt. The bolt reactions from the ANSYS analysis below indicate that the cyclic load is small (10-15% of the bolt pretension), so can be reduced to nearly zero with the use of Belleville washers. To maximize the contact pressure and lift-off margin, without exceeding the maximum allowable bolt loads, the following bolt pretensions were chosen for the upgrade design: 10,000 lbf for the 3/8 bolts; and 27,000 lbf for the 5/8 bolts.

Table IV - Static Bolt Strength and Insert Pull-Out Load Comparison

Design	Bolt Size	Qty/ Joint	Bolt Mat'l	Bolt Yield Strength (psi	Bolt NSTX D.C. Allowable (psi)	Tensile Stress Area (in^2)	Max. Bolt Load	Tap-Lok Insert Outer Thread	Insert Length (in)	Effective Shear Area (in^2)	Copper Alloy	Yield Strength (psi)	Shear Strength (psi)	Insert Pull-out Load (lbf)
Current	3/8-16	4	Inconel 718	185,000	138,750	0.0775	10,753	9/16-16	0.562	0.4864	C10700	36,000	20,772	10,104
Upgrade	3/8-16	4	Inconel 718	185,000	138,750	0.0775	10,753	9/16-16	0.687	0.608	C18150	75,000	43,275	26,311
	5/8-11	2				0.226	31,358	29/32-11	1.125	1.61				120,750

1.3.2.3 2.7 Comparison Summary

In summary, joint pitting damage in the current design occurs with TF fields > .45 T, in lift-off areas predicted by an ANSYS direct-coupled model and verified by in-situ measurements of joint resistivity. No pitting damage occurs in joints further from the plasma that do not lift-off. Bolt pretension, limited to 5000 lbf due to the low shear fatigue strength of the copper threads, is not sufficient to prevent lift-off, given the long lever arm of the TF Radial Flag.

The upgrade flex strap design reduces the lever arm length, minimizing the prying torque. The more robust design , with bolt pretensions limited by the strength of the bolts, also increases the mating torque, resulting in a large positive lift-off margin. A description of the ANSYS multiphysics analysis, used to determine the stresses in the laminations and the minimum local contact pressure in the joints, follows.

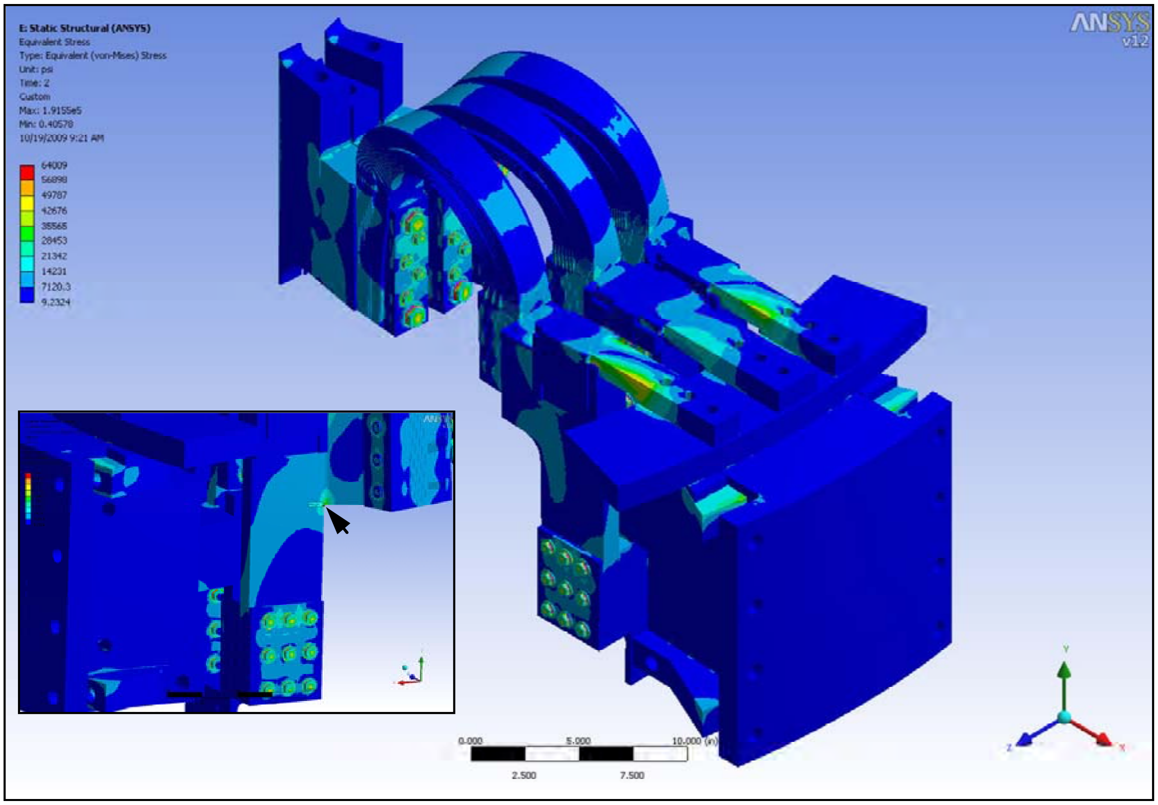

Figure 1.3.2.3-1 Static Structural Analysis Results: von Mises Stress

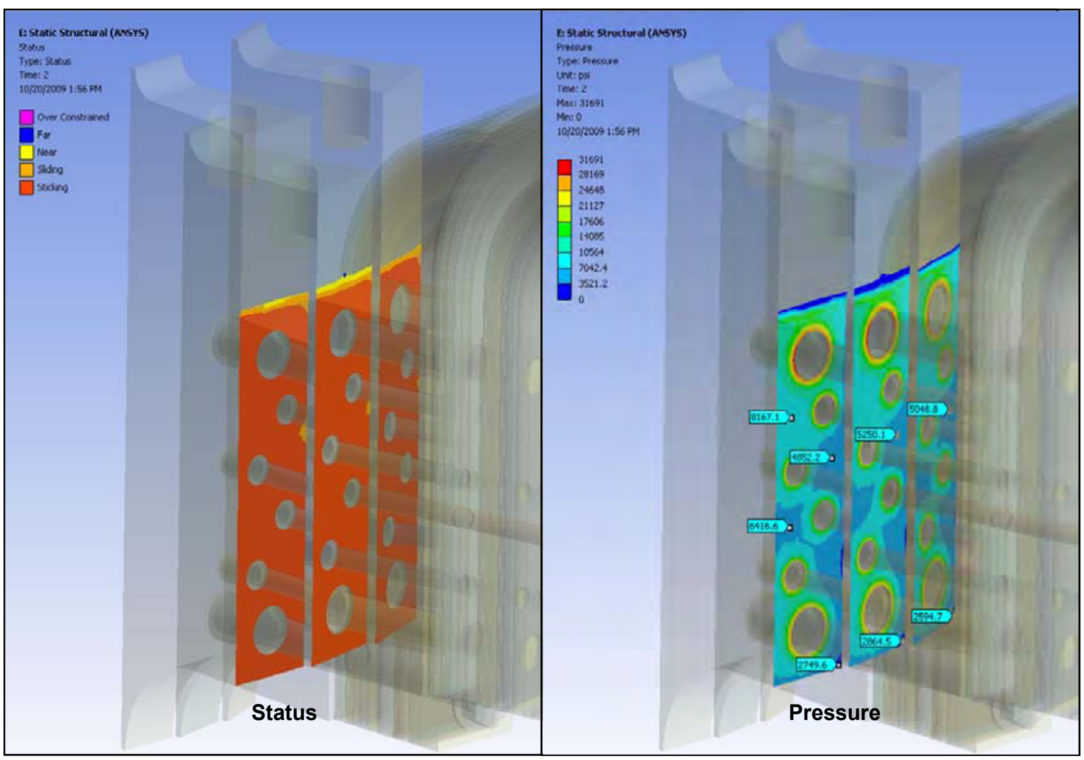

Figure 1.3.2.3Figure Static Structural Analysis Results: TF Bundle Stub Bolted Joint

Contact Pressure

Evaluation of OOP Motions from the Global Model

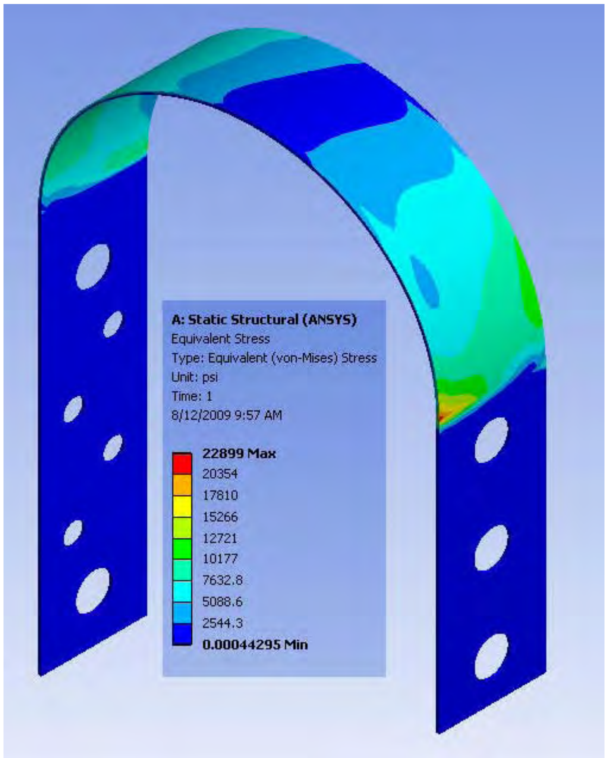

The inner-most lamination stress increases only about 7% with the addition of the 2.5mm torsional displacement: 22899 psi vs 21445 psi

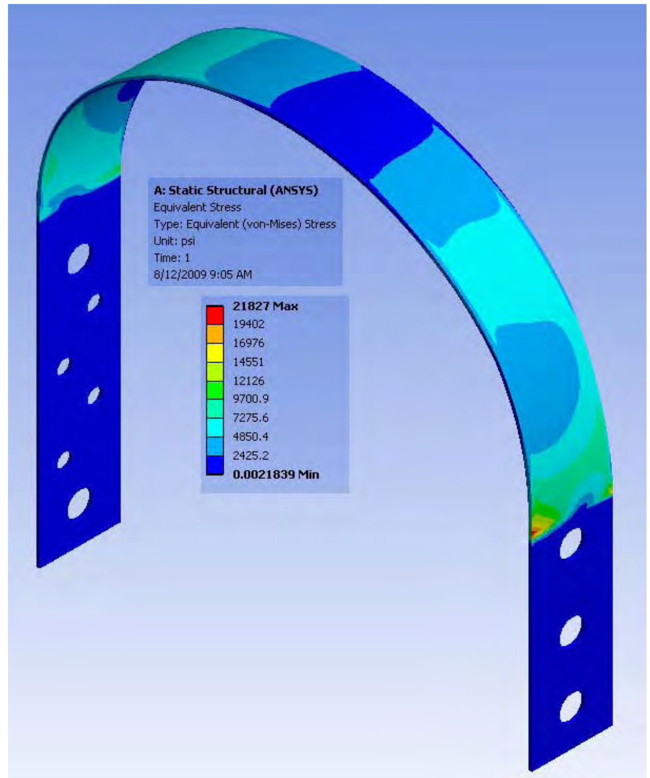

In the Outer-most lamination model with the 2.5mm OOP displacement added to the Emag loads and thermal displacements, the stress increased by only 3% (21827 psi vs 21178 psi). This shouldn't be a problem if we use C15000 copper or better.

1.3.2.3 TF Inner Leg Torsional Shear, Global Model Results

Out-of-Plane (OOP) loads on a toroidal field (TF) coil system result from the cross product of the poloidal field and toroidal field coil current. Support of OOP loads is statically in-determinant, requiring an understanding of the flexibility of the outboard structures and the inboard stiffness of the central column. For NSTX CSU, this is accomplished in the global model. For the worst PF loads considered in the global model, the peak torsional shear stress is 20 MPa – just below the allowable of 21.7 MPa.

Additional Discussions of torsional shear may be found in Bob Woolley's calculation NSTX-CALC-132-003-00 which provides moment calculations which are useful to find the maximums in thte NSTX Design Point spreadsheet. Bob's summation of the outer leg moment is directly useful in evaluations of the up-down asymmetric case that Han is running in the diamond truss/tangential - radius rod calculations. (Section 1.3.2.2)

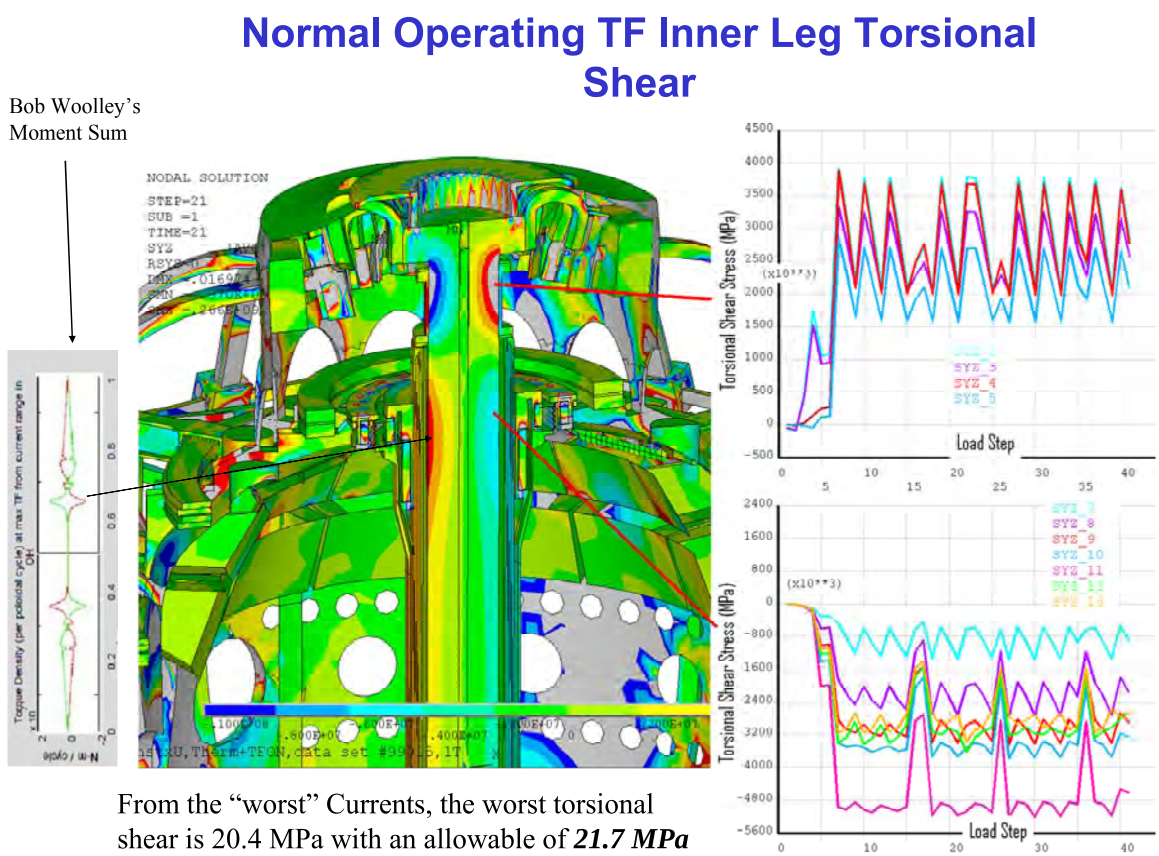

Figure 1.3.2.3-1 Global Model Inner Leg Torsional Shear

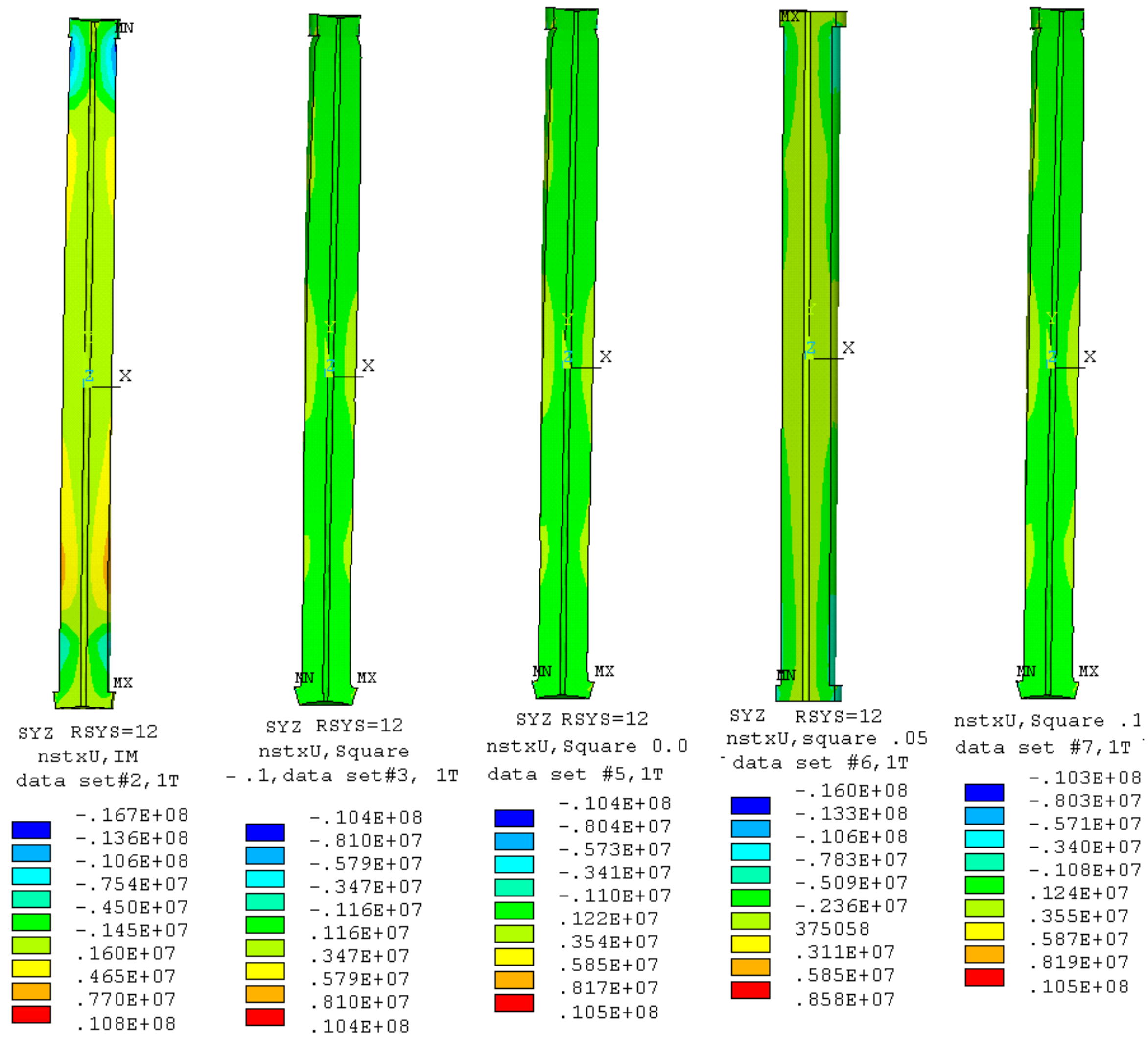

Figure 1.3.2.3-2 Global Model Inner Leg Torsional Shear

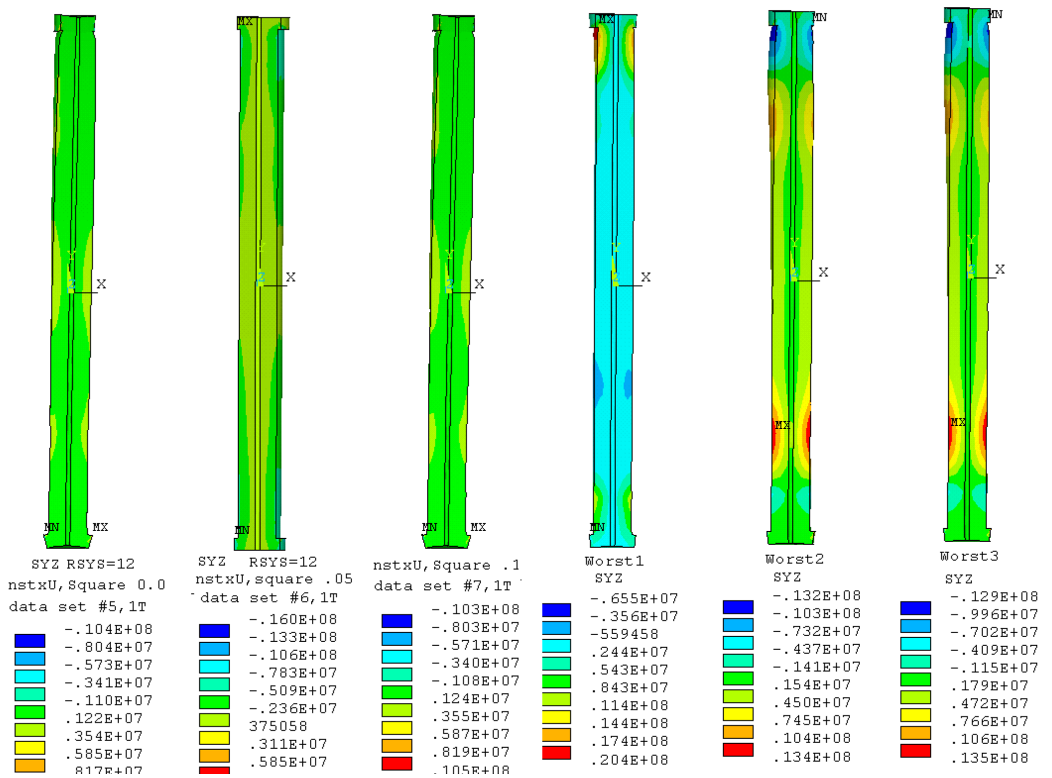

Figure 1.3.2.3-3 Global Model Inner Leg Torsional Shear, Worst Case PF Loads

A simplified method for calculating OOP shear stresses and their distributions, suitable for systems codes, is described here. The TF coil system and structure is modeled as a toroidal shell The poloidal field is calculated at the shell using axisymmetric current loops and an elliptic integral solution. OOP Lorentz forces are computed by crossing the TF current with the poloidal field. The torsional stiffness of segments of the TF shell is computed, adjusting shear modulus and thickness to simulate the stiffnesses of the tokamak. In practice the global finite element model is used as a guide in selecting the shell properties. This kind of approach can be implemented in the Design Pointg

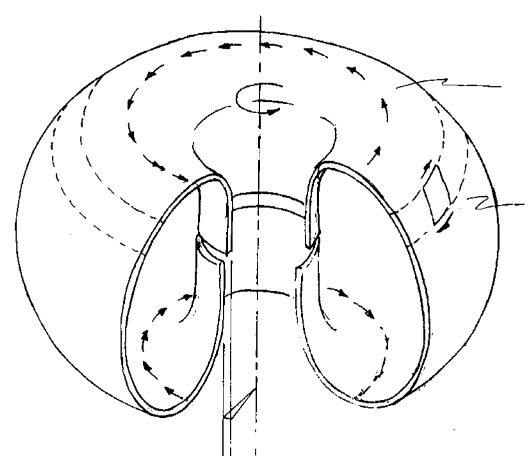

1.3.2.3- 2 Simple Toroidal Shell Model. OOP loads are computed from the TF current and PF currents using an elliptical integral solution for the PF fields. TF OOP loads are assumed to be applied to a toroidal shell – with varying thickness to simulate more complex OOP structures. Shear deformations are accumulated to a split in the shell, then a moment is applied to align the split.

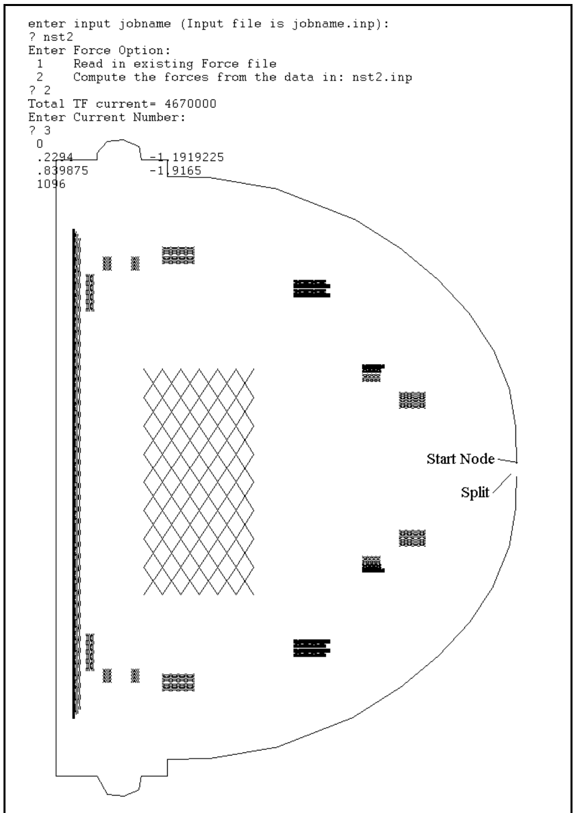

NSTX Shell Model

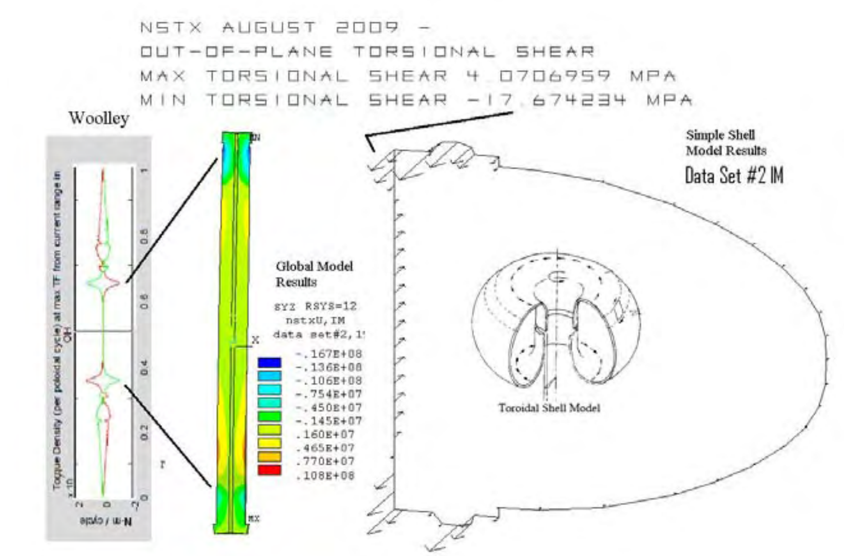

Comparison of Woolley, Global FEA and Simple Shell Analyses

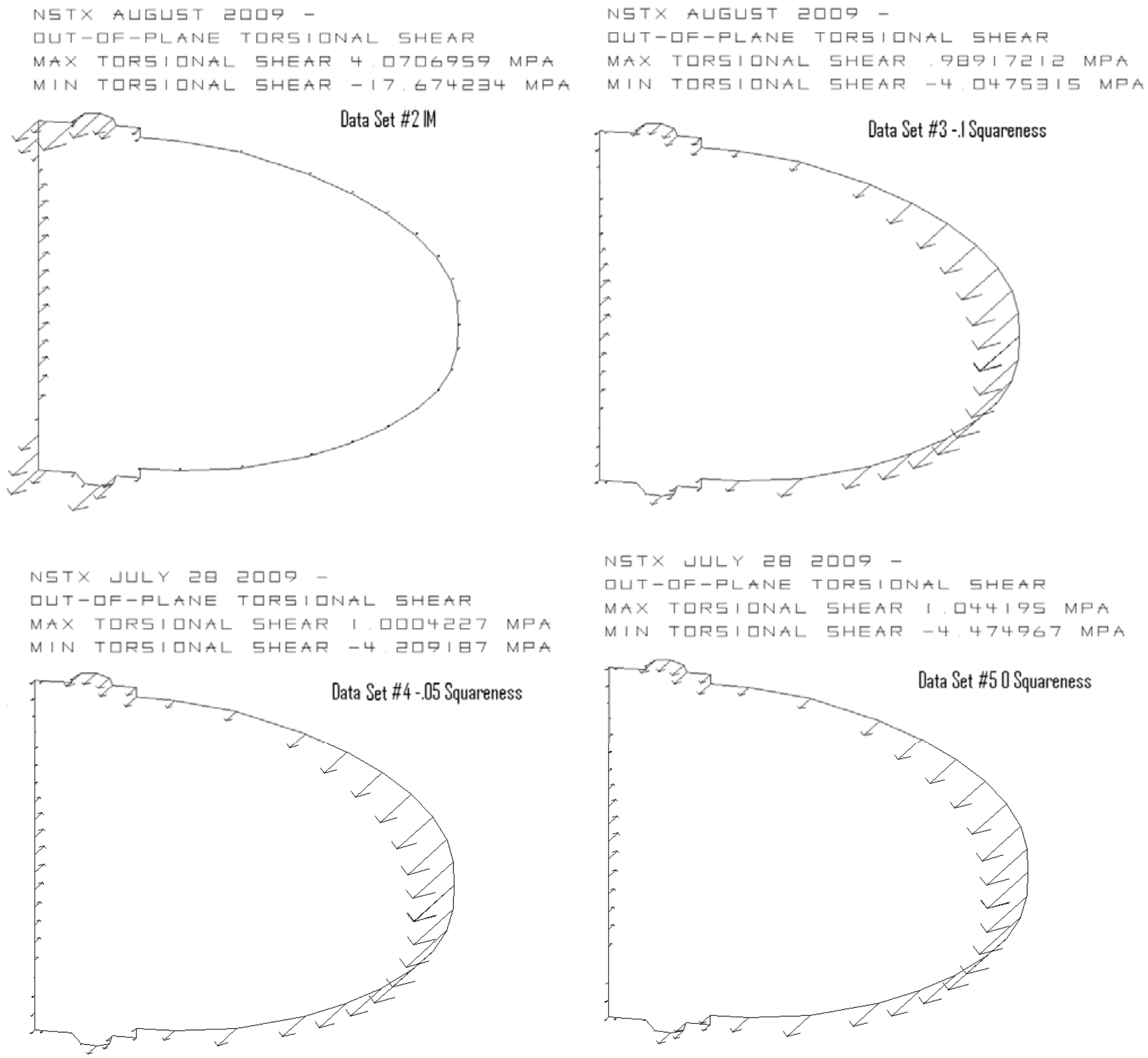

Torsional Shear for IM and some Equilibria

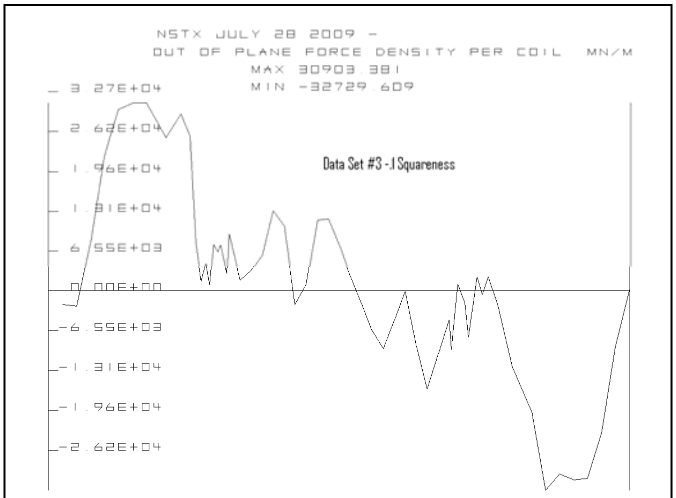

OOP Force Density Along TF CL starting from Outboard Equatorial Plane

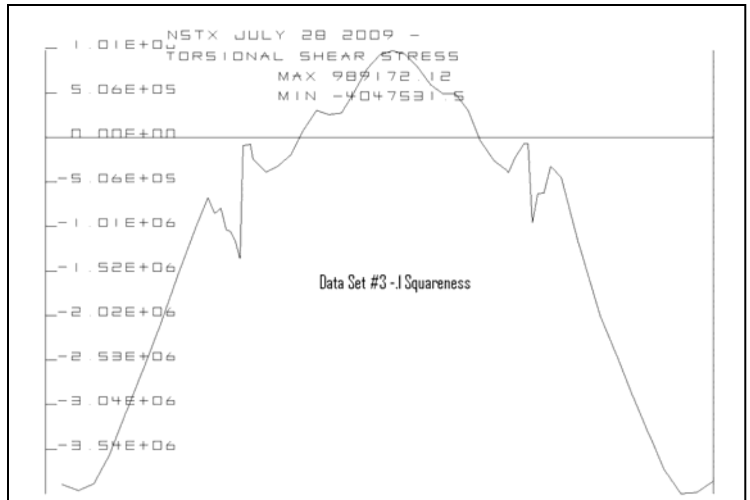

Torsional Shear Stress Aalong TF CL starting from Outboard Equatorial Plane

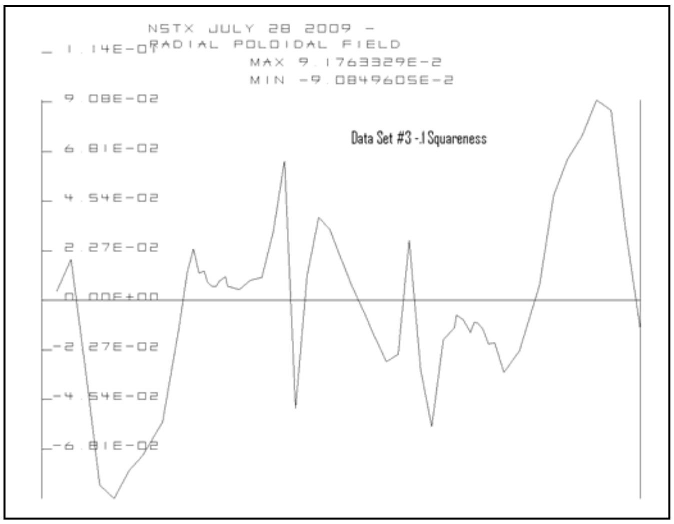

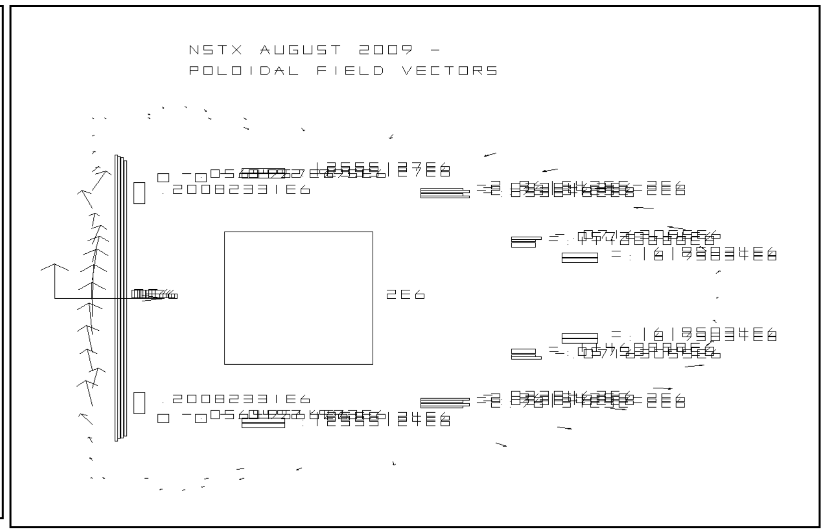

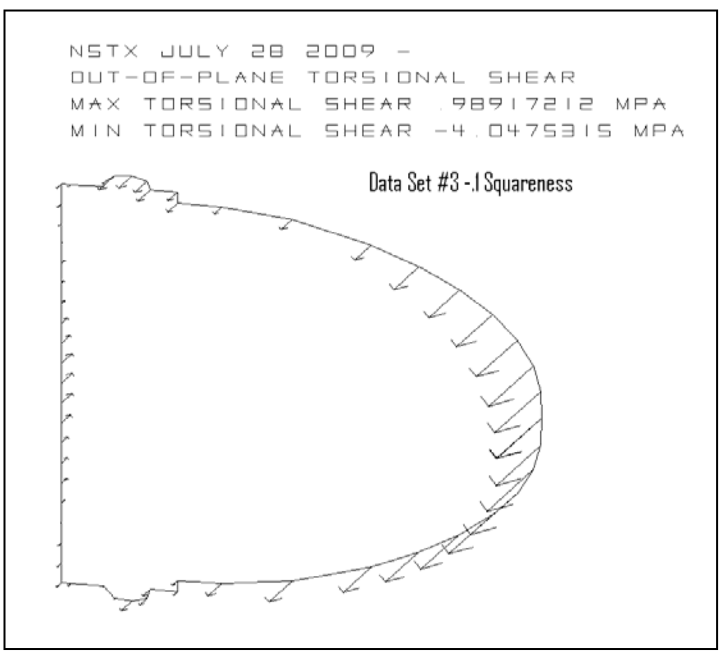

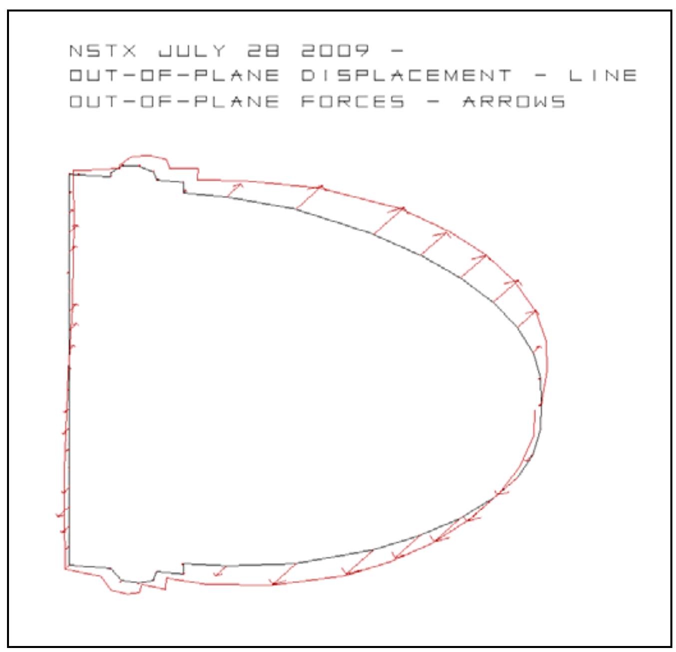

1.3.2.3 TF Outer Leg Reinforcement

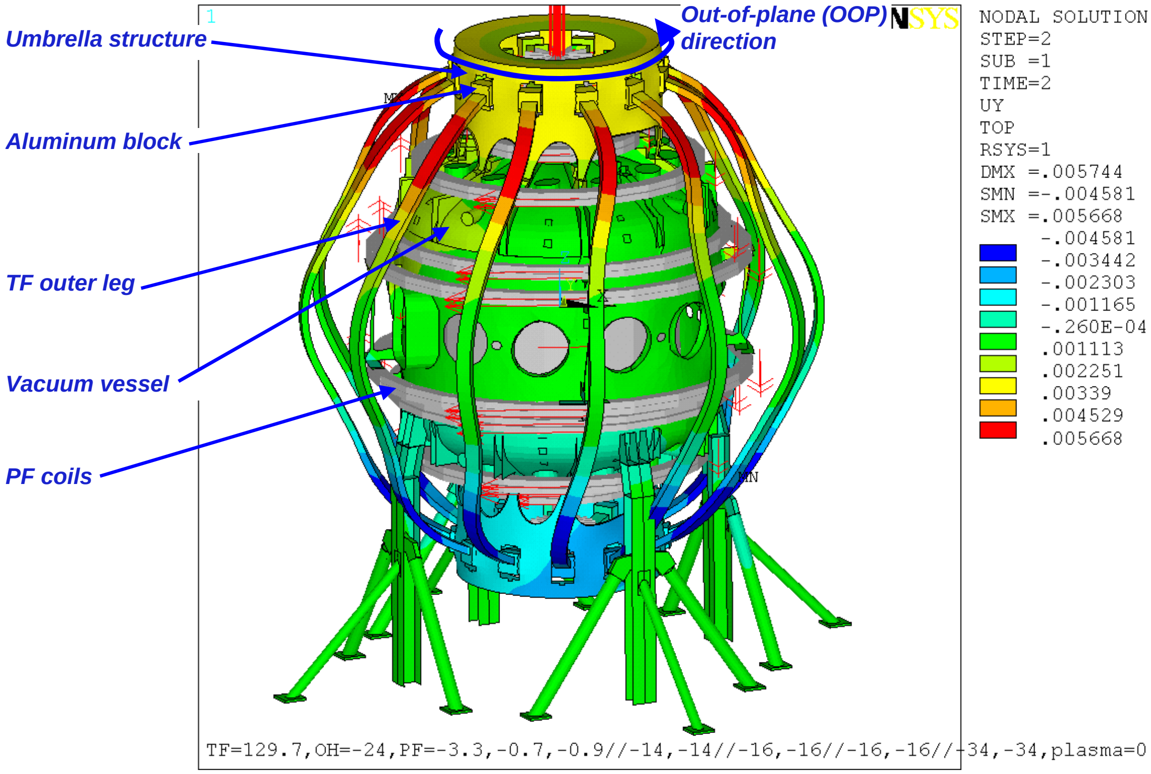

Figure 36: NSTX Machine

The objective of this analysis is to study what kind of additional support structure can help take some of the in-plane and out-of-plane (OOP) force of TF outer leg.

The upgrade of NSTX CSU will increase the TF current to 130KA. Upon TF self field and poroidal field, TF outer leg will have in-plane (i.e. in the plane of TF outer leg) force and OOP (i.e. perpendicular to the plane of TF outer leg) force. The only support structure of TF outer leg is the umbrella structure . From previous analysis, with the worst case PF currents, the umbrella structure will have very high stress of >1GPa (145 ksi). The umbrella structure has a cylindrical shape and radial load should not be a problem. However, the blocks are bolted to the umbrella structure and must take the radial load. Vertical load will be transferred to vacuum vessel. OOP load will cause the rotation of umbrella structure and produce high stress on the arches. So it is necessary to add additional support structure to take some OOP load and so as to reduce the load to umbrella structure.

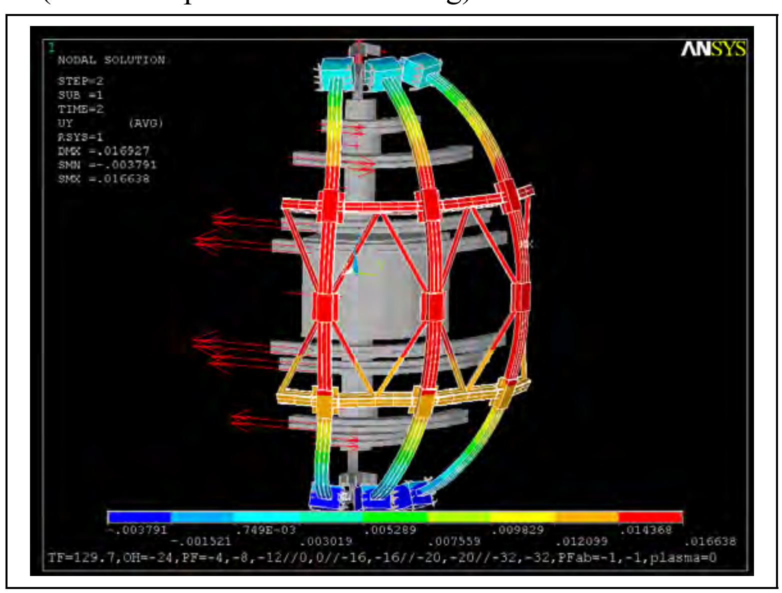

The first idea is to add a stainless steel ring to take in-plane expansion and tie bar connected to vacuum vessel to transfer the load to vacuum vessel. But the tie bar will constrain the TF coil due to vacuum vessel bake out.

The second idea is to use stainless steel ring and diamond truss and there is no link to vacuum vessel. However, the space is quite limited and only a few of diamond truss can be added. The non-uniformly distributed diamond truss will cause the non-axisymmetric coil deformation and high stress points in the coil.

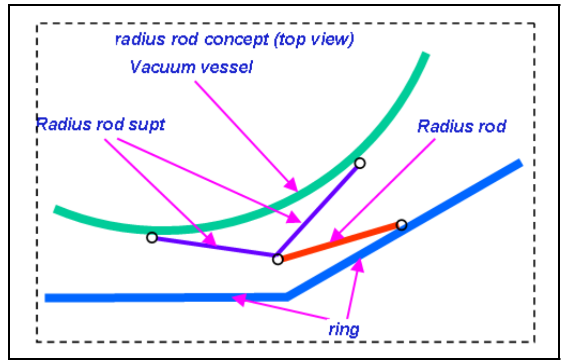

The third idea is to use ring and tangential (or radius) rods. They occupy the space of existing turn buckle and not affected by the vacuum vessel bake out. They can transfer the OOP load to vacuum vessel and effective on both symmetric and asymmetric PF currents. Table 5 shows the stress result based on criteria document. The stresses in TF outer legs are almost within allowable. The highest stress is at the connection between TF coil and ring. The stress in the ring is a maximum of 30 ksi for symmetric and maximum of 32.5 ksi for asymmetric current. For symmetric current, max load in radius rod is 18.4 klbs and min load is 4.5 klbs. For asymmetric current, max load in radius rods is 20.3 klbs and min load is 4 klbs.

Table 5: Stress Evaluation Based on Criteria Document: symm indicated the result is upon up-down symmetric PF currents and asym means up-down asymmetric PF currents.

	Max Tresca (Mpa) [1]	Allowable (Mpa) [1]	Von Mises stress from analysis (Mpa)
TF outer leg at Al. block	173	156	109 (symm) 107 (asym)
TF outer leg at ring	173	156	147 (symm) 158 (asym)
vessel at Al. block	183	183	313 (symm) 329 (asym)
vessel arch	183	183	289 (symm) 273 (asym)
vessel at radius rod support structure	160	160	139 (symm) 144 (asym)

The vessel stress at Aluminum block is too high. It is mainly because the direct coupling of nodes of Al. block and umbrella structure so as to cause element discontinuity. This should be further analyzed by a detailed model. Stress in vessel arch area is too high and requires reinforcement in that area. Vessel stress at radius rod support area is within allowable.

Figure 37: design of stainless steel case

A. current design.

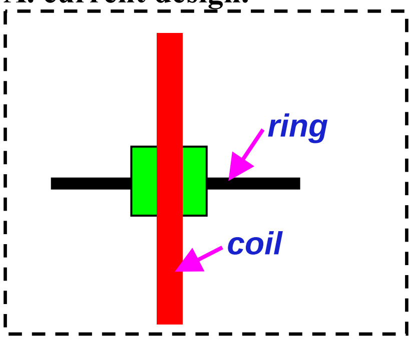

B. improved design.

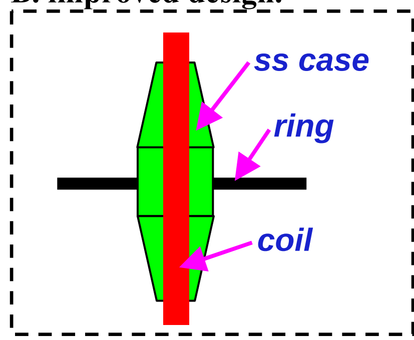

In these analyses, rings were added to reduce the pull-out (in-plane) loads at the umbrella structure. Various trusses (including tie bars, diamond bracing, and tangential rods) were tried reduce out-of-plane loads from the outer TF legs. Since the machine is already crowded, interference was a severe problem limiting the addition of trusses. Although we don't want to transfer more load to vacuum vessel, up-down asymmetric currents and resulting net twist required an attachment to the vessel. Tangential radius rods can take the net twist and also provided adequate OOP support for symmetric case. Tangential radius rods use the existing territory of turn buckle and there is enough room for them. Loads in the tangential radius rods allow attachment to the vessel with only modest modification and local stress of 20ksi. Vessel stresses in the umbrella structure and equatorial plane port region are acceptable or require only modest modification.

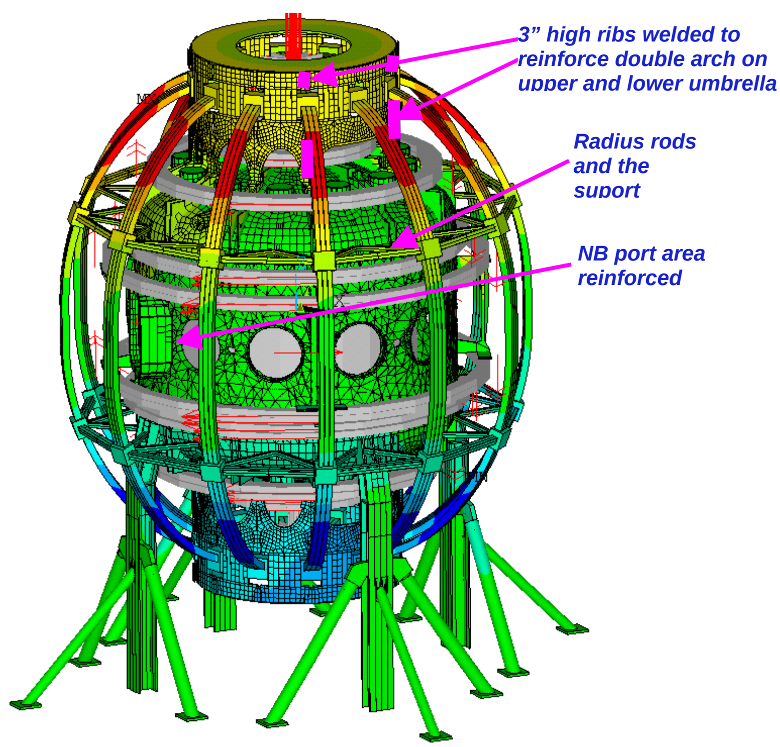

Outer TF, Vessel, Umbrella Structure, Reinforcements

Vessel Stresses With Tangential Radius Rods

Arch Regions Needing Reinforcement

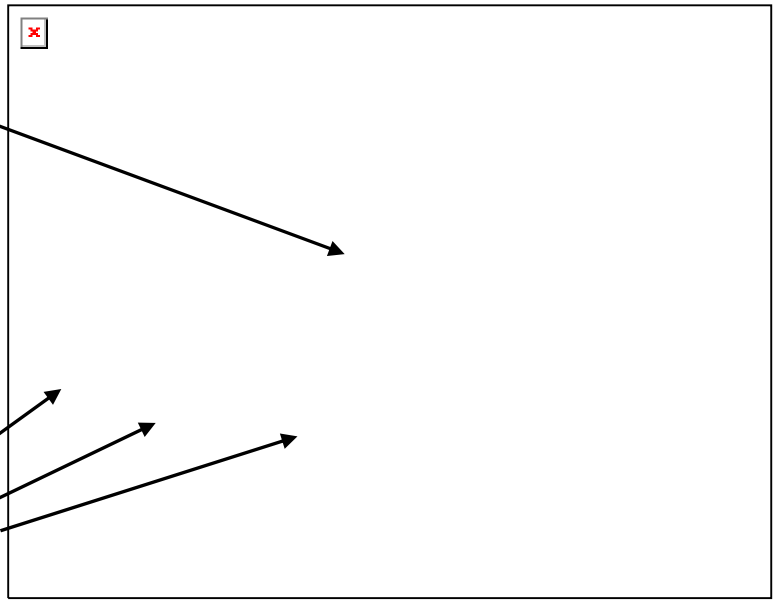

Positions of radius rod support (stress ~139MPa (20ksi)

140 MPa

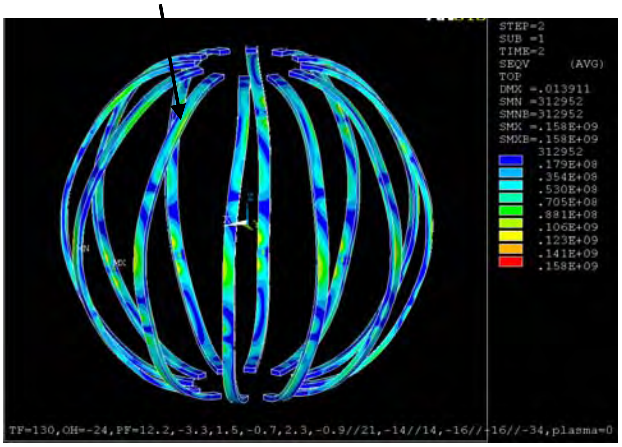

Coil Bending Stress Asymmetric PF currents, H.Zhang

Global Model Upper Outer TF Leg SI

TF Copper

1.5*Sm = 233MPa

Bending Stress =~ 100 MPa

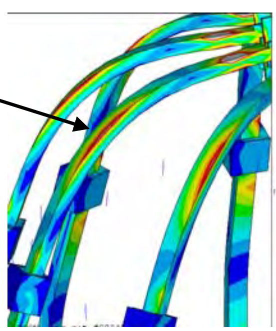

Charlies "Worst"

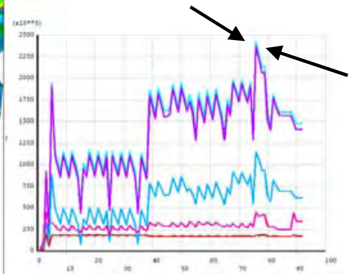

The Global model contains an error that over-estimates the TF leg bending stress by the ratio of section modulus or 237 MPa*(4.5/6)^3 = 100 MPa which is closer to the stress reported by Han

1.3.2.2.2 TF Outer Leg Bond Shear

The existing outer legs will be qualified for the higher loads – as mitigated with the addition of the support rings and tangential radius rods. Bending stresses have been qualified in section 1.3.2.3. Bending related shear stresses must be sustained with a turn to turn bond in the existing coils. The outer leg is made up from 3 turns of copper, each of which is 2 inches thick. The global model TF outer leg contains a dimensional error that over estimates the bending stress and the shear stress. The mid-plane shear was plotted in the figure, and this actually is in the middle of one of the 3 conductors so the global model overestimates the shear in a coupkle of ways. However even with these errors, the shear stress for a range of normal scenarios is 6.25 MPa with a shear alowable that may be as high as 21.7 MPa. Further evaluation will be required to address the worst case loads that have been used to qualify the bending stress

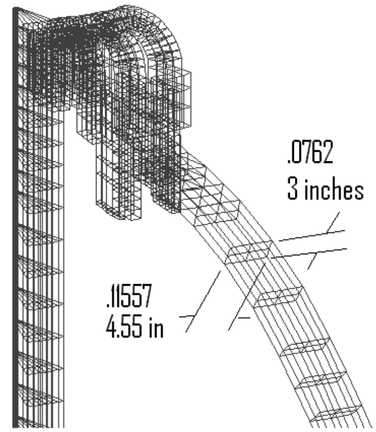

Figure 1.3.2.2.2 The Toroidal Width of the TF Outer Leg Should Be 6 inches. Stresses would scale as the section modulus or by d^3

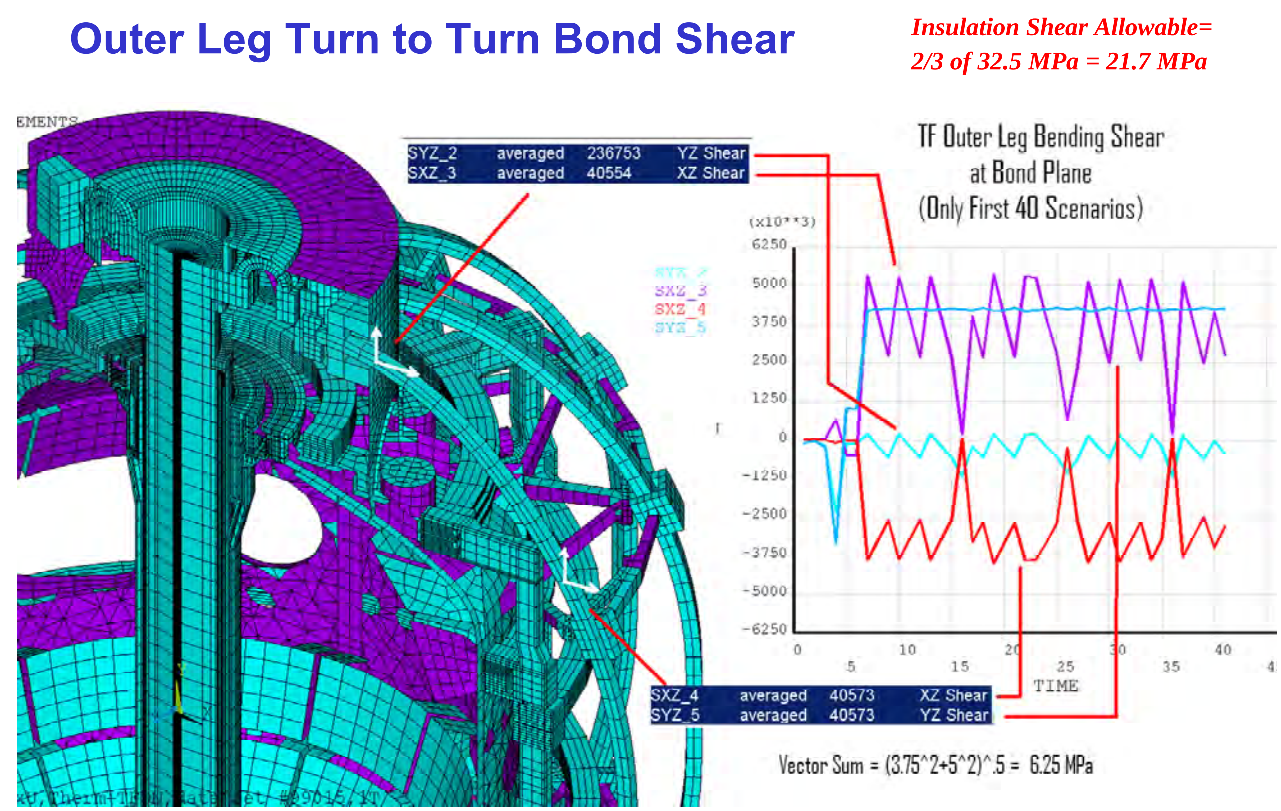

Figure 1.3.2.2.1 Global Model Bending Related Shear

1.3.3.1 OH Analyses in the Centerstack Assembly

The objective of this analysis was to estimate the anticipated stresses in the upgraded NSTX OH coil in various discharge scenarios. Axisymmetric coupled structural /Emag modeling of the OH coil and interaction with PF coils were performed using ANSYS. The OH coil was modeled both as a volume with smeared property and as discrete conductors and insulation volumes. Additionally the maximum stress in the OH coil due to thermal expansion in the TF coils was calculated. This stress results from the fault scenario where the OH coil, which is wound on the TF bundle, fails to energize while TF bundle is energized and expands out thermally.

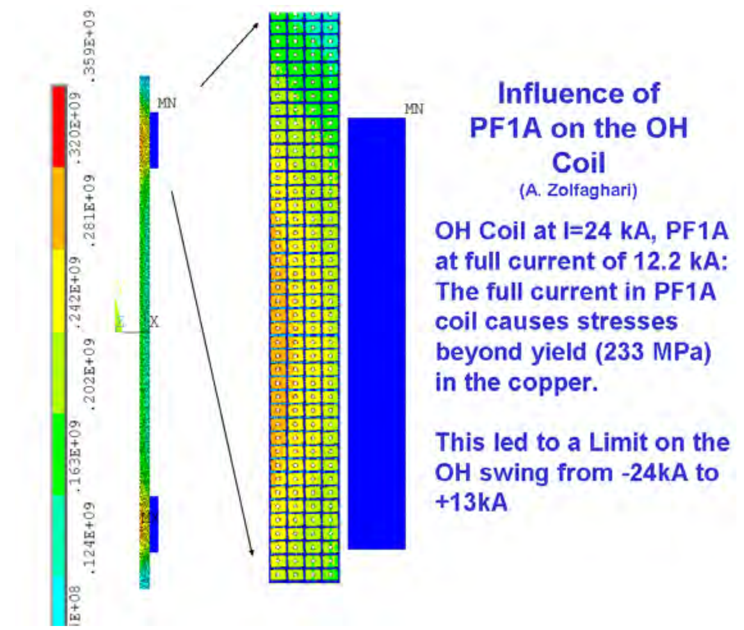

Figure 1.3.3.1-1

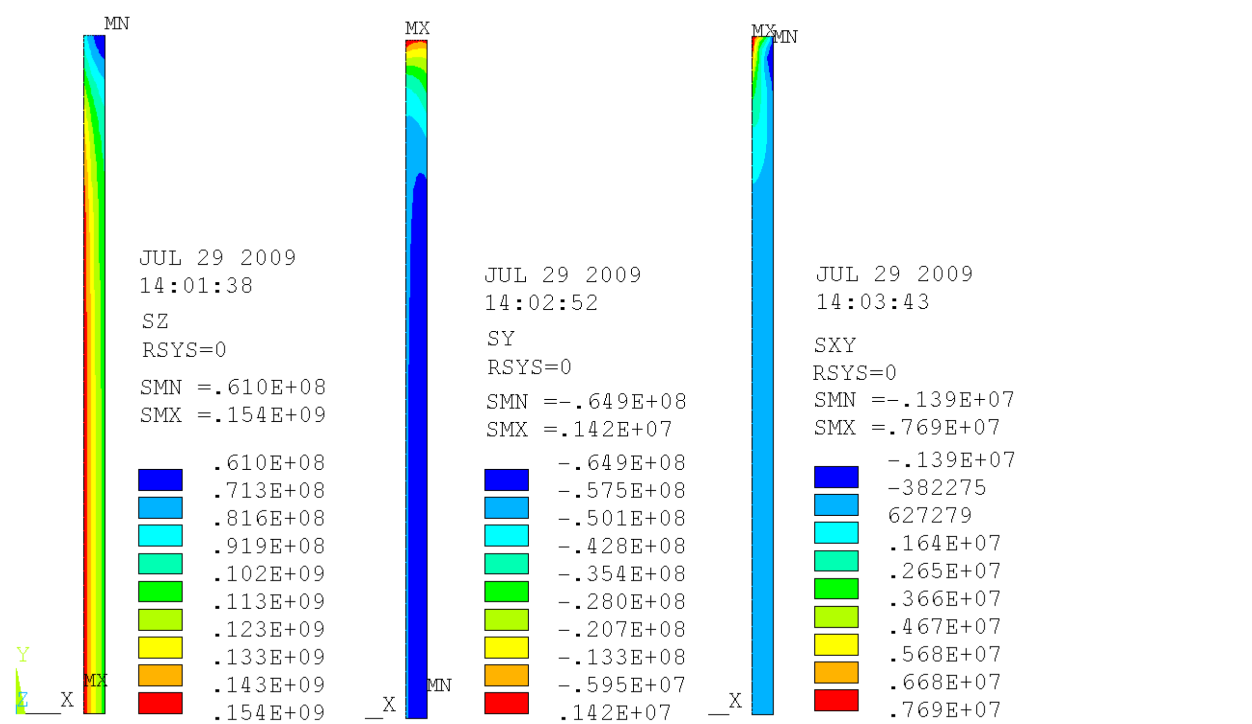

CS Hoop Stress CS Axial Stress CS Shear Stress

Figure 1.3.3.1 -2“Smeared:” Results with only the OH current

Analysis shows that the OH coil can withstand its self hoop stress, shear stress and normal to plane stresses at I=24kA. The analysis also revealed that running the PF1A coil at full 12.2 kA concurrently with the OH coil will cause stresses in the OH conductors beyond yield (233 MPA) in a large fraction of the OH coil cross section inside of PF1A coil. Limiting the OH current

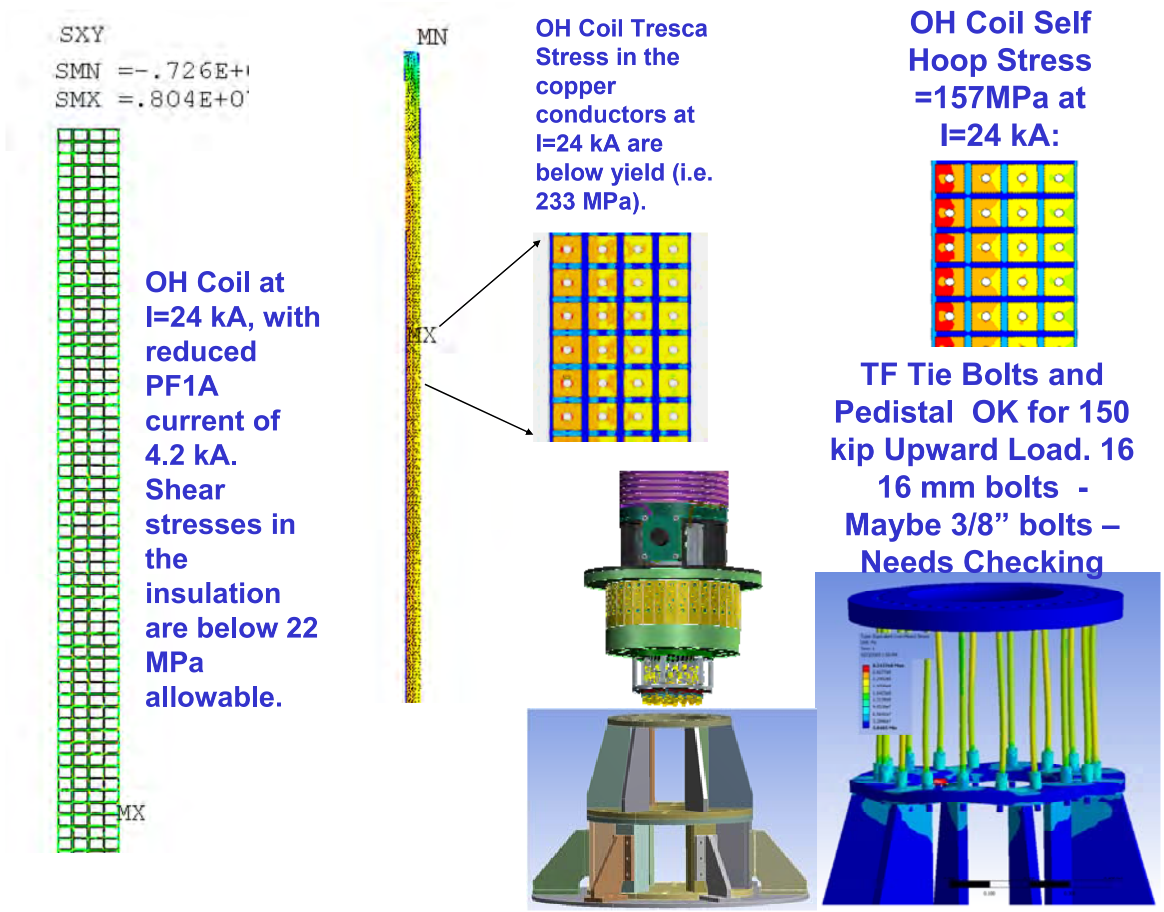

Figure 1.3.3.1 -3

swing from +24kA to -13kA will keep this stress below yield. The stress in the OH coil due to hot-OH cold-TF scenario was found to be acceptable but the frictional shear along the length of the TF-OH interface produces unacceptable vertical tension in the OH coil. Mechanical solutions such as low friction interface and removable interface layer as well as electrical solutions in the coil current control system are being considered for this problem.

CS Structural/Emag Modeling

A. Zolfaghari

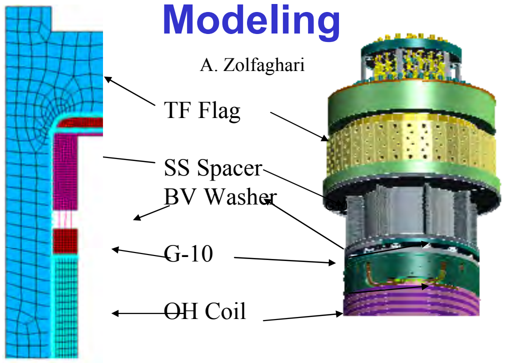

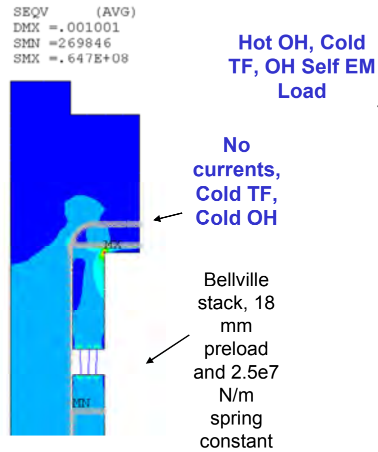

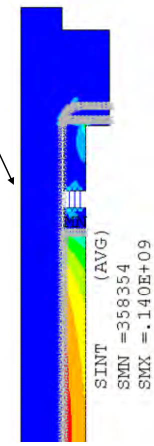

TF Temp.	OH Temp.	TF Current	OH Current	Launch Force	Peak OH Stress	Peak TF Stress	Peak Displacement	OH Lifted?	Case #	Notes
COLD	COLD	OFF	OFF	OFF	7-14 MPA	7-14 MPA	0.6 mm TF	NO	00000	Bellville staff force only
HOT	COLD	ON	OFF	OFF	102-115 MPA	38-51 MPA	8.8 mm TF	NO	10100	TF grows pushing OH laterally
COLD	HOT	OFF	OFF	OFF	10-19 MPA	19-29 MPA	4.6 mm OH	NO	01000	
COLD	HOT	OFF	ON	OFF	125-140 MPA	16-31 MPA	1.6 mm OH	NO	01010	TF was off and OH current was turned on with hoop stress only
COLD	HOT	OFF	ON	ON	123-138 MPA	16-31 MPA	1.9 mm OH	NO	01011	TF was off and OH current was turned on with hoop stress and launch force.
HOT	COLD	ON	ON	ON	117-132 MPA	15-29 MPA	8.2 mm TF	NO	10111	Just in case, OH getting current before heating up
HOT	HOT	ON	ON	ON	110-134 MPA	15-19 MPA	8.3 mm	NO	11111	

Figure 1.3.3.1 -4

Net Load on CS Real Constants 1,2,3,4,5,6,31,32

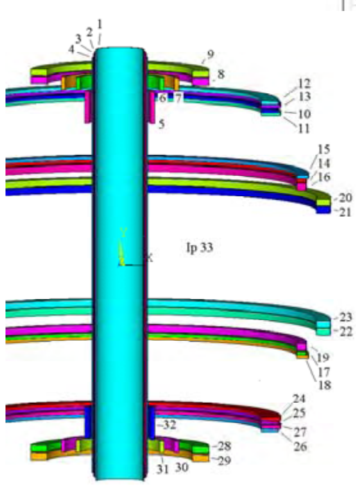

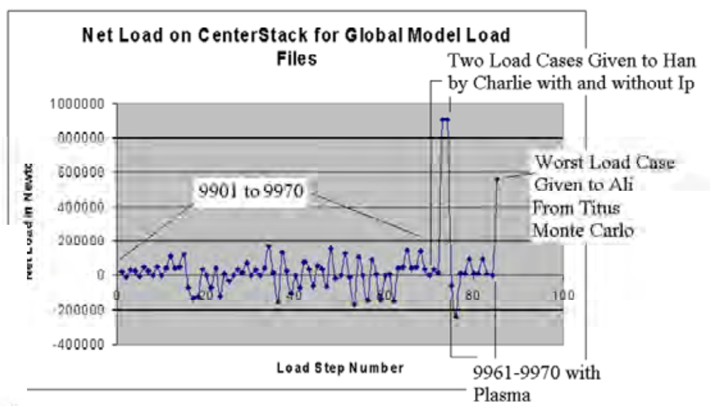

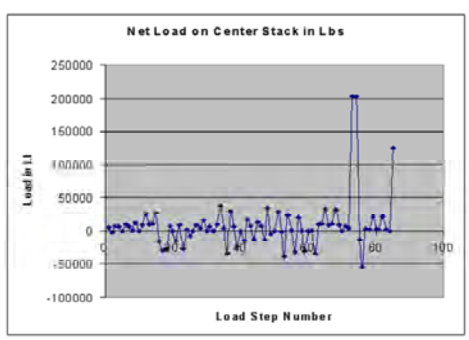

Figure 1.3.3.1 -5

Initial sizing was based on the peak Tresca in the conductor. This is interpreted as having a bending stress like distribution with a nearly linear variation across the build of the coil. The peak Tresca bus pass the bending stress allowable. The average Tresca must also pass the membrane allowable. In figure __ the Tresca stress across the build of the OH coil is plotted and the average of 168 MPa is above the membrane allowable of 155 MPa. (discussed in section 0.17) During preliminary design a bit more capacity will be found – either with an adjustment in build, or copper hardness.

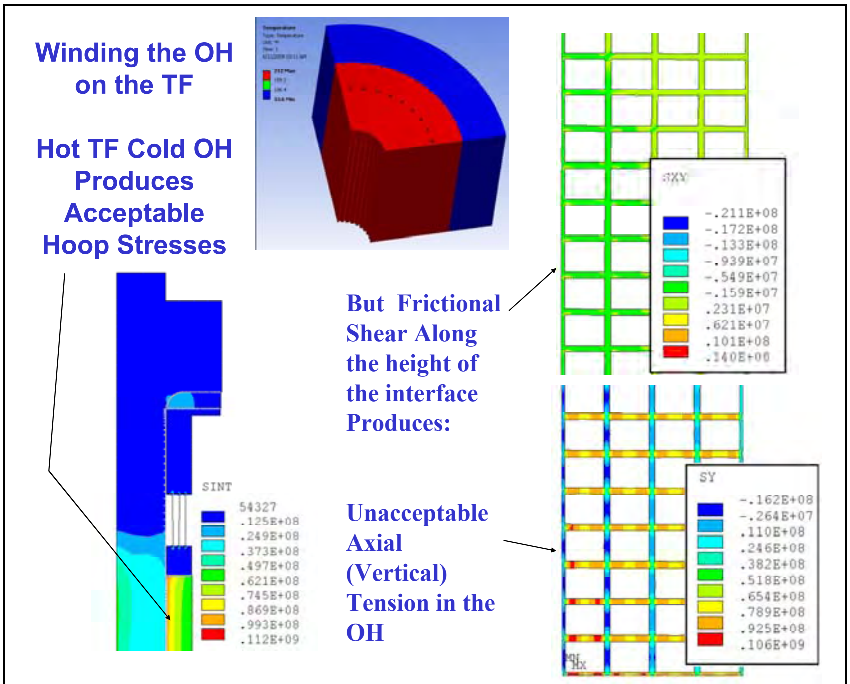

Figure 1.3.3.1-6

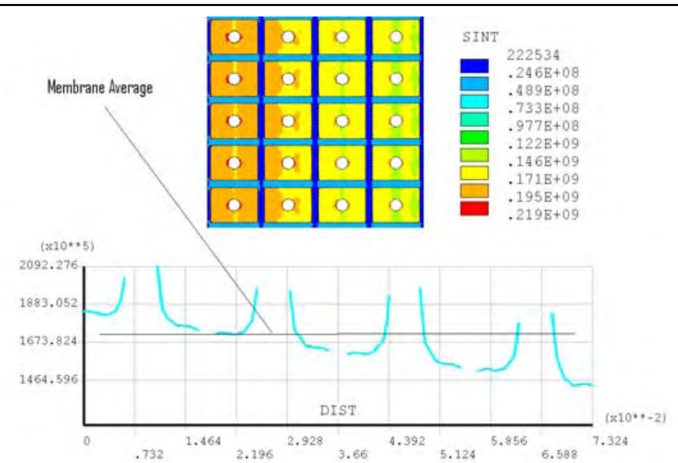

Figure 1.3.3.1 -7 Estimate of Membrane Stress or Average Tresca Across the Radial Build of the M id-Plane of the OH – with only the OH current considered.

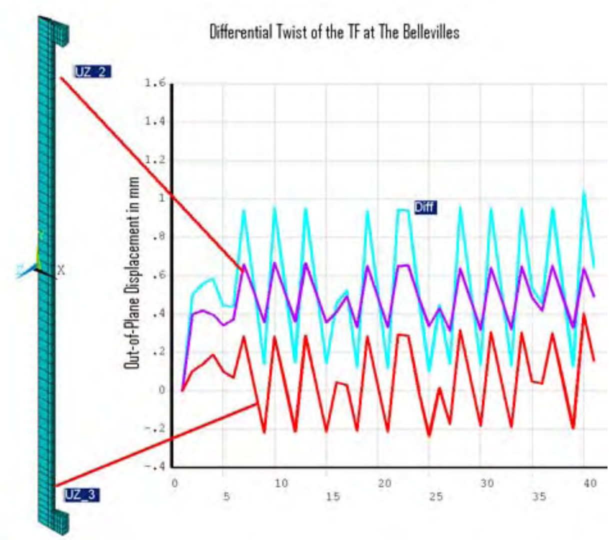

Figure 1.3.3.1 -8 Relative Torsional Displacements that must be allowed by the OH Belleville Precompression devices

1.3.3.2 OH Coolant Hole Optimization

The objective of this analysis was to estimate the anticipated temperature rise in the OH coil in the upgraded NSTX OH coil during a discharge with 24 kA current and a Tesw of 0.85 seconds. The objective also included estimating the cooling time between OH discharges as a function of pressure drop in the cooling pump. Based on these analyses the coolant channel size was to be optimized in order to keep the maximum temperature of the coil to 100° C. The pump pressure required to keep the cooling time less than 20 minutes were to be estimated.

The in-house Fcool code and the Ansys-CFX CFD code were employed to perform the analyses. The results of the analyses showed that a coolant channel diameter of 0.175 in. is optimum in achieving the required Tesw in the coil without exceeding 100° C. The results also show that a 600 PSI pump pressure can provide cooling times less than the 20 minutes required.

Coolant flow through the OH progresses in a wave that imposes a relatively sharp gradient in temperatures axially along the OH. The thermal differentials may introduce unacceptable stresses in the coil. These will be evaluated during preliminary design.

Center Stack
CS Coolant Hole Optimization, CFX, FCOOL –
(Ali Zolfaghari, Fred Dahlgren))

Optimizing the coolant channel diameter:

- Started from 0.188 in. diameter in existing NSTX OH coil. Analysis shows that increasing this diameter leads to coil temp above 100° C for I=24 kA and Tesw=0.8 s and higher.
- Decreasing the coolant channel diameter allows higher Tesw at the expense of cooling time.
- A diameter of 0.175 in. allows a Tesw of 0.85 sec. (I=24 kA) in the coil without exceeding 100° C.

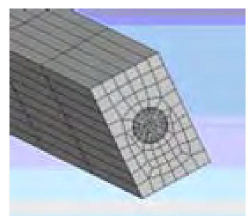

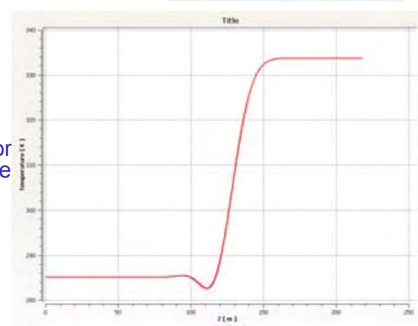

Conclusions:

- 0.175 in. coolant channel diameter is optimal. This value keeps the maximum conductor temperature below 100° C for I=24 kA and Tesw=0.85 s allowing scenarios with OH double swing.
- Using 0.175 in. coolant channel diameter, an effective pressure drop of 500 PSI is needed to keep the coil cooling time below 20 minutes.

Figure 1.3.3.1 -1

1.3.3.3 Inner PF Support Design and Analysis

A structural assessment of the NSTX CSU Inner PF coils (PF1a/1b/1c) Has been performed based on finite element simulations of the coils and their support structure. A parametric 2D ANSYS EM field model is developed and used to calculate Lorentz forces for each of the 96 equilibria (Menard version F). This also serves as a benchmark for the PPPL force calculation. Nine of these 96 cases produce the largest loads on the subject PF1 coils; faulted conditions are not addressed. The "Worst Case" loads in the design point and in the Monte Carlo Simulation are much larger than is deemed feasible to support with the spaces allotted to the inner PF supports and coolant hardware.

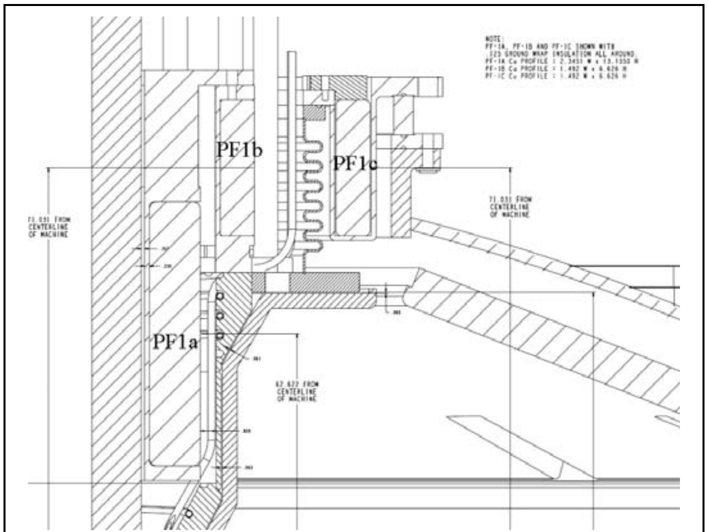

Figure 1.3.3.3 -1

The 2D stress analyses indicates that an 80 kip launching force on PF1c requires a more robust hold-down design to stiffen the open coil case. A full cover is recommended over the four hold-down clips design. The 100 kip centering force on PF1a produces some bobbin flange deformations which would benefit from a slight increase in their thickness and/or stiffening gussets. Cu and insulation stresses are generally OK, but would gain some margin with any increases to the structure discussed above.

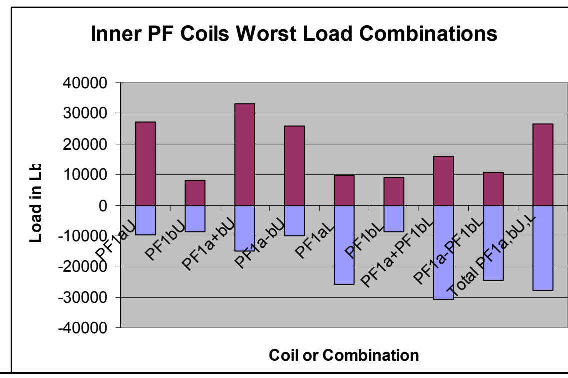

A 3D stress analysis is used to evaluate the non-axisymmetric structural elements of the support design. The model shows that the PF1a gussets which link the coil bobbin to the PF1b bobbin flange should be thickened and radiused. The net vertical loads which pass down through the three legs to ground produces some large bending stresses which must be addressed with a design/analysis cycle. The PF1c case needs a full cover with ID & OD bolt circles.

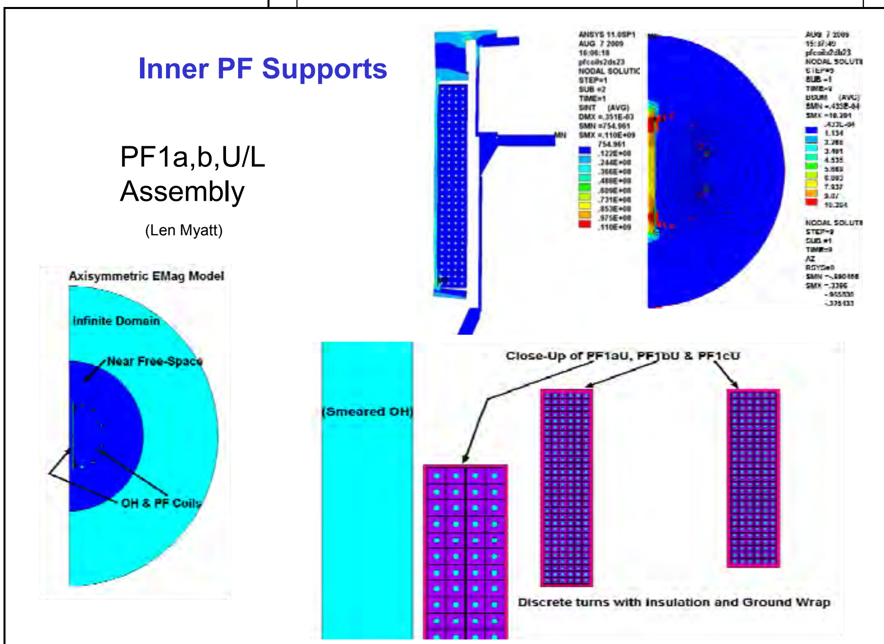

Figure 1.3.3.3 -4

Differential thermal strains can lead to high bending stresses in the shell structure. However, a more detailed and consistent thermal-stress analysis is required.

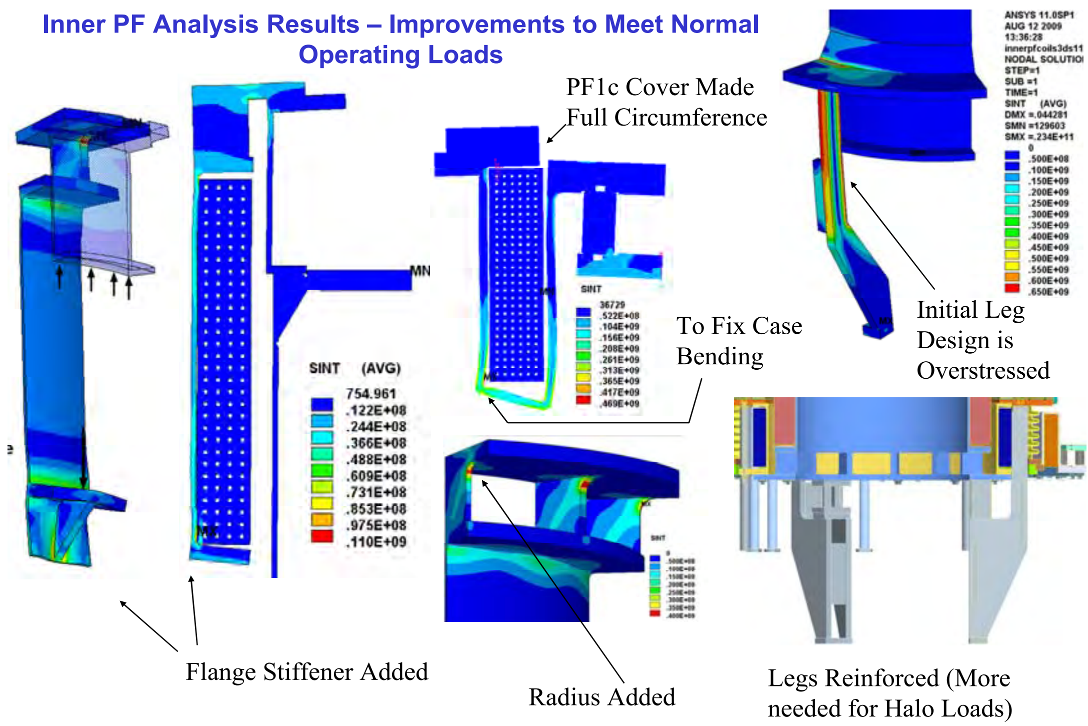

Figure 1.3.3.3 -5

1.3.3.4 PF 2 Support Design and Analysis

As of the CDR, Support of PF2 has not been performed in detail

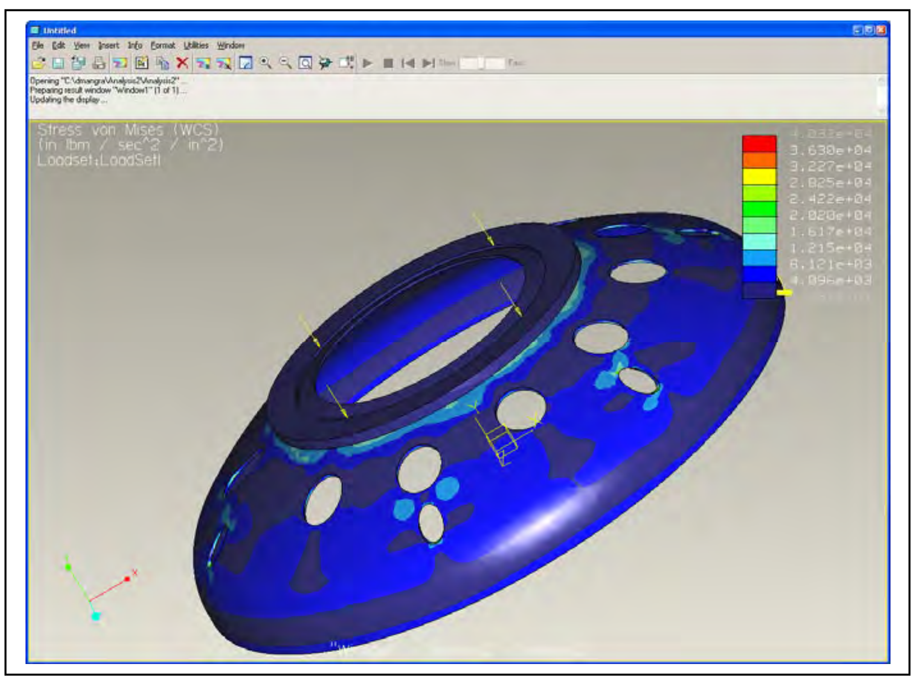

1.3.3.5. PF Coil Hoop Stresses “Worst 1

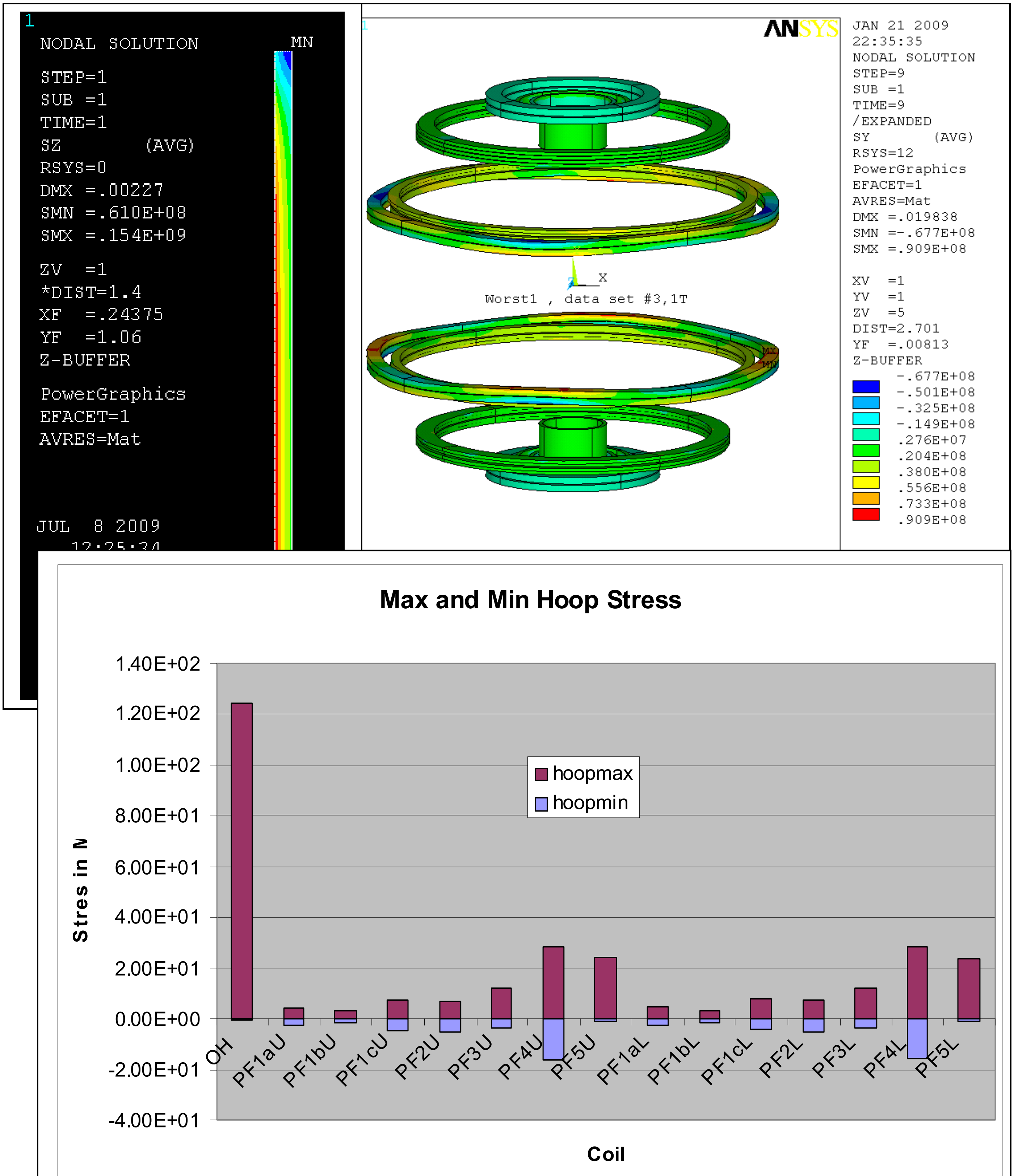

Max and Min Hoop Stresses, Ron Hatcher Influence Coefficients

1.3.3.6 Outer PF Support Cage.

The max and min vertical loads in the structural elements of the proposed outer PF support cage are presented in the figure below. These loads were developed assuming support at the bottom with some sort of column or strut either to the ground or to the vessel support columns/legs. These loads are from the Monte Carlo analysis based on worst case PF power supply capabilities. If this concept is not too excessive it would be worth considering as it de-couples the PF supports from the thermal and mechanical displacements of the vessel.

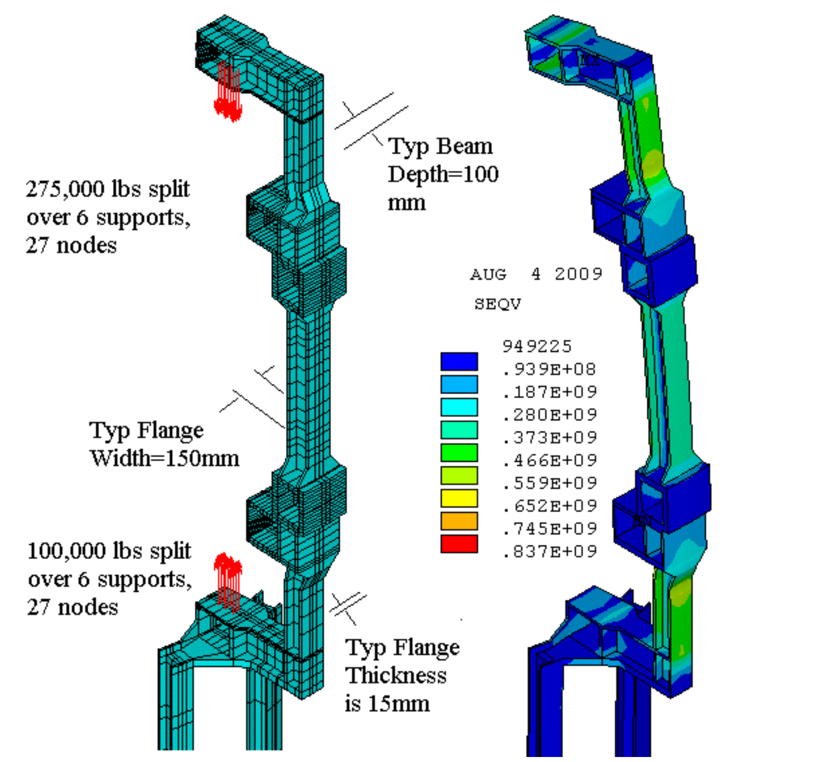

The Min value for PF3U is 140,000 Lbs from C. Neumeyer's design point. With only 6 supports, the support frame would be over-stressed – 12 may be needed

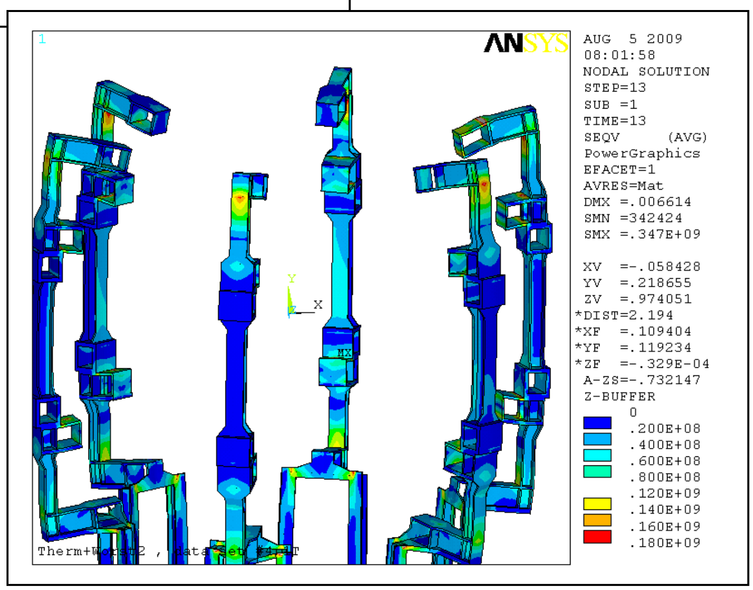

Upper Flex/Diaphram

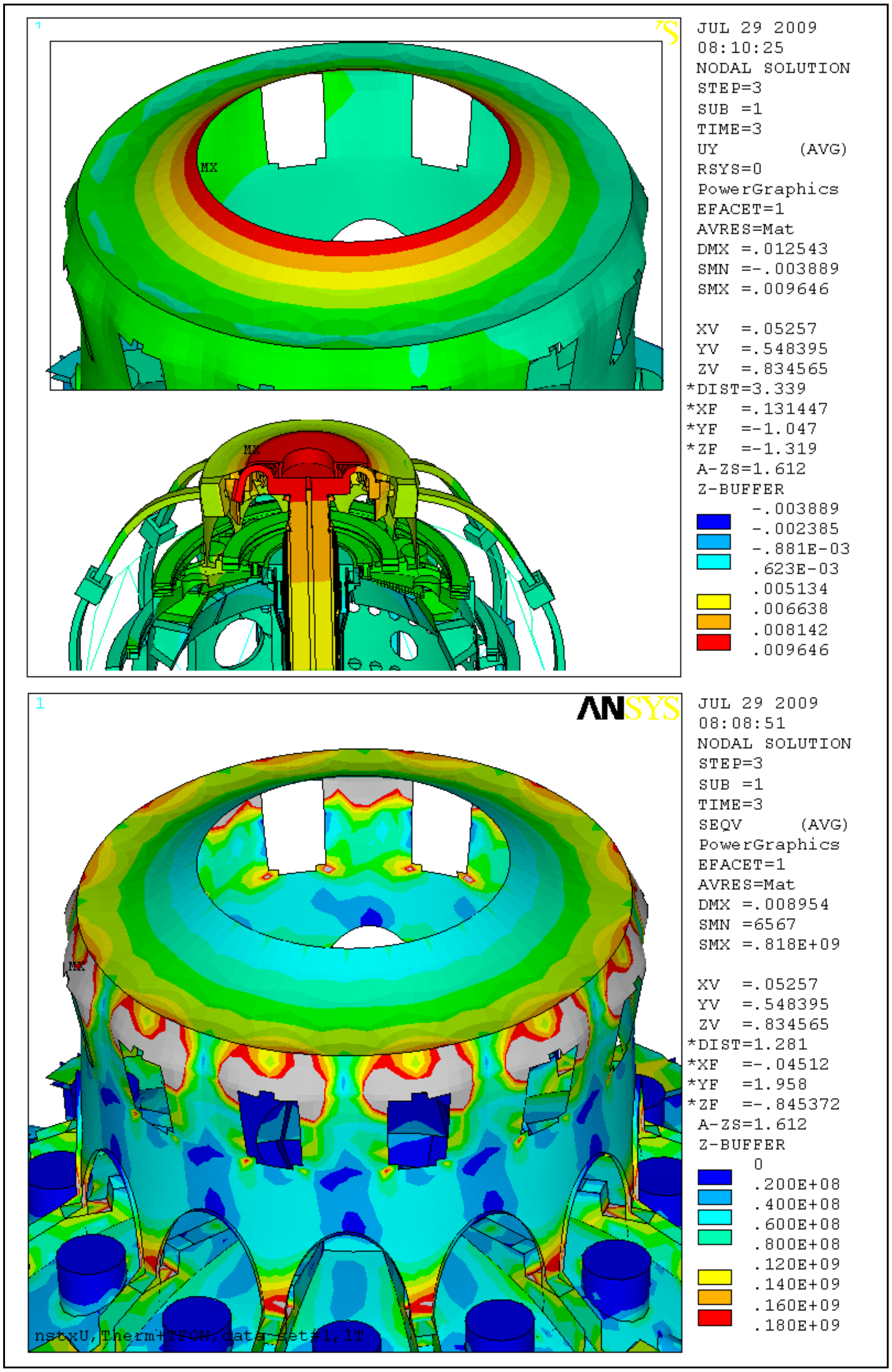

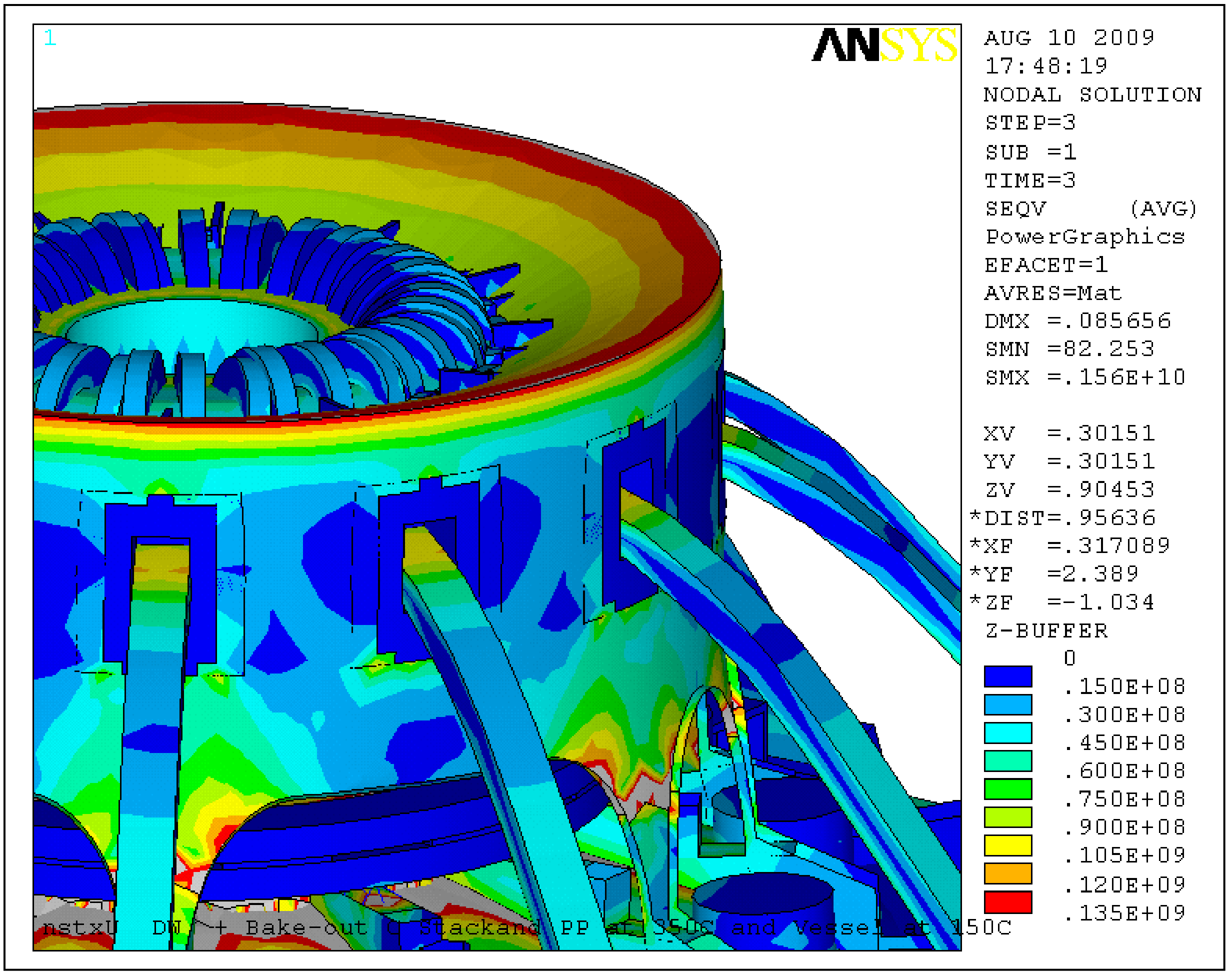
1
ANSYS
AUG 10 2009
17:48:19
NODAL SOLUTION
STEP=3
SUB =1
TIME=3
SEQV (AVG)
PowerGraphics
EFACET=1
AVRES=Mat
DMX =.085656
SMN =82.253
SMX =.156E+10
XV =.30151
YV =.30151
ZV =.90453
*DIST=.95636
*XF =.317089
*YF =2.389
*ZF =-1.034
Z-BUFFER
0
.150E+08
.300E+08
.450E+08
.600E+08
.750E+08
.900E+08
.105E+09
.120E+09
.135E+09
nstxU DW + Bake-out C Stack and PP at 350C and Vessel at 150C

2.0 Plasma Heating & Current Drive Systems

2.1 High Harmonic Fast Wave (HHFW)

The NSTX HHFW Antenna has been operating since 1999. For the 2009 run, it was upgraded from a single feed, bottom grounded strap configuration to a double feed, center grounded current strap.

A finite element electromagnetic model of the antenna was generated using the ANSYS code. The model included four of the 12 antennas, and fully represented the important in-vessel components including the straps, backplates, current straps, and Faraday shields. This analysis, performed to satisfy a CHIT from the final design review, indicated that the stresses in the critical areas near the center post of the strap, and the connection of the strap ends to the feedthroughs , were acceptable.

As part of the NSTX upgrade design, the model was run with ambient fields and plasma current representative of the upgraded NSTX. Critical Hardware details are being evaluated for the higher loads

Reference Drawings:
E-8C3B01, Rev. 2, RF Antenna General Arrangement 12 Antenna Array
E-8C3B02, Rev. 2, RF Antenna 1 through 12 Assembly

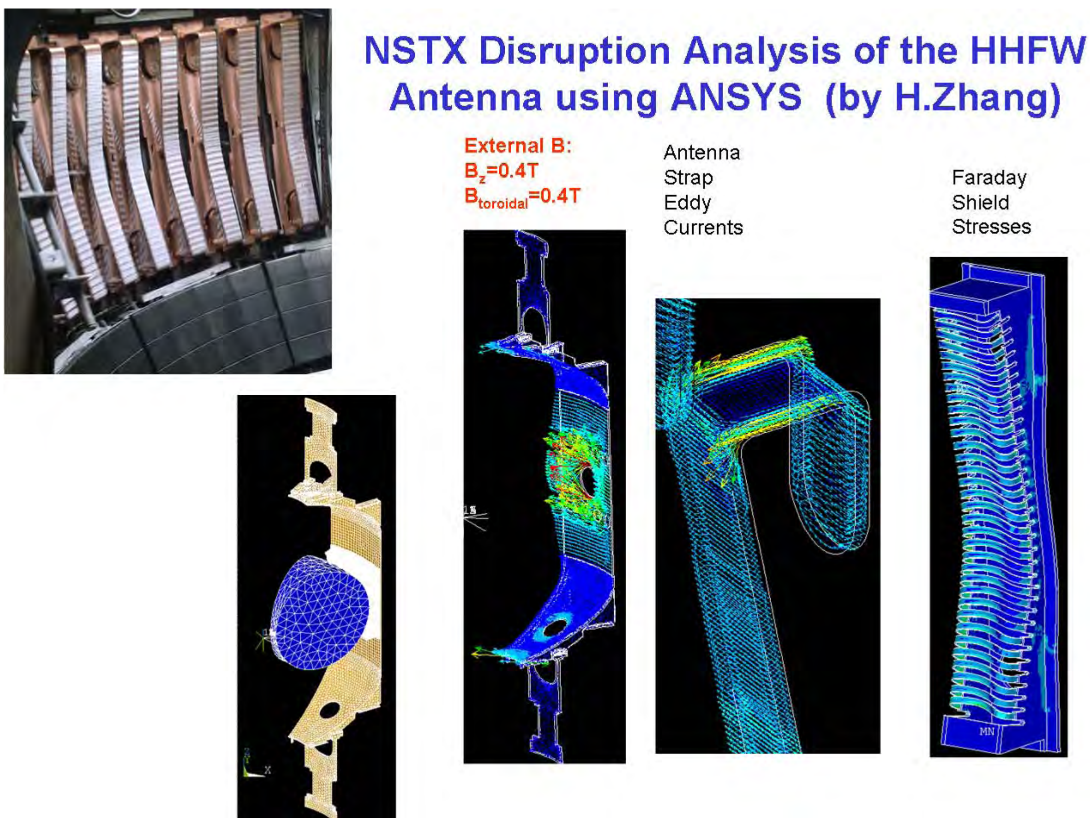

Figure 2.1-1 HHFW Disruption Analysis

2.3 Electron Cyclotron Heating (ECH)

To date, no structural analysis has been performed on the ECH waveguide. This has been carried as a task to recognize that there are many areas in NSTX that may require upgrade to survive the higher background fields,

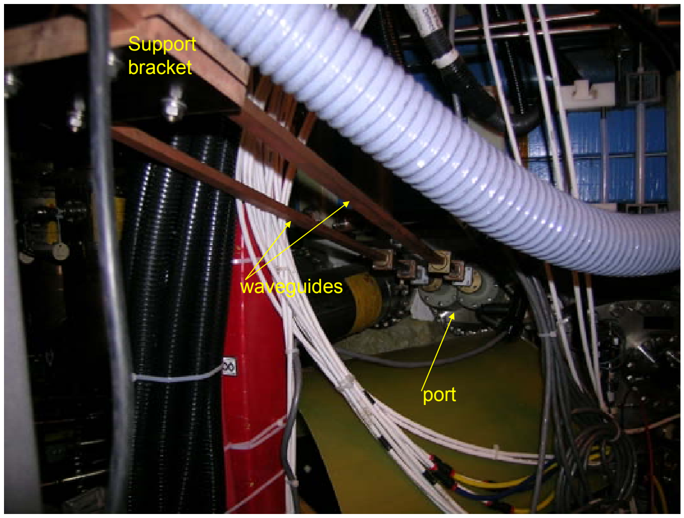

ECH Support Details

Section 7: Power System Upgrades for Centerstack upgrade

NSTX Upgrade CDR

October 2009

Lead Author: Raki Ramakrishnan

1.0 EXISITING POWER SYSTEM

NSTX power system uses the TFTR equipment in D-Site. In D-Site, there are two MG units each with a 475MVA pulsed generator with 2.2 gigajoules of stored energy. Only one MG unit is required for the NSTX with upgrades. The AC distribution system has two 13.8kv 60Hz buses and two variable frequency buses (Figure 8). There are 37 thyristor power supplies, each with two sections each rated for 1kV, 24kA pulsed for 6.6 seconds every 300 seconds (Figures 6,7). NSTX has thirteen circuits using 48 power supply sections at present. For the proposed upgrade per the GRD, we will use a total of 62 power supply sections with appropriate reconfiguration.

2.0 UPGRADES REQUIRED:

Following is the task description for the upgrade:

a) In the upgrade mode the AC system will be used as at present. Four additional AC feeders will be reactivated. The protective relays will be set and tested.
b) TF power loop will be designed to have the capability of a maximum of 129.8 kA ESW for 7.45 seconds every 2400 seconds as compared to the existing capability of 71.2kA for 1.3 seconds every 300 seconds.
c) OH power loop will be upgraded to 8kV +/-24kA as compared to the existing 6kV, +/-24kA.
d) The controls will be upgraded to a PLC system. Currently they are electromechanical relays.
e) The Firing Generator (FG) and Fault Detector (FD) for each power supply will be upgraded with state of the art system. At present the FG/FD is common for both sections of a power supply. This will be changed to have separate FG/FD control & protection for each section of the power supply.
f) A Digital Coil Protection (DCP) will be designed and implemented. The DCP will protect the coils and the coil support systems.
g) About 150 drawings will be generated/revised/changed
f) The upgraded systems will be tested and commissioned.

3.0 GENERAL:

a) NSTX machine is located in the original Neutral Beam Test Cell (currently known as NTC and by itself is small in area. Furthermore there is no free space in the basement of NTC, since the mechanical HVAC equipment of TFTR complex is all located underneath.

b) Unlike the MG Building, the FCPC Building has very limited floor space and the equipment is virtually crammed inside. Also there is no basement provided for this building. Thus the real estate availability to make changes is extremely limited and we have to design upgrades accordingly.

c) At present TF have four parallels. When we double the number of parallels the short circuit current also gets doubled – thus the forces are four times more. Hence the power loop components require appropriate upgrade. Also additional protective measures are required to be taken.

d) A detailed circuit simulation using PSCAD software, has been performed to determine that the circuit will perform as desired with eight parallel supplies. The analysis continues in order to ascertain the fault levels under various scenarios, and measures to be taken for control and protection. With eight parallels in the TF loop, it is important to have reliable and fast protection. Also appropriate values for the DC CLRs will be determined through the PSCAD analysis.

4.0 DETAILS

4.1 TF POWER LOOP (See Figure 1)

a) Four additional PARALELS of Transrex power supplies will be connected in the circuit in parallel to the existing four parallels. Nearly 6000 feet of new power cables need to be installed. Also several hundred feet of old cabling will have to be disconnected and removed. Appropriate Installation Procedures (IPs) and Statement of Work (SOWs) will be written. The job is proposed to be executed through outside contractors. As in the past this task comes under the purview of Davis Bacon requirements.

b) Each parallel will have two 1 kV Transrex power supply sections in series. One of the sections will be kept on electrical bypass thus effectively acting as a diode. This prevents the other parallel supplies from feeding into a fault across the terminals of one parallel.

c) The existing four SDS of the TF with additional parallel supplies will be used. Thus two parallels will feed via each switch. Note that the switches can handle two strings of power supply for the upgrade mode. Limited space makes it very difficult to install additional switches in the first floor.

d) The existing four TF DC Current Limiting Reactors (CLR) and the existing four OH CLRs – a total of eight CLRs will be used for the TF system with one CLR in each parallel path.

e) Install the reactors in the TF wing. For this purpose it is necessary to remove some of the equipment in the isle.
These are:
(1) The PF1a Ripple reduction Reactors are no longer required with the new design of the PF1a coils. Thus the PF1a circuit will be changed eliminating these reactors. For this purpose necessary power cabling changes will be implemented.

(2) Remove the four CICADA Racks in the middle of the isle. After the new design of the Firing Generator and Fault Detector (FG/FD), these CICADA racks will no longer be needed.

f) Installation of additional DCCTs: The basic approach is to have two DCCTs to detect the Total Coil current, and two DCCTs in each of the eight parallel paths. All these DCCTs will be used for control and protection.

g) Install power cabling for the changes within the FCPC. It will be necessary to install nearly 6000 feet of 1000mcm 5kV power cables. The space in FCPC is a premium and with proper design, this can be accommodated. Limited space makes it extremely difficult to install buses instead of cables.

h) In order to meet the requirements in the initial phase of the design of providing 129.8 kA ESW for 7.45 seconds every 2400 seconds, additional power cables are required for the TF power loop from the Transition Area to the PCTS. At present we have 5 /1/c-1000 mcm power cables in each leg of the TF. This shall be increased to 8 1/c-1000 mcm cables to handle the current. Keeping the future plans in view, a total of 6-1/c- 1000mcm cables will be released from other circuits in the run from the TA to PCTS, and connected in the TF loop. (See Figure 5)

i) Modify Power Cable Termination Structure (PCTS) for TF to handle fault currents as well as to accept additional power cables.

4.2 OH POWER LOOP (Figure 2)

a) Two additional sections of power supplies will be introduced in each of the two branches of the OH power supply. This will increase the rating to 8kV +/-24kA.
b) Two new CLRs of optimized values will be purchased and installed for the OH. (Note: The existing reactors are 2 *270uH in each of the two branches of OH. But we propose to re-size the units based on PSCAD analysis)
c) Power cabling as required will be performed.

4.3 REACTOR INSTALLATION (Figure 4)

The reactors are to be re-installed in the TF Wing as shown in the Layout Sketch.
The reactors are required to be physically moved into the space shown in the Layout sketch. However the space between the TF Dummy load enclosure (currently being used as PF1a Ripple Suppression reactors) and the TF PSS is not adequate. Since no ripple suppression reactors are required for the new PF1a coils, this enclosure will be demolished and the PF1a Ripple suppression reactors removed. Also some of the CICADA racks in the isle will be removed since these will no longer be required after the new FG/FD systems are installed.

4.4 Power Cable Termination Structure (PCTS)

The TF Bus bar in the PCTS shall be provided with additional braces with insulators to withstand the additional short circuit forces.

4.5 **<u>DC CURRENT TRANSDUCERS (DCCT)</u>**

a) Two DCCTs in each of the eight branches will be installed within FCPC. One of these sets of DCCTs are for control purposes to establish current balance in the branches. The second set will be used for protection. There are eight existing DCCTs in the TF loop. Additional eight DCCTS (+/-25kA) will be procured and installed.

b) Two fiber optic DCCTs – range +/- 160000Amps – will be purchased and installed in the TFTR Test Cell Basement. These two DCCTs will be used to control and protect the TF Coil.

4.6 HARDWIRED CONTROL SYSTEM (HCS)

Hardwired control system is currently designed with electro-mechanical relays. This is clearly out of date and has inherent time lags. With the design of a new FG/FD, it is appropriate to have the HCS changed to a PLC based system. This design is in progress.

4.7 FIRING GENERATOR (FG) and FAULT DETECTOR (FD) (See Figure 3)

The FG/FD of the TF and OH rectifiers (total of 20 supplies) will be changed. The new FD/FG will provide reliable fast acting system to reflect the new requirements.

4.8 ANALOG COIL PROTECTION SYSTEM (ACP)

Currently NSTX coils are protected using ACP which has been designed in-house. ACP has been successfully operating protecting the coils. Necessary changes in the ACPs will be made to reflect the changes in the coil system. The ACP will trip the power supplies by suppressing the rectifiers and bypassing the load current.

4.9 DIGITAL COIL PROTECTION SYSTEM (DCP)

A DCP will be designed and implemented. The DCP will provide coil protection. In addition, it will also incorporate the protection of the coil support system. Suitable algorithms will be developed based on analysis of the coil thermal characteristics and forces generated in the coil support system by the coil currents. The hardware will be designed to implement the algorithms. Software will be written and implemented. The DCP will invoke the suppression of the rectifiers if excursions beyond set limits are detected.

4.10 KIRK KEY SYSTEM CHANGES

Kirk key changes as required will be incorporated to reflect the new configuration. PPPL has a well designed Kirk Key system which is our first and important step to insure safe operation.

5.0 **COST & SCHEDULE**

A Work Breakdown Structure has been developed for the project under which the Power System is classified as WBS5. Details of the breakdown of the WBS elements with associated cost are given in the table below.

Cost has been developed based on the following:

- Prior Experience
- Similar tasks previously executed
- Input from Vendors

- Engineering Judgment
- Other aspects
- Costs are essentially center -of-the-error bars
- Areas of risk judged ; constraints noted
- Contingency in the spreadsheet based on analysis of risks, general spread in quotes

WBS BREAKDOWN				Cost k$	Cost k$
51	AC POWER			67.8	
	511	Experimental AC Power			67.8
52	AC/DC CONVERTERS			53.3	
	521	Reactivate Converters			53.3
53	DC SYSTEMS			1739	
	531	FCPC DC Systems			
		531.1	NSTX PF1a PS loop changes		255
		531.2	TF PS Power Cabling/Changes		879
		531-3	Removing Cabling		74.9
		531.4	DC Reactors		355
		531.5	TA Cabling Changes		53
	532	TA to NTC and NTC changes			
		532.1	PCTS Changes		122.5
54	CONTROL & PROTECTION SYSTEM			5873	
	541	Electrical Interlocks			733.7
	542	Kirk Key Ingterlocks			81.9
	543	Real Time Control			169.2
	544	PC Link/FD/FG Changes			2813
	545	Instrumentation			622
	546	Coil Protection			194
	547	Machine Protection System			1259
55	System Design & Integration			612.9	
	Ø551	System Design			442.7
	Ø552	System Testing			170.2
FY09	Actual FY09			386	386
GRAND TOTAL				**8732**	**8732**

Note: M&S – 2242k$; Subcontract:1012k$ included above

Schedule:

The schedule has been developed based on the overall project requirements, run plans and shutdowns.

Section 8: Overview of Second Neutral Beam

NSTX Upgrade CDR

October 2009

Lead Author: Tim Stevenson

NSTXU NBI BL2 CDR Overview

For the NSTXU Conceptual Design Review, an overview of the NBI BL2 project was presented. The NBI BL2 project has been divided into sections covering general requirements, NSTX Test Cell general arrangement and equipment relocations, the decontamination effort status and progress to reuse a TFTR BL, and the technical design work necessary to add the second beamline in the NTC, connect services, connect power and control, and provide an interconnecting duct and armor in the vacuum vessel.

The general requirements document GRD indicates the need for injected neutral power in keeping with the existing specifications and operating parameter space of the TFTR and NSTX Beam system. The aiming angles require tangency radii of 110, 120, and 130 cm for the new beamline. This requirement drove the need to make changes to the vacuum vessel and Bay K. This conceptual design accommodates these aiming angles.

At present, the NSTX device uses one Neutral Beam Injection (NBI) beamline (BL) with three sources for NBI experiments injecting power up to 7.4 MW as requested into NSTX plasmas. This beam injection has provided numerous benefits in heating, fuelling, and adding rotation to NSTX plasmas, and has provided diagnostic information intrinsic to the operation of CHERS and MSE. The addition of a second NBI beamline would provide additional power, fuelling, rotation, diagnostics data, and wider tangency radii aiming options. The upgrade would also well match and test the plasma current drive benefits of the proposed upgrade to the Ohmic Heating coil considered elsewhere in project documents.

The NSTX NBI 2nd Beamline Upgrade would add a second BL to the NSTX machine in a V arrangement. The existing BL, which resides in the Northeast (NE) corner of the NSTX Test Cell (NTC), would remain as presently aimed and situated. The additional BL would reside in the Northwest (NW) corner of the NTC and would be aimed at tangency radii more outboard than the first BL.

This upgrade requires the rearrangement of machine equipment and systems to clear the appropriate floorspace for the additional BL and its paraphernalia in the NW area of the NTC. This upgrade requires relocation of various diagnostics so the 2nd BL can make use of the Bay K port on the midplane of the device. This port has already been sized for NBI. Due to the more outboard aiming angles of the 2nd BL the port will require some in situ modifications.

In large part, the 2nd NBI upgrade scope tracks the original NBI upgrade installed on NSTX in 1999 and 2000. This scope includes refurbishing three NBI power systems, one for each source, and installing the associated cabling to the NW location in the NTC, refurbishing three ion sources for operations, refurbishing a TFTR era BL, relocating it and supporting it in the NW area of the NTC, and commissioning it for operations. Auxiliary services will be upgraded to provide water, cryogenics, vacuum, pneumatic, and SF6 services.

A new interconnecting drift duct design and fabrication effort will be required to attach the 2nd BL to the torus vacuum vessel. The beam portion of the design is much like the first, including a new bellows to account for bakeout expansion of the vessel; however, the larger tangency radii desired for the second beam will require modifications to the existing design of duct and port to clear outer legs and provide beam free aperture. Also, the Torus Vacuum Pumping System will be connected to the new duct and its TMPs will be underslung to fit into existing floor space. The existing armor design will be moved to center on Bay H. Armor tile modifications will be required in the NSTX vacuum vessel to accommodate the additional beam trajectory overlapping regions.

New scope required for this 2nd BL upgrade also includes the decontamination of the TFTR era BL prior to refurbishment. The original beamline, which had been used as an ion source test stand, was selected for the first beam upgrade because it had not been used with tritium. The next beamline will have seen active service on TFTR during the TFTR DT campaign. These beams have been on continuous air purge to ameliorate tritium since TFTR was shutdown in 1997. This decon effort has started and shows steady progress. This decon work takes place in the Test Cell where the TFTR BLs are stored. Techniques used during the very successful TFTR DT experimental campaign and the TFTR Decontamination and Decommissioning project will be used to remove as much residual tritium contamination as possible prior to use on NSTX.

Existing infrastructure (stacks and elephant trunk stations) and existing HP coverage is covering this decon effort and the decon of sources. This project may well monopolize the existing staff so some HP staff augmentation may be necessary for appropriate coverage. Additional stack and elephant trunk stations will be required in the NSTX Test Cell and South High Bay areas to allow work on components with minor residual contamination.

This upgrade will bring the NBI power capability to 18 MW. The existing BL has been operated to 7.4 MW at 100 kV but the original TFTR capability of 110 kV and 9 MW was retained in the original NSTX upgrade. This capability would also be retained for the second beamline, raising the total power available to heat plasmas to 18 MW injected.

This upgrade reuses an extensive amount of mothballed NBI equipment that has been preserved as site credit, including the BL, power systems, legacy spare sources from TFTR, and fixtures and support equipment. The existing and operating cryogenics Helium refrigerator will also supply the second NBI making use of some spare capacity.

Further, the existing ion source refurbishment facility has been in operation for the life of TFTR and NSTX and would continue to provide sources as needed for both beamlines for future operations.

The Neutral Beam Injector Upgrade for NSTX reuses the technology of the Tokamak Fusion Test Reactor (TFTR) Neutral Beam Injector. The NBI Upgrade reuses spares and existing equipment where practicable. This upgrade includes the design, procurement, fabrication, assembly and construction activities associated with adding a three source neutral beam injector onto the NSTX machine in the NSTX Test Cell (NTC), located at D site, Princeton Plasma Physics Laboratory.

All work shall comply with applicable DOE Orders, PPPL policy and procedures, the Environment, Safety, & Health Manual ES&HD 5008, NSTX Project Management requirements, and D site Caretaking procedures. The NBI Upgrade project shall utilize Integrated Safety Management guiding principles and core functions using a graded approach to implement all work.

Section 9: Second Neutral Beam Interface to Vacuum Vessel

NSTX Upgrade CDR

October 2009

Lead Author: Craig Priniski

NSTX Neutral Beam 2 Interface

Neutral Beam 2 Interface Overview:

The larger target tangency radii for the second neutral beam present some unique challenges in designing a vacuum vessel port and accompanying beam duct to carry the beam into NSTX. The vacuum vessel was originally configured with a second neutral beam-sized rectangular port at identical tangency radii to the first at Bay K. Unfortunately, this port will not accommodate the wider angle required to meet the physics goal of providing neutral beam heating at 110, 120, and 130 centimeters tangency radii. The direct beam path passes through what is currently the edge of the nozzle/vessel joint (for comparison the original beam is centered at 60 centimeters radius). Additionally, in order to free up a diagnostic port on the machine and free floor space for the second neutral beam box the current Torus Vessel Pumping System (TVPS) was moved to a location under the new beam duct. The goals for the interface design were to solve the bay K geometry problem, to redesign TVPS, and to provide accommodations for the system to fit under the new beam duct.

Vacuum Vessel Modifications:

Structural Issues

Even after optimizing the incoming neutral beam angles, part of the beam still clipped the original nozzle opening, which required opening up the bay K port towards the 24” diagnostic port, bay J, adjacent to K. The result was a keyhole-shaped opening with a 1” strip of metal connecting the upper and lower regions of the vacuum vessel. An effort was made to stiffen this area using internal gussets; however, Ansys analysis showed the stress in the vessel metal was still unacceptable. Additionally, the modified ports were approximately 1” from the main beam footprint too close to survive un-shielded.

Vessel “Cap” Design

In order to satisfy both the problem physical proximity of the vessel to the beam and to provide additional structure, the vessel was extended radially outward around the Bay J-K area. This solution gave more physical separation between the J and K port openings, and the added frame around the opening helped to carry load around the area rather than through it (see figure 1). This configuration also moved the edges of the nozzle outside the expected area of significant neutral beam energy. Further analysis has shown that the additional structure provided from the cap, outweighs the loss of material from the cutout needed to install the cap. Before the vessel is cut, either the finished cap and/or additional temporary supports will be welded to the vessel base metal to minimize any stress-induced distortion during machining. Bay K diagnostics will need to be removed for the upgrade. Bay J’s port cover and diagnostics will be removed and reinstalled in a new port relocated 4.88” further outboard with minimal impact to diagnostics. The Resistive Wall Mode (RWM) coil surrounding J and K will need to be removed and modified and reinstalled once the work on the cap is complete.

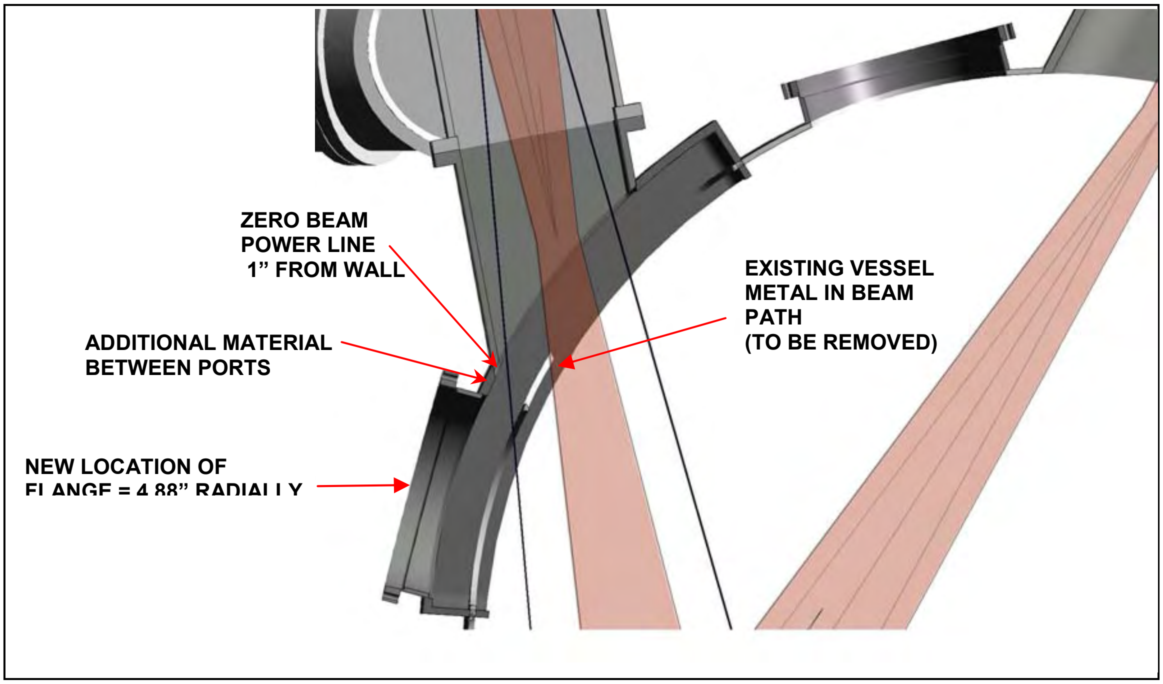

Figure 1: Vessel Cap with Current Vessel

Neutral Beam 2 Transition Duct

The transition duct has three primary functions: 1. Extend the NSTX vacuum vessel to the Neutral beam box, thereby providing a clear path for the neutral beam sources, 2. Provide vacuum, electrical, and mechanical isolation between vacuum vessel and beam line systems, and 3. Create provisions for connecting to a new TVPS system. The duct is split into two portions - a permanently bolted-on port extension for the vessel and a demountable transition duct adapting the 40” diameter neutral beam aperture down to a more conformal rectangular port to get through the Toroidal Field (TF) coils. The transition piece also mates to the TVPS ducts on the bottom of a 40” diameter spool piece.

Transition Duct

The transition duct begins at the exit of the neutral beam box with a new 40” VAT gate valve serving as the isolation valve separating the beam from the NSTX vacuum as needed. In front of this configuration is a set of 40” diameter welded bellows, collapsible to facilitate assembly and removal (see figure 2.). Next, is a large self-supported spool piece. This portion of the duct has two 14” O.D. down-comers that connect up to the TVPS turbo pumps. The face of the spool piece is capped off with a circular flange containing a ceramic break to electrically isolate the beam line from NSTX proper. This flange also starts the transition to a rectangular cross section for the beam. The final component in the transition duct is a large welded rectangular bellows. This set of bellows absorbs any relative motion of the NSTX and vacuum during bakeout. The design of the bellows is a duplicate of the bellows used successfully for 9 years on the first beam line duct. The final flange on the bellows mates up with its partner on the end of the port extension.

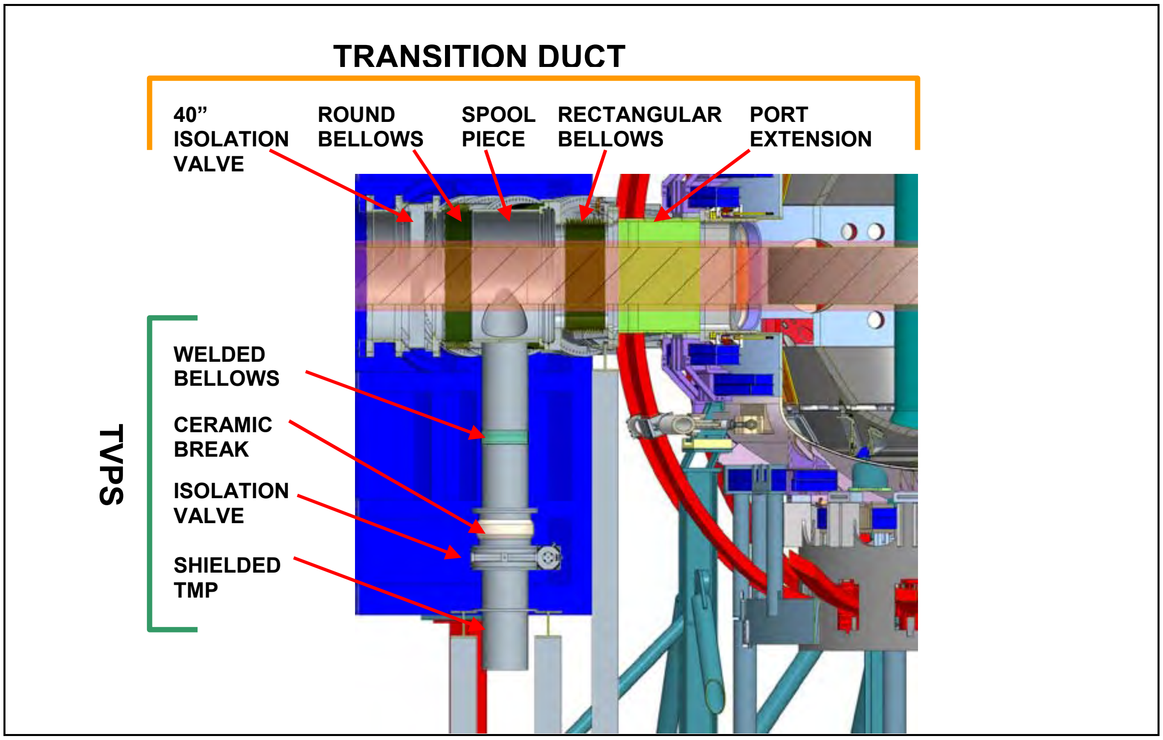

Figure 2: NB2 Transition duct and TVPS pumps below

Port Extension

The bolt up port extension adapts from a TFTR standard neutral beam flange down to a slightly narrower version that mates with the welded on J-K cap (see figure 2). The three neutral beam sources converge in this duct so it is possible to make it narrower than the sections further outboard. The port extension has a paneled, welded duct that conforms to a TF coil that is within 6” of the beam path, making the use of a bellows or flanges impossible in this region. In addition, the extension provides room for tangential diagnostic ports since it will be left in place for maintenance and during operations.

Torus Vessel Pumping System

The intent of relocating the pumping system was two-fold, to maintain independent torus pumping (without beam line pumping) and to free up mid-plane access for diagnostics. The current TVPS design is located at the end of a 17’ long, 24” diameter drift duct that provides magnetic isolation to the turbo pumps near the far end. With the inclusion of a second neutral beam box and supporting equipment in the test cell, there was simply no room to reuse this duct. The present solution has two downcomers, one for each turbo pump, under the spool piece of the transition duct. Each downcomer duct has a welded bellows, ceramic break, and isolation valve for its associated pump, providing the necessary electric and mechanical isolation from the other beam systems (see figure 2). Two smaller sets of bellows and breaks are attractive in that the 14” size becomes a commercial item rather then a custom-engineered part. In addition, the shorter and wider free path back to the torus also provides significant gains in molecular flow conductance, going from around 1000 l/s to close to 4000 l/s. This permits us to upgrade the current 1500 l/s pumps to a pair of 3000 l/s pumps since we are no longer limited by duct conductance. The only drawback to the relocation of the turbo pumps is that the proximity to NSTX coil fields will require magnetic shielding of the pumps. The field in this area is approximately 200 gauss. Most manufactures require 50 gauss or under which should be easily achievable with a Mu metal shield surrounding the pumps (see figure 2).

Section 10: Beam Relocations and Services

NSTX Upgrade CDR

October 2009

Lead Author: Martin Denault

Beam Relocation

The NSTX Upgrade Project requires the relocation of TFTR Neutral Beam 4, now called Neutral Beam 2, into the NSTX Test Cell. The ancillary equipment for this beam must also be moved to new locations. The current plan is to move all components through the door between TFTR Test Cell and the NSTX High Bay area. This will require the removal of the shielding lintels from the doorway and the construction of a steel plate road way. The beam box and lid (in stand) will be moved in separately on roller dollies and individually lifted over the south shielding wall. Clearances for this movement path have been verified and found adequate. Flanges and internal beam components will also be brought in separately and assembled on the beam box. The High Voltage Enclosures will be lifted out of the TFTR basement in sections, follow the same path as NB2, and be reassembled in the NSTX Test Cell.

Beam Services

The NSTX Upgrade Project requires additional services to be brought to the NB2 in the NSTX Test Cell. These services are High Voltage Enclosure Cooling Water, Ion Dump Cooling Water, Ion Source Cooling Water, SF6, Liquid Nitrogen, Liquid Helium, Vacuum Backing, and a Gas Injection System.

HVE cooling water will come from 3 existing pumping skids that will be refurbished. Pipe will be run from the skids, through the Pump Room and MER, and through penetrations in the Test Cell floor. (See: Green path in attached layouts.)

Ion Dump and Source cooling water will require new pumps to be purchased. Pipe will be run from the pumps, through the Pump Room and MER, and through penetrations in the Test Cell floor. (See: Red and Blue paths in attached layouts.)

SF6 piping will be teed from its current termination point in the Test Cell, over head to a new tap point centralized to NB2 and new HVEs. Valving will be utilized to maintain existing tap point. (See: Yellow path in attached layout.)

Liquid Nitrogen will be teed from existing piping and run around the north side of the test cell to the top of NB2. (See: Orange path in attached layout.)

Liquid Helium will be run down the Eastern wall of the TFTR Test Cell and penetrate into the NSTX Test Cell. This path was chosen to minimize heat loads on the system. A warm return line will be added to the South wall of the TFTR Test Cell, allowing for the continued use of the existing refrigeration system. One beam will be cooled then held while the other is cooled. (See: Blue, Green and, Pink paths in attached layout.)

Vacuum Backing lines will be run from the turbo pumps to the existing backing pumps. (See: Purple path in attached layout.)

Gas Injection System will be moved from its current location to outside the North end of the NSTX Test Cell. (See: Dark Green path in attached layout.)

Walk-throughs have been completed for the piping runs of all systems and the routes are mapped. Heat and flow calculations have been performed for water systems and the pipes, pumps, and runs sized accordingly. Cryogenic heat loads have been minimized and found to be acceptable. All planned penetrations have been identified and locations have been approved.

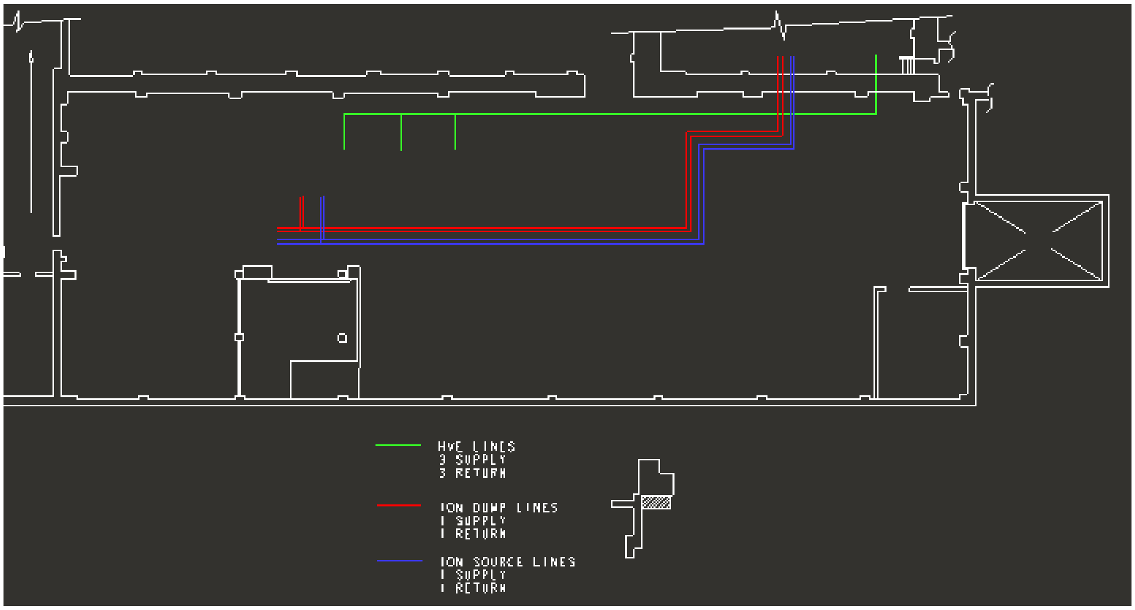

Pump Room

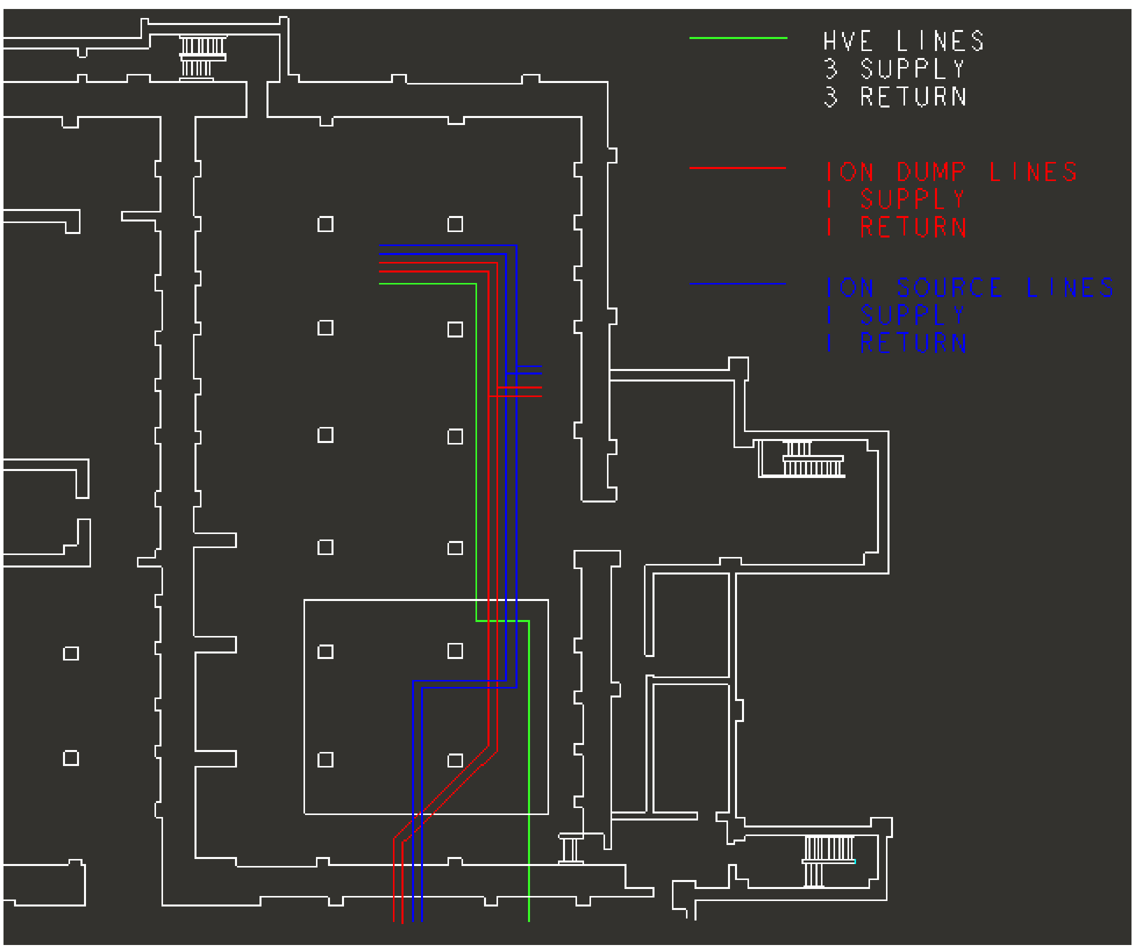

Mechanical Equipment Room

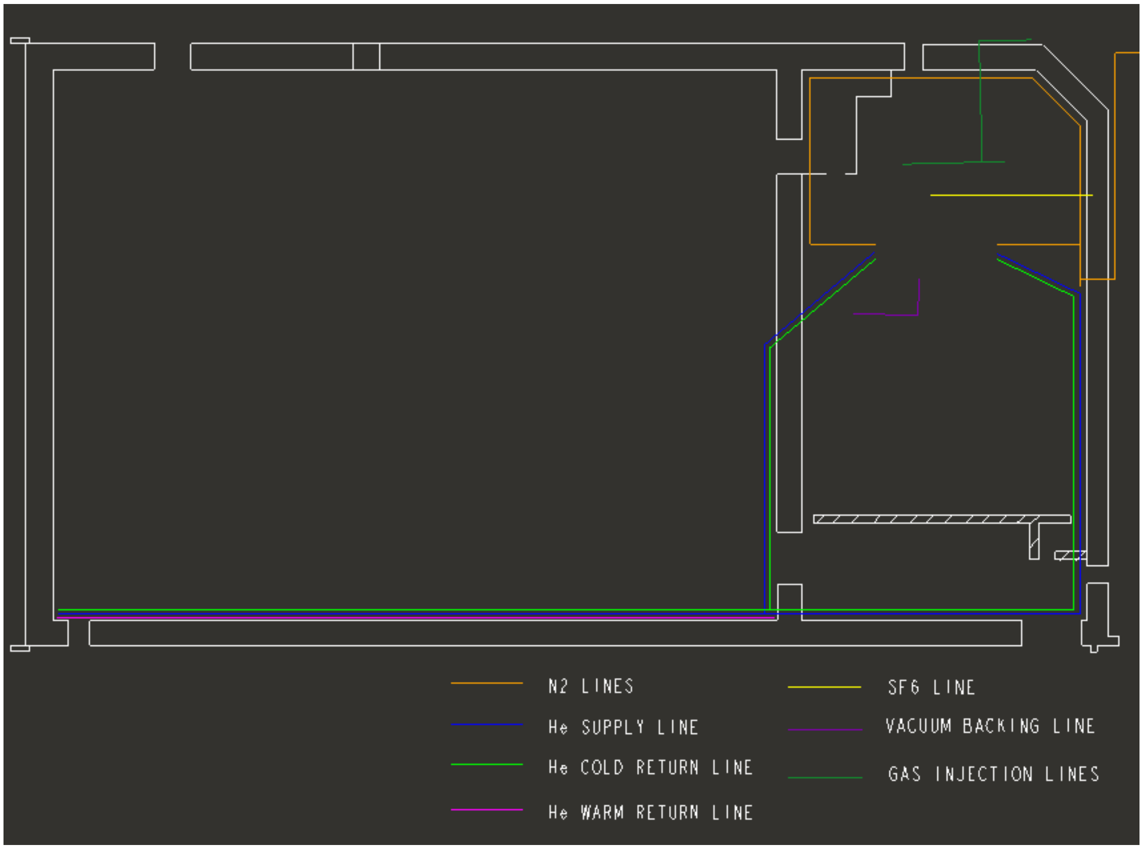

Test Cell

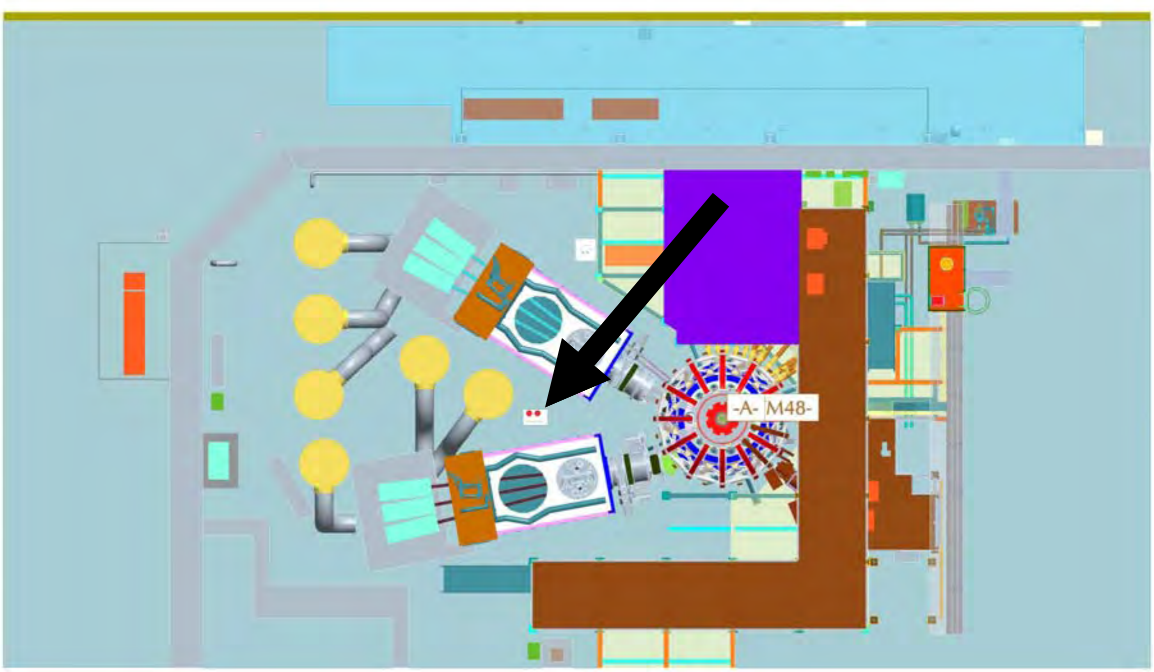

General Arrangement

Section 11: NB2 Armor

NSTX Upgrade CDR

October 2009

Lead Author: Kelsey Tresemer

CDR Report: NSTX-U NBI In-Vessel Armor

The current plan for upgrading NSTX's NBI In-Vessel Armor is to reuse the existing armor array by relocating it to catch all six sources, updating the materials of the carbon tiles and backing plates, and improving the armor's mounting system for accessibility and the certain increase in mechanical loading.

To establish a basis for comparison, we looked at the present, FDR-defined specifications for the NSTX armor. It was designed for a single beamline, three sources, with a worst case "Fault" condition of 2.8 kW/cm^2 for 0.75 seconds per source. Its thermal tiles are made of isothermal graphite or ATJ. After performing an initial thermal analysis using ALGOR, the consequent temperatures and thermally induced stresses were found to be 1985.07 deg C and 109.5 MPa, respectively. This defines an improbable set of conditions which, upon occurrence, would not destroy the armor, but would warrant physical inspection. With the upgraded armor, we sought to meet this same concept of functionality.

To accommodate the addition of the second neutral beam line, the plan is to move the armor array counterclockwise in order to center all six sources on its surface. To verify this concept, three different aspects were examined: beam "footprint" fit on armor array, heat flux overlap, and the efficiency of between-shot cooling using the existing cooling system.

The spread of the source profiles or "footprints" is well-behaved, obeying an elliptical edge-divergence of about 0.5 degrees horizontally and 1.5 degrees vertically. This has been empirically confirmed by observation of armor striping on the present array. (Figure 1) This image shows the lack of white lithium deposition due to the high surface temperature of the tiles where they are being struck by neutral beam sources during aiming and MSE calibrations. Taking this dispersion behavior into account, all six sources were laid across the armor to confirm that they did indeed fit. (Figure 2)

Figure 1: NSTX Armor array showing beam striping due to neutral beam sources.

The beam profiles were split into two distinct areas: the core beam which represents the area with the highest power concentration (~80% of total source power), and the divergent beam which represents the area of high beam scatter, (~20% total source power). With the addition of the second beamline, areas of overlap were created on the armor (Figure 2), which creates larger power densities in those zones. Preliminary analyses of these zones or “hotspots” show that the max temperatures and surface stresses make ATJ an insufficient shielding material. We propose replacing the affected tiles with carbon-fiber composite, a material better equipped to handle the temperature and thermal stresses, and augmenting the stainless steel backing plates with molybdenum in the midplane areas behind the hot spots to give thermal aid. Additionally, we will provide a redundant plasma current interlock to further guard against the fault condition via engineering and administrative control. It should be noted that although the current plan is to design the armor to survive such a fault condition, if such an unlikely event would occur, physical inspection of the armor’s integrity would be required.

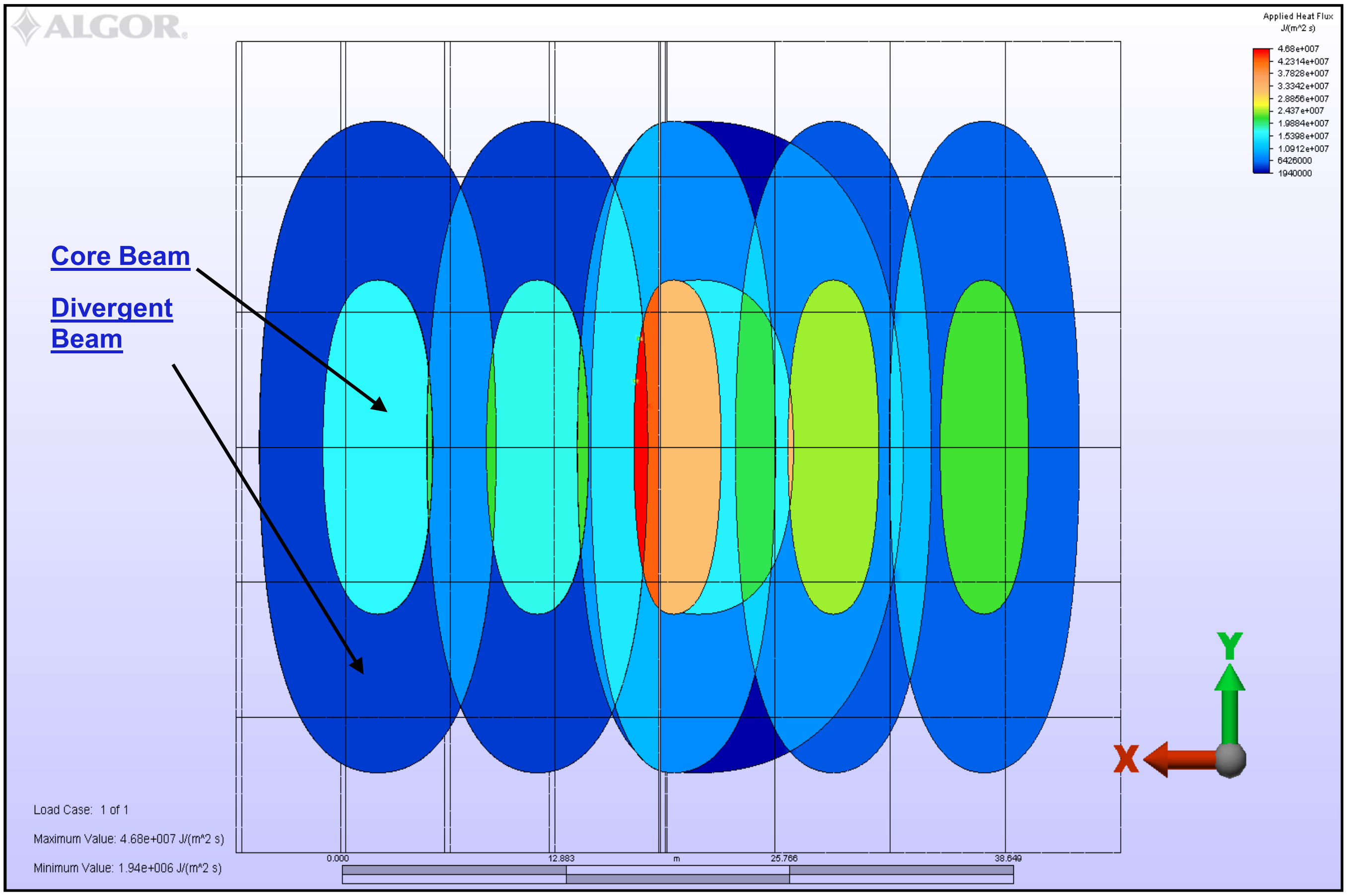

Figure 2: Overlapping beam profiles, showing placement and heat flux.

A preliminary thermal analysis was performed to confirm that the concept to reuse the present in-armor cooling system was viable. A simple, "back of the envelope" analysis with a slice of armor and backing plate, determined the time constant for cooling. Initial results produced a time constant of about 77s, which, since the between shot time for the upgrade was increased from 900s to 1200, suggests that the present cooling system is sufficient. This analysis will be repeated in more depth and the results updated for the PDR.

With the relocation of the armor, we have the opportunity of improving the existing armor design for accessibility as well as the increasing mechanical loads. After the move, the armor will be almost centered on bay H, allowing access to all of the center mounting points. However, as an added improvement, all of the side mounting points on the array can also be accessed via bays G and I. This convenience makes installation and repairs much easier to accomplish as well as allowing room for an increase in fasteners, if needed.

In order to give an estimate of the increase in mechanical loads on the armor due to an increase in electromagnetic forces, we looked at the previous FDR specifications, which, for a 16 mount-point array, stated the conservative number of 13,375 lbs/mount (214,000 lbs total). If we assume that this number will double for the upgrade, we see an estimate of 26,750 lbs/mount, which is an acceptable load. Further analysis is underway and again, we will update these figures for the PDR.

In conclusion, the plan to relocate and reuse the armor array to accommodate the second neutral beam line seems viable. We will make the needed materials improvements, such as changing thermal tile type to carbon-fiber composite and augmenting the backing plates with more material. We will provide increased engineering and administrative control by adding an additional plasma interlock to guard against the fault case. Upon completion of the cooling system analysis, we will verify its re-use for both beamlines and, once the mechanical loads due to electromagnetic fields are confirmed, we will be able to make the appropriate alterations in the mounting scheme.

Section 12: NB2 Power and Controls

NSTX Upgrade CDR

October 2009

Lead Author: Tim Stevenson

Second Neutral Beam Power System

The NBI Power System (NBPS) design for the NSTX upgrade beamline follows the same pattern as with the original existing BL and the TFTR NBPS. The Neutral Beam Ion Source requires power for filament, arc, accel grid, gradient grid, and decel grid, and for the BL bending magnet. The existing TFTR BL4 NBPS for sources AB&C are reusable in their entirety for the upgrade. Thus, three NBPS lineups will be reactivated and updated to the present status as with BL1.

The high voltage Accel and Gradient Grid power require that the N4 ABC switchyard gear be reactivated. These systems are well maintained and available. The surge rooms and modulator/regulators are also available. The mod/reg uses a high voltage switch tube which is a power tetrode originally developed by RCA for TFTR. These tubes provide switching and regulation up to 120 kV and 70 Amperes. The gradient grid dividers will be updated to the present 25 k-ohm air cooled resistive divider design. Some on board electronics will be updated also. These systems feed high voltage to the source on an armored triax cable to the High Voltage Enclosures in the NTC which then communicate that voltage to the ion source via the Transmission Line. The triax cables will be new installations. The HVEs and transmission lines will be reused.

The low voltage arc and filament supplies have useable conductor runs to the TFTR Test Cell Basement. For the upgrade, a junction box will be provided. New conductors will be installed from the junction boxes to the HVEs in the NTC. New Decel and Bending Magnet cables will also be installed to the new BL.

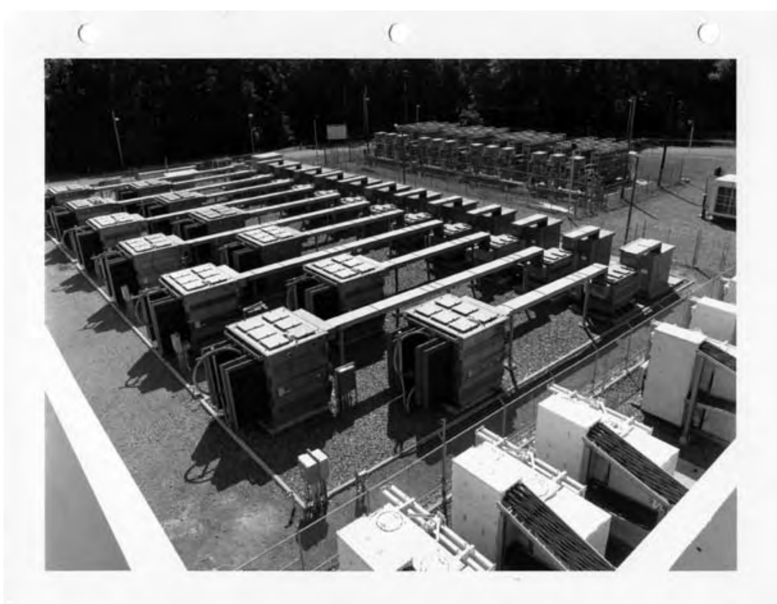

NBPS Switchgear and Transformers

NSTX NBI NBPS One Line Diagram

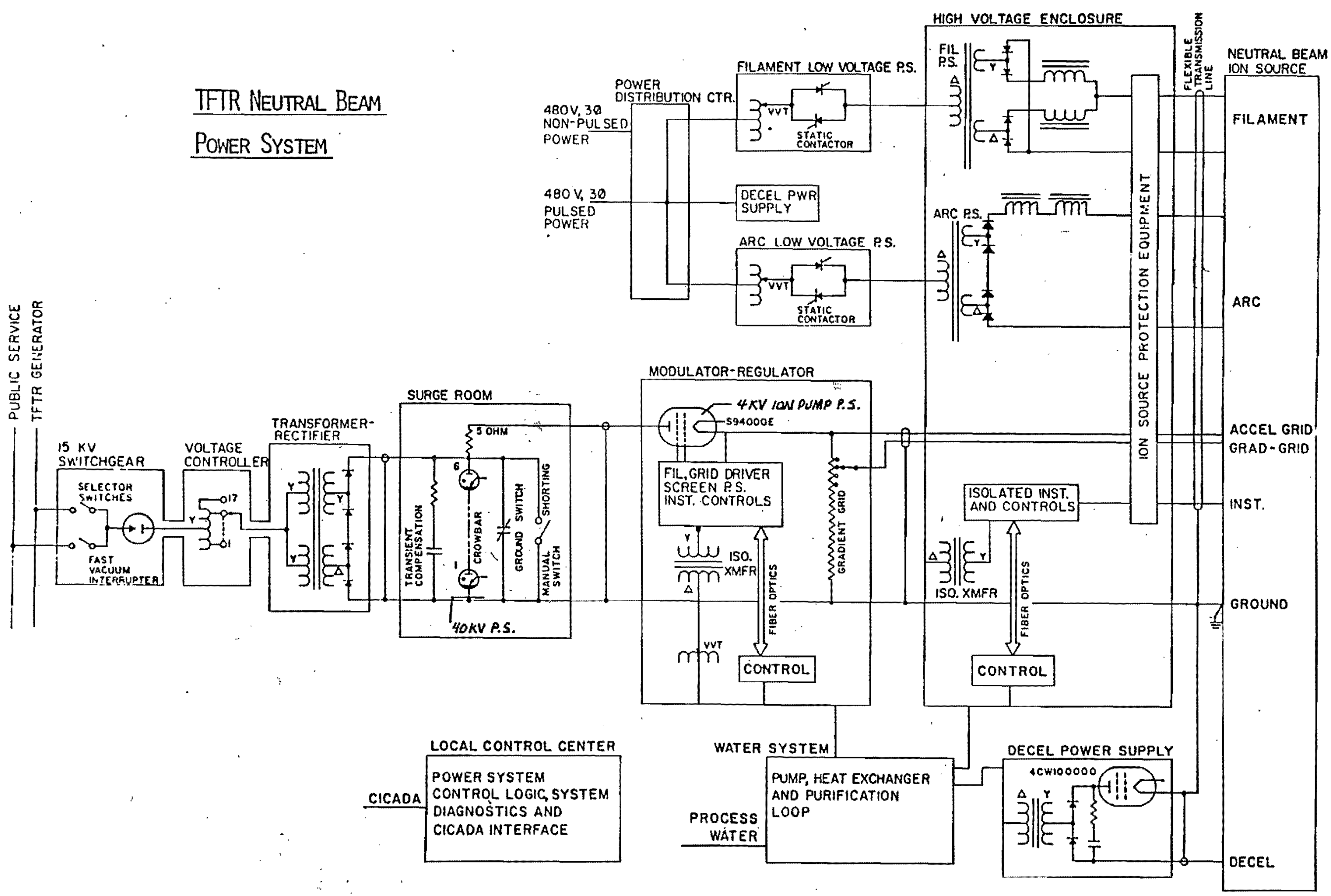

Second Neutral Beam Control System

The control system for the NSTX NBI system is an amalgam of several entities interconnected into a cohesive whole. The beamline, cryogenics plant, and mechanical services are monitored and controlled via an Allen Bradley PLC system and RSView user interface pages. These systems will be expanded using the same technology to include the second beamline. The existing PLC is capable of accommodating two beamlines.

The ion source operator manually controls the ion source at the Local Control Center by adjusting the NBPS settings for best performance and experimental requests. The NBPS is controlled via a local control center, fiber optic telemetry, a fault detector, and a timer. Additional monitoring, timing, interfaces are done through NSTX EPICS. Each of these systems will be mimicked and expanded to include BL2 in like fashion as BL1. Additional racks and fiber optics cables will be installed to connect the controls to the NTC and system. The NTC NBI racks are slated to move into the NTC East gallery.

The Neutral Beam Operations Supervisor presently uses a LabView based monitoring and control system to supervise the sources and to control injection selection. This system will be expanded so that the existing NBI staff can operate both beamlines without additional operators.

In summary, the NBI power and control required for the second beamline follow the existing design quite closely. The N4 system will be reused to power the NBI BL2. The controls will mimic the existing design and will be expanded to accommodate the second beamline. The operations interface will be expanded so that the existing NBI staff can operate both beamlines without additional operators.

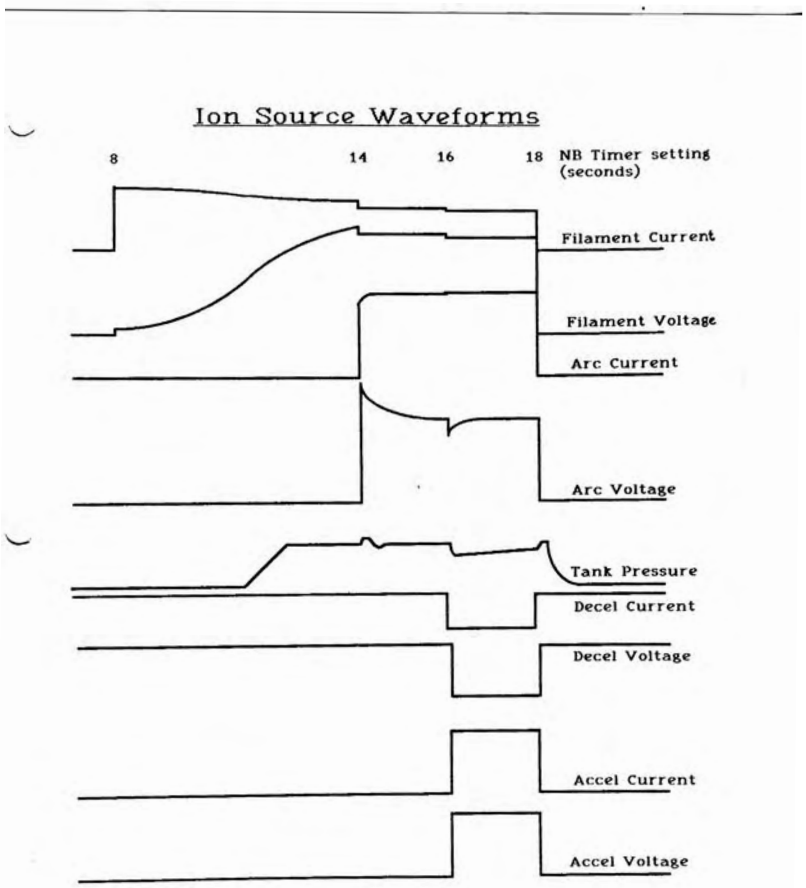

Typical NBI source waveforms for one ion source, monitored and adjusted as required, every source, every shot, by NBI Operations staff due to unregulated arc and filament supplies and emission limited ion source design.

Section 13: Cost and Schedule

NSTX Upgrade CDR

October 2009

Lead Author: Ron Strykowsky

NSTX-U Cost and Schedule Overview

A conceptual design level cost and schedule estimate was prepared, documented and presented as part of the conceptual design review. This consisted of discussions of the formulation process, quantification of cost, schedule, staffing, and funding requirements, and plans forward looking toward the preliminary design review.

Formulation Process

The project scope was defined following the NSTX project WBS structure which resulted in 40 individual "jobs" (cost accounts) being established and assignment of individuals as job managers (CAM's).

The basic cost estimates were gathered following a standard PPPL process that utilized PC based spreadsheet referred to as a Work Authorization Form (WAF). A WAF was prepared for each of the 40 jobs by the job manager assigned. This document is partitioned into 4 major sections that captures and documents the; A) Description of the scope , B) detailed task, resource estimates by skill, basis of estimates, and names of responsible individuals, C) the estimate uncertainty & risk and D) detail backup basis of estimates. Once the WAF form is prepared by the cognizant manager it undergoes an internal engineering review to ensure that; 1) all the scope is properly captured, 2) the estimates provided are reasonable and "center of the error bars" and, 3) all potential risks are identified. This data is entered into a PC based project management software package (Primavera) where the individual tasks are linked, scheduled and the resource estimates "priced" by applying standard PPPL labor and overhead rates. Once integrated in this manner the project was able to generate the initial base cost for the upgrade scope. This data base provided a sound basis for then quantifying the contingency which would establish the cost range for the project. At the time of the CDR the project's Primavera data base consisted of 1457 individual tasks, 1751 links and 2259 individual resource loadings. The resource loaded schedule also provides 1) a model to evaluate alternative approaches and scenarios and 2) the basis for managing and performance monitoring.

The key planning basis and assumptions followed were:

- TPC - from January 1st, 2009
- Institutional Overhead and Labor Rates
- Standard work week 8hrs/day 5 days/ week
- No overtime or Saturday work planned. Overtime and Saturday used to maintain schedule.
- Holidays included
- Task durations based on deliverables and/or tasks identified by the job managers
- Established tasks, internal milestones (PDR's, FDR's, contract awards)
- Task durations based on realistic resource loadings & crew sizes

Contingency

In order to quantify the upper and lower bound of the project cost a contingency methodology was followed that took into account the estimate uncertainty, risks, and critical path schedule contingency. Contingency was quantified by following the following formula;

Lower Range

- Average range of estimate uncertainty [1] (%) x base estimate ($)

  +

- Risk Cost ($) x likelihood *(weighted) (%)*

  +

- Schedule contingency (critical path tasks average uncertainty (%) x total schedule length (mos.) x standing army cost ($/mo.)
-

Upper Range

- High estimate uncertainty [1] (%) x base estimate ($)

  +

- Risk Cost ($) *(not weighted)*

  +

- Schedule contingency (critical path tasks average uncertainty (%) x total schedule length (mos.) x standing army cost ($/mo.)

(1) Estimate uncertainty consistent with AACE cost estimate classification system

Budget Range

In addition to providing an unconstrained budget case ("base case") the project also was responsive to anticipated funding guidance provided by DOE (referred to as the "Constrained case"). It should be noted that the base estimates are somewhat conservative, being based on worst case design points, thus do not reflect the benefit of value engineering exercises that are planned during the preliminary design phase. Results of these two cases are shown in Tables 1 and 2.

Table 1 Summary Cost Profile

TPC ($K)

				No Operations				
Unconstrained Case	**FY2009**	**FY2010**	**FY2011**	**FY2012**	**FY2013**	**FY2014**	**FY2015**	**TOTAL**
Base Estimate	$5,146	$11,469	$12,731	$28,894	$11,765	$249		$70,254
Lower Contingency		$358	$694	$2,436	$1,344	$1,762		$6,593
Total Lower Bound	**$5,146**	**$11,827**	**$13,425**	**$31,330**	**$13,109**	**$2,010**		**$76,848**
Upper Contingency		$1,507	$2,956	$11,020	$6,059	$1,817		$23,359
Total Upper Bound	**$5,146**	**$12,977**	**$15,687**	**$39,914**	**$17,824**	**$2,066**		**$93,613**

					No Operations			
Constrained Case	**FY2009**	**FY2010**	**FY2011**	**FY2012**	**FY2013**	**FY2014**	**FY2015**	**TOTAL**
Base Estimate	$5,146	$10,693	$7,654	$9,418	$27,423	$13,468	$18	$73,820
Lower Contingency		$345	$310	$705	$2,170	$1,494	$1,757	$6,781
Total Lower Bound	**$5,146**	**$11,038**	**$7,964**	**$10,123**	**$29,593**	**$14,962**	**$1,775**	**$80,601**
Upper Contingency		$1,449	$1,314	$3,095	$9,843	$6,794	$1,810	$24,304
Total Upper Bound	**$5,146**	**$12,142**	**$8,968**	**$12,513**	**$37,265**	**$20,262**	**$1,828**	**$98,124**

Table 2 Base Cost Estimate Detail

	NSTX UPGRADE CONCEPTUAL DESIGN COST ESTIMATE								Recommended		CONCEPTUAL DESIGN	
	UNCONSTRAINED CASE				Uncertainty %		Risk		Contingency		ESTIMATE RANGE	
Review Committee	DESCRIPTION	RLM	Job Manager	Base Estimate	Low	High	Gross risk $ (4)	Likelihood	Lower = (2)+(5)	Upper = (3)+(4)	LOWER	UPPER
Nelson/McManamy	Job: 1000 - CSU Analytical Support	Larry Dudek	Pete Titus	$421	-20%	40%			$42	$168	$463	$589
	Job: 1001 - CS Plasma Facing Components		Kelsey Tresemer	$1,776	-20%	40%	40	L	$195	$724	$1,971	$2,500
	Job: 1002 -Passive Plate Analysis & Upgrade Act		Pete Titus	$180	-20%	40%	-		$18	$72	$197	$251
	Job: 1200 - Vacuum Vessel & Structural Support		Danny Mangra	$779	-20%	40%	60	U	$36	$143	$815	$922
	Job: 1201 - Outer TF Structures		Danny Mangra	$701	-20%	40%	-		$70	$280	$771	$981
	Job: 1202 - Outer PF Coil Structures		Danny Mangra	$1,128	-20%	40%	-		$113	$451	$1,241	$1,580
	Job: 1203 - Umbrella Structural Reinforcement		Danny Mangra	$289	-20%	40%	-		$29	$115	$317	$404
	Job: 1204 - CS Support Pedestal		Danny Mangra	$203	-20%	40%	-		$20	$81	$223	$284
	Job: 1205 - Misc VV Structural Support		Danny Mangra	$256	-20%	40%	-		$26	$102	$282	$358
	Job: 1301 - Outer Toroidal Field Coils (incl 1300 CAD sprt)		Jim Chrzanowski	$726	-10%	15%	240	U	$78	$349	$804	$1,075
	Job: 1303 - TF Joint Test Stand & Perform Test		Tom Kozub	$338	-15%	25%	15	VU	$18	$100	$356	$438
	Job: 1304 - Inner TF Bundle (Dsgn/Fab)		Jim Chrzanowski	$1,935	-20%	40%	165	U	$235	$939	$2,170	$2,874
	Job: 1305 - OHMIC Heating Coil (OH) DSGN/FAB		Jim Chrzanowski	$4,004	-20%	40%	550	U	$432	$1,729	$4,436	$5,733
	Job: 1306 - Inner Poloidal Field Coils (Shaping)		Jim Chrzanowski	$536	-20%	40%	125	U	$85	$339	$621	$875
	Job: 1307 - CS Casing Assembly (DSGN/FAB)		Jim Chrzanowski	$892	-20%	40%	-		$89	$357	$981	$1,249
	Job: 1302 - Center Stack Assembly		Jim Chrzanowski	$833	-20%	40%	-		$83	$333	$917	$1,166
	Job: 2300 ECH Analysis		Jim Chrzanowski	$183	-20%	40%	100	U	$43	$173	$227	$357
Kellman/Greenfield	Job: 2420 - 2nd NBI Sources	Tim Stevenson	Mark Cropper	$1,398	-5%	10%	-		$35	$140	$1,433	$1,538
	Job: 2425 - BL Relocation		Martin Denault	$1,707	-15%	25%	-		$85	$423	$1,792	$2,131
	Job: 2430 - 2nd NBI Decontamination		Tim Stevenson	$2,738	-20%	10%	-		-$75	$150	$2,663	$2,888
	Job: 2440 - 2nd NBI Beamline		Martin Denault	$2,534	-10%	15%	(184)	L	-$48	$192	$2,486	$2,726
	Job: 2450 - 2nd NBI Services		Martin Denault	$3,601	-15%	25%	50	U	$189	$931	$3,789	$4,532
	Job: 2460 - 2nd NBI Armor		Craig Priniski	$420	-10%	15%	-		$10	$58	$430	$478
	Job: 2470 - 2nd NBI Power		Raki Ramakrishnan	$3,033	-15%	25%	50	U	$158	$779	$3,191	$3,812
	Job: 2475 - 2nd NBI Controls		Mark Cropper	$1,769	-15%	25%	-		$88	$442	$1,858	$2,212
	Job: 2480 - 2nd NBI/TVPS Duct		Craig Priniski	$2,665	-10%	15%	125	L	$137	$497	$2,802	$3,163
	Job: 2485 - Vacuum Pumping System		Craig Priniski	$319	-5%	10%	-		$8	$32	$327	$351
	Job: 2490 - NTC Equipt Relocations		Erik Perry	$3,314	-20%	40%	366	U	$409	$1,634	$3,723	$4,949
McManamy/Nelson	Job: 3200 - Water Cooling System Mods for CSU	Larry Dudek	Martin Denault	$394	-15%	25%	-		$19	$97	$413	$491
	Job: 3300 - Bakeout System Mods for CSU		Raki Ramakrishnan	$82	-5%	10%	-		$2	$8	$84	$91
	Job: 3400 - Gas Delivery System Mods for CSU		Bill Blanchard	$91	-15%	25%	10	VU	$5	$33	$96	$123
	Job: 4100 - Center Stack Diagnostics for CSU		Bob Kaita	$888	-5%	10%	-		$22	$88	$909	$975
	Job: 5000 - CSU Power Systems		Raki Ramakrishnan	$8,978	-15%	25%			$430	$2,148	$9,408	$11,126
	Job: 5501 - Coil Bus Runs		Jim Chrzanowski	$725	-20%	40%	-		$73	$290	$798	$1,015
	Job: 6100 - Control Sys & Data Acquisition Sys		Paul Sichta	$811	-15%	25%	253	U	$104	$456	$915	$1,267
Haines/Crescenzo	Job: 7100 - Project Mgt & Integration CSU & NBI	Ron Strykowsky	Ron Strykowsky	$4,536	-15%	25%	150	U	$233	$1,128	$4,769	$5,664
	Job: 7200 - Center Stack Management		Larry Dudek	$1,381	-15%	25%	107	U	$96	$452	$1,477	$1,833
	Job: 7300 - NB2 Management		Tim Stevenson	$1,679	-15%	25%	75	U	$100	$479	$1,778	$2,157
	Job: 7400 - Health Physics Support		Tim Stevenson	$2,768	-15%	25%	35	L	$159	$727	$2,927	$3,494
	JOB: 7700 - NSTX Upgrade HP Allocations		Ron Strykowsky	$1,755	-15%	25%	70	L	$130	$509	$1,885	$2,264
	Job: 7710 - Upgrade Allocations		Ron Strykowsky	$918	-15%	25%	20	L	$32	$118	$950	$1,036
Nelson/ McManamy	Job; 8200 - Centerstack & Coil Structural Instal	Larry Dudek	Mike Viola	$5,745	-20%	40%	370	U	$667	$2,668	$6,412	$8,413
	Job: 8250 - Remove/Install Centerstack		Mike Viola	$755	-30%	60%	196	U	$162	$649	$918	$1,404
Haines/ Crescenzo	Job: 7900 - Integrated System		Charlie Gentile	$71	-20%	40%	-		$7	$29	$79	$100
	schedule (months)			48		7.2			$1,746	$1,746	$1,746	$1,746
	Base Estimate =			$70,254			2,988		$6,594	$23,360	$76,848	$93,614
	etc=			$65,108					10%	36%		

Staffing

Based upon the resource loaded schedule it was demonstrated that the project was sufficiently staffed to continue from conceptual into preliminary design. Furthermore the out year staffing requirements for the entire project were determined to be achievable by utilizing existing laboratory staff. Table 3 shows the staff required to support the project schedule (base case) as well as the total compliment of PPPL staff on-board.

Exhibit 3 Project Staffing Requirements

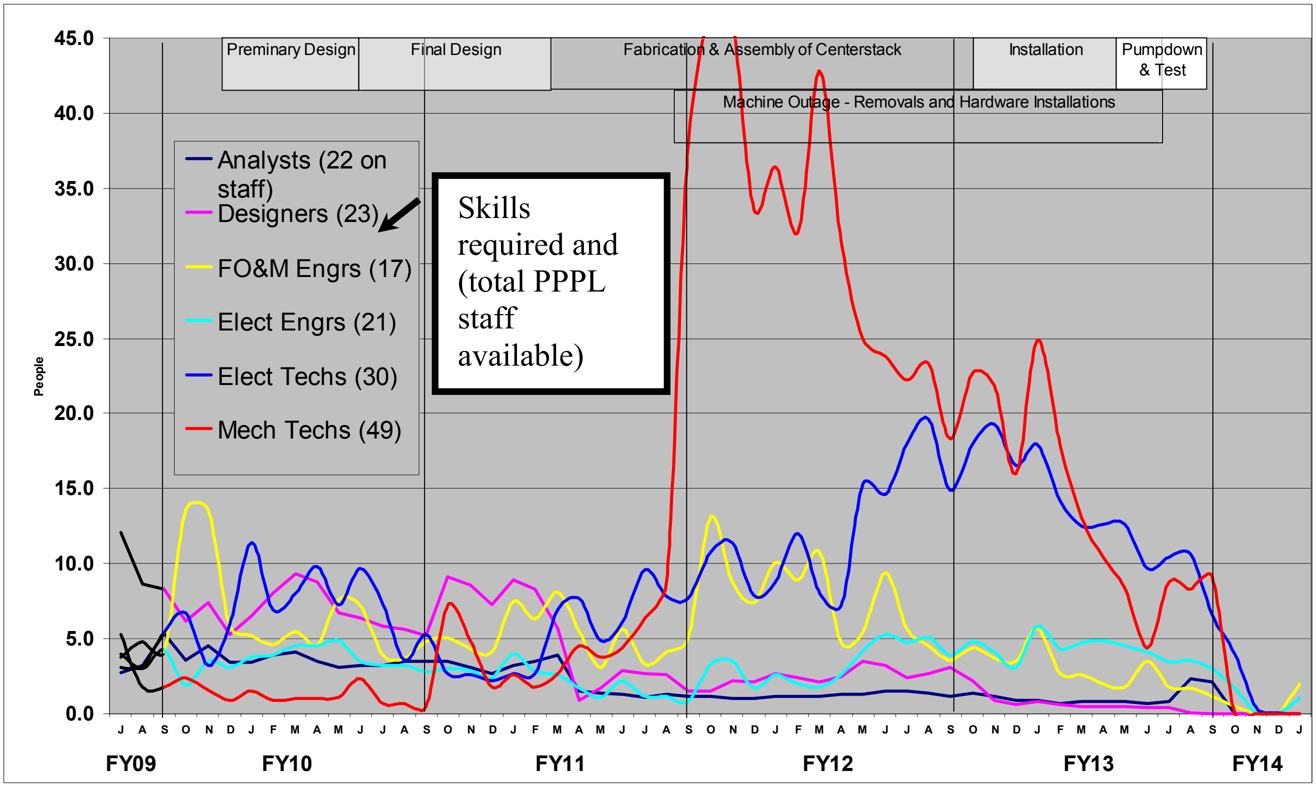

Schedule

The overall project schedule in the unconstrained case is 48 months with 7.2 months of schedule contingency. The critical path for the project goes through the design, fabrication and installation of the new center stack followed by start-up and testing. (See exhibit 4) Key milestones include;

Preliminary design Review	June 2010
Final Design Review	March 2011
Begin Upgrade Outage	August 2011
Resume Operations	October 2013
CD-4	May 2014

Exhibit 4 Summary project Schedule

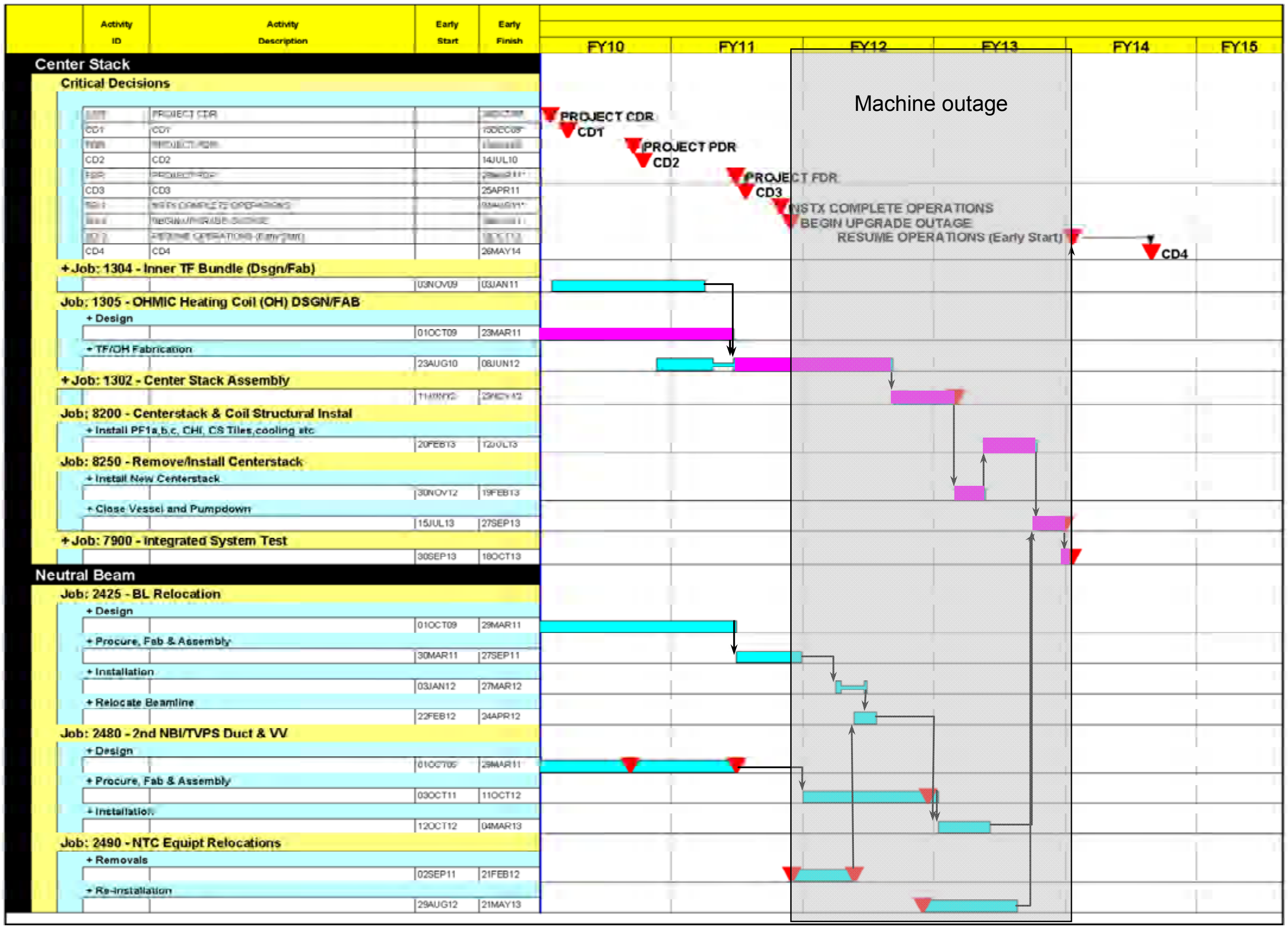

Management

At the conclusion of the conceptual design phase the project is poised to embark onto the preliminary design phase of the project. Starting this fall the project will implement PPPL's project management system process for managing the project. The fundamental processes that will commence include;

- Adopting the conceptual design plan (constrained case) as the baseline through preliminary design (CD-2) (will adjust in response to CDR and OFES findings)
- Monthly progress measurement including;
  - Earned value
  - Risk registry review
  - EAC assessment
- Monthly reporting including
  - Status bar charts
  - Cost performance reports (CPR's) including EAC's
  - Updated risk registry
- Change control process - changes documented via engineering change proposals (ECPs)

Conclusions

The following CDR charges have been satisfied by the project:

- ***Is the proposed cost range adequate for CD-1?***
    - The conceptual design estimate was prepared following a disciplined process and is credible for this stage of the project.
    - The work scope is complete, well organized with clear assignment of responsibilities.
    - A well detailed resource loaded schedule exists and provides the basis for all cost and schedule estimates.
    - The contingency and methodology used to establish the upper and lower cost range is reasonable for this stage of the project.
    -
- ***Is the proposed schedule realistic for CD-1?***
    - The schedule is realistic and achievable based on the resource availability and level of schedule detail.
    -
- ***Is the project organization/staffing appropriate?***
    - Staffing requirements have been clearly defined and are achievable.
    - The project is currently staffed to begin the preliminary design phase.
    - The project has been responsive in addressing both programmatic mission goals (base case) as well as anticipated funding guidance (constrained case).
    - The project is poised to initiate and effectively manage the preliminary design phase of the project.

Section 14: ES&H

NSTX Upgrade CDR

October 2009

Lead Author: Jerry Levine

Environment, Safety and Health Aspects of the NSTX Upgrade Project

The NSTX Upgrades Project is incorporating ES&H into its plans and activities, and will draw on the well-established ISM culture and infrastructure at PPPL.

NEPA

Upgrades to the NSTX experiment had been addressed in the NSTX Environmental Assessment (DOE/EA-1108: FONSI issued 12/8/95). The upgrades covered included plasma currents up to 2 MA and pulse lengths up to 60 seconds. Nevertheless, a formal request for a Categorical Exclusion (CX) for the NSTX Upgrade Project under 10CFR1021 (Appendix B, B3.13) was submitted to the DOE Princeton Site Office (DOE-PSO). A CX determination was granted by the PSO NEPA Compliance Officer on 3/31/09. No further NEPA actions are required.

Nuclear Facility Hazard Classification

An evaluation has been performed on the projected NSTX nuclear facility hazard classification with the upgrades in place. It was assumed for this analysis that a maximum of 4E18 DD neutrons/year would be generated. This evaluation, using DOE-STD-1027, indicated that NSTX would remain a Below hazard Category 3 Facility. Thus, 10CFR830 Subpart B safety analysis requirements are not applicable. The NSTX Safety Certificate (operations authorization) will address the neutron generation limit.

ES&H Considerations

A Preliminary Hazards Analysis (PHA) has been prepared. It was based on current plans using the hazard analysis summary in the current NSTX Safety Assessment Document (SAD). The expected air emissions are 0.19 Ci/year tritium from D-D fusion (site limit is 500 Ci/year). There are no 40CFR61 Subpart H (NESHAPS) issues. It is estimated that these air emissions of tritium will result in 0.0005 mrem/year at the nearest business versus the Subpart H limit of 10 mrem/year and the 0.1 mrem/year threshold for requesting EPA approval.

Radiation exposure to the public is estimated to be 0.006 mrem/year from tritium and direct radiation (site limit: 10 mrem/year). Radiation exposure to workers will be less than the 1000 mrem/year and 600 mrem/qtr limits set by PPPL policy. Collective dose will be controlled ALARA and compliance with occupational radiation exposure (10CFR835) and DOE-approved PPPL Radiation Protection Program will be assured with Health Physics Division support. Radiological conditions after the upgrades will be enhanced compared with current operations, but well within previous PPPL experience during TFTR operations and TFTR D&D.

Non-radiological hazards (electrical, fire, magnetic fields, RF, lithium, etc.) are expected to be comparable to present NSTX operations.

Integrated Safety Management (ISM)

NSTX Upgrade activities will be conducted using PPPL's well-established policies and procedures that apply to the principles and core functions of ISM. The project will follow the DOE approved ISM System Description (ISMS), which is incorporated into the DOE approved Worker Safety & Health Plan (WSHP) per 10CFR851.

Hazard controls will include:
- Installation, test and operating procedures
- Design reviews
- Job Hazard Analysis (JHAs)
- Worker training
- Line managers and workers involvement and responsibility
  - Safety Training Observation Program
- Oversight by ES&H professionals

Assessment and feedback will include:
- Line manager and facility manager walkthroughs
- Laboratory Management Safety Walkthroughs
- Internal audits
- PSO surveillances
- Plan-of-the-day meetings
- Project team meetings

Safety Assessment Document (SAD)

The existing NSTX Safety Assessment Document (SAD) will be revised prior to operating NSTX with the upgrades. The SAD includes descriptions of the NSTX structures, systems and components, with emphasis on environment, safety and health (ES&H) features. It also includes identification of the hazards of NSTX and the methods employed for their mitigation as well as a description of how operations will be conducted (with emphasis on ES&H features).

NSTX Activity Certification Committee (ACC)

The existing independent joint PPPL/PSO Activity Certification Committee will conduct ES&H reviews of planned NSTX operations with the upgrades and make recommendations to PPPL management on whether to approve the start of NSTX operations with the upgrades. They will also make recommendations to PPPL management on any restrictions or limitations associated with NSTX Upgrade operations (e.g. neutron generation limit). The ACC is composed of senior engineers, Physicists and ES&H professionals.

Section 15: Conceptual Design Review Committee Report

NSTX Upgrade CDR

October 2009

Chairman: Joseph Minervini (MIT)

Conceptual Design Review (CDR) Committee Report

for the

National Spherical Torus Experiment (NSTX)

Upgrade Project

Princeton Plasma Physics Laboratory
Princeton, NJ

October 28-29, 2009

Table of Contents

1. Introduction

A Conceptual Design Review was held at the Princeton Plasma Physics Laboratory (PPPL) for the NSTX Upgrade Project on October 28-29, 2009 at the request of Dr. Michael D. Williams, Associate Laboratory Director, Engineering and Infrastructure. The purpose of the review was to assess the project's technical, cost, schedule, and ESH status in preparation for the CD-1 milestone review to be held in December 2009. The committee was asked to review the NSTX center stack upgrade and the addition of a second neutral beam for plasma heating to assess whether; the general requirements have been addressed; the risks have been appropriately identified and adequately addressed by the project plans; there are any "show stoppers"; the ES&H issues have been properly addressed; the cost range is adequate and the proposed schedule realistic for this stage of the project; the project organization and staffing appropriate; and if the project is ready for CD-1.

The NSTX is the world's highest performance Spherical Torus (ST) research facility and is the centerpiece of the U.S. ST research program. Since starting operation in 1999, NSTX has established the attractiveness of the low-aspect-ratio tokamak ST concept characterized by strong intrinsic plasma shaping and enhanced stabilizing magnetic field line curvature. The purpose of the NSTX Center Stack Upgrade project is to expand the NSTX operational space and thereby the physics basis for next-step ST facilities.

The plasma aspect ratio (ratio of plasma major to minor radius) of the upgrade is increased to 1.5 from the original value of 1.26, which increases the cross sectional area of the center stack by a factor of ~ 3 and makes possible higher levels of performance and pulse duration. The project intends to replace the NSTX "center stack" in order to effectively double the magnetic field and plasma current (from 0.5T to l.0 T, and l.0 MA to 2.0 MA, respectively), increase the plasma pulse length (from nominally 1 second to 5 seconds), and add an additional neutral beam injector to effectively double the neutral beam heating power.

The NSTX Upgrade Project team presented to the review committee technical details of the center stack upgrade task including, TF, OH, PF coils, and structure modifications; the task for the addition of the second neutral beam; ES&H issues; project cost and schedule, and; readiness for CD-1. All presentations were very comprehensive in content, well organized, and professional in presentation, which allowed the committee to understand the complexity of the upgrade project and the supporting programmatic and administrative requirements. The presentations were supported by extensive project documentation provided to the committee including Work Approval Forms (WAFS), costs, and project schedule broken down by WBS, etc.

The committee was very impressed with the level of effort and comprehensiveness of the design effort to date, and commends the project management and team for their dedication to making this project a success. The committee appreciates the support given to the committee and the responsiveness of the project team during this review.

2. Summary of Response to the Charge

A summary of the review committee response to the charge is given below. Further details of committee report are given in the following sections.

1. *Have the requirements for the NSTX Upgrade Project, delineated in the General Requirements Documents, been addressed?*

   Yes, GRDs have been generated for both the Center Stack and the Second Neutral Beam. The design and analysis to date address the requirements at an appropriate level for this stage of conceptual design.

2. *Does the Conceptual Design Review satisfy the objectives of PPPL Procedure ENG-033, "Design Verification", Attachments 4 and 6, "Design Review Objectives and Input Documentation" and "Human Performance Improvement/Factors Considerations in Design Reviews"?*

   Yes, successful technical reviews have been completed to this stage;
   bottoms-up cost and schedule details have been generated for all jobs

3. *Have risks been appropriately identified? Are project plans adequate to address/retire the identified risks? Are there any "show stoppers?" Are ES&H issues properly addressed?*

   Yes, the risks identified at CD-0 and forward are being appropriately addressed. The Risk Registry is established and is in constant update as new risks are identified with mitigation plans being developed (to be completed before CD-1 Review). There are no apparent "show stoppers" at this stage; ES&H is being appropriately addressed in designs and the Preliminary Hazard Analysis is based on current plans using the hazard analysis summary in the NSTX Safety Assessment Document.

4. *Is the proposed cost range adequate (for CD-1)? Is the proposed schedule realistic (for CD-1)?*

   Yes, a well detailed ~1500 WBS element project schedule has been developed and resource loaded. WAFs have been generated and provide the basis for all cost and schedule estimates. The resource loaded project schedule is realistic for this project stage at CD-1.

5. *Is the project organization/staffing appropriate?*

   Yes, laboratory management have established an appropriate project organization and applied sufficient design/analysis staffing for the conceptual design phase. Future staffing requirements needed for the next phase of the project have been generated as part of the project plan. Staff have been identified and project management have determined that these resources are available as required.

6. *Is the project ready for CD-1 per DOE Order 413.3A?*

Yes, the project is ready for CD-1 as described next, assuming the recommendations in Section 4.3 and the CD-1 requirements in Section 4.4 are completed before the December 2009 Lehman Review.

3. Technical Systems Evaluations

The following sections provide the findings, comments, and recommendations broken down for the major program elements of Center Stack Upgrade, Second Neutral Beam, and Cost and Schedule.

3.1. Center Stack Upgrade

Findings

A comprehensive amount of detailed design and technical analysis was presented for a CDR level review. The project has chosen a very conservative design philosophy based on designing the coils and structure to handle maximum output from power supplies. If the conservative design cost becomes to expensive, the fallback position will be to design to the required operational levels and loads, which will be agreed upon doing preliminary design.

The Center Stack upgrade scope includes the following items:

- Inner TF bundle (centerstack)
- TF Flex bus
- OH coil
- Inner PF coils
- Enhance outer TF supports
- Enhance PF supports
- Reinforce umbrella structure
- New umbrella lids

The project team plans to fabricate the new TF inner leg bundle in-house and then wind the OH coil directly on top of the TF legs. Estimates are based on the actual costs of designing, fabricating and installing the current center stack. These are considered to be conservative allowing opportunities for further cost reduction.

The new TF coil flexible joint appears to be greatly improved from the previous version, although it was unclear what load cases and fault conditions the machine was being designed for. Potential problem areas/ risks have been identified for the design, manufacture, and assembly and are being addressed. Issues for the design life remain to be addressed for the legacy components, i.e. TF outer legs and PF coils.

Since CD-0, 10 risks have been addressed and retired and about 50 new ones have been added to the Risk Register.

The critical path runs through the copper for the inner TF legs and OH conductor, including long lead procurement time, machining, and stir welding of the joint. The project will request an early procurement of the copper

Comments

There appear to be no show-stoppers in the chits. In-line braze joints in central solenoid conductor may be eliminated using the CONFORM™ continuous extrusion process presently being used by Luvata in Finland. If joints are kept, then careful NDT of the joint is needed.

Stress in the epoxy insulation of ~22MPa appears too high for this material at 100°C for routine operation. Few, if any, fusion magnets have ever been proposed using VPI epoxy resin operating at 100°C.

Friction stir welding seems a good solution for joining the flags to the wedges and it is good to see new manufacturing techniques being developed and applied.

Much effort appears to have been directed at the TF joint design but it is important not to lose sight of the other critical areas of the machine. The tradeoff appears to be the captured OH coil on the TF center-stack. This can create problems if severe thermal stresses on the OH coil if TF-only shots are performed with TF inner leg temperatures reaching 100C while the OH coil is cold. Running TF only shots needs to be assessed on the OH. Perhaps a trade off study between radial build and optimal performance is warranted.

The fault load cases that have been analyzed for stresses are overly conservative when compared to the design basis. Some structures are designed to the Monte Carlo/excel solver routines (which result in much higher electromagnetic loading) while others are designed according to the 96 specified plasma scenario load cases. A clear design basis is required for design operations and fault conditions. The interface between machine protection system and design needs to be clearly defined.

Another issues is the how to handle the existing cycle count on legacy hardware i.e., how much fatigue life has been used in the outer TF legs and PF coils? Also, a fault occurred at one point in the life due to the TF leads that needs to be accounted for in the current cycle count.

Performance (in general) appears to have been favored over technical functionality.
The support structures for the PF coils and TF outer legs need continued evolution in the design process. In particular, the lower TF supports and the interfaces between the TF and PF need attention. The present structural support system seems to have grown spatially and while being constrained by the legacy components, e.g. TF outer legs and supports, PF coils and supports, vacuum vessel, etc. This makes adding new support structure for the significantly higher loads (~3.5 times greater) non-ideal, unsymmetrical, and likely requires complex 3-D FEA.

Heat loads in the divertor area develop temperatures that may require an engineered cooling solution. Upgrade of the divertor to accept higher heat loads is not included in this upgrade project. If it is found necessary, it will have to done in the physics operational phase.

The machine cannot meet the design criteria under static-only loading cases. Dynamic impulse analysis is being used to meet the design criteria for the structure. Thus, it is very important that this dynamic analysis be performed correctly by properly specifying the input load durations and time dependencies.

Error fields from the eddy current loop created by vacuum vessel patch for the new NB port have not been performed yet, although the project team believes these will not significantly affect the plasma.

High pressure in small cooling channels seems excessive. The inlet pressure of 550 psi in the cooling channels may present as a personnel hazard.

Recommendations

Slip plane
Consider improving the design of the slip plane to give sufficient strain isolation between the solenoid and centre rod to allow TF only operation. Consider using removable axial strips, as demonstrated on Alcator C-mod and MAST, to give a small radial gap. This may mean adding a few mm to this slip plane at the expense of reduced I^2t in the solenoid.

Solenoid conductor braze joints
It may be possible to eliminate the need for these in-line braze joints by forming the conductor using a continuous extrusion process called CONFORM. This process has been developed by Luvata in Finland for copper and allows very long lengths of high conductivity copper to be produced. However, the silver content in the copper may be limited to very small amounts which may lead to larger volumes of annealed copper at the interlayer braze joints.

If the in-line joints cannot be eliminated then careful NDT of each joint is needed i.e. X-ray of the braze joint in two directions. If in-line ferrules are used in these joints they may give rise to stress concentrations that can limit the fatigue life so fatigue tests of the joints should be considered.

Manufacture of centre rod wedge conductors
Consider asking Kabelmetal at Osnabruck, Germany, to quote for the extrusion of the wedges. They have previously made the wedges for MAST centre rod, which included the cooling channel inside the wedge, which reduces machining and soldering. Consider not machining the main side faces of the wedges to avoid the possible deformation due to residual stresses.

Centre stack and solenoid insulation
Operation of the insulation at 100°C and at a shear stress of 22MPa appears to be too high for routine operation. Various alternatives/changes should be considered including:

- Use of B-stage insulation for the centre stack, which should offer higher temperature operation.
- Alternative primers for the copper conductors that offer higher operating temperatures than the conventional DZ80 primer.
- If VPI epoxy is used, consider increasing the curing temperature or add a post cure cycle to increase the glass transition temperature. However, this may also reduce the fracture toughness of the material.
- Consider reducing the maximum operating temperatures of the copper conductors.

Need to bring together what little test data exists for epoxy at 100°C and then determine what further static and fatigue tests, especially for shear strength, need to be carried out to qualify this material at the required temperature, stress levels and number of cycles. Tests on alternative primers and cure cycles may also be needed.

Reconsider radial build of the center stack to allow a more effective slip plane between the components even if there is some loss of i^2t capability on the solenoid.

Structural Design

Develop criteria for allowable load conditions that require protection by the MPS, as soon as possible, to be used for preliminary design. Write a design specification to collect and identify all design critical components that exceeded allowables that would guide the MPS design.

Establish, document, and carryout a supporting R&D program for all components and processes as required.

3.2. Second Neutral Beam

Findings

The second neutral beam scope includes:
- Disassemble and evaluate a TFTR beamline
- Decontaminate
- Refurbish for reuse
- Relocate pump duct, 22 racks and numerous diagnostics to make room in the NSTX Test Cell
- Install new port on vacuum vessel to accommodate NB2
- Move NB2 to the NSTX Test Cell
- Run services (power, water, cryo and controls)

Estimates are based on the actual costs of designing, refurbishing, and installing NSTX Neutral Beam #1. The beamline decontamination estimates are based on actual experience with TFTR neutral beams. The project believes these estimates to be conservative. They include costs for making new parts that might be able to be decontaminated for reuse. Whenever decontamination succeeds this results in opportunities for reducing costs.

Some of the risks identified at CD-0 have been retired.

The plan for re-using an old contaminated beamline seems to be appropriate, although the decontamination is a necessary, time-consuming part of the task. The human effort is significant and the safety aspects are crucial.

The beamline armor appears to take quite a lot of power. The visual evidence of the beam footprint was very illuminating. Perhaps some real-time monitoring of the power is advisable.

The proposed NB port modification of the vacuum vessel creates a new worst case for wall stabilization, error fields, weld stresses, etc.

Comments

The operation and maintenance of the new beamline must be handled differently than the first, due to the lingering tritium contamination. Care must be taken to strictly enforce different procedures, especially with respect to personnel working on or near the beamlines.

The general requirements mentioned that the radiological impact on NSTX operation was not significantly impacted by the upgrade. However, the plasma current, toroidal field, injected power, and pulse length are all much bigger. There definitely IS a radiological impact.

How is the decommissioning of the contaminated beamline determined to be complete? How is success measured there? How will long-term beamline surface contamination or cooling down be measured?

The committee feels a more modest modification should be considered instead of the proposed large cutout of the vacuum vessel for the new beamline. The committee is concerned that the vacuum vessel (and beamline) support systems may not be able to react the load sufficiently for the new beamline on the same side of the vessel caused by the asymmetry of the pressure.

It was not made clear whether the beamline internal copper components (collimators) will be replaced or if they will be decontaminated, refurbished, and re-used. The project should consider the difference in the effort and cost for each option.

Bellows (especially large ones) are risks. Are all the bellows associated with the transition duct necessary for the second beamline? The present design includes two large ones and two smaller ones for the vacuum lines. Also, the support system for the transition duct was not shown in the presentation. The bellows and ceramic breaks cannot take the weight, so extra supports are required. It was reported that the extra supports are included, but they were not presented at the review.

Recommendations

Perform eddy current/error field analysis on the new very large vessel cutout port box assembly.

Consider replacing data acquisition and I&C CAMAC systems with a more modern and reliable solution.

Incorporate better interlocks (Ip and density) and monitoring (real-time pyrometers) of the beam armor tiles.

Install and maintain strict procedures for radiological control for contaminated beamline maintenance.

Installation procedure recommendations for the large beam port:

- Increase port width as needed
- Remove diagnostic port
- Reinforce vessel wall with insert welded into the diagnostic port hole
- Replace curved plate leak check fixture into vessel for use in checking port welds
- Position and weld NB port box
- Leak check port box welds
- Consider option to install smaller or relocated diagnostic port
- Cut the leak check plate if required for removal

4. Cost and Schedule

4.1. Findings

Cost Estimates

A project plan with ~1500 WBS elements has been developed and resource loaded. Excellent process has been put in place for estimating costs and a bottoms-up cost estimate has been performed for all scope. Lead engineers have developed Work Authorization Forms (WAFs) for their task areas. A top-down review of each WAF was performed by the AD and the Department Heads. The Levels of WAF completion and consistency, however, are uneven (*e.g.,* quantifying bases of estimates, risk likelihood and impacts), and will be further developed.

The cost estimate is in the range $71M-$95M with project completion in 2014 for the baseline case.

Schedule
Bottoms-up staffing estimates have been loaded to the Project schedule.
A detailed near-term staffing plan has been developed through CD-1.

Risk Management
Excellent process, guidelines, and risk registry are established.
Some documentation of plan is given in the WAF and in the PPEP.
Few "opportunities" to reduce cost are listed in risk registry.
Risk registry largely is incomplete.
The contingency estimate is based on risk and uncertainty roll up.

DOE relationship and communication appears to be very good
The local Site Office is satisfied with the Project performance at this stage.

4.2. Comments

It is essential that all Job Managers "own" their Project assignments, as evidenced by preparation of a complete WAF, and intimate knowledge of resource-loaded schedules and milestones. Incomplete risk and opportunity assessments limit contingency justification and distribution estimates. NCSX Lessons Learned appear to have been appropriately applied. This needs to be continued, *e.g.,* developing a detailed near-term staffing plan that will meet the CD-2 milestone on time in June 2010. Deployed staffing levels are appropriate, and need to be continued

4.3. Recommendations

The following recommendations should be completed before the December 2009 Lehman Review.

1) Complete all elements of all WAFs, maintaining a common, crisp format.
2) Complete all fields in the risk registry.
3) Document the risk management plan (a CD-1 requirement) in the PPEP
4) Establish and implement a staffing plan to CD-2 that accounts for monthly assignments of specific tasks, self-consistent with the resource-loaded schedule.
5) Continue to implement PU Advisory Board recommendations to refine and improve the rigor of the risk/contingency development in advance of CD-2. Also, consider using risk matrix deadline dates to inform contingency distribution plan before Lehman CD-1 review and, continue to develop more "opportunities."

4.4. Findings for CD-1 Requirements

- Conceptual Design Report not drafted yet; plan to start and complete by Nov 17.
- Acquisition Strategy: Major procurements identified and scheduled; DOE approval (CD-2a and 3a?) expected at CD-1.
- Preliminary Project Execution Plan draft prepared; risk management plan is at very high level, and does not describe methodology used.
- Integrated Project Team (IPT) formed and Federal Project Director named. IPT meeting regularly.
- NEPA: Categorical Exclusion requested and granted by DOE.
- Preliminary Hazard Analysis Report generated and submitted to DOE for approval.
- Preliminary Security Vulnerability Assessment Report: Not examined at this review.
- Initial Cyber Security Plan: Not examined at this review.
- QA Program: Not examined at this review.

5. Appendices

5.1. Charge Letter

PRINCETON
UNIVERSITY

Plasma Physics Laboratory
James Forrestal Campus
P.O. Box 451
Princeton, New Jersey 08543

July 31, 2009

Dr. Joseph Minervini
Massachusetts Institute of Technology
Plasma Fusion Center
Room NW22-129
77 Massachusetts Avenue, NW16
Cambridge, MA 02139

Dear Dr. Minervini,

The Princeton Plasma Physics Laboratory (PPPL) is planning a Conceptual Design Review for the NSTX Upgrade Project on October 28-29, 2009. We would be honored and grateful if you could agree to serve as the Chairman of the Review Committee. To help you with the administrative aspects of this responsibility, I intend to appoint Mr. Al von Halle of PPPL as Vice-Chair.

The NSTX Upgrade Project intends to replace the NSTX "center stack" in order to effectively double the magnetic field and plasma current (from 0.5T to 1.0T and 1.0 MA to 2.0 MA respectively), increase the plasma pulse length (from nominally 1 second to 5 seconds) and add an additional neutral beam injector to effectively double the neutral beam heating power. Additional pertinent information will be provided prior to the review.

If you have any questions, please contact me (at 609-243-2866 or williams@pppl.gov) or Erik Perry (at 609-243-3016 or eperry@pppl.gov). Please let me know of your intentions by August 14, 2009.

Sincerely,

Michael D. Williams
Associate Laboratory Director
Engineering and Infrastructure

cc: A. Cohen
E. Perry
S. Prager
S. Smith (PU)

5.2. CDR Charge

1. Have the requirements for the NSTX Upgrade Project, delineated in the General Requirements Documents (attached), been addressed?
2. Does the Conceptual Design Review satisfy the objectives of PPPL Procedure ENG-033, "Design Verification", Attachments 4 and 6, "Design Review Objectives and Input Documentation" and "Human Performance Improvement/Factors Considerations in Design Reviews" (attached)?
3. Have risks been appropriately identified? Are project plans adequate to address/retire the identified risks? Are there any "show stoppers?" Are ES&H issues properly addressed?
4. Is the proposed cost range adequate (for CD-1)? Is the proposed schedule realistic (for CD-1)?
5. Is the project organization/staffing appropriate?
6. Is the project ready for CD-1 per DOE Order 413.3A? Is the required documentation for this phase in order?

5.3. Review Participants

CDR Committee:

Joe Minervini (MIT), Chair	minervini@psfc.mit.edu	617-252-5503 (Cell: 978-821-6391)
Tim Scoville (GA)	scoville@fusion.gat.com	858-455-3596 (Cell: 619-889-9914)
Paul Anderson (GA)	anderson@fusion.gat.com	858-455-4748 (Cell: 858-775-6640)
Gary Voss (UKAEA)	garry.voss@ukaea.org.uk	+44 (0)1235 466553
Kevin Freudenberg (ORNL)	freudenbergk@ornl.gov	865-574-1310
Don Rej (LANL)	drej@lanl.gov	505 665 1883
Bob Parsells (Consultant)	rparsells@verizon.net	609-213-4400

PPPL/PU Resource Team:

Mike Bell	mbell@pppl.gov	609-243-3282
Charlie Gentile	cgentile@pppl.gov	609-243-2139
Geoff Gettelfinger	gettelf@Princeton.EDU	609-258-4404
Steve Raftopoulos	sraftopo@pppl.gov	609-243-3626
William Sands	wsands@Princeton.EDU	609-258-4918
Al von Halle	avonhalle@pppl.gov	609-243-2618

5.4. Review Agenda

NSTX Upgrade Project
Conceptual Design Review
October 28-29, 2009
Agenda

Wednesday October 28th

0800	Executive Session	
0830	Welcoming remarks and introductions	
0845	Project Overview	Perry
0900	Motivation for upgrade and selection of design point	Menard
0920	Overview of centerstack upgrade	Dudek
0940	Analysis summary	Titus
1025	Break	
1045	TF, OH and inner PF coils	Chrzanowski
1130	TF Flex joint and TF bundle stub	Willard
1150	Outer TF/PF structure	Dudek
1210	Power and controls	Ramakrishnan
1230	Lunch	
1330	Neutral Beam overview and status of decontamination Stevenson	
1410	Beamline relocation and services	Denault
1430	Beamline duct and vacuum vessel modifications	Priniski
1500	In-vessel armor	Tresemer
1515	Beamline power and controls	Stevenson
1600	Executive session	

Thursday October 29th

0800	Executive session	
0830	Cost and Schedule	Strykowsky
0900	CD-1 Readiness	Perry
0930	Tour of NSTX	
1030	Additional presentations as requested by reviewers	
1130	Preparation of closeout presentation by reviewers	
1500	Closeout meeting	

Section 16: Design Review Chits

NSTX-U Project Reviews Recommendations Log

Item	Ref.	Concern/Recommendation	Responsibility / WBS or Job	Comment/Action	Current Status
200911-01	CDR Chit-01	Castellated ends of center rod may generate stress concentrations due to transient loads, which causes cracks to propagate especially between two adjacent conductors. Consider alternate designs.	Chrzanowski		Will examine present design and consider changing ends of TF bundle to accommodate transient loads
200911-02	CDR Chit-02	Consider using "CONFORM" extrusion process to make long conductors to avoid in-line braze joints. Luvata (Finland) have developed conform for copper conductors but may need to limit the silver content.	Chrzanowski	investigate process, including the impact of reduced silver content.	Good suggestion- This process will be invesigated in regards to the OH conductor-
200911-03	CDR Chit-03	Allowable shear stress of ~ 22MPa seems too high for epoxy resin at 100C under stress and fatigue loading. Check if a lower value is more appropriate. Is DZ80 primer used?	Chrzanowski	verify vendor test data on this application, and to further document design details for the preliminary design.	Will contact CTD if data is available for 100C application. Have considered using DZ80 or alternative primer to enhance bond strength with conductor
200911-04	CDR Chit-04	Determine shear strength of CTD101 epoxy resin at 100C by direct measurement. Explore making winding stack impregnated sample of conductor/insulation and test for fatigue at 100C. Also, consider shear and creep at 100C.	Chrzanowski	Concur. See chit #3	See Chit #4
200911-05	CDR Chit-05	TF Outer legs should be characterized for present mechanical strength since they will be subject to higher point loads at support points. Consider using the TF leg removed because of the water leak to get samples for static and fatigue testing.	Dudek	consider tests on the unused outer TF leg to evlauate delamination, coil movement, etc.	This will be evaluated as part of the preliminary design. The plan was to repair this leg once off and keep as a spare. It that plan is not implemented we can perform the test. (Action: Mangra and Chrzanowski)
200911-06	CDR Chit-06	Better determine the strength of the CD107 copper alloy at 100C by either direct measurement or published data specific for this alloy,	Chrzanowski		Will contact Copper Dev Assoc for additional data on 107 at 100C
200911-07	CDR Chit-07	Interface between TF and OH, if TF is run and OH is not, what happens? Is this a bad condition?	Neumeyer	Analysis indicates that this is a problem for full power TF only operation. Investigate design options that decouple the TF & OH. Action: C. Neumeyer/P. Titus/ J. Menard	Inclusion of a small gap is a desirable feature which will be investigated. The gap should be sufficiently large that, when the TF and OH coils are cooled with 12 degC water, and then the TF is pulsed with its maximum I2T including L/R decay, while the OH remains cool, the gap should not close. The gap should be slightly larger than this minimum amount considering realistic manufacturing tolerances on coil roundness, straightness, etc., to ensure that gap is realized. Gap should not be larger than this because it can lead to lack of concentricity of TF inner leg and OH coil, resulting in field error. Method needs to be developed to introduce gap during manufacturing process. Action to be taken by J. Chrzanowski to calculate required gap including tolerances and to develop manufacturing technique.

NSTX-U Project Reviews Recommendations Log

Item	Ref.	Concern/Recommendation	Responsibility / WBS or Job	Comment/Action	Current Status
200911-08	CDR Chit-08	The machine Protection System is discussed but the philosophy is unclear. Is the design requirement based on this protection? Clarification is needed.	Neumeyer	specify system	Machine Protection System (MPS) has been budgeted and R. Woolley has been assigned the task of writing a requirements document. Design philosophy will be clarified via a revision of the General Requirements Document (GRD). Implementation of the MPS will allow the structural design to proceed based on normal operation with headroom. Failure of the MPS will be classified as an "Extremely Unlikely Event" and the structural design will not be required to consider worst case power supply current combinations.
200911-09	CDR Chit-09	Loads on TF – PF bracket unclear if degree of freedoms are satisfied. This is probably reasonable for the CDR level.	Titus	The appropriate number of degrees of freedom are restrained. The mechanics of the tangential radius rods is the same for both the TF to vessel connection and the PF cage to TF ring connection. A similar mechanical connection could be achieved with a sliding capture of the vessel gussets as suggested by Phil at the peer review. Vertical mis-match is accomodated with the spherical ball ends on the radius rods. If the cage is omitted, then the extra mechanism to maintain coincentricity is not needed.	Analysis to be completed as design matures towards a PDR.
200911-10	CDR Chit-10	Make sure that long lead time items are accounted for (for example; CFC tiles for armor)	Strykowsky		Lead times for procurements in the project schedule are based on experience with similar procurements or vendor quotes.
200911-11	CDR Chit-11	Vertical support for PF's need added supports. Stated design/analysis is in the works but not shown at this review.	Dudek	investigate need for additional supports	Were are in the process of redesigning at the operational Limits which are lower (Action: Mangra)
200911-12	CDR Chit-12	On friction stir welding: does the vendor who is supplying the Cu inner TF conductor know that they have to provide a tab (of sorts) to provide a cutoff portion for the welding.	Chrzanowski		Yes, this has been discussed with vendor during initial trials.
200911-13	CDR Chit-13	Impact of as-built on analysis. Buckling failure mode sensitive to geometry. Fatigue failure mode sensitive to current cyclic life.	Titus	This is being addressed as out-of round/or other imperfections are found in, primarily, the vessel. So far these are not an issue. One point raised in this discussion at teh CDR was the shift in current centers and the magnetic stability of neighboring coils that are not perfectly concentric. This is being addressed analytically to assess resulting loads on the coils and the ability of the supports to take the lateral loads.	Analysis to be completed as design matures towards a PDR.
200911-14	CDR Chit-14	Concern about the differential thermal expansion at the interface between Cu and CuCrZr due to different electrical resistivity and other properties. Will there be high local stress on the friction stir welded joint?	Dudek	consider/analyze/test as we approach a preliminary design.	As part of the preliminary design the stress will calculated and evaluated. (Action: T. Willard)

NSTX-U Project Reviews Recommendations Log

Item	Ref.	Concern/Recommendation	Responsibility / WBS or Job	Comment/Action	Current Status
200911-15	CDR Chit-15	In Tom Willard's presentation on slide "Current Joint Design vs. Upgrade Comparison", there's an error in Table 1. The current design flattop is ~.5 seconds, not 5 seconds as shown. This may propagate to table 3.	Dudek	Typo. correct and evaluate impact on table 3	This was just a typo in the table and has been corrected.
200911-16	CDR Chit-16	NBI vessel port cut-out presented introduces a new "worst case" hole in the vessel wall that affects plasma wall stabilization, vessel stress, etc. Design needs to consider and minimize these impacts.	Menard	consider impact on wall stabilization, as well as impact on RWM/EFC coil performance	
200911-17	CDR Chit-17	Analysis should be done on the error fields generated by the new (large) NB port box attachment caused by eddy currents and/or non-axisymmetric toroidal geometry.	Bell	Concur. See above chit # 16	
200911-18	CDR Chit-18	The bellows for the 2 neutral beams produce loads on the vessel that are additive and will contribute to horizontal displacement. This should be evaluated.	Mangra	The vacuum vessel will see a slightly higher load because the NB duct has a larger cross section than the existing pumpduct. However, it is the vacuum vessel supports that must react the additional load (the neutral beam box is more rigidly attached to the building).	This will be incorporated into the preliminary design.T
200911-19	CDR Chit-19	As shown, the NB armor blocks portions of bay G, which is the main diagnostic port. Consider alternate mounting schemes to reduce impact on this region.	Priniski	investigate with the help of B. Stratton (Diagnostics0	Due to the domed design of the port, a scalloped cut placed at the midplane in the support should maintain current diagnostic sightlines, this was planned, but not incorporated in cad model, will verify any other impacts.
200911-20	CDR Chit-20	The RWM coils have a nut plate which is approximately ¾" thick. (It sits under the coil.) It may have to be reworked to clear the vessel bumpout.	Dudek		This will be reviewed as part of the preliminary design review
200911-21	CDR Chit-21	Consider including an interlock on plasma density as well as current, since new beams will be injecting through edge of plasma and overlapping strike point areas will increase power on armor tiles. (A redundant interlock to a pyrometer)	Stevenson	investigate variety of interlock schemes.	An interlock and operational strategy will be evaluated and delineated for PDR but the strategy still remains that the NBI armor is a sacrificial backstop to avoid heating the vessel in the event of a full power shot in the absence of plasma and with the failure of any and all interlocks. In this very unlikely event, the carbon tiles may need to be inspected and replaced
200911-22	CDR Chit-22	Consider employing pyrometer(s) to monitor the surface of the neutral beam armor tile hot spots for a real-time interlock to terminate the beam pulse.	Stevenson		An interlock and operational strategy will be evaluated and delineated for PDR but the strategy still remains that the NBI armor is a sacrificial backstop to avoid heating the vessel in the event of a full power shot in the absence of plasma and with the failure of any and all interlocks. In this very unlikely event, the carbon tiles may need to be inspected and replaced

NSTX-U Project Reviews Recommendations Log

Item	Ref.	Concern/Recommendation	Responsibility / WBS or Job	Comment/Action	Current Status
200911-23	CDR Chit-23	The OH cooling system is designed for 600PSI water. This upgrade from 400PSI will increase flow about 20%. 600PSI is a high pressure. Suggest considering resizing holes to operate at 400PSI with back pressure to prevent any boiling.	Neumeyer	Menard/C. Neumeyer to evaluate design points and consider trade-offs.	A trade-study will be performed to quantify the relationship between pressure, hole size, cooldown time, and magnetic flux for the design with 24kA per turn and an alternate at ~ twice the current, ~ ½ the turns, which would have ~ ½ the winding length. Depending on the outcome, it may be necessary to revert to the higher current design to achieve cooldown within 400 psi constraint.
200911-24	CDR Chit-24	Consider alternate solutions to the I&C system other than CAMAC. It is old and frought with problems and difficult to debug failures. Now may be the time to replace	Sichta	evaluate.	Value Engineering will be used to develop the Preliminary Design; this is a tradeoff between cost (M&S, engineering) and quality of service (performance, reliability).
200911-25	CDR Chit-25	Presentation of Design before analysis in reviews would be an improvement.	n/a	Out of Scope for this review. PPPL to consider for future reviews.	Closed
200911-26	CDR Rec CS-01	Develop criteria for allowable load conditions that require protection by the MPS as soon as possible to be used for preliminary design.	Neumeyer	See 200911-08	See 200911-08
200911-27	CDR Rec CS-02	Write a design specification to collect and identify all design critical components which exceeded allowables that would guide MPS design.	Titus		The Machine Protection System has been adopted and incorporated into the baseline design. A design load specification will be written to identify and collect the critical components which rely on the protection of the MPS. The specification will be presented as part of the Preliminary Design.
200911-28	CDR Rec CS-03	Reconsider radial build of the centerstack to allow a more effective slip plane between the components even if there is some loss of i^2*t capability on the solenoid.	Neumeyer	See 200911-07	See 200911-07
200911-29	CDR Rec CS-04	Develop a supporting R&D program	Chrzanowski		I will develop document outlining R&D requirements for Upgraded Centerstack.
200911-30	CDR Rec NB-01	Consider a more modest modification of the proposed large cutout of the vacuum vessel for the new beamline.	Stevenson	Smaller cuts in the vessel were evaluated prior to arriving at the present design solution. The increased tangency radii are necessary for current drive and higher performance which are key goals of the upgrade. The increased tangency radii, the NBI fan array, and the TF outerleg at Bay K require a change to the Bay K opening because the beam trajectory cuts across the interstitial wall of the vacuum vessel between Bay K and Bay J. Because of the removal of the metal in the area to allow beam passage a cap was added to move the vacuum boundary out and to carry the stresses in this region. Rather than lose Bay J for diagnostics, the port was added to the cap also. These issues drove the size of the cap and the size of the VV hole.	Closed.

NSTX-U Project Reviews Recommendations Log

Item	Ref.	Concern/Recommendation	Responsibility / WBS or Job	Comment/Action	Current Status
200911-31	CDR Rec NB-02	Perform eddy current/error field analysis on the new very large vessel cutout port box assembly.	Bell		See 200911-17
200911-32	CDR Rec NB-03	Consider replacing data acquisition and I&C CAMAC systems with something more modern and reliable.	Sichta	See 200911-24	See 200911-25
200911-33	CDR Rec NB-04	Incorporate better interlocks (Ip and density) and monitoring (real-time pyrometers) of the beam armor tiles.	Stevenson	See 200911-22	See 200911-22
200911-34	CDR Rec NB-05	Install and maintain strict procedures for radiological control for contaminated beamline maintenance.	Stevenson	The existing beamline is assumed to be contaminated and is already treated as a radiologically contaminated beamline with full ES&H radiological procedure adherence now due to the presence of contaminated ion sources. Strict procedures exist and are employed on the existing beamline until it is show by surveys and samples to be not contaminated. This procedural approach will continue on with the new beamline also where the full regimen of HP RWP postings and support will be required for maintenance. So, due to the aforementioned sources, the very necessary procedures advocated by this chit have been in use for some time and fully meet the recommendations of the chit.	Closed
200911-35	CDR Rec C&S-01	Complete all elements of all WAFs, maintaining a common, crisp format.	Strykowsky		In process. Will be completed for the PDR in December
200911-36	CDR Rec C&S-02	Complete all fields in the risk registry.	Perry	Completed	Closed
200911-37	CDR Rec C&S-03	Document the risk management plan (a CD-1 requirement) in the PPEP	Perry	Completed	Closed
200911-38	CDR Rec C&S-04	Establish and implement a staffing plan to CD-2 that accounts for monthly assignments of specific tasks, self consistent with the resource-loaded schedule.	Strykowsky	Staffing plans will be prepared that show individuals by name and their loadings by month. These will be prepared on a 6-12 month rolling wave to better ensure the acheivability of the schedule.	In preparation for the December 2009 OFES review.
200911-39	CDR Rec C&S-05	Continue to implement PU Advisory Board recommendations to refine and improve the rigor of the risk/contingency development in advance of CD-2.	Strykowsky		Supplemental contingency methodologies will be explored and utilized prior to CD-2.
200911-40	CDR Rec C&S-06	Also, consider using risk matrix deadline dates to inform contingency distribution plan before Lehman CD-1 review	Strykowsky	Distribution of contingency as a function of time will be tempered by when risk are likely to occur.	Will be incorporated into future analyses.